

INFORMATION TO USERS

This manuscript has been reproduced from the microfilm master. UMI films the text directly from the original or copy submitted. Thus, some thesis and dissertation copies are in typewriter face, while others may be from any type of computer printer.

The quality of this reproduction is dependent upon the quality of the copy submitted. Broken or indistinct print, colored or poor quality illustrations and photographs, print bleedthrough, substandard margins, and improper alignment can adversely affect reproduction.

In the unlikely event that the author did not send UMI a complete manuscript and there are missing pages, these will be noted. Also, if unauthorized copyright material had to be removed, a note will indicate the deletion.

Oversize materials (e.g., maps, drawings, charts) are reproduced by sectioning the original, beginning at the upper left-hand corner and continuing from left to right in equal sections with small overlaps. Each original is also photographed in one exposure and is included in reduced form at the back of the book.

Photographs included in the original manuscript have been reproduced xerographically in this copy. Higher quality 6" x 9" black and white photographic prints are available for any photographs or illustrations appearing in this copy for an additional charge. Contact UMI directly to order.

UMI

A Bell & Howell Information Company
300 North Zeeb Road, Ann Arbor MI 48106-1346 USA
313/761-4700 800/521-0600



Université d'Ottawa • University of Ottawa

**Effects of Water Balance, Decomposition of Organic
Matter and Photosynthesis on the Chemistry and
the Carbon Cycle in the Upper St. Lawrence River
(Canada)**

Johannes A.C. Barth

A thesis submitted to the school of Graduate Studies and Research in partial
fulfillment of the requirements for the Ph.D. degree: Faculty of Science

Ottawa-Carleton Geoscience Centre

University of Ottawa

© Johannes Barth, Ottawa, Canada, 1998



National Library
of Canada

Acquisitions and
Bibliographic Services

395 Wellington Street
Ottawa ON K1A 0N4
Canada

Bibliothèque nationale
du Canada

Acquisitions et
services bibliographiques

395, rue Wellington
Ottawa ON K1A 0N4
Canada

Your file Votre référence

Our file Notre référence

The author has granted a non-exclusive licence allowing the National Library of Canada to reproduce, loan, distribute or sell copies of this thesis in microform, paper or electronic formats.

The author retains ownership of the copyright in this thesis. Neither the thesis nor substantial extracts from it may be printed or otherwise reproduced without the author's permission.

L'auteur a accordé une licence non exclusive permettant à la Bibliothèque nationale du Canada de reproduire, prêter, distribuer ou vendre des copies de cette thèse sous la forme de microfiche/film, de reproduction sur papier ou sur format électronique.

L'auteur conserve la propriété du droit d'auteur qui protège cette thèse. Ni la thèse ni des extraits substantiels de celle-ci ne doivent être imprimés ou autrement reproduits sans son autorisation.

0-612-36764-9

Canada

In memory of my father, Peter F.A. Barth

1932 -1977

Acknowledgments

I am indebted to Ján Veizer for his tremendous support, patience and encouragement. This research was supported by a grant from the Institute for Research on Environment and Economy (IREE) as well as NSERC research funds.

For invaluable advice with the manuscript, many useful discussions and technical support, I am truly grateful to my friends and colleagues Natalie Morisset, Patricia Wickham, Kelli Powis, Kenneth Hooper, Bernhard Mayer, Steven Turgeon, Kevin Telmer, Ajaz Karim, Mark Mihalaski, Bahram Daneshfar and François Richard.

For assistance with field work, special thanks to Lee Willard and James Abbott, as well as to Stephane Lorrain and Serge Lepage from the Centre St. Laurent in Montréal and Hans Biberhofer from the Canadian Inland Waters Directorate in Burlington. For support and training in the laboratory work, I thank Gilles St-Jean, Wendy Abdi, Natalie Morisset (G. G. Hatch Isotope Laboratories at the University of Ottawa), Bernhard Mayer (Isotope Laboratory at the Ruhr Universität, Bochum), Frances Pick (Department of Biology at the University of Ottawa), Judy Vaive and Gwendy Hall (Laboratory of Applied Geochemistry at the Geological Survey of Canada) and John Loop (Geochemistry Laboratory of the Ottawa-Carleton Geoscience Centre). For advice and help in the construction of various glass devices a special thanks to John Hopkins from the glass shop in the Department of Chemistry (University of Ottawa).

For every day support and encouragement a big thanks to Hélène de Gouffe, Sylvie Downing, Jean-François Tardiff, Andreas Prokoph and André Lalonde in the Department of Geology, University of Ottawa.

For numerous useful discussions and for nourishing my interest, I thank Ian Clark, Peter Fritz, Fred Michel, Ralf Kretz, Michel Robin, André Desrochers, Yves Goddérés and Olaf Podlaha.

Special thanks also to Harald Strauss and Dieter Buhl at the Ruhr-Universität Bochum for opening this opportunity for me; and finally, for continuous support and for providing me with an understanding of sportsmanship in science, an enormous thanks to my brothers Nikolaus and Thomas Barth, my mother Annegret Barth and my friends Klaus Pirke, Peter Duncan and Paul Waque.

Abstract

Temporal and spatial investigations of seven ecosystems in the St. Lawrence River (the 'Main Channel', a creek, a wetland and embayments) near the city of Cornwall, Ontario revealed more intense biogeochemical activity in near-shore ecosystems. The resulting gradients between near-shore ecosystems and the 'Main Channel' exist despite the Great Lakes' strong buffering effect, which is reflected in the well mixed water masses of the 'Main Channel', with consistent average $\delta^{18}\text{O}_{\text{H}_2\text{O}}$ and $\delta\text{D}_{\text{H}_2\text{O}}$ values of -6.9 and -50 ‰ VSMOW, respectively. These isotopic compositions also reflect lake-surface evaporation. The evaporated water is then added to atmospheric vapor and produces a deuterium excess of -11.8 ± 1.4 ‰ in local rain at Cornwall that indicates admixture of evaporated Great Lakes water to the local precipitation.

Precipitation over the Great Lakes catchment area contributes 3.9 % of Mg^{2+} and 31.2 % of SO_4^{2-} to the major ion flux of the 'Main Channel', with other major elements (Ca^{2+} , Na^+ , K^+ , Cl^- , SiO_2) falling between these two end-members. The precipitation input of total inorganic nitrogen is 9.4 times larger than the nitrogen output at Cornwall, indicating that the Great Lakes-St. Lawrence catchment area is a nitrogen sink. Based on major inorganic species, most samples are dominated by bicarbonate and calcium, showing that limestone weathering exerts the principal control on the water chemistry of the river.

The pCO_2 of waters ranges from values close to atmospheric equilibrium, 358 ppmV in the 'Main Channel', to as high as ~5450 ppmV in near-shore ecosystems indicating their higher groundwater influx and more active decomposition of organic matter. This gradient is also manifest in isotopic compositions of dissolved inorganic carbon, with $\delta^{13}\text{C}_{\text{DIC}}$ values ranging from +2.2 to -13.7 ‰ VPDB for the 'Main Channel' and near-shore ecosystems, respectively. High pCO_2 and negative $\delta^{13}\text{C}_{\text{DIC}}$ values in the 'Hoople Creek' were inherited mostly from the respiration dominated baseflow, as evidenced by the resemblance of $\delta^{18}\text{O}_{\text{H}_2\text{O}}$ to local groundwater (-9.9 to -11.3 ‰ VSMOW), but abundant organic matter in the creek (DOC up to 38.3 mg/L) causes additional decomposition, resulting in even higher pCO_2 and more negative $\delta^{13}\text{C}_{\text{DIC}}$ values. The embayment sampling stations 'Hoople Bay' and 'Long Sault Island', on the other hand, are dominated by photosynthesis during the warm seasons, as indicated by pCO_2 values of less than atmospheric equilibrium and O_2 oversaturations. This is further supported by enriched $\delta^{13}\text{C}_{\text{DIC}}$ values and by chlorophyll-a (chl-a) contents as high as 63.0 mg/L.

Photosynthesis and detrital inputs are both significant contributors to the POC pool in the isolated embayments. The former dominates during warm seasons, with POC concentrations up to 2663 $\mu\text{g/L}$. Near-shore ecosystems have a wide range of $\delta^{13}\text{C}_{\text{POC}}$ values (-31.5 to -16.3 ‰), but this variability is not reflected in the 'Main Channel'. There, the $\delta^{13}\text{C}_{\text{POC}}$ signal is uniformly close to -27 ‰, in accord with estimates from earlier studies on the river's estuary. This suggests that the POC contribution from near-shore ecosystems is minor. Although the 'Main Channel' has low chl-a concentrations, model calculations suggest that most of its POC originates from photosynthetic activity, probably within the Great Lakes.

The carbon cycle studies are the most essential part of this work and outline three major ecosystems for the St. Lawrence River: (1) The 'Main Channel' and related ecosystems that are dominated by the Great Lakes and exchange processes with the atmosphere; (2) near-shore ecosystems (creeks and wetlands) that are dominated by groundwater and decomposition of organic matter; (3) isolated embayments that, during the warm season, also have a strong photosynthetic component. The latter two types of ecosystems are the most active in carbon recycling, indicating their importance in terms of net primary productivity. They also mark the locations with the highest vulnerability to anthropogenic influences.

Résumé

Un suivi temporel et spatial de sept écosystèmes du fleuve Saint-Laurent (la partie centrale du fleuve, un ruisseau, un marais et des baies) à proximité de la ville de Cornwall en Ontario a révélé l'existence d'activité biogéochimique plus prononcée dans les écosystèmes à proximité de la rive. Les gradients résultants s'observent malgré le puissant effet tampon dû à la présence des Grands Lacs. Les masses d'eau bien mélangées de la partie centrale du fleuve illustrent cet effet tampon, le $\delta^{18}\text{O}_{\text{H}_2\text{O}}$ et le $\delta\text{D}_{\text{H}_2\text{O}}$ ayant respectivement des valeurs constantes de -6.9 et -50 ‰ VSMOW. Ces compositions isotopiques reflètent également l'évaporation à la surface des lacs. L'eau évaporée s'ajoute à la vapeur d'eau atmosphérique et produit un excès de deutérium de -11.8 ± 1.4 ‰ dans les pluies locales à Cornwall.

Les précipitations sur le bassin de réception des Grands Lacs contribuent respectivement à 3,9 % et 31,2 % des flux totaux de Mg^{2+} et SO_4^{2-} dans la partie centrale du fleuve. Les contributions des autres éléments majeurs (Ca^{2+} , Na^+ , K^+ , Cl^- , SiO_2) sont comprises entre ces deux extrêmes. L'apport total d'azote inorganique par les précipitations est 9.4 fois plus important que la perte au niveau de Cornwall. Ceci indique que le bassin de réception des Grands Lacs et du Saint-Laurent constitue un puits d'azote. L'étude des espèces inorganiques majeures montre que la plupart des échantillons d'eau sont dominés par le bicarbonate et le calcium, suggérant que la dissolution des carbonates contrôle largement la chimie aquatique du Saint-Laurent.

Les valeurs mesurées du pCO_2 aqueux vont de ~358 ppmV dans la partie centrale du fleuve jusqu'à ~5450 ppmV dans les écosystèmes à proximité de la rive. Le premier chiffre démontre l'équilibre avec l'atmosphère, et le second, la décomposition active du carbone organique et l'influence d'eau souterraine. Ce gradient s'observe également en termes de composition isotopique du carbone inorganique dissous: les valeurs de $\delta^{13}\text{C}_{\text{DIC}}$ s'étendent de +2,2 ‰ VPDB dans la partie centrale du fleuve à -13.7 ‰ dans le ruisseau Hoople. Les valeurs extrêmes de pCO_2 aqueux et du $\delta^{13}\text{C}_{\text{DIC}}$ dans le ruisseau Hoople proviennent essentiellement de l'eau souterraine marquée par la respiration, ce qu'indique clairement la similitude du $\delta^{18}\text{O}_{\text{H}_2\text{O}}$ entre le ruisseau Hoople et les eaux souterraines locales (-9,9 à -11,3 ‰). Cependant, la décomposition des matières organiques qui abondent dans le ruisseau Hoople (DOC max. 38,3 mg/L) y a encore accentué le signal provenant de la respiration (pCO_2 plus élevé et $\delta^{13}\text{C}_{\text{DIC}}$ plus négatif). Les baies Hoople et Long Sault Island sont quant à elles dominées durant les mois chauds par l'activité photosynthétique, mise en évidence par des supersaturations en oxygène et des concentrations de CO_2 plus basses que la valeur d'équilibre avec l'atmosphère. Ceci s'observe également dans des valeurs enrichies de $\delta^{13}\text{C}_{\text{DIC}}$ et des concentrations de chlorophylle-a (chl-a) allant jusqu'à 63 $\mu\text{g/L}$.

La photosynthèse et l'apport détritique contribuent de façon importante au carbone organique particulaire (POC) dans les baies isolées. La photosynthèse domine durant les saisons chaudes, produisant des concentrations de POC allant jusqu'à 2663 $\mu\text{g/L}$. Bien que les écosystèmes proches des rives affichent un large éventail de valeurs de $\delta^{13}\text{C}_{\text{POC}}$ (de -31,5 à -16,3 ‰), cette variabilité n'est pas observée dans la partie centrale du fleuve. Le $\delta^{13}\text{C}_{\text{POC}}$ y est uniformément égal à environ -27 ‰, en accord avec des estimations publiées dans des études

sur l'estuaire du fleuve. Ce résultat suggère que l'apport de POC en provenance des écosystèmes des rives est de faible importance. Quoique la partie centrale du fleuve contienne peu de chl-a, les modélisations suggèrent que la plupart de son POC origine d'activité photosynthétique, probablement dans les Grands Lacs.

L'étude du cycle du carbone est la partie la plus essentielle de ce travail et marque trois écosystèmes majeurs dans le fleuve Saint-Laurent: (1) la partie centrale du fleuve et les écosystèmes reliés, qui sont dominés par les Grand Lacs et les processus d'échange avec l'atmosphère; (2) les écosystèmes à proximité de la rive (ruisseaux et marais), qui sont dominés par l'influence de l'eau souterraine et la décomposition de la matière organique; (3) les baies isolées qui, dans les saisons chaudes, sont marquées fortement de la photosynthèse. Les deux derniers types d'écosystèmes sont ceux qui recyclent le carbone le plus activement, indiquant leur importance en termes de production primaire. Ils représentent par ailleurs les parties du fleuve qui sont les plus vulnérables aux activités humaines.

Table of Contents

Acknowledgments	I
Abstract	II
Résumé	IV
Table of Contents	VI
List of Figures	IX
List of Tables	X
List of Appendices.....	XI
1. Introduction	1
1.1 Previous and ongoing work on the St. Lawrence River	2
1.2 Objectives and description of the monitoring.....	4
1.2.1 Description of the sampling sites	8
1.3 Original contributions	10
1.4 Overview of the Great Lakes-St. Lawrence Catchment area.....	11
1.4.1 General characteristics of the Great Lakes-St. Lawrence system.....	11
1.4.1.1 Great Lakes	11
1.4.1.2 St. Lawrence River	12
1.4.1.3 Climate, natural vegetation and topography of the region	13
1.4.2 Anthropogenic influences.....	14
1.4.2.1 Agriculture and forestry	15
1.4.2.2 Mining	16
1.4.2.3 Manufacturing and industry.....	16
1.4.3 Description of the study area at Cornwall.....	17
2. Geology of the Great Lakes-St. Lawrence catchment basin.....	18
2.1 The St. Lawrence Platform and its History.....	18
2.2 The Michigan Basin.....	24
2.3 The Canadian Shield surrounding the Great Lakes	26
2.4 Quaternary Deposits	29

2.5 Local Geology at Cornwall.....	31
3. Methodology.....	33
3.1 General notes	33
3.1.1 Resolution of the samples in time and space.....	33
3.1.2 Precision and Accuracy.....	34
3.1.3 Sampling containers and their preparation	36
3.1.3.1 Field sampling bottles.....	36
3.1.3.2 Subsampling bottles	37
3.2 On site procedures.....	37
3.2.1 Temperature	38
3.2.2 Dissolved oxygen.....	38
3.2.3 pH.....	39
3.2.4 Eh	40
3.2.5 Alkalinity	40
3.2.6 Conductivity	41
3.3 Field procedures within six hours after sampling	41
3.3.1 Filtration.....	41
3.3.2 Sample preservation.....	42
3.3.3 Photometric determination of the dissolved NO_3^- -N, NO_2^- -N, NH_4^+ -N, PO_4^{3-} and SiO_2	43
3.4 Laboratory procedures	44
3.4.1 Major cations.....	44
3.4.2 Major anions.....	45
3.4.3 Dissolved organic carbon (DOC)	45
3.4.4 Chlorophyll-a.....	46
3.4.5 Isotopic composition of the dissolved inorganic carbon ($\delta^{13}\text{C}_{\text{DIC}}$)	46
3.4.6 Particulate organic carbon (POC) and its isotopic composition ($\delta^{13}\text{C}_{\text{POC}}$).....	47
3.4.7 Isotopic composition of oxygen in water($\delta^{18}\text{O}_{\text{H}_2\text{O}}$).....	48
3.4.8 Isotopic composition of hydrogen in water ($\delta\text{D}_{\text{H}_2\text{O}}$).....	48
3.4.9 Trace- and rare earth elements	48

3.4.10 Summary	49
4. Oxygen and Deuterium Isotopes.....	51
4.1 Results	52
4.2 Isotopic composition of local meteoric waters	52
4.3 Isotopic composition of surface water.....	57
4.4 Residence time in the 'Hoople Creek' system.....	64
5. Major ion and nutrient chemistry	69
5.1 Results	70
5.1.1 Major ions	70
5.1.2 Nutrients	71
5.2 Average composition of the upper St. Lawrence River water	71
5.3 Atmospheric deposition of major ions	73
5.4 Classification of the St. Lawrence water	76
5.5 Grouping of major ions.....	80
5.5.1 Sodium, chloride and potassium.....	80
5.5.2 Sulfate	85
5.5.3 Calcium and magnesium.....	87
5.5.4 Bicarbonate	90
5.6 Dissolved inorganic nitrogen species.....	94
6. Carbon cycle	97
6.1 Seasonal dynamics of carbon dioxide and oxygen.....	100
6.2 Isotope constraints	108
6.3 Biogeochemical classification of ecosystems	115
6.4 Origin of particulate organic carbon in the upper St. Lawrence: Isotopic constraints	122
6.4.1 Results.....	124
6.4.2 Discussion	125
6.4.2.1 Sources of particulate organic carbon.....	125
6.4.2.2 Isotopic constraints	129
6.4.2.3 Theoretical fractionation by algae.....	133
7. Conclusions.....	138

7.1 Water balance.....	138
7.2 Major element and nutrient chemistry	140
7.3 Upper St. Lawrence River carbon cycle.....	141
References.....	144

List of Figures

Fig. 1.1 Overview of the St. Lawrence River and the sampling stations at Cornwall.....	6
Fig. 2.1 Overview of the geologic regions in the Great Lakes-St. Lawrence catchment basin.....	19
Fig. 2.2 Elements of the St. Lawrence Platform.....	20
Fig. 2.3 Subdivision of the Canadian Shield surrounding the Great Lakes	27
Fig. 4.1 Daily precipitation together with temperature curves and $\delta^{18}\text{O}_{\text{H}_2\text{O}}$ values.....	53
Fig. 4.2 Local meteoric water line for precipitation collected at Cornwall between 1995 and 1996.....	55
Fig. 4.3 Average $\delta^{18}\text{O}_{\text{H}_2\text{O}}$ compositions of the seven sampling stations.....	58
Fig. 4.4 Local meteoric water line in comparison to surface water samples.	59
Fig. 4.5 Temporal $\delta^{18}\text{O}_{\text{H}_2\text{O}}$ variations at the seven sampling stations.....	61
Fig. 4.6 Mixing proportions between groundwater, 'Hoople Creek' and the 'Main Channel' in 'Hoople Bay'.....	63
Fig. 4.7 Temporal $\delta^{18}\text{O}_{\text{H}_2\text{O}}$ variations in 'Hoople Creek'	65
Fig. 4.8 Three scenarios for time delays between the $\delta^{18}\text{O}_{\text{H}_2\text{O}}$ curves of precipitation and those of 'Hoople Creek' waters.	66
Fig. 5.1 Piper diagram of major ions.....	79
Fig. 5.2 River classification modified after Meybeck (1986).....	81
Fig. 5.3 Temporal trends of Na^+	82
Fig. 5.4 Scatter plot of Cl^- versus Na^+	83
Fig. 5.5 Scatter plot of SO_4^{2-} versus Na^+	88
Fig. 5.6 Temporal trends of SO_4^{2-}	89
Fig. 5.7 Scatter plot of HCO_3^- versus DOC.....	92
Fig. 5.8 Weathering model with DOC and HCO_3^-	93

Fig. 5.9 Temporal trends of NO_3^-	95
Fig. 6.1 Location of the sampling sites near Cornwall, with their average annual pCO_2	99
Fig. 6.2 Temporal variations of the pCO_2 in the ecosystems studied.....	101
Fig. 6.3 Differences between calculated and atmospheric pCO_2 plotted versus the differences between measured pO_2 and atmospheric pO_2	105
Fig. 6.4 Plot of chlorophyll-a versus the partial pressure of oxygen.....	107
Fig. 6.5 Measured $\delta^{13}\text{C}_{\text{DIC}}$ compared to expected values for equilibrium with the atmospheric CO_2	111
Fig. 6.6 Differences between the calculated and measured $\delta^{13}\text{C}_{\text{DIC}}$	112
Fig. 6.7 Differences between the calculated and measured $\delta^{13}\text{C}_{\text{DIC}}$ plotted versus the $\delta^{18}\text{O}_{\text{H}_2\text{O}}$ signal of the water samples.	114
Fig. 6.8 Correlation between DOC and $\delta^{13}\text{C}_{\text{DIC}}$	117
Fig. 6.9 Temporal variations of the $\delta^{13}\text{C}_{\text{DIC}}$ and DOC signals in the ecosystems studied.....	118
Fig. 6.10 Ternary plot of relative proportions of the DOC, $\delta^{13}\text{C}_{\text{DIC}}$ and chl-a.....	121
Fig. 6.11 Location map and annual average concentrations of POC	123
Fig. 6.12 Temporal distributions of chlorophyll-a contents and POC.....	126
Fig. 6.13 POC/chl-a ratio versus $\delta^{13}\text{C}_{\text{POC}}$	130
Fig. 6.14 Temporal variations of $\delta^{13}\text{C}_{\text{DIC}}$ and $\delta^{13}\text{C}_{\text{POC}}$	132
Fig. 6.15 Theoretical and measured fractionations, ϵ , between C_e (= $\text{CO}_2(\text{aq})$) and phytoplanktonic POC	135

List of Tables

Table 3.1 Diurnal variations of biologically dominated parameters in Hoople Bay.....	34
Table 3.2 Reagents, reaction times, wavelengths and precisions for the photometric field procedures.....	43
Table 3.3 List of analytical methods and instruments used, including their precisions.	50
Table 4.1 Parameters of the Cornwall meteoric water line in comparison to the data from the literature.....	56
Table 5.1 Comparison between the average composition of world river water and upper St. Lawrence River.	72

Table 5.2 Major ion fluxes of the upper St. Lawrence River and their contributions to the global world river flux.	73
Table 5.3 Precipitation input of major ions to the Great Lakes and the percent contributions to the major ion flux in the 'Main Channel'.	74
Table 5.4 Precipitation input of major ions to the Great Lakes catchment area and the percent contributions to the major ion and nutrient flux in the 'Main Channel'.....	76

List of Appendices

A 1 Trace and rare earth element data	12 p.
A 2 Field measurements	4 p.
A 3 Deuterium and Oxygen isotope data and calculations	
A 3.1 Isotope data of precipitation	1 p.
A 3.2 $\delta^{18}\text{O}_{\text{H}_2\text{O}}$, $\delta\text{D}_{\text{H}_2\text{O}}$ and Cl^- for surface water samples	4 p.
A 3.3 Calculation of the mixing of water masses in 'Hoople Bay'	2 p.
A 4 Major ion and nutrient data and calculations	
A 4.1 Surface water data.....	4 p.
A 4.2A Calculation of precipitation flux over the Great Lakes	2 p.
A 4.2B Calculation of precipitation flux over the Great Lakes catchment area	2 p.
A 4.2C Atmospheric corrections	1 p.
A 5 Carbon cycle data and calculations.....	
A 5.1 List of relevant data for the carbon cycle.....	4 p.
A 5.2.A POC and relevant data	1 p.
A 5.2.B Calculation of theoretical fractionation byalgae	3 p.

1. Introduction

During the past few decades chemical and geochemical aspects of rivers have received increasing attention in the scientific community. This has led to numerous publications (e.g. Livingstone, 1963; Gibbs, 1970; Meybeck, 1979, 1980, 1984, 1986; Holland, 1978; Stallard and Edmond, 1983; Wadleigh et al., 1985; Berner and Berner, 1987; Négrel et al., 1993; Edmond et al., 1995; Tardy et al., 1995; Cameron et al., 1995; Allègre et al., 1996; Louvat and Allègre, 1997). These studies outlined chemical weathering processes and helped to understand transport of chemical elements from land to ocean. Additionally, since rivers are potential sites for pollutant disposal, growing environmental concern led to investigations of their ecology and biogeochemistry. Within this field the understanding of riverine carbon cycles is of particular interest, because they reflect transport of carbon from land to ocean as well as the state of life and biodiversity within rivers and their catchment areas (Degens et al., 1991; Ludwig et al., 1996; Probst et al., 1992; Pawellek and Veizer, 1995; Flintrop et al., 1996; Buhl et al., 1991; Mook and Tan, 1991). One of the most intriguing findings in this type of research was that many rivers have significantly higher partial pressures of CO₂ in their water column than the atmosphere (e.g. Kempe, 1982; Gao and Kempe, 1987; Probst et al., 1992; Amiotte Suchet and Probst, 1995; Ludwig et al., 1996; Telmer, 1996; Tardy et al., 1993), leading to discussions of their contribution to the greenhouse effect. This contribution gains particular weight when considering that biogeochemical arrays within rivers may reflect processes of entire drainage areas.

The St. Lawrence River represents a low energy system, caused by its source in the Great Lakes and by a series of dams. These lacustrine environments reflect upon the river's biogeochemical characteristics, which, in contrast to many other major river systems, is marked by equilibration with the atmosphere and surface water evaporation (Yang et al., 1996).

1.1 Previous and ongoing work on the St. Lawrence River

Water chemistry data from 1870 are among the earliest measurements reported for the St. Lawrence River (Meybeck, 1979; Weiler and Chawla, 1969). In recent decades the St. Lawrence River and the Great Lakes were subject to intensive monitoring of their environmental quality by Environment Canada and various other governmental and educational institutions. Among the published data are those of the Envirodat Water Quality Database (Environment Canada, 1992) and various water quality reports (e.g. Lamarche, 1992; Désilets and Langlois, 1989; Cluis et al., 1990; Rondeau, 1993; Houle et al., 1995). Considerable work was also undertaken on trace metals and rare earth elements in the St. Lawrence River (Sloterdijk, 1991; Quémerais et al., 1996; Carignan et al., 1994). The particulate organic carbon in the St. Lawrence estuary was studied in detail by Pocklington (1985), Pocklington and Tan (1987), Tan and Strain (1983) Tan (1987), Lucotte (1989) and Lucotte et al. (1991) and the dissolved inorganic carbon along the St. Lawrence course by Yang et al. (1996). Experiences and ideas were also exchanged at numerous conferences on the Great Lakes-St. Lawrence River system, such as the 'Symposium on the Saint-Lawrence' (Messier et al., 1990), the international 'Sharing Knowledge, Linking Science' conferences in 1994, 1995 and 1996 in Cornwall, and the

Great Lakes Research Consortium Conferences of 1996, 1997 and 1998 in Syracuse, NY. In the recent project under the auspices of the Institute for Research on the Environment and Economy (IREE) at the University of Ottawa, 18 publications and 49 working papers appeared, all related to the environmental situation of the St. Lawrence River near Cornwall.

The IREE Project also led to the establishment of the St. Lawrence River Institute in Cornwall that provides environmental information and participates in the Cornwall and Massena Remedial Action Plans to restore damaged local ecosystems, such as contaminated sediments. In other ongoing work, the Centre Saint-Laurent (established in 1988) in Montréal monitors sediment and water chemical dynamics of the St. Lawrence River, with some of their programs taking place in Lake St. Francis in the Cornwall area. Furthermore, the 'Biosphere Ecowatch Centre' in Montréal has established a long-term monitoring network of the St. Lawrence-Great Lakes ecosystems, involving a number of individuals, schools, colleges, universities and research centres. A number of eight provincial and federal governmental organisations, including the Canadian Inland Waters Directorate (Burlington), the Centre Saint-Laurent and the Ministère de l'Environnement et de la Faune du Québec, amongst others, participate in an environmental plan known as 'St. Lawrence Vision 2000'. This program is dedicated to monitoring of the ecology and the restoration of the health of the river system.

Among the body of literature on the St. Lawrence River the publication by Yang et al. (1996) is the one most related to this study, because it applies many of the same parameters. This work also provides an excellent overview of the biogeochemistry of the

entire Great Lakes-St. Lawrence system, thus laying the foundations for the local monitoring conducted in this thesis.

1.2 Objectives and description of the monitoring

Most of the work outlined above is either related to the entire St. Lawrence River or its lower parts (i.e. downstream of Montréal) and focuses on the river's main channel. However, biogeochemical studies of the Great Lakes-dominated upper St. Lawrence River and its marginal ecosystems is essential if we are to understand the dynamics of the riverine system. For this reason, a local monitoring program was established near the city of Cornwall in order to answer the following questions:

- What is water balance in the seven ecosystems studied?

This question implies the objective to investigate the origin of water in the seven sampling stations in order to map the relative importance of precipitation, baseflow and Great Lakes water. Furthermore, the influence of surface water evaporation has to be established for the studied sampling sites.

- What are the chemical characteristics of the upper St. Lawrence River and its near-shore ecosystems in the Cornwall area?

This question implies the objectives to classify the water chemically and to narrow down specific sources of major ions, such as rock weathering, anthropogenic and biological influences. Additionally, major ion flux balances of the 'Main Channel' are to be compared to average major world river in order to elucidate the influence of

precipitation inputs of major ions to the Great Lakes-St. Lawrence River catchment basin.

- What are the major influences on the riverine carbon cycle in the Cornwall area?

This question implies the task to investigate the CO₂ budget of the river by targeting locations with higher than the 'Main Channel' pCO₂. With CO₂ budgets and other tools, such as the isotopic composition of the dissolved inorganic carbon ($\delta^{13}\text{C}_{\text{DIC}}$) one can then establish the relative importance of mixing, atmospheric equilibration, influx of groundwater, interaction with organic matter and photosynthesis on the riverine carbon cycle. In particular, the role of in situ generation of particulate organic carbon (POC) by photosynthesis versus terrestrial influences is to be investigated with chlorophyll-a measurements as well as the isotopic composition of the POC ($\delta^{13}\text{C}_{\text{POC}}$).

Specifically this study investigates whether there are any biogeochemical differences between the main river and its adjoining near-shore ecosystems and, if so, how they compare to the down-river evolution. This study also explores seasonal variations and their effect on the aqueous biogeochemistry of the studied ecosystems. Comparison between near-shore ecosystem and the 'Main Channel' is most important in order to test the vulnerability of the study area to environmental influences and to be able to protect the St. Lawrence River in the future.

In order to fulfill these objectives, a total of 165 water samples were collected in the Cornwall area between May 1994 and June 1996 (Fig. 1.1). Based on a reconnaissance study during the first sampling year, some sampling localities

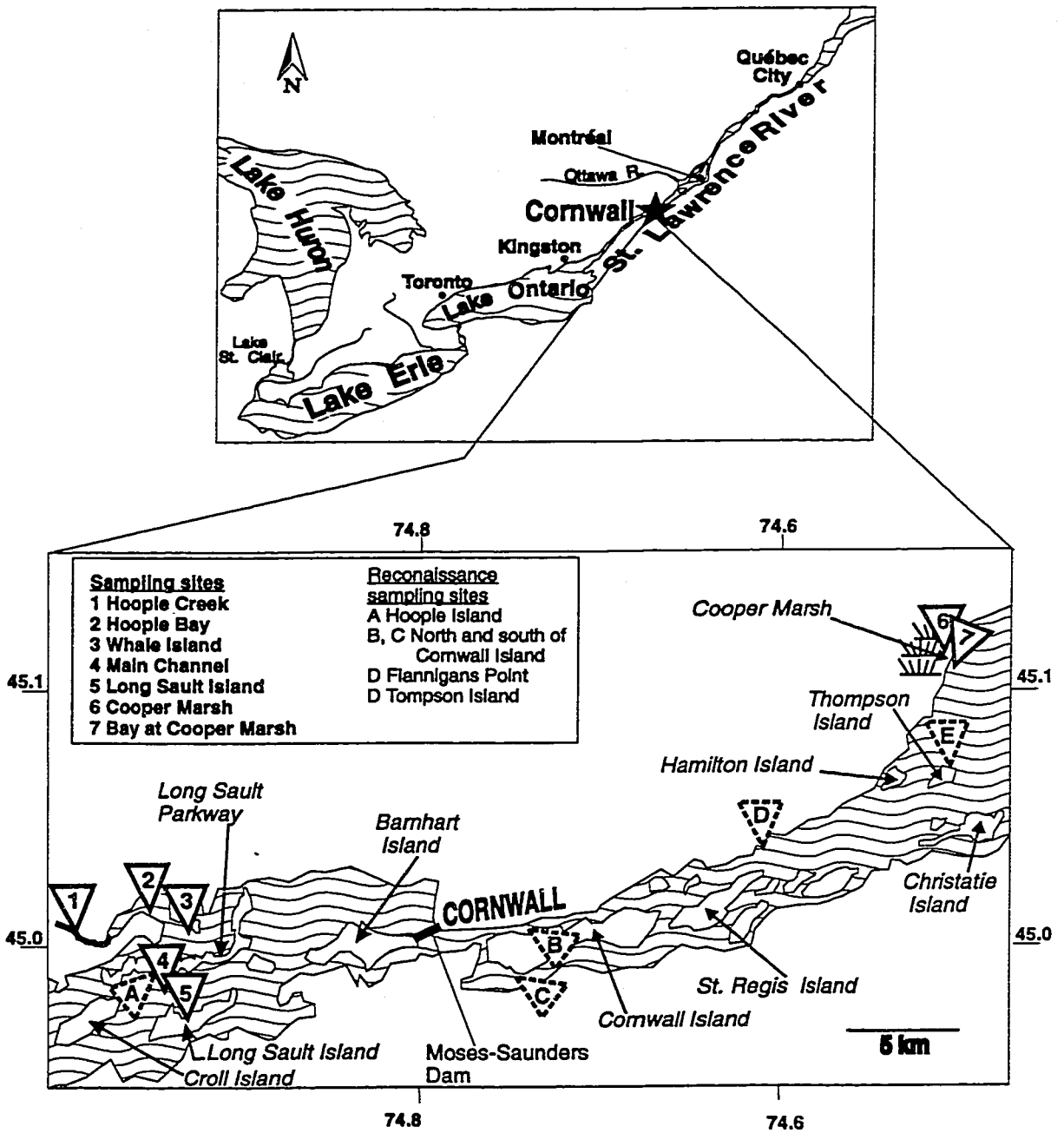


Fig. 1.1 Overview of the St. Lawrence River and the sampling stations at Cornwall.

(‘Hoople Island’, two stations north and south of Cornwall Island, ‘Flannigans Point’, and ‘Thompson Island’ Fig. 1.1), proved superfluous for the purposes of this study, because their water chemistry was almost identical to the ‘Main Channel’ waters. These stations were therefore not further sampled and are not discussed throughout this thesis, but their data are still listed in the appendices and considered in a separate report (Barth et al., 1996). Between May 1995 and June 1996 the main monitoring took place with two-week interval sampling at the seven locations ‘Hoople Creek’, ‘Hoople Bay’, ‘Whale Island’, ‘Long Sault Island’, ‘Bay at Cooper Marsh’, ‘Cooper Marsh’ and the ‘Main Channel’ (Fig. 1.1). Sampling was interrupted between December 1995 and April 1996 due to ice cover and too expensive sampling logistics. Within this period, the most critical time was during formation and break up the ice cover, because it would have been too dangerous to go on the river by boat. The reader should be aware that the omission of one entire season (winter) may weaken some conclusions for the seasonal aspects of this work. Nevertheless, in many cases, the temporal trends may be extrapolated from the late fall to early spring for the missing season. The parameters analyzed were the following:

- field parameters (temperature, dissolved oxygen, pH, Eh, alkalinity, conductivity)
- major anions, cations and nutrients (Cl^- , SO_4^{2-} , Ca^{2+} , Mg^{2+} , Na^+ , K^+ , dissolved nitrogen species and PO_4^{3-}),
- chlorophyll-a (chl-a), dissolved organic carbon (DOC), particulate organic carbon (POC),
- isotopic compositions of the dissolved inorganic carbon ($\delta^{13}\text{C}_{\text{DIC}}$) and the particulate organic carbon ($\delta^{13}\text{C}_{\text{POC}}$),

- isotopic signature of the water ($\delta^{18}\text{O}_{\text{H}_2\text{O}}$, $\delta\text{D}_{\text{H}_2\text{O}}$),
- trace metals (Fe, Mn, Al, Cd, As, Cr, Pb, etc.),
- and rare earth elements (La, Ce, Nd, Sm, Tb, etc.),

The trace and rare earth elements are not further discussed here, because they were found to be fairly homogenous and below the limits of the Canadian recommended surface fresh water quality objectives (Barth et al., 1996). Nonetheless, they are listed in Appendix 1. Also note that this work neglects investigations at the sediment water interface. One should keep in mind that this could weaken some of the conclusions, particularly for the discussion of the riverine carbon cycle.

In addition to the river water, a total of 57 precipitation samples were collected in Cornwall between July 1995 and August 1996 in order to characterize their stable isotope compositions ($\delta^{18}\text{O}_{\text{H}_2\text{O}}$, $\delta\text{D}_{\text{H}_2\text{O}}$).

1.2.1 Description of the sampling sites

Although scattered data were obtained from other sampling sites, this section describes only the seven sampling stations of the main monitoring (Fig. 1.1).

'Hoople Creek' is a small stream of 0.5 to 0.7 m depth. However, during high runoff events in the spring and fall, the water stand of this creek reached depths of approximately 1.5 m, while at the end of August 1995 the water was less than 0.3 m deep. The creek water is non-turbid but has a slight brownish color. During summer, submersed macrophytes and algal mats were attached to rocks in the creek while reed canary grasses (*Phalaris arundinacea*) and sedges (*Scirpus validus*) grew at its sides.

'Hoople Bay' covers an area of about 1 km² in size and has a lake-like character with normally calm waters ranging between 2 and 2.5 m depth. The bottom sediments are muddy to sandy and the waters are turbid with a greenish color. Turbidity increases were observed after storm events, likely caused by re-suspension of bottom sediments. The embayment is surrounded by few family homes and cottages. The northern parts of the embayment are very shallow with reeds and rushes of various kinds growing on the shorelines.

The sampling station at 'Whale Island' has a constant water depth of approximately 4 m. Its waters were clear, and during the warm seasons submersed macrophytes grew close to the shore of the island.

The 'Main Channel' sampling station has a depth of about 30 m with turbulent water flow. During every sampling event, the water collected was crystal clear with no turbidity or color.

The 'Long Sault Island' sampling station was located at the end of an elongated embayment of about 800 m length and 150 m width. The water depth varied between 0.5 and 1.5 m, depending on the water stand of the river. The muddy to sandy bottom sediments are partially covered with tree stumps, still present from before the flooding of the area. The waters at this site can be very turbid, particularly during times of phytoplankton growth and after storm events.

The 'Cooper Marsh' wetland lies on the north-shore of the river, about 3 km south-west from the mouth of the Raisin River. The sampling station was located in a drainage canal with a water depth of about 1 m. The water level is regulated using water from the St. Lawrence River. At times, floating algal mats and duckweed (*Nymphaea*) and

Frogsbit (*Hydrocheris morsus-ranae*) were present, while cattails (*Typha*), willows (*Salix*), sedges and grasses and Purple Loosestrife framed the sides of the 4 m wide drainage canal during most of the sampling season.

The sampling station 'Bay at Cooper Marsh' was established 100 m south of the wetland. This site had a water depth of 2.5 m, and during summer a field of rushes (*Junkus*), partially coated by algal mats, grew at this location. Like most other sampling stations related to the main stem of the river the waters had little turbidity and clear color.

1.3 Original contributions

The original contributions to research on the St. Lawrence River from this study include:

1. Description of the methodology, including sampling of river water, field measurements, filtration and chemical and isotopic laboratory procedures (Chapter 3).
2. Evaluation of the $\delta^{18}\text{O}_{\text{H}_2\text{O}}$ and $\delta\text{D}_{\text{H}_2\text{O}}$ compositions of upper St. Lawrence River water, including estimates of mixing with near-shore ecosystems (Chapter 4).
3. Estimates of $\delta^{18}\text{O}_{\text{H}_2\text{O}}$ and $\delta\text{D}_{\text{H}_2\text{O}}$ compositions of local precipitation at Cornwall, contributing to the network of other stations (i.e. Ottawa, Simcoe) in the Great Lakes-St. Lawrence watershed (Chapter 4).
4. Comparison of the upper St. Lawrence River major element chemistry to average world river water (Chapter 5).
5. Calculation of the major element and nutrient flux in the upper St. Lawrence River with respect to inputs by precipitation (Chapter 5).

6. Combined consideration of $\delta^{13}\text{C}_{\text{DIC}}$ with dissolved organic carbon (DOC) and chlorophyll-a (chl-a) with particular emphasis on peripheral ecosystems (Section 6.1, also submitted to *Chemical Geology*; authors: Johannes Barth, Ján Veizer).
7. Evaluation of particulate organic carbon (POC) and its isotopic composition ($\delta^{13}\text{C}_{\text{POC}}$) in the upper St. Lawrence River and its near-shore ecosystems (Section 6.2, submitted to *Earth and Planetary Science Letters*; authors: Johannes Barth, Bernhard Mayer, Ján Veizer).

1.4 Overview of the Great Lakes-St. Lawrence Catchment area

The study area at Cornwall should not be considered in isolation, because it is tied into the entire Great Lakes-St. Lawrence catchment basin. A brief description of the latter helps to understand the riverine processes that will be discussed in the subsequent chapters of this thesis.

1.4.1 General characteristics of the Great Lakes-St. Lawrence system

1.4.1.1 Great Lakes

By surface, the Great Lakes form the greatest connected area of fresh water on earth. The drainage basin of the five lakes, including their water surfaces, covers about 765 990 km² (United States Environmental Protection Agency and Government of Canada, 1995), with three fifths of this watershed in the United States and two fifths in Canada (Compton's Encyclopedia, 1994). Of this area, two thirds consists of land and one third of water surface. The shoreline of the Great Lakes skirts the eight states Minnesota,

Wisconsin, Michigan, Illinois, Indiana, Ohio, Pennsylvania, and New York as well as the Canadian province of Ontario.

Precipitation amounts to an annual average of 840 mm in the catchment area (Environment Canada, 1994). Streams draining adjacent land are the second largest source of water supply. While no major rivers empty into the Great Lakes, the runoff carried by thousands of brooks, creeks, and small rivers is large in total. The streams emptying into Lake Superior, for example, discharge the equivalent of about 460 mm of the lake's average depth (Compton's Encyclopedia, 1994). The Nipigon River is the largest tributary, flowing 65 km from Lake Nipigon, Ontario, into Lake Superior. A third natural source of water supply is groundwater, while relatively small amounts of water are added to the Great Lakes through artificial channels and by pumping. For example, the Long Lake and Ogoki projects of the Ontario Hydro-Electric Power Commission divert water from the Hudson Bay watershed into Lake Superior. Water is also removed from the Great Lakes, such as from channels that divert water from the Lake Michigan basin into the Mississippi River system. However, this water output is minor when compared to that of the St. Lawrence River. About 650 mm/year of water are estimated to be lost from the Great Lakes surface by evaporation (United States Environmental Protection Agency and Government of Canada, 1995).

1.4.1.2 St. Lawrence River

The St. Lawrence is part of a large seaway from the Atlantic Ocean to the Great Lakes, ranking in importance with the Suez and Panama canals. In 1959, the Canadian and United States governments established the St. Lawrence Seaway, opening the Great Lakes

to ocean vessels and harnessing the river's hydroelectrical power. The river proper stretches 1197 km from about 44°N near Kingston to approximately 50°N near Sept-Îles, where it empties into the 800 km long Gulf of St. Lawrence (Canadian & World Encyclopedia, 1997). The chief tributaries from the north are the Ottawa, St. Maurice and Saguenay rivers; from the south, the St. Francis and Richelieu rivers, however the largest proportion of water originates from the Great Lakes. The river leaves Lake Ontario, widening into the Thousand Islands section during its next 109 km. In the following 185 km it drops 69 m passing the Iroquois Dam and Lake St. Lawrence, which ends at the Moses-Saunders Power Dam at the city of Cornwall. Then it flows through the 48 km long Lake St. Francis and the 26 km long Beauharnois Canal, which bypasses the Lachine Rapids at Montréal and drains into Lake St. Louis. For about 45 km between Sorel and Trois-Rivières the river stretches through Lac St-Pierre leading to the city of Québec, where it broadens into the St. Lawrence Estuary. Compared to other major world rivers, the St. Lawrence ranks 15th in terms of its catchment basin and 13th in terms of its discharge (St. Lawrence Centre, 1993).

1.4.1.3 Climate, natural vegetation and topography of the region

The St. Lawrence lowland region of Ontario and Québec have a cool continental climate, characterized by hot summers and cold winters. Near the city of Québec, the temperature averages -11.5°C in January and 19.3°C in July, while the annual precipitation is 1060 mm, a large part of which falls as snow (Compton's Encyclopedia, 1994). The region roughly corresponding to the Canadian Shield has a cold continental climate, with long, cold winters and short, hot summers, with mean temperatures of -20°C in January

and 17.5°C in July (United States Environmental Protection Agency and Government of Canada, 1995). The mean annual precipitation of the Great Lakes region lies between 810.5 and 870.7 mm (Environment Canada, 1994).

The natural vegetation on most of the Canadian Shield in the catchment area consists of mixed forest with patches of boreal and broadleaf forest (National Atlas Information Service, 1993). In northwestern and central Ontario as well as in Québec lies a belt of mixed coniferous and deciduous forest, while southern Ontario and the Michigan Peninsula have small wooded areas that are the remains of what once was a large deciduous forest.

The topography in the Catchment basin is relatively moderate with the Canadian Shield reaching maximal elevations of 600 m above sea level (Compton's Encyclopedia, 1994; United States Environmental Protection Agency and Government of Canada, 1995). Altitudes in the St. Lawrence lowlands range from 15 m above sea level along the St. Lawrence River near Montréal to approximately 150 m along the borders with the Laurentian Mountains to the N, the Adirondacks to the S, the gradual transitions to the Appalachians in the SE and the Precambrian shield of Ontario in the W (Canadian & World Encyclopedia, 1997).

1.4.2 Anthropogenic influences

In 1535, Jacques Cartier arrived at the St. Lawrence River and its lowlands, which at this time were only inhabited by a small population of the Iroquois people (Canadian & World Encyclopedia, 1997). Cartier named a bay on the north shore of the river in honor of the third-century saint and martyr Laurentius (St-Laurent), a name that was transferred

to the entire river by Samuel de Champlain in the 17th century. This marked the start of European colonisation of the region. Today, over 41 million inhabitants live in the Great Lakes-St. Lawrence catchment area (St. Lawrence Centre, 1993), and land use can be grouped into three major categories: (1) agriculture and forestry, (2) mining, and (3) manufacturing and industry. Further anthropogenic influence may be caused by urban pollution and landfill sites.

1.4.2.1 Agriculture and forestry

Almost all farming in the Great Lakes-St. Lawrence drainage area is practiced in the lowland areas of Ontario, Québec and the U.S. states that skirt the Great Lakes. The region hosts not only mixed farmlands with grain cultivation (wheat, oats, flax, and canola) and livestock farms (cattle, poultry, eggs, pork), but also specialty farming (fruit trees, tobacco, vegetables). In recent years farming in Québec has been increasingly converted into larger dairy operations, specializing more than half of the commercial farms in the province on dairy products (Compton's Encyclopedia, 1994). The largest tobacco growing area in Canada is on the north shore of Lake Erie, and most of the country's production of Table and wine grapes is grown in the narrow strip of lake-level land in the Niagara peninsula (Canadian & World Encyclopedia, 1997).

A large part of the boreal forest in the catchment area is used as lumber and plywood for furniture making and the pulp and paper industry. Inexpensive newsprint from Canada has become the material used to print almost half the newspapers in the western world (Compton's Encyclopedia, 1994).

1.4.2.2 Mining

Next to copper, nickel, zinc, gold, silver and uranium, mining operations of iron ores are the most important in the Great Lakes-St. Lawrence drainage basin. For instance the Mesabi and Gogebic iron mines on the shores of Lake Superior supply a large part of the U.S. iron industry. One of the most significant gold deposits in Canada was found in 1981 at Hemlo on the north shore of Lake Superior. Furthermore, the asbestos deposits in the Eastern Townships (Québec) are the world's largest, accounting for about 85 percent of Canada's asbestos production. Additionally, there is substantial mining of coal, gas and petroleum in the Michigan Basin. Furthermore, the Sifto salt mine at Goderich, Ontario, is one of the largest mining operations in the region (Environment Canada, 1994).

1.4.2.3 Manufacturing and industry

The cities of Toronto and Montréal account for more than a third of Canada's manufacturing with cereal processing, breweries, and industries of electrical appliances, clothing, publishing and aircrafts. Chicago has a diversified industry, producing machine tools, plastic and rubber goods. Detroit in the United States, Oshawa, Oakville, Brampton, and Windsor in Ontario and Ste-Thérèse in Québec are automobile and truck centers; Hamilton (Ontario), Contrecoeur (Québec) are known as 'Steel Cities', while Sarnia (Ontario) has petrochemical and salt processing facilities. In the cities of Beauharnois, Baie-Comeau, Bécancour and Shawinigan in Québec aluminum and other metal alloys are being produced along with chemical products. Finally, the numerous rivers draining into the St. Lawrence system as well as the St. Lawrence River itself have a large hydroelectric power potential.

1.4.3 Description of the study area at Cornwall

The city of Cornwall (Ontario) has approximately 47,000 inhabitants and is situated at 74.73°W and 45.01°N on the St. Lawrence River, about 85 km south-east of Ottawa. The local industry at Cornwall consists of Domtar Fine Papers and the chemical company Courtaulds Fibre, which was recently closed. Upstream of the Moses-Saunders Dam, at Ingelside, a factory of Kraft Foods Ltd. is located in the vicinity of 'Hoople Creek', while south of the river in Massena the two major industries are General Motors, and Aluminum Co. of America. According to the International Joint Commission, Cornwall belongs to one of the 18 worst polluted areas in the Great Lakes-St. Lawrence catchment region (Wallace and Millvard, 1985). This is largely attributed to PCB contaminated sediments on the U.S. side of the river, a problem that is now addressed by sediment dredging and clearing programs.

Downstream of the Moses-Saunders Dam, the Akwesasne Indian Reserve is spread over the Cornwall and St. Regis Islands, which are followed by a series of smaller islands (e.g. St. Regis, Hamilton, Christatie and Thompson Island). South of the Akwesasne Islands, the Wiley Dondero Canal bypasses the merchant ship traffic past Cornwall. Upstream of the Moses-Saunders Dam a series of islands are connected by the Long Sault Parkway. Other important upstream islands are Barnhart Island on the Canadian side and Long Sault Island on the U.S. side (Fig. 1.1). With the establishment of the Moses-Saunders Dam in 1958 some areas upstream of Cornwall were flooded, leading to resettlement and the creation of new islands and embayments. For instance, the river area north of the Long Sault Parkway is artificial and old roads and railway lines are present under the water cover.

2. Geology of the Great Lakes-St. Lawrence catchment basin

The Great Lakes-St. Lawrence catchment basin consists of three major geologic regions: (1) the Canadian Shield surrounding the north-west and lying to the north of the Great Lakes, (2) the Michigan Basin underlying the area inbetween and underneath Lake Michigan and Lake Huron, and (3) the St. Lawrence Platform (Fig. 2.1). This chapter presents an overview of the most important rock types of these regions. Knowledge about the geological setting of the Great Lakes-St. Lawrence watershed will become important for consideration of the major ion chemistry (Chapter 5), which is largely influenced by rock weathering.

Sedimentary rocks are particularly important for this process with the water chemistry at Cornwall being most strongly influenced by rocks of the St. Lawrence Platform. The latter region will therefore be discussed in greater detail in this chapter. Downstream of Montréal, the St. Lawrence Lowlands are bordered by the Canadian Shield to the North and the Appalachian Mountains to the South (Fig. 2.1). These areas, as well as the Ottawa River Basin, are not discussed here, because they do not influence the water chemistry of the upper St. Lawrence River at Cornwall.

2.1 The St. Lawrence Platform and its History

The St. Lawrence Platform hosts sedimentary strata of early Ordovician to late Devonian age and consists of a western and a central part separated by the Frontenac Arch (Fig. 2.2).

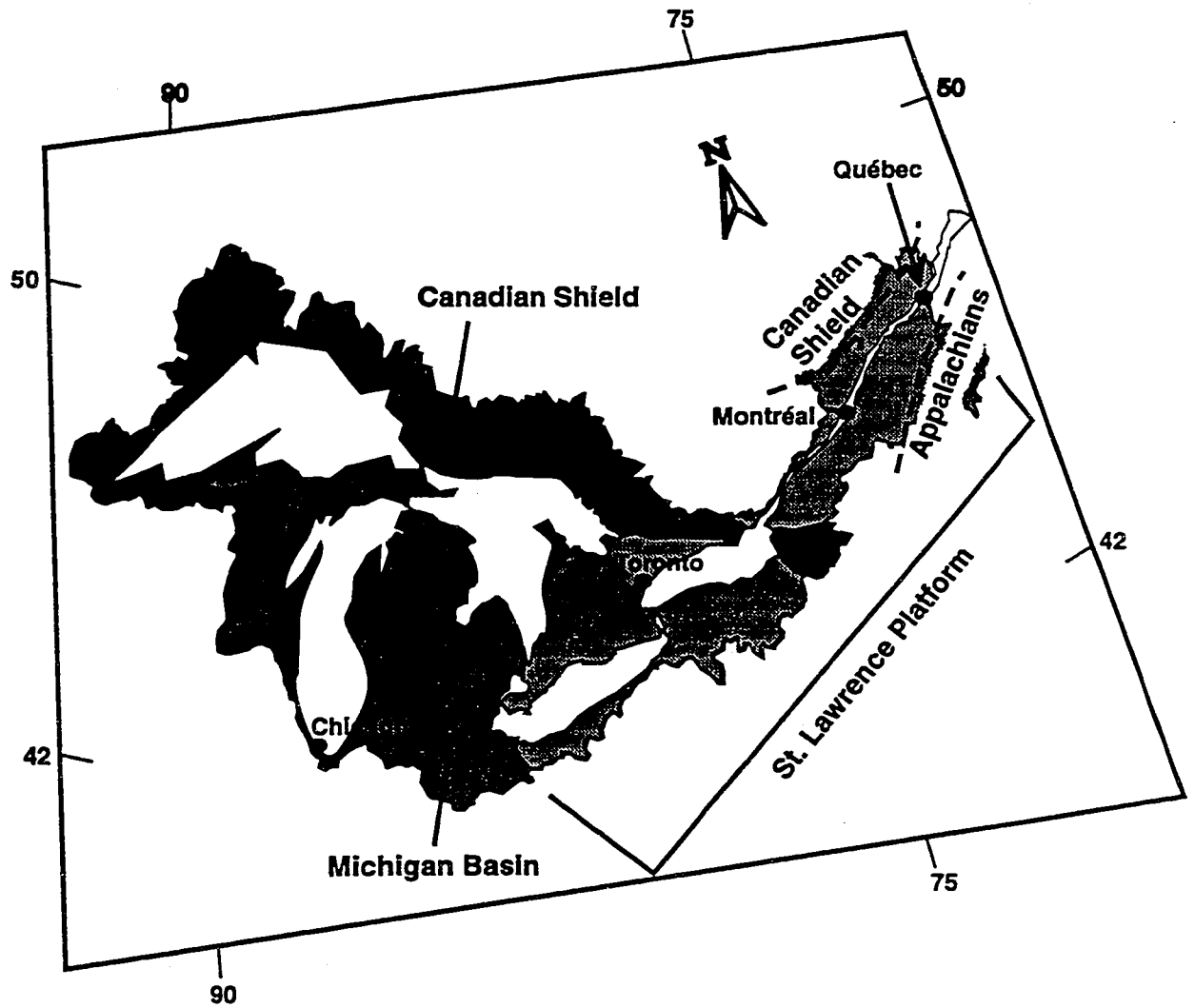


Fig. 2.1 Overview of the main geologic regions in the Great Lakes-St. Lawrence catchment basin.

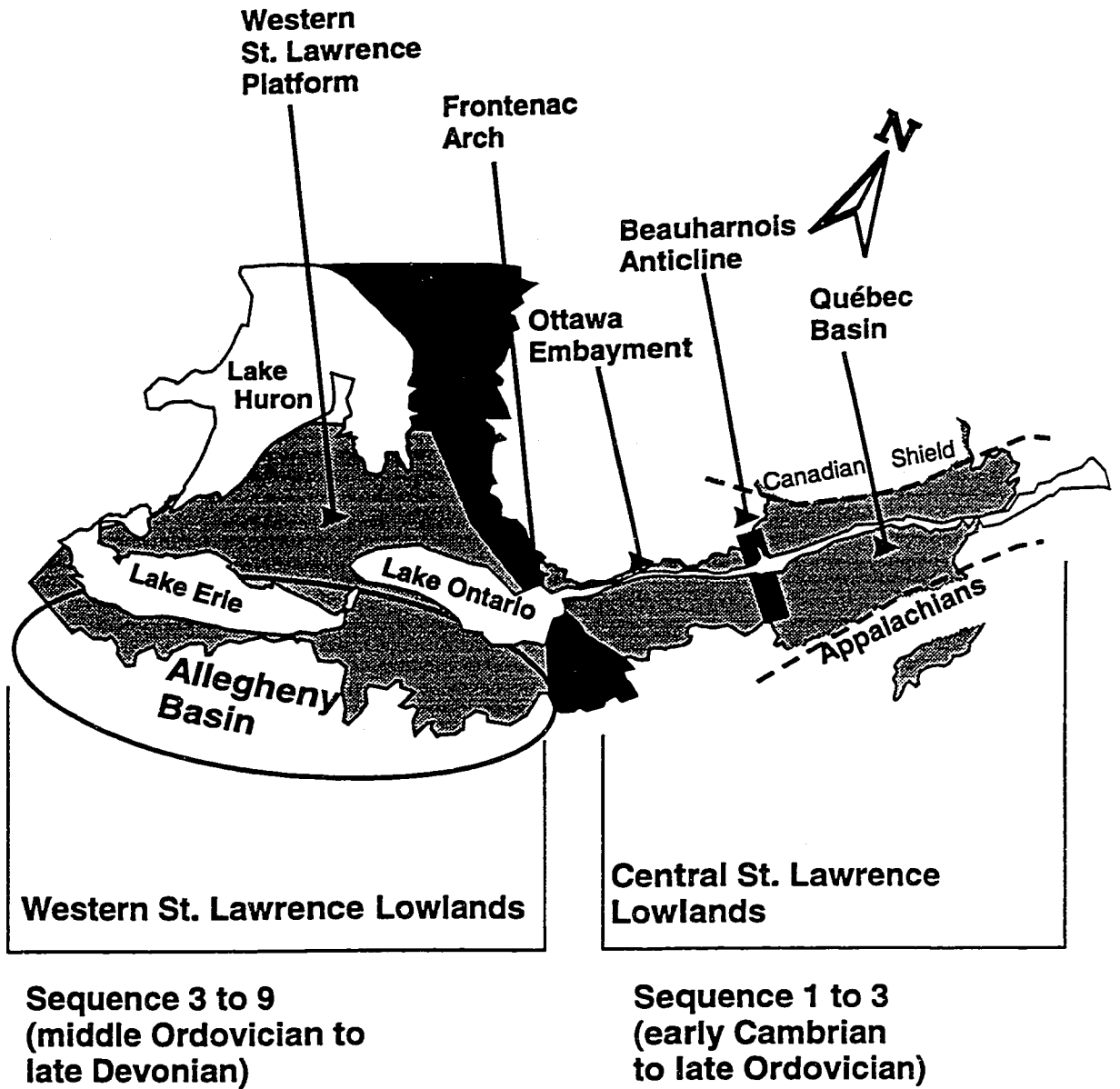


Fig. 2.2 Elements of the St. Lawrence Platform.

The central part is further subdivided by the Beauharnois Anticline into the Québec Basin and the Ottawa Embayment (Sanford, 1993). The latter will receive particular emphasis in this section, because some of its strata are present at Cornwall. It should be noted, however, that the formations of the Québec Basin resemble those of the Ottawa Embayment, but have a generally greater thickness. The Western St. Lawrence Lowlands can further be subdivided into the Western St. Lawrence Platform and the Allegheny Basin, both having similar lithologies. For the description of the St. Lawrence Platform and its basic history, the depositional sequence stratigraphy of Johnson et al. (1992) was applied. This stratigraphy subdivides the continent-wide sequences by Sloss (1963) into 10 subsequences.

Sequence 1 marks the time from Early Cambrian to Early Ordovician (545 - 478 Ma), with the opening of the Iapetus Ocean leaving the St. Lawrence Platform as a passive continental margin, which functioned as a broad continental shelf with shallow marine conditions, and favored the deposition of carbonates with minor intercalations of shield-derived orthoquartzitic sandstones (Sanford, 1993). In the Ottawa Embayment, sandstones and conglomerates dominate the lithology of this sequence and are known as the about 20 m thick Covey Hill and the 200 m thick Nepean sandstones that both belong to the Potsdam Formation (Sanford, 1993; Baer et al., 1971).

During sequence 2 (early to middle Ordovician, 478 - 450 Ma), the Iapetus seafloor began to converge against the North American margin, initiating the Taconian Orogeny. With this, the broad shelf of the St. Lawrence Lowlands changed into a trough and formed a NW trending foreland basin, in which sandstones and dolomites were deposited. A subsequent marine transgression caused the deposition of predominantly carbonates. Examples for these two depositional environments are the 30 m thick sand- and dolostones of the March

Formation and the 115 m thick dolostones of the Oxford Formation in the Ottawa Embayment (Sanford, 1993; Baer et al., 1971).

In middle Ordovician times, the North American margin commenced with subduction, causing the rise of the Taconian Orogen. This time span, between 450 and 438 Ma, is known as sequence 3, with deposition of mainly orogen derived clastic sediments and carbonates and fine to coarse-grained clastics as the dominant facies. The associated formations belong to the Chazy Group and consist of shales, sandstones and few carbonates that are known as the up to 50 m thick Rockliffe Formation in the Ottawa Embayment (Sanford, 1993; Baer et al., 1971). Continuation of the orogeny caused the trough axis to migrate northwestward, resulting in dominant sedimentation of flysch and shale. After a minor marine regression the sea transgressed from west of the Frontenac Arch and led to the deposition of limestone beds belonging to the Black River and Trenton groups (Cane, 1996a), which together are about 210 m thick (Sanford, 1993). On the Western St. Lawrence Platform, these limestones are also exposed and present the first significant Palaeozoic sediments west of the Frontenac Arch, with a thickness of approximately 280 m (Sanford, 1993; Ontario Geological Survey, 1991). Overlying shales result from subsequent deep water conditions and, in the Ottawa Embayment, are known as the Billings, Carlsbad, Russell and Queenston shales, having a cumulative thickness of about 300 m (Sanford, 1993). Similar formations with a thickness of 240 m lie concordantly on the Trenton Group limestones on the Western St. Lawrence Platform and dip slightly westwards (Ontario Geological Survey, 1991). Due to erosion, marine transgressions later than the upper Ordovician are not preserved in the Central St. Lawrence Lowlands.

Due to relatively subdued orogenic activity along the Appalachian front, a mixed deposition of siliciclastic orogen-derived rocks, marine shales and dolostones took place in

Early to Middle Silurian times (Llandovery). This interval (438 - 432 Ma) is referred to as depositional sequence 4, and its formations are known as Whirlpool-Sandstones, Manitoulin-Dolostones, Cabbot Head-Shales and the shaly Grimsby Sandstones on the Western St. Lawrence Platform. Together they reach a maximal thickness of 90 m (Johnson et al., 1992).

During sequence 5 (middle Silurian, 432 to 417 Ma) a phase of reef growth in the Great Lakes region and reactivation of the arches dominated the geologic setting of the St. Lawrence Platform. Perhaps the most famous Silurian formation of this phase is the Lockport Formation, a dolomitic limestone that forms the upper layer of the Niagara Falls. With the exception of the Rochester Formation (argillaceous limestones) and the Thorold Formation (quartzitic sandstones and shales), the other units of sequence 5 consist of limestones and dolostones with various admixtures of argillaceous material. The maximum cumulative thickness of these strata reaches about 190 m, and together with the formations of sequence 4, forms the Niagara Escarpment (Johnson et al., 1992).

Sequence 6 (417 to 401 Ma) reflects activities of the late Taconic and early Acadian orogenies that resulted in an uplift of the arches and led to restricted inter-basin circulation. This resulted in depositions of evaporites mixed with dolostones and shales known as the 430 m thick Salina Formation in the Western St. Lawrence Platform (Sanford, 1993; Ontario Geological Survey, 1991).

Sequence 7 (early to middle Devonian, 401 to 380 Ma) is characterized by first movements of the Acadian Orogeny, causing the deposition of redbeds. However, more importantly for the western parts of the St. Lawrence Platform, in Early Devonian times seaways extended far across the Canadian Shield, connecting the St. Lawrence and Hudson platforms and causing deposition of carbonates, shales and evaporites. The latter are only

preserved in the Devonian strata of the Michigan Basin, while a band of sandstones, dolostones and limestones with a cumulative thickness of 350 to 380 m is exposed on the Western St. Lawrence Platform (Sanford, 1993; Johnson et al., 1992).

The sedimentary formations of sequence 8 (380 -358 Ma) reach a maximum thickness of 340 m and are marked by the onset of the Acadian Orogeny during Late Devonian times. The strata are known as the shales and limestones of the Hamilton Group, which is topped by black and grey shales of the Kettle Point and Bedford formations, followed by shaly sandstones and black shales of the Berea and Sunbury formations.

Between Carboniferous and Early Permian times (Sequence 9) the Alleghenian Orogeny (320 to 280 Ma) caused deposition of clastic sediments in the St. Lawrence Lowlands. Carboniferous sediments may have covered a substantial part of the St. Lawrence Platform, but are largely eroded by now. Only the area south of Lake Erie exposes some Carboniferous sandstones (Sanford, 1993).

Sequence 10 lasts from Middle Jurassic to Late Cretaceous times (186 to 91 Ma) and is separated from the subjacent sequence by a hiatus. However, there is no record of sedimentation of these strata in the St. Lawrence Lowlands.

In summary, the history of repeated tectonism caused by uplift and collisional forces at the Appalachian plate margin influenced sedimentation and facies in the St. Lawrence Basin with sequential deposition of sandstone, carbonate, shale and evaporite facies.

2.2 The Michigan Basin

This circular basin underlies the area inbetween and underneath Lakes Michigan and Lake Huron and also crops out on Manitoulin Island and the Bruce Peninsula between

Georgian Bay and Lake Huron. It contains a sequence of Phanerozoic sediments that have similar lithologies when compared to the strata of the St. Lawrence Platform (Bally, 1989). Cambrian, Ordovician and Silurian strata are exposed west and north of Lake Huron as well as on Manitoulin Island and the Bruce Peninsula, while Silurian, Devonian and Carboniferous rocks crop out between Lake Michigan and Lake Huron. The entire sequence is over 5000 m thick and has been described by Fisher et al. (1988).

The Lower Cambrian strata consist chiefly of sandstones with a maximal thickness of 600 m and are topped by carbonate and shale deposits that contain sandstones and glauconitic dolomites. The carbonate and sandstone facies were deposited within Late Cambrian and Early Ordovician times and reach a maximum thickness of 850 m. Subsequently, until the Upper Ordovician, a series of sandstones with a maximum thickness of 900 m was deposited. These series are topped a ~1300 m thick series of evaporite-rich shales and carbonates that span most of the Silurian era and are the equivalent to the Salina Formation on the St. Lawrence Platform. The Devonian is marked by ~1200 m thick series of dolomites, limestones and few sandstones that contain some evaporites. From the Middle Devonian onwards, the lithology changes again to shales with increasing amounts of sandstone by mid Mississippian times. This change to siliciclastic sedimentation probably happened in response to the rising Appalachians in the East. The maximum thickness of the Mississippian is about 600 m. The Pennsylvanian is characterized by a typical Carboniferous coal bearing sequence of sandstones, shales and limestones with a maximal thickness of 230 m.

2.3 The Canadian Shield surrounding the Great Lakes

The rocks of the Canadian Shield surrounding Lake Superior belong to the Archean Superior Province, while parts of Lake Huron border the Proterozoic Southern Province. The Grenville Province extends from east of Lake Huron to the Adirondack Mountains, which start southeast of the St. Lawrence River (Fig. 2.3).

The Superior Province is composed of sub-parallel east-northeast trending belts of contrasting lithology, age and metamorphic grade and consists of metasedimentary accretionary prisms, island arch plutons and supercrustal belts with granulite grade gneisses (Hoffman, 1993). Only four of these subprovinces fall into the Great Lakes Basin (Fig. 2.3). The Wabigoon Subprovince has a circa 3 billion-year old granitic basement and greenstones of the same age (Blackburn et al., 1991). Its dominant lithology consists of metavolcanic and subordinate metasedimentary rocks that are surrounded and cut by granitoid batholiths. The Quetico Subprovince consists mainly of metamorphosed turbiditic wacke and silts, which were deposited during and after a climax period in volcanic activity in the neighboring Wawa, Wabigoon and Abitibi subprovinces. The youngest sediment deposition was dated at 2.698 Ga, while the oldest granitoid intrusion happened 2.688 Ga ago (Percival and Sullivan, 1988). The oldest stage of supracrustal development in the Wawa Subprovince was dated 2.89 Ga, and its major lithology consists of greenstone belts that are interlaced with gneiss, granodiorite and granite facies (Williams et al., 1991). The western Abitibi Subprovince is separated from the Wawa province by the Kapuskasing Structural Zone.

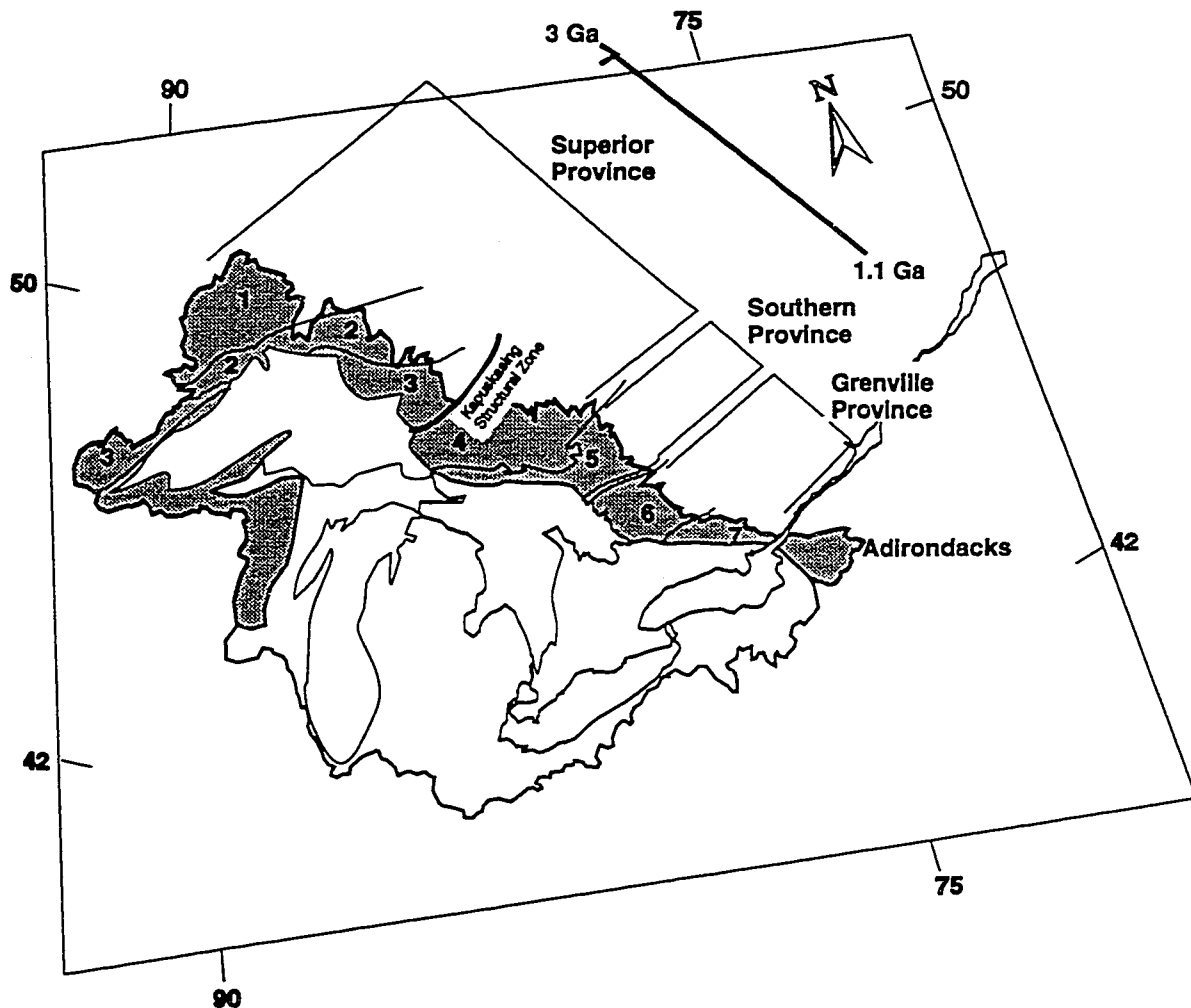


Fig. 2.3 Subdivision of the Canadian Shield surrounding the Great Lakes modified after Thurston (1991a,b). Subprovinces are as follows: 1 = Wabigoon, 2 = Quetico, 3 = Wawa, 4 = Abitibi, 5 = Southern Province, 6 = Central Gneiss Belt, 7 = Central Metasedimentary Belt.

Its 2.75 to 2.65 Ga old granite-greenstone dominated lithology hosts metavolcanic rocks, fluvial-alluvial metasediments and granodiorite intrusions (Jackson and Fyon, 1991).

The 2.5 to 2.2 Ga old Huronian Supergroup is the main subdivision of the Southern Province in the Great Lakes catchment basin and extends from the east shore of Lake Superior along the north shore of lake Huron to beyond Sudbury. It consists cycles of conglomerate, mudstones, siltstones and arenites, with volcanics at the base (Bennett et al., 1991). The other subdivision of the Southern Province that falls within the Great Lakes basin is the 1.85 Ga old Sudbury Structure consisting of the Sudbury Igneous Complex as well as breccias, mudstones, and wackes (Dressler et al., 1991).

The Grenville Province is a complex orogenic belt of ca. 1.1 Ga age (Easton, 1991), and is separated from the Southern Province by the Grenville Front Tectonic Zone (Fig. 2.3). The Central Gneiss Belt is one of the major units in the Grenville Province, hosting amphibolite to quartzofeldspathic gneisses of chiefly igneous origin as the most abundant rock type. The other major unit is the Central Metasedimentary Belt with Mesoproterozoic accumulations of supracrustal rocks invaded by syn- and post-tectonic plutons. The metamorphic grade varies from greenschist to granulite facies (Easton, 1991).

The lithology of the Adirondack Mountains, south of the St. Lawrence, is an assemblage of anorthosite-gabbro batholiths, pyroxene granitoids, quartzite, marble and paragneiss (Hoffman, 1993).

The shield area between Lake Superior and Lake Michigan consists of various rock units with greenstones and gneisses of Archean times. Another unit found in this area is the Animikie Basin with stratified rocks from early Proterozoic times (Sims, 1993). The latter includes major iron formations in a sedimentary sequence of quartzites and slates.

2.4 Quaternary Deposits

During the Quaternary, several ice sheets formed the present morphological structures of the Great Lakes-St. Lawrence catchment area. With the retreat of the Laurentide Ice sheet at the end of Wisconsinian times (13,200 to 10,000 BP), large volumes of meltwater accumulated in glacial lakes along the ice front, forming the pre-stages of the present Great Lakes. Subsequent isostatic rebound and shifting of the ice fronts caused dramatic changes in the drainage patterns of the glacial lakes. Drainage occurred variously through the valleys of the Illinois River (towards the Mississippi), the Hudson River, the Trent River and the Ottawa River, before the establishment of the outlet through the St. Lawrence River (United States Environmental Protection Agency and Government of Canada, 1995). The main type of deposit resulting from glaciations are tills, which are defined as poorly sorted sediments that were transported and deposited by and from glacier ice (Dreimanis, 1982). Tills that are derived from Paleozoic sediments are usually more silty and have higher carbonate contents when compared to tills from the Canadian Shield, which are more sandy in nature (Barnett, 1991). Between 12,000 and 9,000 B.P. the Champlain Sea covered large areas of the St. Lawrence Lowlands (Ramesh and Anglejan, 1995). During this episode, marine, glacial and, to a limited extent, also non-glacial sediments were deposited.

The St. Lawrence Lowlands have three major types of Quaternary deposits, 1) non-glacial terrestrial deposits, 2) glacial deposits and 3) Champlain Sea deposits. The latter pre-date the glaciations while the non-glacial terrestrial deposits occur after glaciations and consist of lacustrine, fluvial, eolian silts and sands and organic material such as peat. Next to ice contact deposits, glaciolacustrine and glaciofluvial deposits, the main type of glacial

deposits are tills (Ochietti, 1989). In the Ottawa Embayment these tills are known as the clayey Malone Tills that are overlain by the more sandy Fort Covington Tills reaching a cumulative thickness of 24 m (MacClintock, 1958; Fullerton, 1980; Clark and Karrow, 1984; Dreimanis, 1985).

Marine sediments of the Champlain Sea consist of a sequence of glaciomarine deposits, overlain by marine sediments, which in turn are topped by a regression facies. The glaciomarine deposits occur locally and consist of submarine fans containing gravels and sands (Rust, 1977). The marine sediments are up to 100 m thick clay series with admixtures of silt and occasionally fine sands. They are covered by crossbedded stratified sands and silts of the regression facies with some decimetres to metres thickness (Ochietti, 1989). The massive to color-banded marine clays are by far the most abundant units of the Champlain Sea and are referred to as Leda Clays (Barnett, 1991). Due to their characteristics, when disturbed, they are classified as quick clays and numerous landslides have occurred along slopes cut into these sediments. At Casselman (~50 km north of Cornwall) the Leda Clays consist of about 30 m thick silty and sandy clays, occasionally carrying H₂S odors (Gadd, 1986).

The Great Lakes subregion between Lake Ontario and Lake Huron was not affected by the Champlain Sea, and its Quaternary deposits consist of extensive clay and silt deposits of glacial and glaciolacustrine origins and glacial moraines (Farvolden and Cherry, 1988). For instance in the Toronto area, tills were reported to range between ~30 to 80 m in thickness with clayey and sandy components (Karrow, 1984). Most of the area south of Lake Superior is dominated by end moraines of similar thickness that are interlaced by sand and gravel deposits with maximum thicknesses exceeding 100 m (Richmond and Fullerton, 1983a). The Michigan Basin is predominantly covered by outwash (sand and gravel) of up to 20 m and end moraines

of up to 35 m thickness (Richmond and Fullerton, 1983b). Only the western parts of Lake Huron are framed by lacustrine clay and silt deposits with thicknesses between 1 and 10 m (Farrand and Bell, 1982). The sedimentary cover south of Lake Erie changes from a ground moraine (1-10 m) to a loamy till end moraine (2-6 m) that also covers large areas south of Lake Ontario (Fullerton and Richmond, 1991). The Canadian Shield in the Great Lakes area exposes predominantly bedrocks (Dyke et al., 1989), with its sparse Quaternary coverage consisting mainly of sandy tills and few glacial lake deposits (Dredge and Cowan, 1989).

Sediments within Lake Ontario have been described as carbonate-poor glacial tills, glaciolacustrine clays and postglacial muds, with quartz and feldspar more abundant in coarser inshore sediments and clay minerals and organic carbon dominating finer offshore sediments (Thomas et al., 1972). Similar lake sedimentologies were reported for Lake Erie (Bolsenga and Herdendorf, 1993) and are likely of the same nature in the other lakes.

2.5 Local Geology at Cornwall

The bedrock geology at Cornwall is much the same as some of the lower Ordovician strata described for the Ottawa Embayment (Section 2.1), but the formations have partially local names (Cane, 1996b; Porter, 1996). The strata dip slightly north-westwards and begin with a series of limestones and dolostones known as the 198 m thick Beekmantown Group that crops out the southern part of the St. Lawrence River as well as Cornwall Island (Cane, 1996b; Williams et al., 1985). This unit is unconformably overlain by the 113 m thick Rockcliffe Formation, which consists of grey-green shales with sandstone pods. They crop out in a ~1.5 km wide area at the north shore of the St. Lawrence, including Cornwall and crossing the river just below the Moses-Saunders Dam

(Cane, 1996b; Wilson, 1946). The ~47 m thick St. Martin Formation crops out in an about 2 km wide southwest-northeast trending band north of Cornwall and cuts through the St. Lawrence River upstream of the Moses-Saunders Dam at Barnhart Island and Long Sault Island (Cane, 1996b). Its lithology consists of a thick bedded impure gray limestone sequence that is interspersed with gray shale beds (Wilson, 1946). The north-western parts of the study area (i.e. 'Hoople Creek' and 'Hoople Bay') are underlain by the Ottawa group limestones which are 212 m thick (Hewitt, 1972), and are the dominant bedrocks of the ambient hinterland north of the St. Lawrence (Cane, 1996b).

Glacial till covers most of the area around Cornwall. It consists of a clay rich sequence at the base that can be up to 15 m thick and is topped by up to a 9 m thick series of sandy till, containing several crystalline pebbles (Terasmae, 1965). Alluvial sands and Champlain marine clays and silts with thicknesses of several metres cover some areas at the river front east of Cornwall. Between 5 and 10 km northwest of Cornwall a series of peatlands and an inlier of marine sands are embedded in the till sequence (Cane, 1996a).

3. Methodology

After discussing some general concerns of sampling and data treatment, this chapter chronologically lists a typical water sampling campaign, starting from preparation of the sampling bottles, to field procedures (on-site measurements, filtration, preservation), to laboratory analyses.

3.1 General notes

3.1.1 Resolution of the samples in time and space

The longest time period between sampling events within 1995 and 1996 was four months during times of ice coverage; however, most sampling events were separated by two week intervals. This gives reason to the assumption that important biogeochemical processes may have been missed, particularly diurnal signals in biologically active ecosystems, such as 'Hoople Bay'. In order to test if diurnal biologically dominated processes are stronger than the seasonal trends, Hoople Bay was sampled at 12 hour intervals in three different sampling campaigns during the late spring and early summer. The parameters tested were temperature, O₂ content, pH, alkalinity and $\delta^{13}\text{C}_{\text{DIC}}$. These parameters would most readily respond to different biological activities, such as photosynthesis. As can be seen from Table 3.1, the parameters studied differ less between day and night sampling than between sampling events that were two weeks apart. During the last night sampling it rained heavily, while the following day the weather was sunny. Yet, even in this case no strong difference between day and night were observed for the given parameters.

Another concern is the spatial variability of the chosen sampling sites. In other words, "how representative is the water chemistry for the area around the spot of sampling?" In order to answer this question, conductivity measurements were taken in a radius of 100 to 200 m around the usual spot of sampling, but showed little variation of this parameter. This test is based on the assumption that conductivity is representative of the water chemistry, which is true for conservative parameters, such as Cl⁻. For less conservative parameters, such as dissolved oxygen, dissolved nitrogen species, or sulfate, a greater spatial variability is possible; however, they were not tested on this scale.

date	time	Temp. [°C]	pH	diss. oxygen [mg/L]	d ¹³ C _{DIC} [‰]	HCO ₃ ⁻ [mg/L]
1-Jun-96	night	17.0	nm	10.0	-6.72	162.1
2-Jun-96	day	17.1	nm	9.5	-6.36	160.9
15-Jun-96	night	20.0	nm	nm	-4.99	159.7
16-Jun-96	day	20.5	nm	8.9	-4.55	143.8
29-Jun-96	night	19.0	8.03	7.0	nm	131.6
30-Jun-96	day	19.2	7.95	7.3	nm	125.5

Table 3.1 Diurnal variations of biologically dominated parameters in Hoople Bay.

The vertical stability of the water column was tested with dissolved oxygen measurements, but even in the ~30 m deep 'Main Channel' the oxygen content was only 0.4 mg/L lower than at the surface. This suggests almost complete vertical mixing of the water column.

3.1.2 Precision and Accuracy

It is a general misconception that a method is as precise as the analytical instrument used. In reality, most analyses stand at the end of a lengthy procedure of sampling, filtering, conservation and transport to the laboratory. One has to be aware that

many errors can be introduced in this whole procedure and, therefore, the precision of the laboratory instrument can rarely be transposed to the whole method.

In order to test the precision of the whole method for the determination of a parameter, repeat measurements were run on a regular basis and multiple measurements were performed on field standards and blanks. Multiple measurements have to be interpreted as a statistical sample that is biased because it can only give an estimate of the population studied (Robin, 1996; Davis, 1986). For this reason the frequency that is used to calculate the standard deviation for each parameter has to be 'n-1', with 'n' being the number of measurements performed on the standard. The standard deviation then is multiplied by two in order to obtain '2 σ ', a measure of the precision at a confidence level of 95 %. If several sets of standards at various concentrations were measured for one parameter, each of these sets were treated as different statistical samples. In this case, it would be incorrect to determine the standard deviation of the method by averaging all standard deviations of each statistical sample, because all mathematical manipulations, such as averaging, should be performed on the variance (Robin, 1996). Therefore, the mean standard deviation had to be calculated as follows: first, the variance of each statistical sample for each test at a specific concentration was computed; then, a weighted average of all these variances was calculated by using the frequencies 'n-1'; and finally, the square root of this weighted average was taken in order to give the averaged standard deviation of all multiple measurements. For the determination of some parameters, such as the deuterium and oxygen isotopes and chlorophyll-a, not enough field standards were sampled to allow the computing of reasonable standard deviations. In these cases multiple measurements of laboratory internal standards were used to calculate 2 σ . Although this

does not produce the true precision for the whole procedure, it gives a better idea of the quality of extraction procedures for the isotope measurements and constrains the precision values to the given data set.

The photometric determinations were the only measurements for which direct accuracy corrections were necessary. They were performed by measuring standard samples at various concentrations and plotting the measured versus the expected values. The equation resulting from a linear regression of these data points was then applied to correct the measurements of the given parameter. Polynomial regressions were not considered necessary, since the r^2 value for all linear regressions was larger than 0.93. This accuracy correction procedure was applied to all photometric tests, except for the determination of NO_2^- . For the latter no reasonable dilution series with values between 0 and 0.3 mg/L NO_2^- could be established. Other accuracy corrections were not necessary, but most measurements were monitored with standards and blanks and all instruments used were calibrated on a regular basis.

3.1.3 Sampling containers and their preparation

3.1.3.1 Field sampling bottles

The field sampling bottles for the major cations, trace- and rare earth elements consisted of 1L Nalgene high density polyethylene bottles, whereas the samples for all other parameters were collected in 2.5 L glass bottles. These two types of primary sampling bottles were washed with a soap solution, rinsed with tap water, then soaked in 10 % aqua regia, and finally rinsed and soaked with de-ionized water. This cleaning procedure was carried out only once at the beginning of the field season, because for the

rest of the time the bottles were only in contact with St. Lawrence water, so that no contamination could have occurred.

3.1.3.2 Subsampling bottles

The 100 mL brown glass bottles for the $\delta^{13}\text{C}_{\text{DIC}}$ samples were the only subsample bottles that were re-used and were pretreated in the same manner as the field sampling bottles in order to remove mercury residue and carbonate dust particles.

Nalgene high-density polyethylene bottles with a volume of 30 mL were used for the dissolved organic carbon (DOC) and the anion samples, while the same type of bottles with a volume of 125 mL were used for the major cations, rare earth and trace elements. The δD and $\delta^{18}\text{O}$ samples were collected into 15 mL polyethylene vials. All plastic bottles were rinsed three times with filtered sample water before being filled. One may argue that the omission of the usual acid washing procedure may have enhanced water-wall interactions between bottle and sample. This potentially contaminating process is of particular concern for trace- and rare earth element samples. However, since the bottles were new and the storage time was kept within a few weeks, no such contamination was found. The validity of the above procedure was also confirmed by blank samples of de-ionized water that were treated in the same manner as real samples and never showed any concentrations above the detection limit for the elements of concern.

3.2 On site procedures

Rain samples for the $\delta\text{D}_{\text{H}_2\text{O}}$ and $\delta^{18}\text{O}_{\text{H}_2\text{O}}$ were collected in a container equipped with a funnel system. After entering the system, the sample water was always covered

with an ~0.5 cm paraffin oil layer in order to avoid evaporative losses. Snow samples were collected in a metal bowl, then melted at room temperature and filled into sampling vials.

For the river water collection, all sampling bottles and beakers were rinsed thoroughly with sampling water on site. Sampling bottles were attached to a metal weight and lowered 2 m below the water surface, where possible. The stations 'Hoople Creek', 'Long Sault Island' and 'Cooper Marsh' were too shallow for this depth, allowing sample collection only at 0.5 to 0.75 m below the water surface. Measurements for the following parameters were then carried out in succession.

3.2.1 Temperature

Temperature measurements were carried out with the integrated temperature probe of a YSI oxygen meter (model 51B) with a precision of $\pm 0.2^{\circ}\text{C}$. The probe was left in the water for at least two minutes in order to ensure stable readings. This procedure shows no interferences.

3.2.2 Dissolved oxygen

The dissolved oxygen was determined with the same instrument by lowering the probe to the depth of sampling and moving it gently until the reading stabilized. The measurements were temperature corrected for the permeability of the probe membrane by adjusting to the previously determined temperature with a dial system. The precision of the instrument was determined to be ± 0.2 mg/L, and interferences due to high salinity did not apply to the dilute St. Lawrence waters. The on-site calibration of the instrument with an oxygen saturated solution assured accurate readings and automatically adjusted the readings to the ruling barometric pressure and the given altitude.

3.2.3 pH

Sørensen (1909) defined the pH as the negative decadic logarithm of the hydrogen ion concentration. The logarithmic nature of this definition implies that a change of one pH unit represents a ten-fold change in the hydrogen ion activity, and thus special caution has to be taken with pH measurements. The pH was determined on site with a Hach instrument that was calibrated before every measurement, utilizing two standard buffer solutions of pH 7.00 and 10.00 (at 25°C). Before the measurement the probe and the beaker were washed several times with sample water. The probe was then placed in the sample and stirred gently until the reading was stable. Subsequently, a control solution of pH 8.3 was measured in order to confirm the measurement. The pH values for the buffer and control solutions refer to 25°C and change with different temperatures. Although the Hach instrument automatically performs a temperature compensation, the calibration was always carried out at temperatures similar to the sample water in order to avoid secondary temperature effects that occur at the glass membrane. High ionic strength can cause interferences with pH measurements; however, all samples showed low to moderate ionic strength, so that this type of interference need not be of any concern. The 2σ precision of this method was determined to be ± 0.03 pH units by multiple measurements of standards in the field and in the laboratory.

According to Mc Gaha Miller (1988), the Hach electrode type has the advantage of a continually renewing liquid junction when compared to conventional ceramic type electrodes. The porous reference cell junctions of the latter may clog up with time and thus can hamper the electrolyte diffusion (Illingworth, 1981).

3.2.4 Eh

This parameter describes the redox capacity of a solution and was measured with a Hach (model 44480) Ag/AgCl-electrode that was connected to the pH meter after switching it to mV mode. The electrode potential of 200 mV was added to all readings in order to express them with respect to the standard hydrogen electrode potential. No interferences are quoted for Eh measurements (Hach Company, 1993b), while the precision of this method is ± 0.2 mV.

3.2.5 Alkalinity

This parameter describes the acid neutralizing capacity of water and was measured by titration with 1.6 N sulfuric acid on 100 mL of sample water. The indicator used was Bromcresol Green-Methyl Red. The results, expressed in mg/L CaCO_3 (Hach Company, 1992), were divided by a factor of 0.8205 in order to express them in HCO_3^- . The reason for this conversion is that, at given pH values generally between 7.2 and 9.5, HCO_3^- controls almost the entire acid-neutralizing capacity in the dissolved inorganic carbon pool. Repeat measurements of standards at various concentrations revealed precision and accuracy values of 1.5 mg/L HCO_3^- that conform to the recommended precision in the Compilation of EPA's Sampling and Analysis Methods (1996). Interferences can occur when the water is turbid or strongly colored by organic molecules, such as tannic or humic acids. Occasionally, the samples of 'Hoople Creek', 'Hoople Bay', 'Long Sault Island' and 'Cooper Marsh' showed such characteristics and, therefore, were filtered and titrated again by measuring the end point with the pH meter. However, even with these improvements no difference greater than 1.5 mg/L HCO_3^- could be found. Note that other

species, such as HS^- , can also contribute to the alkalinity of water (Drever, 1988), but in the St. Lawrence waters these species are negligible so that HCO_3^- can be regarded as the representative species of the alkalinity. Titrations to the pH end point of 8.3 did not produce any changes of the phenolphthalein indicator, thus showing that the carbonate alkalinity is negligible.

3.2.6 Conductivity

These measurements were performed with an automatically temperature compensating Hach instrument (model 44600). The instantaneous readings, expressed in $\mu\text{S}/\text{cm}$, were taken in a beaker that was washed thoroughly with sample water beforehand. Periodically, the meter was calibrated with a pure NaCl solution, but only minor drifts from the expected value were observed, so that accuracy corrections remained negligible. The precision of this method is $\pm 0.1 \mu\text{S}/\text{cm}$. Possible interferences due to ingassing of CO_2 , high OH^- contents, or oils (Hach Company, 1989) did not apply for the water samples of this study.

3.3 Field procedures within six hours after sampling

After their collection, the samples were immediately cooled and transported to the field laboratory in a dark container. They were filtered, preserved and tested for their content of NO_3^- -N, NO_2^- -N, NH_4^+ -N and SiO_2 within six hours of sampling.

3.3.1 Filtration

In terms of filtration, two types of samples have to be differentiated: (1) water samples that were filtered through $0.45 \mu\text{m}$ pore-size acetate-cellulose filter papers, and

(2) filtrate samples that were kept on 0.2 μm pore-size glass microfibre filter papers, such as the samples for chlorophyll-a (chl-a) and particulate organic carbon (POC).

Most water samples were filtered through a Nalgene pressure-filter apparatus, using compressed air. The $\delta^{13}\text{C}_{\text{DIC}}$, $\delta\text{D}_{\text{H}_2\text{O}}$ and $\delta^{18}\text{O}_{\text{H}_2\text{O}}$ were filtered by syringe to avoid contamination by CO_2 and moisture present in the compressed air.

For the filtrate samples, at least 1.5 L river water was filtered in order to capture enough material on the filter paper. Prior to filtration of the POC samples, the filter papers were sterilized by heating at 500°C overnight.

3.3.2 Sample preservation

The filtered samples for the major cation, trace and rare earth element determinations were acidified with one mL of ultra pure 8 molar HNO_3 per 125 mL of sample. This acidification was carried out using a pipette dispenser with sterile tips in order to avoid contamination.

The samples for $\delta^{13}\text{C}_{\text{DIC}}$ were preserved in 100 mL brown glass bottles and poisoned with 1.5 mL of a concentrated HgCl_2 solution in order to avoid any biological activity that could shift the carbon isotopic signal. The bottles were then closed with an air-tight polyethylene cap and kept cool until the analyses.

All other water samples were kept in the refrigerator at 4°C until analysis without any addition of preservatives. The filtrates for chlorophyll-a and POC were frozen immediately after filtration at -18°C .

3.3.3 Photometric determination of the dissolved NO_3^- -N, NO_2^- -N, NH_4^+ -N, PO_4^{3-} and SiO_2

The accuracy of all photometric procedures was ascertained by running standards at different concentrations and from different batches of reagents for each parameter. Corrections were made where necessary. Before the analyses the samples were syringe-filtered through an 0.45 μm acetate-cellulose filter paper. The samples were then measured in 1 cm cuvettes with a Hach DR 2000 spectrophotometer at specific wavelengths, after being reacted with chemicals for defined periods. Table 3.2 lists the required reagents, reaction times and wavelengths for each method. 2σ values of ± 0.0012 , 0.063 and 0.014 mg/L applied NO_2^- -N, NO_3^- -N and NH_4^+ -N, respectively. PO_4^{3-} was always at the detection limit of 0.1 mg/L, thus not allowing the determination of its analytical precision.

Parameter	Reagents used	Reaction times	Wavelength
NO_2^- -N	Nitri Ver 3	15 min	507 nm
NO_3^- -N	Nitra Ver 6	5 min	507 nm
	Nitri Ver 3	10 min	
NH_4^+ -N	Ammonia-Salicylate	3 min	655 nm
	Ammonia-Cyanurate	15 min	
PO_4^{3-}	Phos Ver 3	5 min	890 nm
SiO_2	Molybdenum 3	4 min	815 nm
	Citric Acid	1 min	
	Amino Acid F	1 min	

Table 3.2 Reagents, reaction times, wavelengths and quoted precisions for the photometric field procedures (Hach Company, 1993a).

The photometric procedures advise to zero the instrument with the original sample in order to eliminate color interferences (Hach Company, 1993a). Furthermore, all Hach reagents contain built-in pH buffers that avoid pH dependent interferences. Large amounts of dissolved Cl^- , NO_2^- , NO_3^- , PO_4^{3-} , SO_4^{2-} , sulfides, Ca^{2+} , Mg^{2+} and SiO_2 can cause

interferences in all these tests; however, this is of no concern for the dilute St. Lawrence samples.

3.4 Laboratory procedures

Measurements for the major cations, trace- and rare earth elements and for the dissolved organic carbon were carried out at the Laboratory of Applied Geochemistry at the Geological Survey of Canada. The major anions were measured in the Geochemistry Laboratory of the Ottawa-Carleton Geoscience Center, while chlorophyll-a was determined at the Laboratory of Aquatic Ecology and Toxicology at the Department of Biology (University of Ottawa). The stable isotopes of the dissolved inorganic carbon ($\delta^{13}\text{C}_{\text{DIC}}$) and the water ($\delta^{18}\text{O}_{\text{H}_2\text{O}}$, $\delta\text{D}_{\text{H}_2\text{O}}$) were measured in the G.G. Hatch Laboratory, University of Ottawa. The analyses of the particulate organic carbon (POC) and its isotopic composition ($\delta^{13}\text{C}_{\text{POC}}$) were carried out in the stable isotope facilities of the Geological Institute at the Ruhr-Universität in Bochum, Germany.

3.4.1 Major cations

The concentrations of these elements were determined by direct flame atomic absorption spectrometry (FAAS) with a Perkin-Elmer spectrophotometer at wavelengths of 422.7 nm, 285.2 nm, 766.5 nm, and 589.0 nm for the determination of Ca^{2+} , Mg^{2+} , K^+ , and Na^+ , respectively. In order to avoid ionization of these species, 8 mL of a 1250-6250 mg/mL Cs-La buffer solution was added for each 2 mL of sample. The determined analytical precisions for each of these parameters are ± 0.65 , 0.08, 0.05, and 0.58 mg/L for Ca^{2+} , Mg^{2+} , K^+ , and Na^+ , respectively.

3.4.2 Major anions

The concentrations of the dissolved Cl^- , SO_4^{2-} , F^- and Br^- were determined by high pressure liquid chromatography (HPLC). The instrument used was a Dionex (Model DX-100) chromatograph that determines the anion concentrations by time-integrated conductivity measurements, after their separation through a resin filled column (Dionex, 1992). The transport medium for these ions was composed of a $\text{NaHCO}_3/\text{Na}_2\text{CO}_3$ eluent solution. The 2σ precisions, as determined by multiple measurements of field repeats, were ± 0.7 , 0.8 and 0.16 mg/L for Cl^- , SO_4^{2-} and F^- , respectively. The concentrations of Br^- were always at the detection limits of 0.05 mg/L, thus not allowing any determination of its analytical precision.

3.4.3 Dissolved organic carbon (DOC)

The DOC content was analyzed with a Shimadzu TOC-5000 instrument by combusting a small water sample volume at a temperature of 680°C (Shimadzu Corporation, 1991). This turned the total carbon (TC), organic as well as inorganic, into CO_2 , which was then measured by an infrared gas analyzer. In a second run, all inorganic carbon in the sample is turned into CO_2 by a reaction with phosphoric acid (H_3PO_4), yielding the amount of total inorganic carbon (TIC). The amount of total organic carbon (TOC) is calculated as the difference between TC and TIC. For the samples of this study, this difference equals the amount of dissolved organic carbon (DOC), because of filtering with 0.45 μm pore size filter paper. In order to monitor the drift of the instrument, total carbon and inorganic carbon standards were analyzed during each analysis along with

blank and control measurements. The 2σ precision from DOC repeat measurements in this study was ± 0.6 mg/L.

3.4.4 Chlorophyll-a

The pigments of chlorophyll-a (chl-a) were extracted from the filter papers by leaching with concentrated Dimethyl Sulfoxide at 60°C and subsequent rinsing with 90 % acetone, following the method of Burnison (1980). The absorptions of the leachate were then determined with a Pye Unicam double beam spectrophotometer (model SP8-100) according to guidelines of Jeffrey and Humphrey (1975), and the chlorophyll-a content was calculated using a formula described by Wetzel and Likens (1991). The 2σ precision of the chl-a measurements was determined to be ± 0.18 mg/m³ by multiple measurements of standards, while good accuracy was assured by recalibrating the instrument every 10 measurements.

3.4.5 Isotopic composition of the dissolved inorganic carbon ($\delta^{13}\text{C}_{\text{DIC}}$)

The dissolved inorganic carbon of the samples was turned into CO_2 by acidification with 80 % H_3PO_4 and purified under vacuum by utilizing a series of cryogenic cold traps. Subsequently, the isotopic composition of the extracted CO_2 was determined on a triple collector VG SIRA 12 mass spectrometer, which was calibrated against the NBS-19 calcite standard. The results are expressed with reference to the Vienna Pee Dee Belemnite standard (VPDB) and the 2σ analytical precision of this method was determined with ± 0.3 ‰.

3.4.6 Particulate organic carbon (POC) and its isotopic composition ($\delta^{13}\text{C}_{\text{POC}}$)

After filtration, filter papers with sample often weighed less than before. This phenomenon was caused by a substantial weight loss of the outer rim during pressure filtration, leading to difficulties in the determination of the weight of the filtrate. This problem was solved by removing the outer 1.5 mm of blank and sample filter papers with a stainless steel cutter, following a method described by Tan and Edmond (1992). The weight of the filtrate could then be determined by subtracting the average weight of blank filter paper cores from those of sample filter papers.

Prior to analysis, the filtrate was acidified with 10 % HCl in order to eliminate any particulate inorganic carbon, then dried at 70°C overnight. The filtered suspended material and the filter paper could not be separated and therefore were ground up and analyzed together. The POC and $\delta^{13}\text{C}_{\text{POC}}$ measurements were performed at the Isotope Laboratory of the Ruhr-Universität, Bochum (Germany) by continuous flow isotope ratio mass spectrometry (CF-IRMS). The instrument used was a Carlo Erba elemental analyzer (Model 1110) connected to a Finnigan MAT mass spectrometer (Model delta C), connected to a Finnigan ConFlo II interface. Note that the results reflect filter paper and sample material. The true POC contents were calculated by subtracting average readings from multiple measurements of blank filter papers. The true $\delta^{13}\text{C}_{\text{POC}}$ was then determined by mass and isotope balance calculations. The precisions for the C-content and its $\delta^{13}\text{C}$ value were determined from duplicate and triplicate measurements of samples as well as from multiple measurements of blanks. The 2σ precisions were ± 0.02 mg/L and ± 0.5 ‰ VPDB for the POC and the $\delta^{13}\text{C}_{\text{POC}}$ measurements, respectively.

3.4.7 Isotopic composition of oxygen in water ($\delta^{18}\text{O}_{\text{H}_2\text{O}}$)

Due to condensation problems it is not possible to analyze the water directly on a mass spectrometer. For this reason, the isotopic fingerprint of the oxygen in the water was transferred to CO_2 at 25°C following the method by Epstein and Mayeda (1953). The equilibrated CO_2 was then analyzed for the oxygen isotopic composition on a triple collector VG SIRA 12 mass spectrometer. The results are expressed in ‰ versus VSMOW, and the 2σ analytical precision was determined with ± 0.2 ‰.

3.4.8 Isotopic composition of hydrogen in water ($\delta\text{D}_{\text{H}_2\text{O}}$)

In this method, the hydrogen was split from the water molecule via zinc reduction at a temperature of 500°C . For each sample, a vacuum breakseal was filled with 110 mg of zinc granules, and $3\ \mu\text{L}$ of sample water were added under vacuum. The evacuated breakseal was then heated for 30 minutes. The zinc acts as a catalyst and causes the water molecules to release H_2 , while the oxygen forms an oxide compound with the zinc. The isotopic composition of the generated hydrogen gas was determined on an automated double collector VG 602D mass spectrometer and is reported relative to Vienna Standard Mean Ocean Water (VSMOW). The precision of this routine was determined as ± 3 ‰ by repeat measurements of laboratory internal standards.

3.4.9 Trace- and rare earth elements

These analyses were performed with a Fisons inductively coupled plasma analyzer with an integrated mass spectrometer (ICP-MS). Sample water was introduced by dispersion into a stream of gas that injects into a high temperature plasma core. This results in ionisation of the species that are subsequently transferred into a low vacuum

region. The positively charged ions are then extracted by a system of electrostatic lenses and channeled to a quadrupole filter that selects ions of defined mass-to-charge ratio. The concentration of specific ions was then determined with an ion detector by integrative counting. The analytical precisions of the various trace- and rare earth elements are listed in Table 3.3. Note that for the elements Tm, In and Ag no precision values could be determined because their measurements were always at the detection limit.

3.4.10 Summary

The following Table represents a summary of the analytical instruments and methods and their precisions.

parameter	analytical instrument	2 σ precision
temperature	YSI temperature probe	$\pm 0.2^{\circ}\text{C}$
dissolved oxygen	YSI oxygen meter	± 0.2 mg/L (6.25 E-3 mmol/L)
pH	Hach pH meter	± 0.03
Eh	Hach Eh probe and voltmeter	± 0.1 mV
alkalinity	Hach digital titrator	1.5 mg/L HCO_3^- (0.0246 mmol/L)
conductivity	Hach conductivity meter	0.1 mS/cm
NO_2^-	Hach photometer	± 0.0012 mg/L (8.65 E-5 mmol/L)
NO_3^-	Hach photometer	± 0.063 mg/L (4.515 E-3 mmol/L)
NH_4^+	Hach photometer	± 0.014 mg/L (9.97E-4 mmol/L)
SiO_2	Hach photometer	± 0.09 mg/L (1.797 E-3 mmol/L)
Ca^{2+}	Perkin-Elmer flame spectrophotometer	± 0.65 mg/L (0.0162 mmol/L)
Mg^{2+}	Perkin-Elmer flame spectrophotometer	± 0.08 mg/L (3.33 E-3 mmol/L)
K^+	Perkin-Elmer flame spectrophotometer	± 0.05 mg/L (1.28 E-3 mmol/L)
Na^+	Perkin-Elmer flame spectrophotometer	± 0.58 mg/L (0.0252 mmol/L)
Cl^-	DIONEX HPLC	± 0.7 mg/L (0.0197 mmol/L)
F^-	DIONEX HPLC	± 0.16 mg/L (8.43 E-3 mmol/L)
SO_4^{2-}	DIONEX HPLC	± 0.8 mg/L (8.33 E-3 mmol/L)
Lu	Fisons ICP-MS	± 0.001 ppb
Ho	Fisons ICP-MS	± 0.002 ppb
Eu	Fisons ICP-MS	± 0.003 ppb
Ti	Fisons ICP-MS	± 0.005 ppb
Gd, Er, Yb, Pr, Dy,	Fisons ICP-MS	± 0.01 ppb
Tb		
Sm, Be, Cd	Fisons ICP-MS	± 0.02 ppb

parameter	analytical instrument	2 σ precision
Y	Fisons ICP-MS	± 0.03 ppb
La	Fisons ICP-MS	± 0.04 ppb
Nd, Ce, U, Sb, Co,	Fisons ICP-MS	± 0.1 ppb
Mo, Pb, V, Rb	Fisons ICP-MS	± 0.2 ppb
Li, Se, As	Fisons ICP-MS	± 0.3 ppb
Cr, Cu	Fisons ICP-MS	± 0.4 ppb
Ti	Fisons ICP-MS	± 0.9 ppb
Ni	Fisons ICP-MS	± 2 ppb
Zn, Ba	Fisons ICP-MS	± 3 ppb
Mn	Fisons ICP-MS	± 4 ppb
Al	Fisons ICP-MS	± 20 ppb
Fe	Fisons ICP-MS	± 26 ppb
Sr	Fisons ICP-MS	± 39 ppb
DOC	Shimadzu TOC-5000	± 0.6 mg/L
chlorophyll-a	PYE UNICAM spectrophotometer	± 0.18 mg/m ³
POC	Carlo Erba elemental analyzer	± 0.02 mg/L
$\delta^{13}\text{C}_{\text{POC}}$	Carlo Erba elemental analyzer with on-line Fisons mass spectrometer	± 0.05 ‰
$\delta^{13}\text{C}_{\text{DIC}}$	VG SIRA mass spectrometer	± 0.3 ‰
δD	VG 602D mass spectrometer	± 3 ‰
$\delta^{18}\text{O}$	VG SIRA mass spectrometer	± 0.2 ‰

Table 3.3 List of analytical methods and instruments used, including their precisions.

4. Oxygen and Deuterium Isotopes

The ^{18}O : ^{16}O and the deuterium:hydrogen (D:H) ratios of the water molecule are useful tracers of water provenance and also allow one to estimate surface water evaporation, because associated fractionation affects these ratios in a typical manner (Craig, 1961; Dansgaard, 1964). Usually, the aqueous isotopic composition is representative for defined water masses and can therefore be used as an excellent conservative tracer in mixing processes (Kendall et al., 1995). The latter have important implications for the study of the carbon cycle in the upper St. Lawrence River and its near-shore ecosystems in the Cornwall area (Chapter 6). The objectives of these water isotope studies were:

- (1) to explore effects on the isotopic composition of precipitation at Cornwall in comparison to earlier studies on meteoric waters in the Great Lakes-St. Lawrence catchment area in order to estimate the origin and mixing of meteoric waters, and
- (2) to evaluate the influence of local versus Great Lakes waters on the seven St. Lawrence ecosystems studied.

Furthermore, the relationship between the isotopic compositions of surface waters and precipitation can be used to evaluate the residence time of water in small catchment basins (Burgman et al., 1987; Pearce et al., 1986). This evaluation was attempted by utilizing the time delay between peaks of the $\delta^{18}\text{O}_{\text{H}_2\text{O}}$ curves of 'Hoople Creek' and the local precipitation.

4.1 Results

The isotopic compositions of precipitation collected at Cornwall range from -29.6 to +3.1 ‰ and from -216 to -4 ‰ for $\delta^{18}\text{O}_{\text{H}_2\text{O}}$ and $\delta\text{D}_{\text{H}_2\text{O}}$, respectively (Appendix 3.1). Snow is generally more depleted in ^{18}O and deuterium when compared to rain. Necessary meteorological data were obtained from the NOAA internet site (U.S. Department of Commerce/ NCDC/ NOAA, 1998) for a climatological station at Massena near Cornwall.

The $\delta^{18}\text{O}_{\text{H}_2\text{O}}$ values of surface water samples of the seven ecosystems studied range between -12.2 and -4.3 ‰, while their $\delta\text{D}_{\text{H}_2\text{O}}$ compositions lie between -87 and -40 ‰ (Appendix 3.2). The 'Main Channel' waters have little seasonal variation in their isotopic composition with average values of -6.9 and -50 ‰ for $\delta^{18}\text{O}_{\text{H}_2\text{O}}$ and $\delta\text{D}_{\text{H}_2\text{O}}$, respectively, and conform to results by Yang et al. (1996).

4.2 Isotopic composition of local meteoric waters

Isotopic compositions of single precipitation events appear to be uncorrelated to the amount of precipitation (Fig. 4.1A), while they correlate only somewhat with the seasonal temperature (Fig. 4.1B). This variability may result from different provenance of atmospheric water masses, including varying rain-out histories on their trajectories. Additionally, precipitation originating from strongly convective systems (i.e. thunder clouds and cold fronts) can cause large isotopic differences between precipitation events (Gat, 1996).

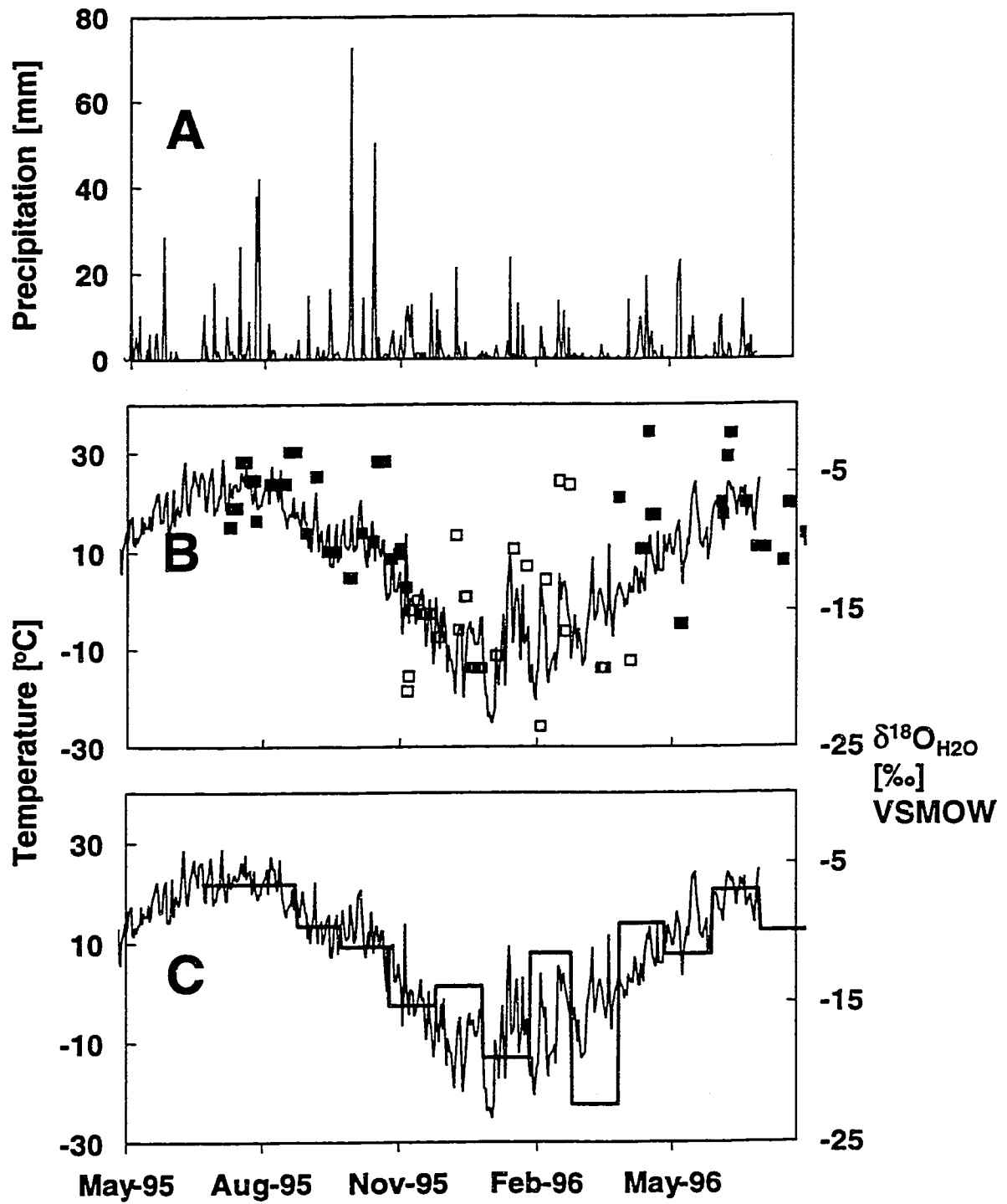


Fig. 4.1 (A) Daily precipitation together with temperature curves and $\delta^{18}\text{O}_{\text{H}_2\text{O}}$ values, (B) the latter unweighted, and (C) weighted by monthly precipitation.

The growth of snow and ice particles under non-equilibrium conditions during winter (Jouzel and Merlivat, 1984) and partial re-evaporation of falling rain, known as the 'amount effect' during summer (Dansgaard, 1964; Clark and Fritz, 1997), may add further variability to the data set. Nevertheless, after weighing $\delta^{18}\text{O}_{\text{H}_2\text{O}}$ compositions by the amount of precipitation on a monthly basis, the temperature and isotope curves move almost in parallel (Fig. 4.1C), indicating that temperature exerts a strong influence on the isotopic composition of precipitation.

A linear regression of the $\delta\text{D}_{\text{H}_2\text{O}}$ and $\delta^{18}\text{O}_{\text{H}_2\text{O}}$ values of snow and rain samples collected at Cornwall (Fig. 4.2) yields an equation that conforms to local meteoric water lines at Ottawa and Simcoe (Table 4.1). This observation indicates that atmospheric waters in the eastern part of the Great Lakes-St. Lawrence watershed are well mixed.

The weighted average of all Cornwall precipitation samples has $\delta^{18}\text{O}_{\text{H}_2\text{O}}$ and $\delta\text{D}_{\text{H}_2\text{O}}$ isotopic compositions of -10.45 ‰ and -71.60 ‰, respectively, leading to a deuterium excess ($d = \delta\text{D}_{\text{H}_2\text{O}} - 8 * \delta^{18}\text{O}_{\text{H}_2\text{O}}$; Dansgaard, 1964) of -12.0 ± 1.4 ‰ for the whole year. This value can be used to calculate the contribution of Great Lakes evaporation to the atmospheric moisture (Gat et al., 1994). Note, however, that only rain data should be used in order to avoid elevated d-excess values in snow that result from kinetic effects in supercooled vapor (Jouzel and Merlivat, 1984). Respecting the latter principle, the weighted $\delta^{18}\text{O}_{\text{H}_2\text{O}}$ and $\delta\text{D}_{\text{H}_2\text{O}}$ averages of rain are -9.21 and -61.93 ‰, respectively, yielding an average deuterium excess of -11.8 ± 1.4 ‰. The Cornwall precipitation therefore conforms to previously determined d-excess values (Table 4.1).

On average, these d-excess values prove to be 3.5 percent higher than their counterparts outside the Great Lakes-St. Lawrence catchment area.

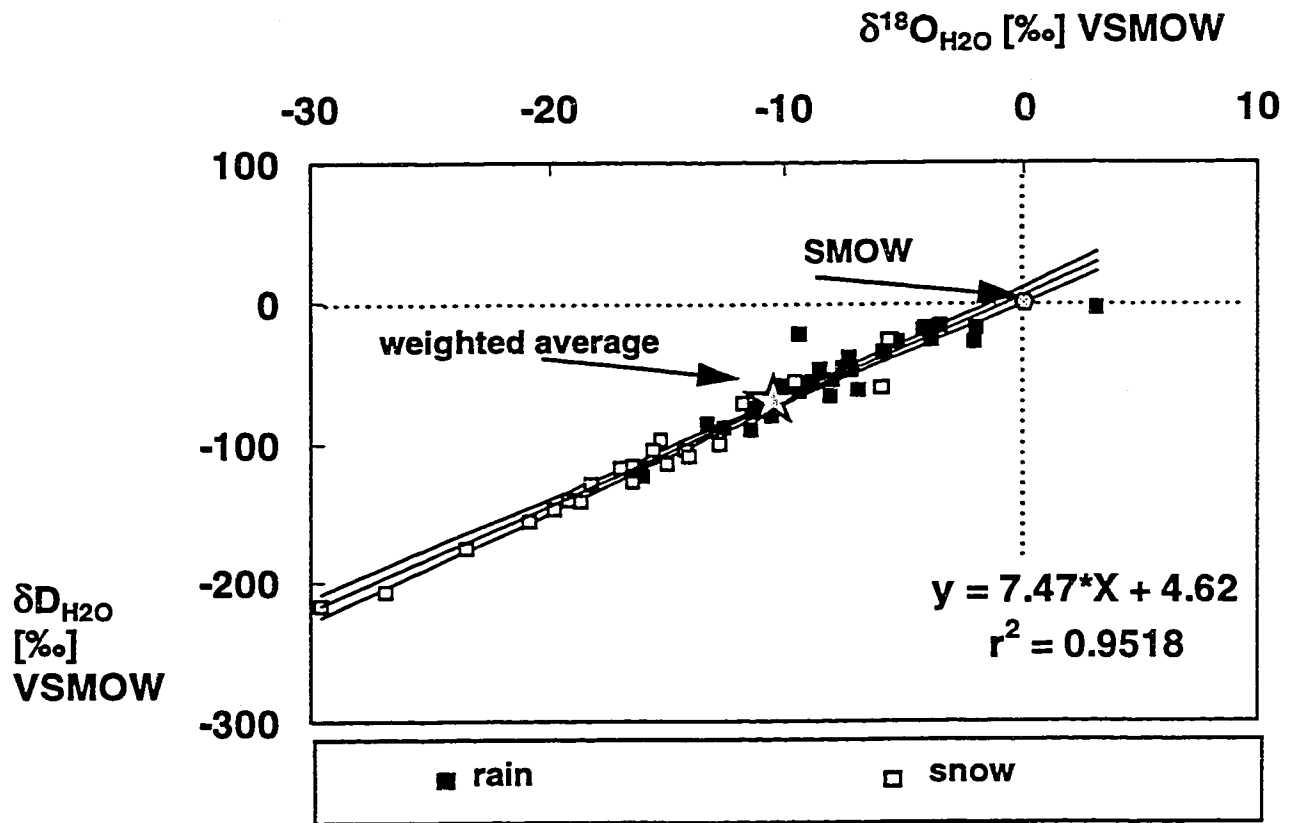


Fig. 4.2 Local meteoric water line for precipitation collected at Cornwall between 1995 and 1996. The confidence limits were calculated according to Payne (1992).

By comparing this higher d-excess to a scaling factor (d-excess of the evaporation flux minus d-excess of atmospheric moisture), Gat (1994) concluded that 4.6 to 15.7 % of the atmospheric water content over the Great Lakes region must be derived from lake evaporation during summer. Machavaram and Krishnamurthy (1995) produced a very similar estimate of 9 to 16 % evaporative contribution to atmospheric moisture in the Lake Michigan area. These atmospheric admixtures appear to be reasonable estimates, considering that the evaporative loss from the Great Lakes surface is $\sim 158.5 \text{ km}^3/\text{year}$ (United States Environmental Protection Agency and Government of Canada, 1995), a trend also noticeable in the enrichment of ^{18}O and deuterium in the Great Lakes-St. Lawrence waters (Yang et al., 1996). Atmospheric admixture of Great Lakes evaporative water to the precipitation at Cornwall is not surprising, because the principal wind direction is from west to east (Morin et al., 1994). This movement adds moisture from the Great Lakes to local precipitation at Cornwall, while the air flow over Lake Ontario is, in turn, significantly influenced by nearby bays and lakes, such as Georgian Bay and Lake Erie (Comer and McKendry, 1993).

location	slope	intercept	average d-excess for rain
Cornwall	7.47	4.62	-11.8 \pm 1.4
Ottawa	7.63 (1)	6.53 (1)	-11.2 (2)
Simcoe	7.92 (1)	10.53 (1)	-12.4 (2)

Table 4.1 Parameters of the Cornwall meteoric water line in comparison to the data from the literature, (1) = (Fritz et al., 1987), (2) = (Gat et al., 1994). The error on the d-excess was calculated following the formula of Robin (1996) for the propagation of error with $\sqrt{-8 * v\delta^{18}\text{O} + v\delta\text{D} + 16 * \text{cov}(\delta^{18}\text{O}, \delta\text{D})}$; $v\delta^{18}\text{O}$ and $v\delta\text{D}$ are the variance of multiple measurements of $\delta^{18}\text{O}_{\text{H}_2\text{O}}$ and $\delta\text{D}_{\text{H}_2\text{O}}$ standards with 0.01, and 2.25 ‰, respectively, and $\text{cov}(\delta^{18}\text{O}, \delta\text{D})$ being the covariance between these measurements.

4.3 Isotopic composition of surface water

The 'Main Channel', 'Whale Island', 'Long Sault Island' and 'Bay at Cooper Marsh' sampling stations appear to have similar $\delta^{18}\text{O}_{\text{H}_2\text{O}}$ compositions, scattering around an average of -6.9‰ with little seasonal variation (Fig. 4.3).

In contrast, the 'Hoople Creek', 'Hoople Bay' and 'Cooper Marsh' sampling sites are characterized by seasonal variations that spread with maximal 2σ values of $\pm 4.6\text{‰}$ around their averages. The latter are also more negative than the 'Main Channel' average. This variability among the ecosystems studied results from the influence of different water masses.

The $\delta^{18}\text{O}_{\text{H}_2\text{O}}$ and $\delta\text{D}_{\text{H}_2\text{O}}$ compositions of the 'Main Channel' waters plot below the local meteoric water line (Fig. 4.4), reflecting the influence of evaporation from the Great Lakes surface waters. This observation can be taken as a further proof that the Great Lakes are the principal source of upper St. Lawrence River water. The similarity of the isotopic composition between 'Whale Island', 'Long Sault Island', 'Bay at Cooper Marsh' and the 'Main Channel' indicates that almost all water in these ecosystems is essentially Great Lakes water. Samples from 'Hoople Creek', and at times 'Hoople Bay' and 'Cooper Marsh', show varying isotopic compositions that mostly plot along the local meteoric water line (Fig. 4.4). This implies that their waters consist of local precipitation and/or baseflow. Some samples of 'Hoople Creek' have also more positive isotope signals that plot below the local meteoric water line (Fig. 4.4), reflecting isotope enrichment due to surface water evaporation during late summer and early fall. Shallow water levels of less than 0.3 m and sluggish water movement during this time support this interpretation.

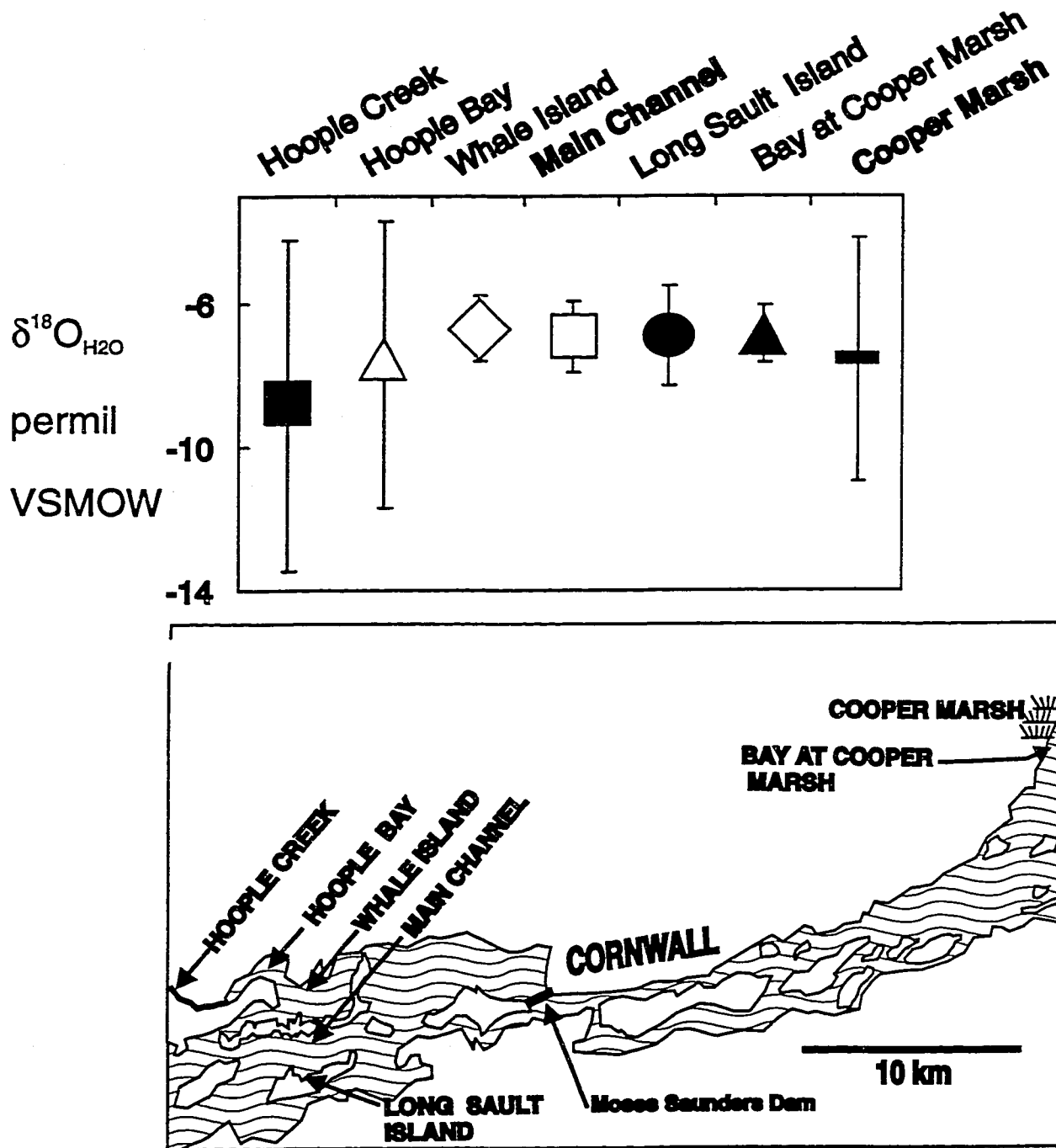


Fig. 4.3 Average $\delta^{18}\text{O}_{\text{H}_2\text{O}}$ compositions of the seven sampling stations with the 2σ error bars indicating their annual variations.

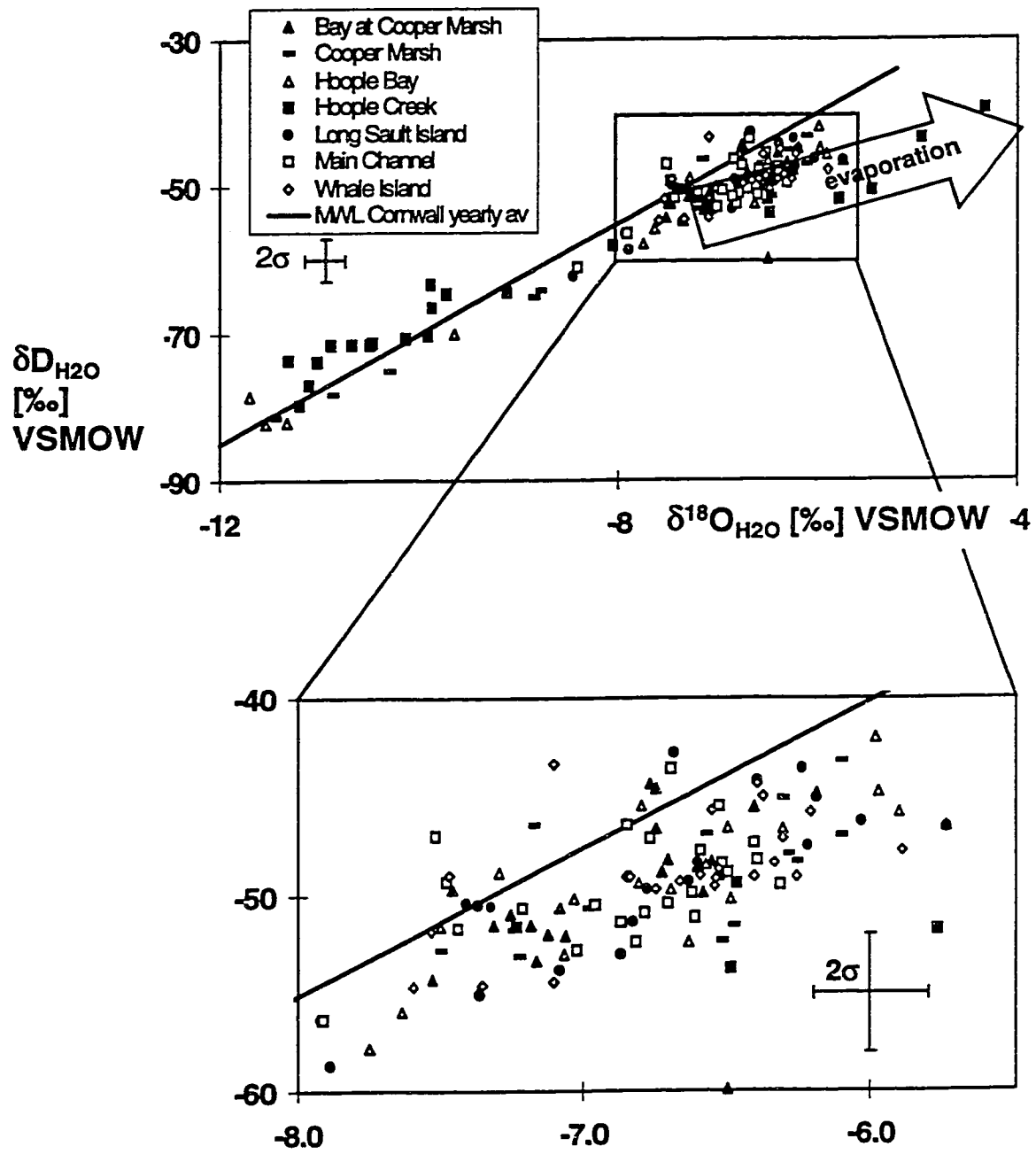


Fig. 4.4 Local meteoric water line in comparison to surface water samples.

The seasonal distribution of the $\delta^{18}\text{O}_{\text{H}_2\text{O}}$ signal in the seven sampling stations can be divided into two groups, the 'Main Channel' and related ecosystems (Fig. 4.5A) and the 'Hoople Creek' and 'Hoople Bay' ecosystems (Fig. 4.5B). As expected, most water samples scatter around the average isotopic composition of the 'Main Channel' waters. Note, however, that during fall and spring, the 'Long Sault Island' and 'Cooper Marsh' ecosystems show more negative $\delta^{18}\text{O}_{\text{H}_2\text{O}}$ compositions, reflecting stronger influx of baseflow (Fig. 4.5A). The more negative $\delta^{18}\text{O}_{\text{H}_2\text{O}}$ values in spring likely result from snow melt contributions.

Interestingly, the $\delta^{18}\text{O}_{\text{H}_2\text{O}}$ of two 'Main Channel' samples from April 1996 are also more negative than usual and almost identical to samples from the bay at 'Long Sault Island' (Fig. 4.5A). Residual amounts of pack-ice and increased baseflow drifting into the 'Main Channel' may have caused these short term influences.

The 'Hoople Creek' and 'Hoople Bay' show much stronger seasonal variations than the ecosystems described above (Fig. 4.5B). The $\delta^{18}\text{O}_{\text{H}_2\text{O}}$ composition of 'Hoople Bay' waters lie mostly between those of the 'Hoople Creek' and the 'Main Channel', indicating mixing of the latter two. A third component that may contribute to the mixing in 'Hoople Bay' is local baseflow that is different from the 'Hoople Creek' waters. By assuming that these three components represent the major end members, their relative proportions can be estimated from three equations with two conservative parameters. They are dissolved chloride (Cl^-) and $\delta^{18}\text{O}_{\text{H}_2\text{O}}$, as determined in this study for the surface water end members. The necessary Cl^- and $\delta^{18}\text{O}_{\text{H}_2\text{O}}$ data for baseflow were taken from the literature (Cane, 1996b; Fritz et al., 1987; Charron, 1978).

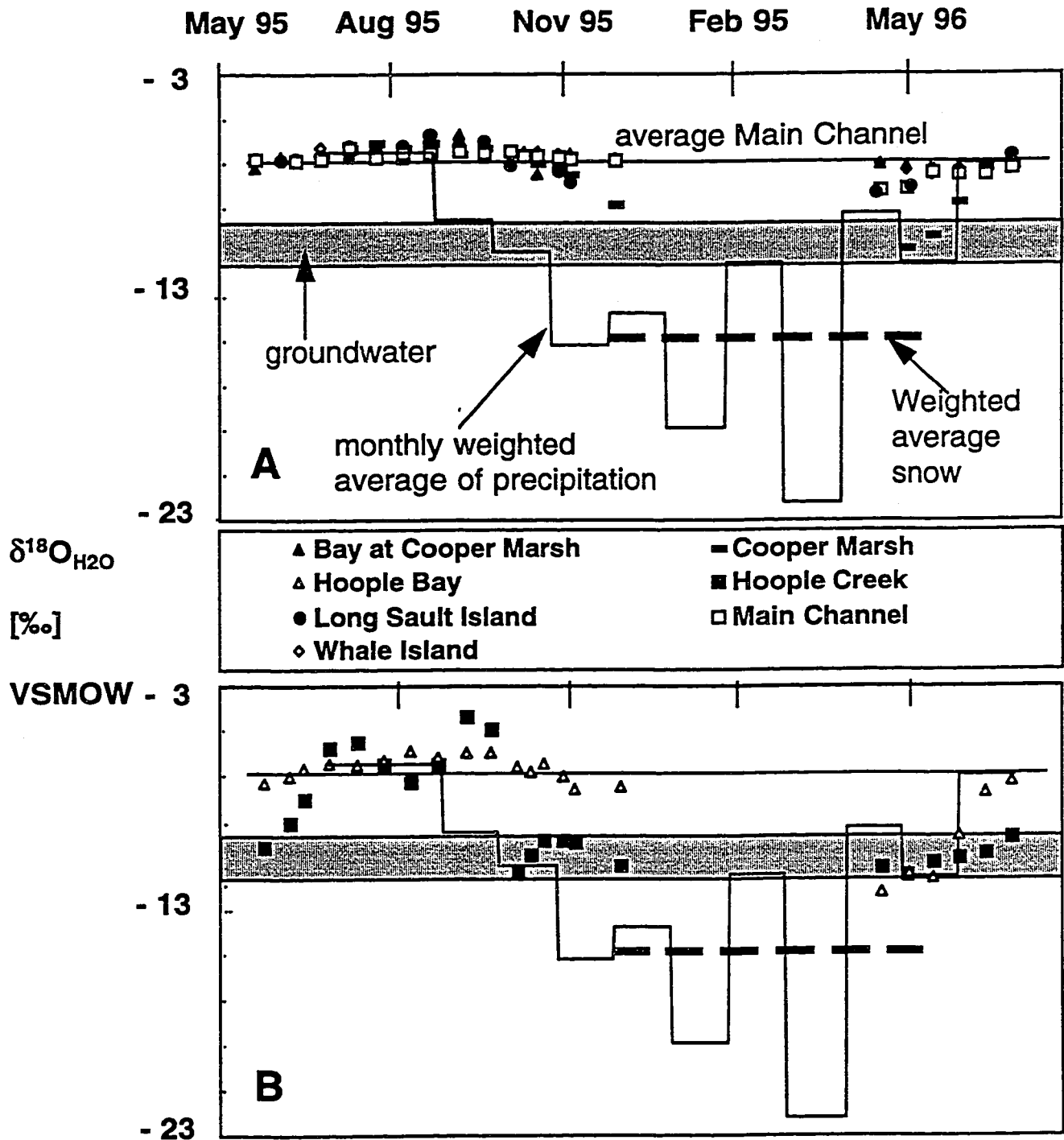


Fig. 4.5 Temporal $\delta^{18}\text{O}_{\text{H}_2\text{O}}$ variations at the seven sampling stations. A = 'Main Channel' and related ecosystems, B = 'Hoople Creek' and 'Hoople Bay'.

With this input, the equations were solved by matrix operations (Appendix 3.3). Note, that better estimate could have been achieved if runoff data of the 'Hoople Creek' were available, however no stream gauges were established at this stream.

The results of these calculations show that the contribution of groundwater is small compared to the influences of the other two end members, with the 'Main Channel' contributing amounts larger than 50 % most of the time (Fig. 4.6). This influence was reversed at times of high discharge in 'Hoople Creek', that is, during periods of snowmelt (April and May, 1996), causing the water to flush out of 'Hoople Bay' into the 'Main Channel'. Strictly, the mixing should have been calculated by factoring in the $\delta^{18}\text{O}_{\text{H}_2\text{O}}$ and Cl^- characteristics of the melting snow during spring. One has to be aware that complete mixing of the water masses in 'Hoople Bay' is a basic assumption for this exercise (Appendix 3.3), but by calculating with monthly averages, this assumption is likely to be valid. However, both parameters are not easy to estimate due to partial melting of the snow package (Kendall et al., 1995) and due to road salting, which complicates quantification of Cl^- input. The calculation with constant input from the local groundwater therefore provides the best estimate. Note also that the mixing proportions in August and September 1995 are identical, because during this time the only reasonable results could be obtained by using two month averages of the $\delta^{18}\text{O}_{\text{H}_2\text{O}}$ and Cl^- values. This necessity indicates a slower mixing rate in 'Hoople Bay' caused by lower than usual water levels during late summer and early fall.

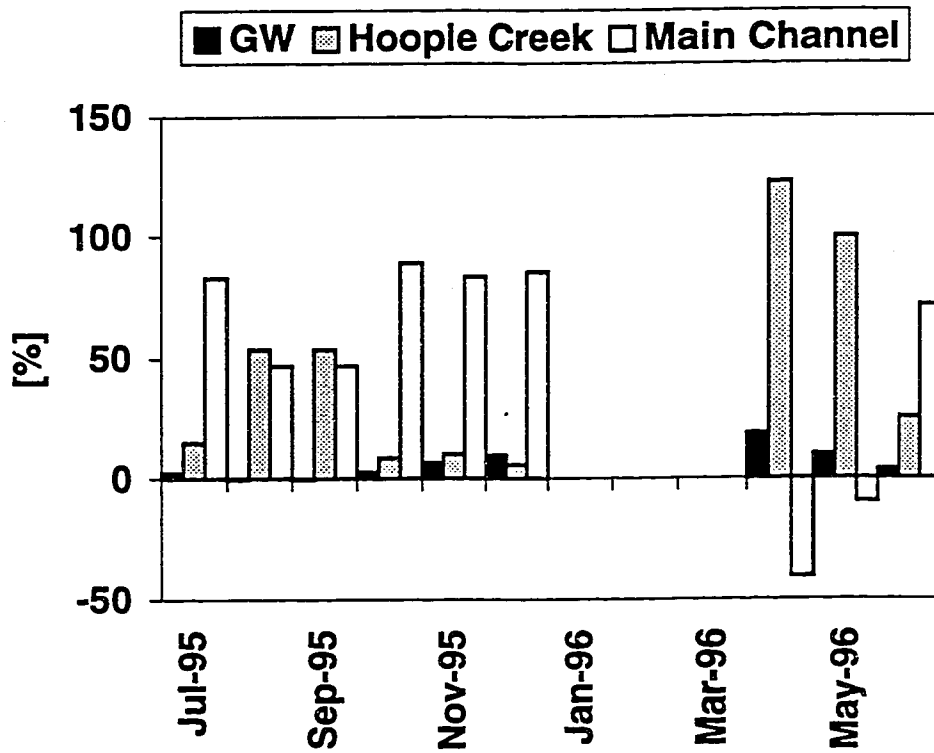


Fig. 4.6 Proportions of the three end members groundwater (GW), 'Hoople Creek' and 'Main Channel' waters for the mixing in 'Hoople Bay'. Negative values imply outflow into the 'Main Channel'.

4.4 Residence time in the 'Hoople Creek' system

The residence time of water in small catchment basins can be determined by a technique known as 'amplitude damping' (Burgman et al., 1987; Pearce et al., 1986; Leopoldo et al., 1992). For this technique, a continuous long term record, over several years, of surface water and precipitation is necessary to establish sinusoidal $\delta^{18}\text{O}_{\text{H}_2\text{O}}$ or $\delta\text{D}_{\text{H}_2\text{O}}$ curves. In this study, the surface water sampling was interrupted during winter, thus preventing the establishment of the necessary sinusoidal curve for the 'Hoople Creek' waters. Another technique that would help to identify the time delay of precipitation reaching the creek is called hydrograph stream separation (Fritz et al 1976, Sklash 1976, Sklash 1978). However, this technique requires detailed information of the stream and groundwater discharge that were not available at this point. In lack of these two techniques, the time delay between the creek and precipitation isotope curves was utilized to estimate the water's residence time in the 'Hoople Creek' catchment.

The seasonal $\delta^{18}\text{O}_{\text{H}_2\text{O}}$ patterns in 'Hoople Creek' follow somewhat those of the local precipitation (Fig. 4.7A), except in spring when the $\delta^{18}\text{O}_{\text{H}_2\text{O}}$ composition of 'Hoople Creek' is fairly homogenous (Fig. 4.7B). Again, this likely reflects the influence of melting snow, a process that controls the discharge during spring and homogenizes the baseflow input to the creek. In contrast, influx of soil waters, reflecting local precipitation, is the probable reason for the similar $\delta^{18}\text{O}_{\text{H}_2\text{O}}$ curves in summer and fall (Fig 4.7A).

Notably, the soil waters must enter the creek with a relatively short retention time, because $\delta^{18}\text{O}_{\text{H}_2\text{O}}$ peaks in the 'Hoople Creek' isotope curve closely follow those of the precipitation curve.

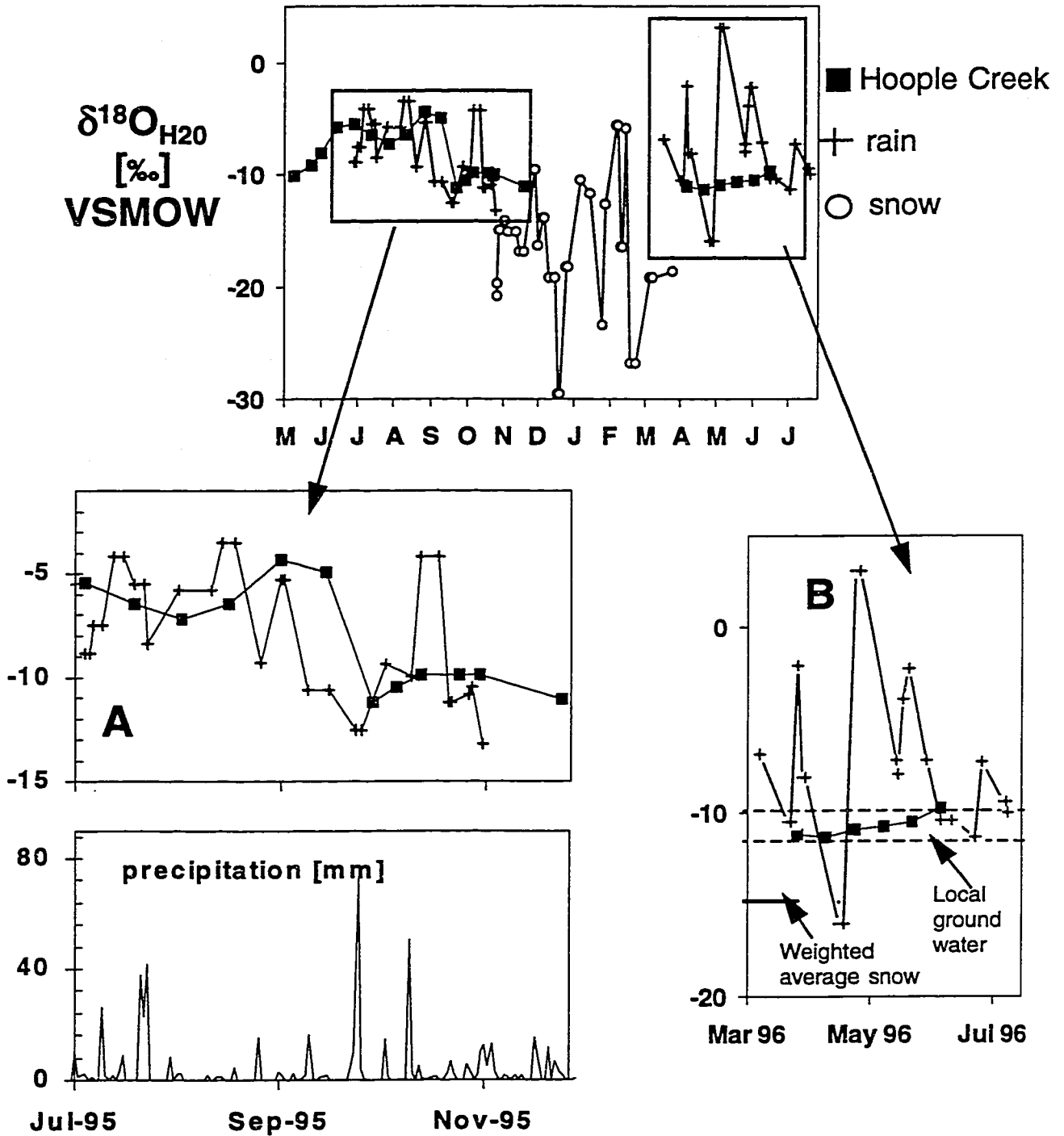


Fig. 4.7 Temporal $\delta^{18}\text{O}_{\text{H}_2\text{O}}$ variations in 'Hoople Creek' in comparison to the local precipitation values (A = summer and fall, B = spring).

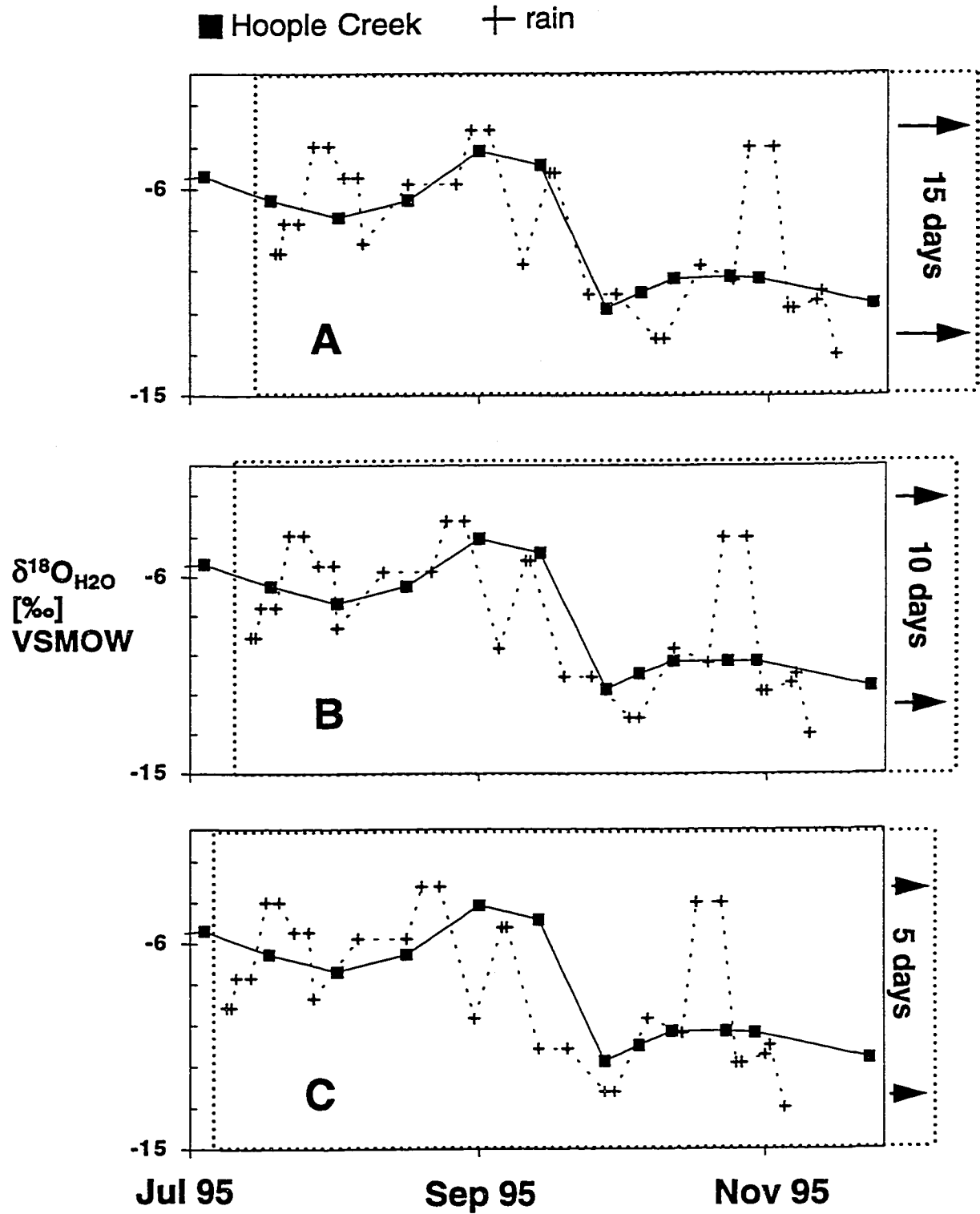


Fig. 4.8 Three scenarios for time delays between the $\delta^{18}\text{O}_{\text{H}_2\text{O}}$ curves of precipitation and those of 'Hoople Creek' waters.

The time delay can be visualized by advancing the precipitation curve on the x-axis (i.e. in time), thus attempting to find the best fit (Fig. 4.8). The increments were chosen to be 5 days, allowing speculation on several possibilities. It is important to consider several scenarios, because of the uncertainty induced by groundwater influx, which may blur the reflection of the precipitation in the isotopic composition of 'Hoople Creek'.

It is also unclear if the unusually positive 'Hoople Creek' values from August and September 1995 (Fig. 4.7A) result primarily from surface water evaporation, or if they simply reflect isotopically enriched summer precipitation. The latter would be supported by a 15 day time delay (Fig. 4.8A), because in this scenario the summer rain and creek samples are almost identical. In contradiction to this, the $\delta^{18}\text{O}_{\text{H}_2\text{O}}$ and $\delta\text{D}_{\text{H}_2\text{O}}$ values of 'Hoople Creek' waters in summer and early fall plot below the meteoric water line (Fig. 4.4), thus indicating that surface water evaporation must be a reality. Considering the latter argument, the best fit would be a 5 day time delay (Fig. 4.8C), indicating that the 'Hoople Creek' is a fast responsive system that is mostly influenced by soil waters. It should be noted, however, that the response time is no fixed entity and may also be influenced by variable soil moisture contents, precipitation amounts and groundwater influx rates.

In summary, the $\delta^{18}\text{O}_{\text{H}_2\text{O}}$ and $\delta\text{D}_{\text{H}_2\text{O}}$ isotope considerations have shown that there are essentially two different water masses in the river area at Cornwall, (1) Great Lakes waters, and (2) local waters, such as precipitation, baseflow and snowmelt. The Great Lakes waters are represented by the 'Main Channel', while the local waters are most clearly present in 'Hoople Creek'. The isotopic compositions of the other five sampling stations 'Hoople Bay', 'Whale Island', 'Long Sault Island', 'Bay at Cooper Marsh' and 'Cooper Marsh' rank between these two end members, with the Great Lakes waters being the dominant component. The isotopic characterisation of water masses in the studied ecosystems is a very useful tool for the understanding of the major element and nutrient chemistry (Chapter 5) and the carbon cycle (Chapter 6).

5. Major ion and nutrient chemistry

Earlier St. Lawrence River studies focused on the downriver evolution of the major element chemistry and on evaluations of the flux into the ocean by the entire river (Yang et al., 1996; Berner and Berner, 1987). However, no estimates exist about contributions from the upper St. Lawrence. This flux needs to be considered separately, if one wants to characterize major ion contributions of the Great Lakes. The monitoring at Cornwall is ideal for an estimate of this type, because most of the upper St. Lawrence in this area consists of well mixed Great Lakes waters (Chapter 4).

The flux of major ions from the upper St. Lawrence River originates from three major sources: precipitation, rock weathering and anthropogenic inputs. The input via precipitation is of particular importance, considering the large drainage area of the Great Lakes and the upper St. Lawrence River. The Great Lakes cover approximately one third of this area and the major ion input by precipitation should therefore be considered in two different ways, (1) for the part of the basin covered by water, and (2) for the entire watershed. This separate consideration is important, because some major elements, such as K^+ , are held back by vegetation on land but not in surface waters. It has long been recognized that the major ion input via rock weathering is not easily quantified in large catchment areas (Gibbs, 1970; Stallard and Edmond, 1983). This is due to the presence of various rock types and difficulties with the estimation of their spatial distributions and weathering rates. In this chapter the influence of rock weathering is evaluated qualitatively, by combining the river classification scheme of Meybeck (1986) with mineral weathering reactions. Anthropogenic influences that contribute to the major ion chemistry

of the upper St. Lawrence River are also difficult to quantify. Nevertheless, potential sources are discussed by considering temporal variations of elements such as Na^+ and SO_4^{2-} . In these qualitative considerations, particular attention is paid to near-shore ecosystems.

In the same manner as for the major elements, the atmospheric contributions to the total nitrogen flux of the upper St. Lawrence 'Main Channel' were calculated for the Great Lakes surface and for the entire catchment area. Within the river, particular attention was given to the dissolved nitrate (NO_3^-), the most common nutrient. Consideration of its seasonal and spatial variations helps one to understand other than atmospheric influences, such as the role of riverine recycling, particularly in near-shore ecosystems.

5.1 Results

5.1.1 Major ions

The major element concentrations of the 'Main Channel' and related ecosystems are comparable to previous studies of the St. Lawrence River at Cornwall (Rondeau, 1993; Yang et al., 1996). All major ions in the 'Main Channel' and related ecosystems ('Whale Island', 'Long Sault Island', 'Bay at Cooper Marsh') showed little seasonal variation over the one year of sample collection. Dissolved Cl^- and Na^+ scattered around 0.5 mmol/L, while Ca^{2+} , Mg^{2+} , K^+ and SO_4^{2-} had mean concentrations of 0.89, 0.34, 0.035 and 0.26 mmol/L respectively (Appendix 4.1). More variability existed for HCO_3^- (1.40 to 2.29 mmol/L) and SiO_2 (0.003 to 0.031 mmol/L) in the 'Main Channel'-related ecosystems. Except for Cl^- and Na^+ in 'Hoople Creek', the near-shore ecosystems 'Hoople

Creek', 'Hoople Bay', and 'Cooper Marsh' showed higher concentrations with larger seasonal variabilities for all major elements.

With a few exceptions, the major ion charge balance lies below 5 %, indicating reliable analytical work (Appendix 4.1). Larger charge balances, such as for some 'Hoople Creek' samples, seem to indicate an excess of cations, but rather originate from the presence of organic anions. These were not measured directly, but can be inferred from dissolved organic carbon contents in 'Hoople Creek'.

5.1.2 Nutrients

The only detectable nutrients were the dissolved inorganic nitrogen species (NO_3^- , NO_2^- and NH_4^+), while reactive phosphate could not be detected with the given instrumentation (Hach field spectrophotometer) and is not further discussed here. The nitrate concentrations of the 'Main Channel' and related ecosystems were slightly lower than 0.01 mmol/L during the warm seasons (May to October) and up to three times as high during cold seasons (November to April). Similar trends exist for 'Hoople Creek', 'Hoople Bay' and 'Cooper Marsh', with cold season concentrations reaching peak values of 0.189 mmol/L. Nitrite and ammonium mimic these trends at order of magnitude lower concentrations. Nitrate concentrations in the 'Main Channel' are in accord with previous data (Yang et al., 1996; Rondeau, 1993).

5.2 Average composition of the upper St. Lawrence River water

Comparison between the composition of average world river and upper St. Lawrence water shows that, with the exception of SiO_2 , the concentrations of major elements in the 'Main Channel' are up to 2.4 times larger (Table 5.1). For Ca^{2+} , Mg^{2+} and

HCO_3^- this is likely a result of large contributions by carbonate weathering in the catchment area, while anthropogenic influences may have increased Cl^- and SO_4^{2-} .

However, the latter two anions may also originate from evaporites, such as the Salina formation in the Michigan Basin and the St. Lawrence Lowlands. The SiO_2 content in the upper St. Lawrence is about 10 times lower than in average world river water (Table 5.1), resulting from smaller proportions of silicate weathering or from silica consumption by diatoms in surface waters (Berner and Berner, 1996). The latter process was estimated to reduce the SiO_2 content in the St. Lawrence River by about 8 %, with most of this activity taking place in the Great Lakes (Meybeck, 1984).

	World mmol/L	'Main Channel' mmol/L	ratio 'Main Channel' / world river water
Ca^{2+}	0.367	0.872	2.4
Mg^{2+}	0.152	0.336	2.2
Na^+	0.313	0.471	1.5
K^+	0.036	0.035	1.0
Cl^-	0.234	0.558	2.4
SO_4^{2-}	0.120	0.263	2.2
HCO_3^-	0.869	1.746	2.0
SiO_2	0.173	0.010	0.1

Table 5.1 Comparison between the average composition of world river water (Berner and Berner, 1996) and upper St. Lawrence River.

With an average annual discharge of $236 \text{ km}^3/\text{year}$ (Morin et al., 1994), the upper St. Lawrence River accounts for $\sim 0.63 \%$ of the average world river flux of $37,400 \text{ km}^3/\text{year}$ (Meybeck, 1979). Multiplying these discharges with the average concentrations of Table 5.1 yields the global and upper St. Lawrence fluxes of major elements, respectively (Table 5.2). This calculation shows that the upper St. Lawrence contributes

between ~0.04 and 1.5 % of the global dissolved major element flux to the ocean (Table 5.2).

	World flux [mol/year]	Main Channel flux [mol/year]	% of world flux
Ca ²⁺	1.37E+13	2.06E+11	1.500
Mg ²⁺	5.69E+12	7.93E+10	1.392
Na ⁺	1.17E+13	1.11E+11	0.948
K ⁺	1.34E+12	8.35E+09	0.624
Cl ⁻	8.76E+12	1.32E+11	1.504
SO ₄ ²⁻	4.48E+12	6.21E+10	1.386
HCO ₃ ⁻	3.25E+13	4.12E+11	1.267
SiO ₂	6.47E+12	2.30E+09	0.036

Table 5.2 Major ion fluxes of the upper St. Lawrence River and their contributions to the global world river flux.

5.3 Atmospheric deposition of major ions

Even though the concentrations in snow and rain are low, considerable amounts of major ions must be added to the system via precipitation on the large surface area of the Great Lakes. This necessitates the evaluation of this type of major ion input with respect to the flux of the 'Main Channel' (Appendix 4.2A). Note, however, that some of the major ions in precipitation are derived from human activities, which drastically increased during the last century. This period roughly corresponds to the cumulative residence time of water in the Great Lakes (~127 years; United States Environmental Protection Agency and Government of Canada, 1995); however, precipitation that reached the Great Lakes this time ago was certainly less affected by anthropogenic influences than nowadays. In other words, the contributions, as calculated from major ion concentrations in present-day precipitation (Environment Canada, 1994), likely exaggerates the overall atmospheric flux. A good example of this exaggeration is the atmospheric contribution of sulfate, which largely results from human activities (Berner and Berner, 1996) and drastically increased

in the atmosphere during the last few decades. Dry deposition of major elements over the Great Lakes imposes additional uncertainty in the given evaluation, but this process is only documented with sparse and variable data. Maximum estimates of NO_x and sulfur dry deposition roughly equal the deposition by precipitation, but the admitted uncertainties are large, particularly for inputs over the Great Lakes surface (Shannon and Voldner, 1992). Due to these limitations, dry deposition was not included in the atmospheric flux evaluations of this study.

	precipitation Input mol/year	% contribution to 'Main Channel'
Ca ²⁺	4.842E+09	2.4
Mg ²⁺	1.334E+09	1.7
Na ⁺	2.332E+09	2.1
K ⁺	7.290E+08	8.7
Cl ⁻	3.566E+09	2.7
SO ₄ ²⁻	8.259E+09	13.3
SiO ₂	1.743E+08	7.5

Table 5.3 Precipitation input of major ions to the Great Lakes and the percent contributions to the major ion flux in the 'Main Channel' (calculation in Appendix 4.2A).

Ca²⁺, Mg²⁺, Na⁺ and Cl⁻ in precipitation over the Great Lakes contribute between 1.7 and 2.7 % to the major ion flux of the 'Main Channel' (Table 5.3). These contributions originate mostly from wind mobilized dust or anthropogenic activity, such as agricultural practices, road salting and open pit mining. Another atmospheric source of these elements is ocean spray (cyclic salt), which is minor due to the distance of the Great Lakes from the coast.

The lions share of the 13.3 % atmospheric SO₄²⁻ input over the Great Lakes (Table 5.3) results from the oxidation of sulfur dioxide gas emitted to the atmosphere during coal burning in power plants, but also from smelting and oil refining (Berner and Berner, 1996). Many of these operations are practiced in the Great Lakes region, which is one of

the most populated and industrialized areas in North America. Additionally, winds add SO₂ from industrial regions south of the catchment area in the mid-eastern United States. Natural sources of sulfate in precipitation are cyclic salts, volcanic emissions, biogenic sulfur gases, soil dust, forest burning and plant aerosols. In the case of the Great Lakes area, these processes can be assumed to play a subordinate role (Environment Canada, 1994).

Compared to the above, silica and potassium originating from precipitation over the Great Lakes exert intermediate influences on the upper St. Lawrence major element flux (Table 5.3). Their sources are wind-mobilized dust, while additional K⁺ may originate from agricultural practices. The consumption of 8 % SiO₂ in the Great Lakes (Meybeck, 1984) roughly equals the silica input by precipitation (Table 5.3). Assimilation by aquatic plants in the Great Lakes may also have reduced the atmospheric K⁺ contribution to the St. Lawrence River. However, assimilation by phytoplankton is known to be negligible (Wetzel, 1983), leaving only macrophytes in the littoral zone to utilize the potassium. Given the comparatively small area of the littoral zone, relative to the pelagic zone, this process is probably of minor significance.

Contributions of bicarbonate by precipitation are not discussed here, because at pH values below 4.5 (Environment Canada, 1994) its concentrations are between 10⁻⁶ to 10⁻⁷ mol/L (Telmer, 1996) and can therefore be neglected when compared to inputs from weathering in soils and groundwater.

Naturally, precipitation does not fall only over the Great Lakes, and evaluation of the major ion input by precipitation has to be integrated over the entire catchment area (Appendix 4.2B). The larger surface area of this calculation leads to larger estimates of the

contributions by precipitation (Table 5.4). Note that sluggish ground- and soil water movements increase the cumulative residence time in the catchment basin, leading to larger overestimates of the major ion flux by precipitation, particularly for anthropogenic elements, such as sulfate.

The potassium contribution by precipitation from this estimate is probably unrealistic, because most of it is assimilated by land plants (Berner and Berner, 1996). For this reason, the potassium value of Table 5.3, for contribution over the Great Lakes only, should be more reliable.

	Input mol/year	% contribution to 'Main Channel'
Ca ²⁺	1.096E+10	5.3
Mg ²⁺	3.114E+09	3.9
Na ⁺	5.337E+09	4.8
K ⁺	1.621E+09	19.4
Cl ⁻	8.237E+09	6.3
SO ₄ ²⁻	1.939E+10	31.2
SiO ₂	3.869E+08	16.8

Table 5.4 Precipitation input of major ions to the Great Lakes catchment area and the percent contributions to the major ion and nutrient flux in the 'Main Channel' (calculation Appendix 4.2B).

Despite all limitations in the above evaluations, the consideration of major ion deposition by precipitation is useful in highlighting the importance of surface area in the Great Lakes-St. Lawrence water chemistry. Nevertheless, these calculations demonstrate that the bulk of the river's major ions must originate from soil and groundwater as well as from anthropogenic influences.

5.4 Classification of the St. Lawrence water

All samples, except those of 'Hoople Creek', occupy the same area in the Piper diagram (Fig. 5.1). According to Back (1961) they can be classified as bicarbonate-

chloride-sulfate types for the anions and as calcium-sodium types for the cations. Most 'Hoople Creek' samples fall within the same field for the anion characterisation, while their cation concentrations are of calcium-magnesium type water. Some 'Hoople Creek' samples had higher SO_4^{2-} concentrations and therefore plot within the chloride-sulfate-bicarbonate field. This classification provides an overview from the water chemistry point of view, but proves insufficient for the description of important processes, such as anthropogenic influences and rock weathering. This classification is also not corrected for major ion input by precipitation.

The application of several river classification schemes was attempted in this study, but none yielded a clear quantification as to the weathering of different rock types. The river classification of Gibbs (1970) proved as ineffective for this local study, because it compares rivers from a global perspective. It has also been criticized for lack of atmospheric input corrections. This deficiency led to the development of a more detailed classification scheme by Stallard and Edmond (1983), which is tailored to the Amazon River. However, different climatic conditions and associated weathering reactions make its application to this study questionable. Meybeck (1986) provides a classification scheme based on the chemistry of several monolithologic and relatively unpolluted rivers in France.

This classification scheme has the advantage of comparable climatic regime to the Great Lakes-St. Lawrence area and was applied to this study after corrections for atmospheric input (Appendix 4.2C). In terms of the sum of major cations (Ca^{2+} , Mg^{2+} , Na^+ , K^+), most samples fall between 2000 and 5000 $\mu\text{eq/L}$ (Fig. 5.2). According to Meybeck (1986) this indicates a dominance of carbonate weathering, which is no surprise

given the abundance of Paleozoic limestones on the St. Lawrence Platform and in the Michigan Basin (chapter 2). The weathering of glacial tills with higher carbonate contents can also contribute to this trend. Nevertheless, pure carbonate weathering leads to a $\text{Ca}^{2+}/\text{Na}^+$ ratio of about 100 (Meybeck, 1986).

Clearly, all samples plot below this ratio (Fig. 5.2) and are therefore also influenced by other rock types, such as Canadian Shield rocks or St. Lawrence Platform and Michigan Basin non-carbonate sediments (i.e. shales, clayey tills, sandstones). According to this classification, higher cation contents and $\text{Ca}^{2+}/\text{Na}^+$ ratios in 'Hoople Creek' samples seem to originate from local evaporites, a proposition that will be considered more closely in section 5.5.2.

It is not possible to determine the relative influence of the different rock types, because of variable weathering rates and spatial bedrock distribution. Additionally, this classification is based on relatively unpolluted rivers, which may not be the case for the St. Lawrence. For these reasons, it is instructive to interpret the major elements in groups that reflect weathering reactions and possible anthropogenic influences.

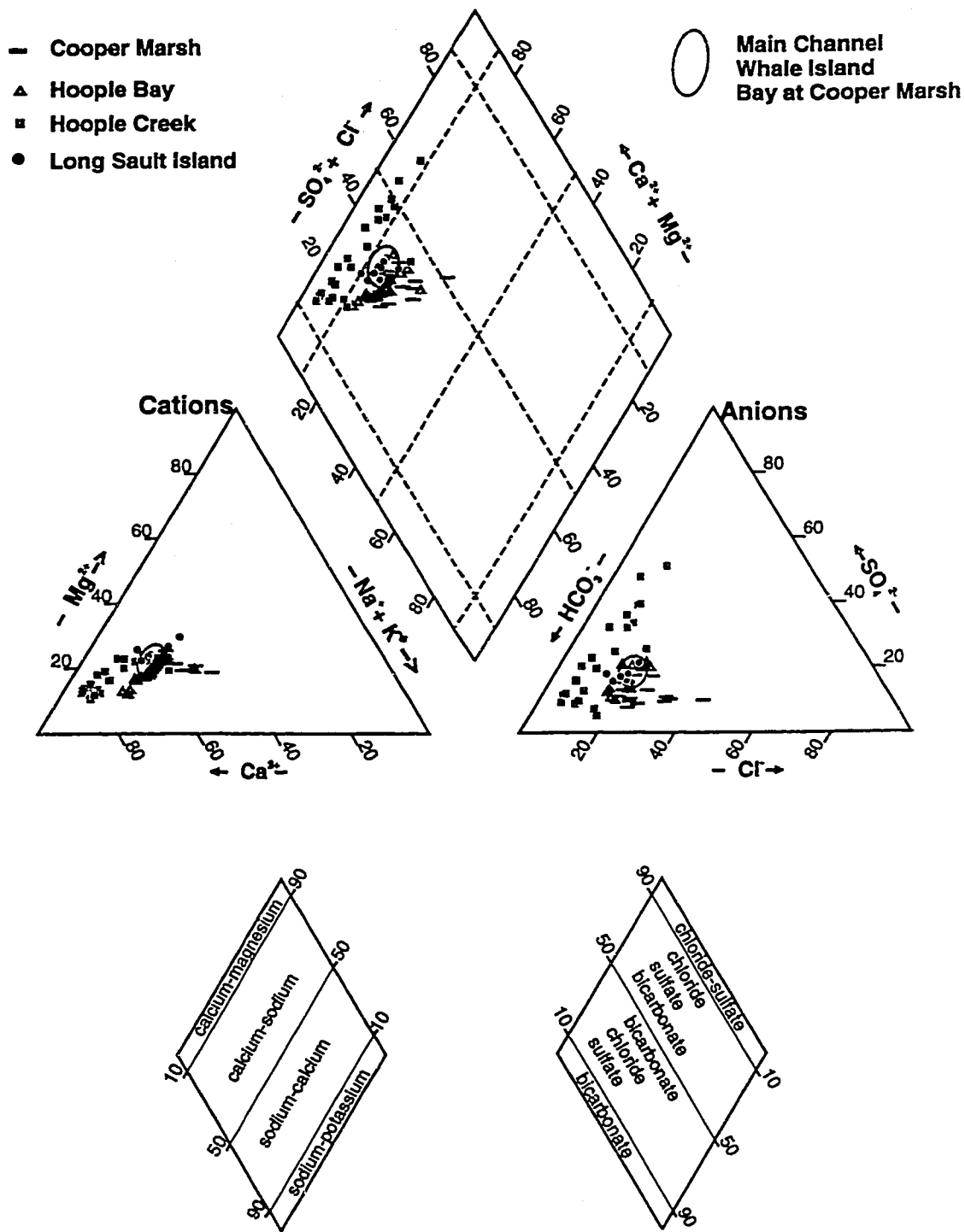


Fig. 5.1 Piper diagram of major ions with classification according to Back (1961).

5.5 Grouping of major ions

5.5.1 Sodium, chloride and potassium

The primary natural sources of sodium and chloride are (1) halite (NaCl) that occurs in bedded evaporites or dispersed in shales, and (2) the influx of brines through fault systems. Anthropogenic sources are mining, road salting, and discharge of domestic and industrial sewage.

As a result of road salting, one would expect higher concentrations of Na^+ and Cl^- in winter, however, with the exception of 'Cooper Marsh', seasonal variations of Na^+ lie within the analytical error (Fig. 5.3). Nonetheless, Na^+ and Cl^- pulses through the ecosystems during February, March, and April, when the stations were not sampled, are likely. It is also not clear why the Na^+ concentrations in 'Hoople Creek' do not increase during early spring, because the sampling station is located only ~200 m away from highway 417.

The non-seasonal temporal Na^+ pattern in 'Hoople Creek' may indicate other local anthropogenic sources, such as discharge of sewage, household and industrial waste water. These influences may have overridden possible seasonal trends caused by road salting.

Dissolution of albite ($\text{NaAlSi}_3\text{O}_8$) can also contribute sodium to river water, but if this process were significant, there should be an excess of Na^+ over Cl^- . Nonetheless, the opposite is true, with many samples having a slight excess of Cl^- over Na^+ (Fig. 5.4). This phenomenon originates either from the 'membrane effect' or from anthropogenic Cl^- inputs.

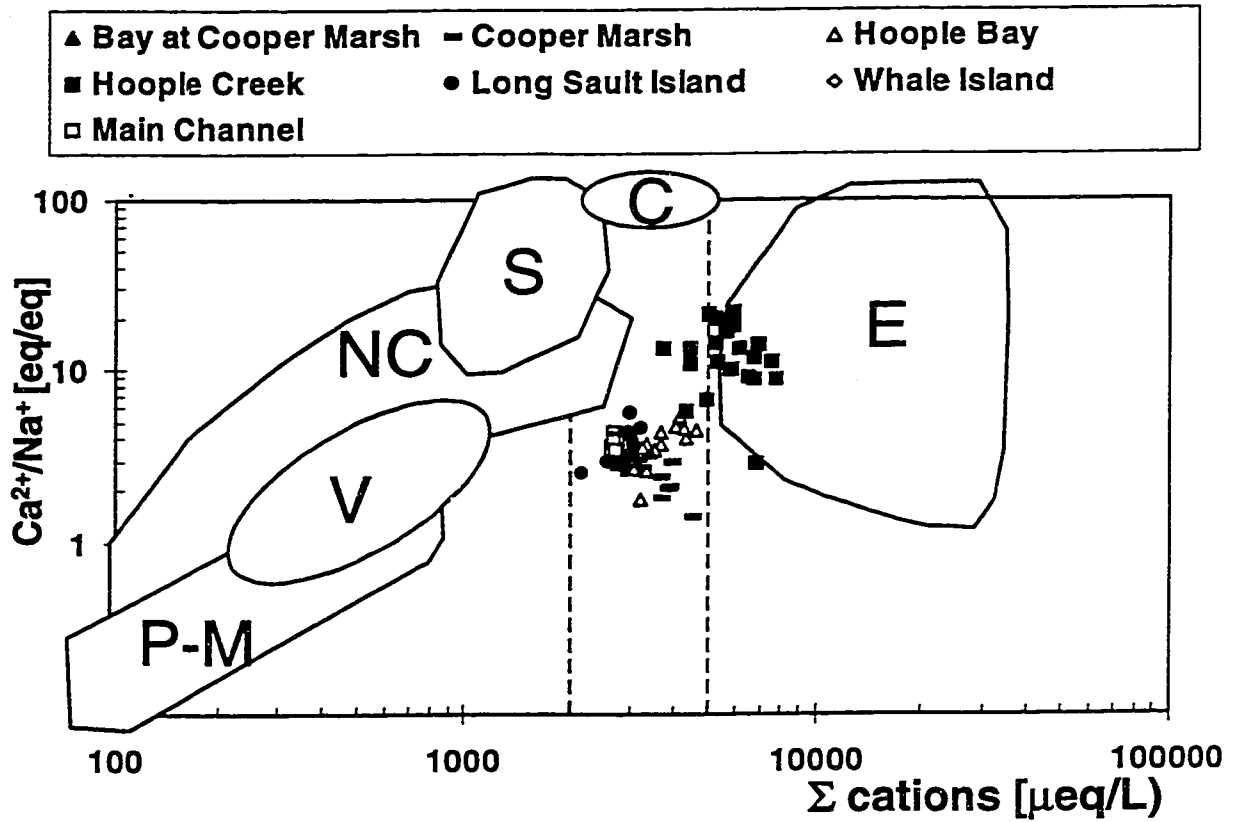


Fig. 5.2 River classification modified after Meybeck (1986). C = carbonates; S = molasse, marls, carbonaceous sandstones; E = evaporites P-M = plutonic and metamorphic rocks (granite, gneiss, micaschist, amphibolites, serpentinite); V = volcanic rocks (basalts, rhyolites, andesites..); NC = non-carbonates (sandstone, greywacke, clays, shales).

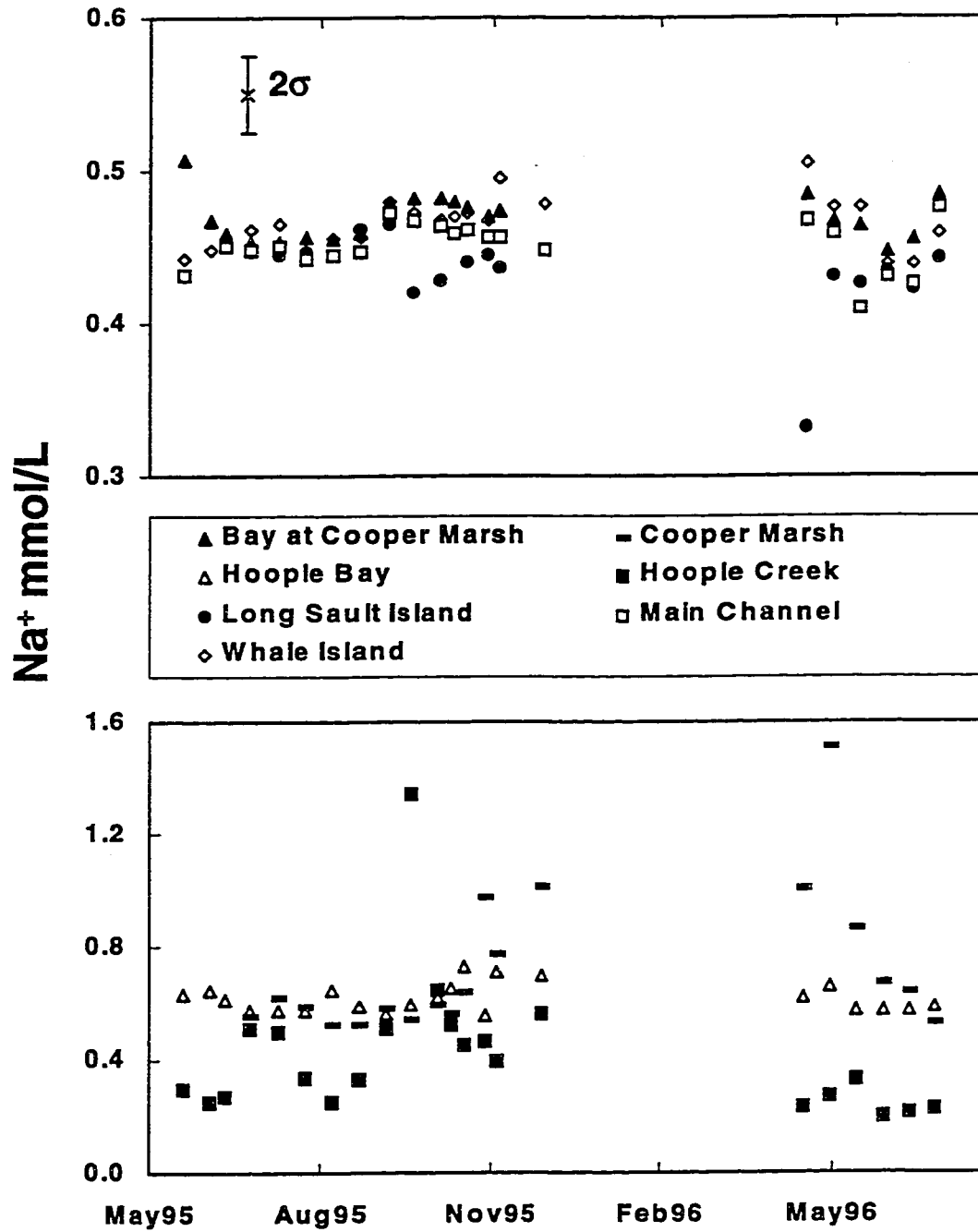


Fig. 5.3 Temporal trends of Na⁺.

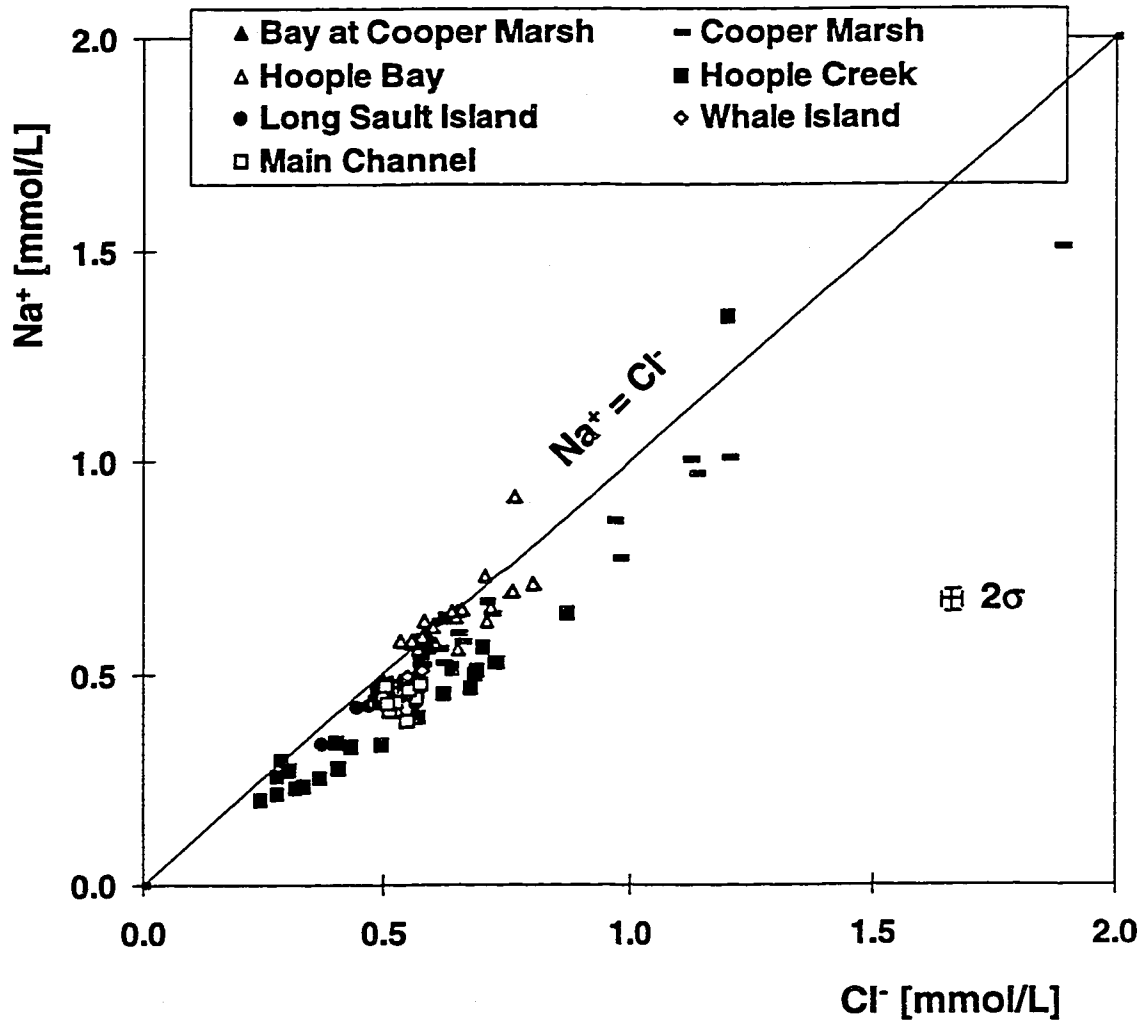


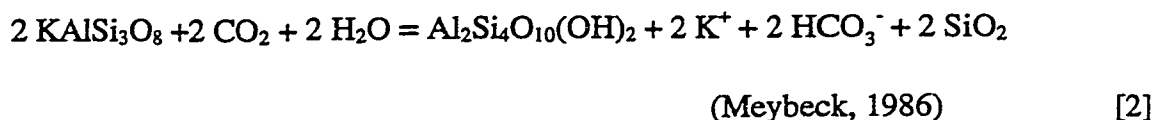
Fig. 5.4 Scatter plot of Cl^- versus Na^+ .

The 'membrane effect' occurs during compaction of clay minerals as the charged layers of their surfaces are squeezed together, leading to 'anion exclusion' from pore water (Drever, 1988). The excluded anions (i.e. Cl⁻) may partition into percolating groundwater and end up in the river. An anthropogenic cause of the chloride excess is chlorination as a tool for disinfection and oxidative removal of Fe, Mn and S in water treatment plants. The reaction for chlorination is:



Another chloride input that is not balanced by sodium is the discharge of waste hydrochloric acid. Altogether, given the large abundance of shales and clays in the Great Lakes-St. Lawrence catchment area (i.e. Billings, Carlsbad, Russell and Queenston shales, Leda clays), it is likely that the membrane effect caused most of the Cl⁻ excess in the 'Main Channel' and associated ecosystems. In the near-shore ecosystems 'Hoople Creek' and 'Cooper Marsh', the Cl⁻ excess is even more pronounced and probably reflects anthropogenic influences.

The dissolution of sylvite (KCl) can also contribute chloride, but it has long been recognized that over 90 % of potassium originates from the dissolution of silicates, such as micas and K-feldspar (Berner and Berner, 1996; Holland, 1978). The weathering for the latter can be formulated as:



Micas and feldspars are present in crystalline rocks (i.e. granites, gneisses, and schists of the Canadian Shield) as well as in sedimentary rocks (i.e. arkosic sandstones, and

shales of the St. Lawrence Platform). Meybeck (1984) estimated that, after atmospheric correction, 75 % of K^+ in rivers results from silicate weathering in sedimentary rocks, while the remaining 25 % originates from igneous and metamorphic silicates. These proportions depend on the distribution of rock types in riverine catchment basins. With the large distribution of shales, clays, clayey tills and sandstones in the drainage area (chapter 2), an even higher contribution of K^+ from sedimentary rock types is possible. Potassium in rivers also originates from fertilizers in agriculture, but the contribution from this anthropogenic source is difficult to estimate.

5.5.2 Sulfate

After atmospheric correction, the sources of sulfate in river water are (1) dissolution of evaporites, (2) oxidation of pyrites and (3) anthropogenic inputs. The latter result from mining and smelting of sulfidic ore, refining of petroleum and from chemical industries.

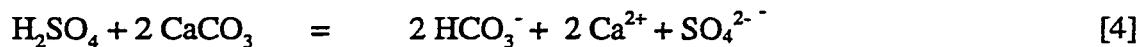
The weathering of gypsum and anhydrite contributes sulfate and calcium in equal proportions to aqueous systems, but is relatively rare due to the sparsity of evaporite series on the earth's surface. The Silurian Salina Formation of the western St. Lawrence Platform and in the Michigan Basin as well as the evaporite series in the Devonian strata of the Michigan Basin may have contributed to the sulfate budget of the upper St. Lawrence. Gypsum lenses that were reported in the March and Oxford formations of the Ottawa Embayment (Hofmann, 1972) represent another source of SO_4^{2-} to the river.

Alternatively, the oxidation of pyrite and other sulfides that are present in clays and shales may add sulfate to rivers. This mechanism is probably the dominant contributor of

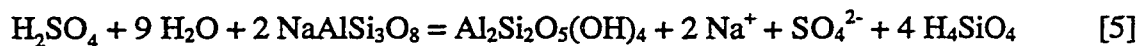
sedimentary sulfate to the St. Lawrence River, given the wide spatial distribution of clays and shales on the St. Lawrence Platform (Chapter 2). The oxidation of pyrite constitutes a representative reaction for this type of weathering:



The sulfuric acid liberated in this reaction causes other reactions such as:



or



Dolomites, K-feldspars, amphiboles and pyroxenes can react in similar ways with sulfuric acid. Consequently, weathering involving H_2SO_4 as a result of pyrite oxidation can contribute Ca^{2+} , Mg^{2+} , Na^+ , K^+ to river water at difficult to estimate proportions. For this reason, the relative contributions of sulfate from evaporite and sulfide weathering are difficult to estimate.

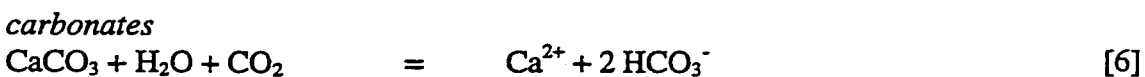
According to Yang et al. (1996), sulfates originating from pollution play a major role in the St. Lawrence sulfur budget. Unfortunately, because they are usually not counterbalanced by cations (such as from direct discharge of sulfuric acid), it is impossible to quantify their influence without consideration of industrial discharge data that are difficult to obtain for the entire catchment area.

As mentioned above, higher sulfate concentrations in 'Hoople Creek' may originate from evaporites, but usually the dissolution of gypsum and anhydrite is accompanied by halite dissolution (Meybeck, 1986). This relationship suggests that higher sulfate contents from evaporite weathering should be associated with higher Na^+ contents. Clearly this is not the case for the 'Hoople Creek' samples (Fig. 5.5), indicating that these

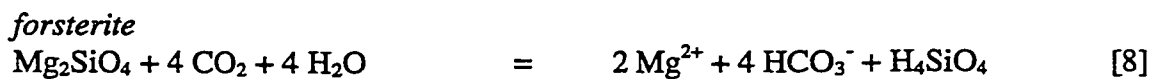
higher sulfate concentrations originate rather from the oxidation of sulfide minerals or from anthropogenic influences. Charron (1978) described a well with high hydrogen sulfide concentrations very close to 'Hoople Creek', which suggests that sulfates originate predominantly from oxidation of sulfides in surrounding clay rich tills. Clays, such as the Leda Clay, are known for a distinct H₂S smell indicating the presence of reduced sulfur that is oxidizable to SO₄²⁻. Nevertheless, the highly variable temporal SO₄²⁻ concentrations in 'Hoople Creek' (Fig. 5.6) may be indicative also of some anthropogenic influences.

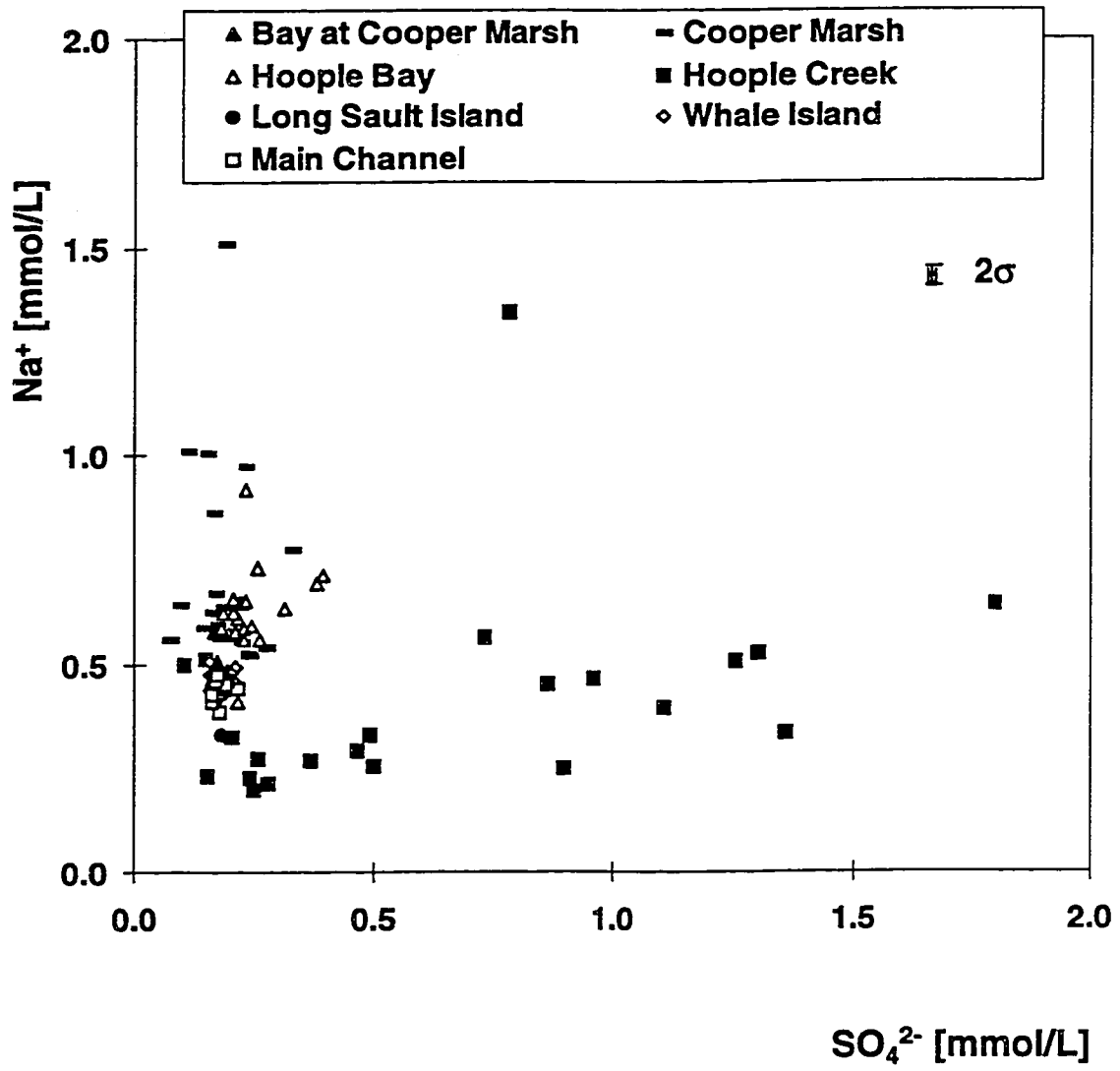
5.5.3 Calcium and magnesium

The following reactions can be formulated for the contribution of Ca²⁺ and Mg²⁺ (Meybeck, 1986; Garrels and Mackenzie, 1971; Garrels, 1976):



Note that, as mentioned above, carbonates can also weather by sulfuric acid (eq. [4]) or by other organic acids. Ca²⁺ and Mg²⁺ may also originate from the weathering of silicates, such as for instance:





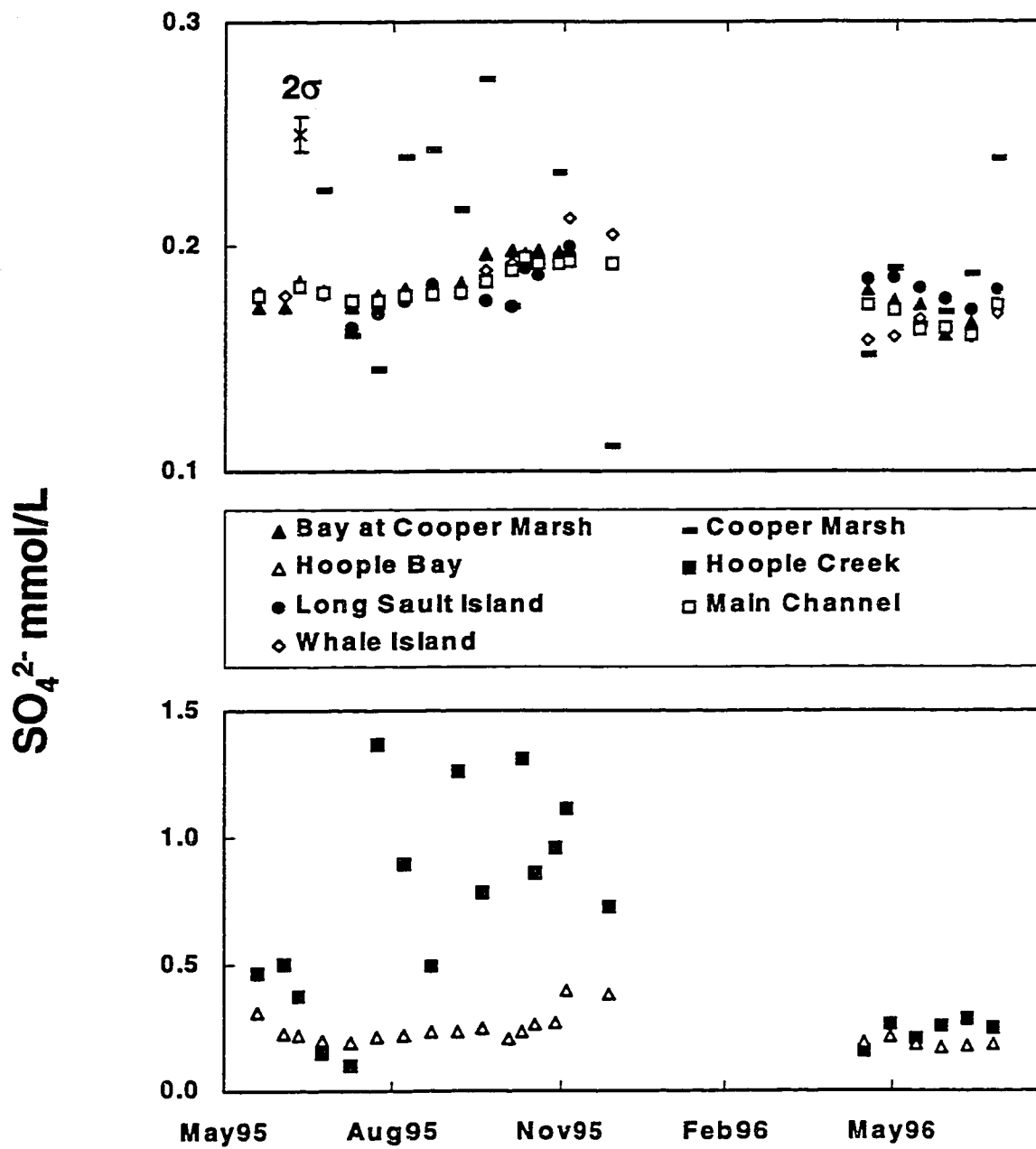
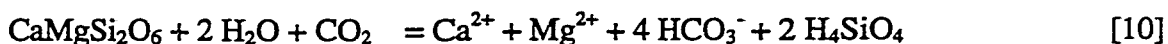


Fig. 5.6 Temporal trends of SO_4^{2-} .

Berner and Berner (1996) formulate a simplified reaction for the weathering of iron free pyroxenes as:



Note that other weathering reactions, involving micas, amphiboles, smectite, vermiculite etc., are also possible. Although the last five reactions are written with CO_2 as the reactive agent, other pathways involving sulfuric or organic acids are also possible. These reactions were not formulated here, because their products are similar.

With the help of strontium isotopes, Yang et al. (1996) attributed 74 % of the Ca^{2+} and Mg^{2+} flux in the St. Lawrence River to carbonate weathering (reactions [4], [6] and [7]) and 26 % to silicate weathering (reactions [8] to [10]). After atmospheric corrections, this estimate can be refined to contributions of 70.4 and 24.7 % for carbonate and silicate weathering, respectively. Note that this evaluation ignores the contribution of Ca^{2+} from weathering of gypsum and anhydrite. If these evaporites were the only contributors of sulfate in the St. Lawrence river, correction could easily be performed by subtracting the equivalents of sulfate from the total Ca^{2+} load. However, sulfate inputs from human activity and from sulfides in shales (reactions [3] to [5]) make this estimate impossible. For this reason, the above proportions have to be interpreted as maximal estimates.

5.5.4 Bicarbonate

Bicarbonate is the major anion in all river water samples collected and its principal source is the weathering of carbonates and silicates (reactions [4] and [6] to [10]). Ultimately, most riverine HCO_3^- originates from soil CO_2 produced during biological

processes, such as root respiration and bacterial activity. Within the river, respiratory activity consumes organic matter and leads to higher contents of CO_2 . The latter is then transformed into HCO_3^- at pH values between 6.4 and 10.3. The same process may occur on an inorganic basis by simple oxidation of organic matter. During warm seasons these processes may be counteracted by algal photosynthesis. As will be seen, both of these in situ processes exert important secondary influences on the dissolved carbon budget (Chapter 6).

The wide range of HCO_3^- and DOC concentrations over the seven sampling locations suggests two endmembers, with the 'Main Channel' at the lower end and the 'Hoople Creek' at the high end (Fig. 5.7). Although, more organic material seems to augment the respiration rate and adds CO_2 to the system, one cannot conclude that respiration is the main contributor of HCO_3^- . A large part of HCO_3^- must also originate from weathering reactions outside the river in order to explain the Ca^{2+} and Mg^{2+} concentrations in the water column that are largely balanced by HCO_3^- . For this reason, a model involving both processes needs to be established. In this model, organic matter in soils either disintegrates into its organic anions and protons or is transformed to CO_2 via respiration (Fig. 5.8A). Both, CO_2 and protons, cause further weathering and therefore contribute to the HCO_3^- pool in aqueous solutions (Fig. 5.8B and 5.8C).

In this example, the reactant was chosen to be CaCO_3 , but could be any other mineral from reactions [4] to [10]. Naturally, the reaction pathways from Figure 5.8 occur more readily where more organic matter is present, part of which is leached and

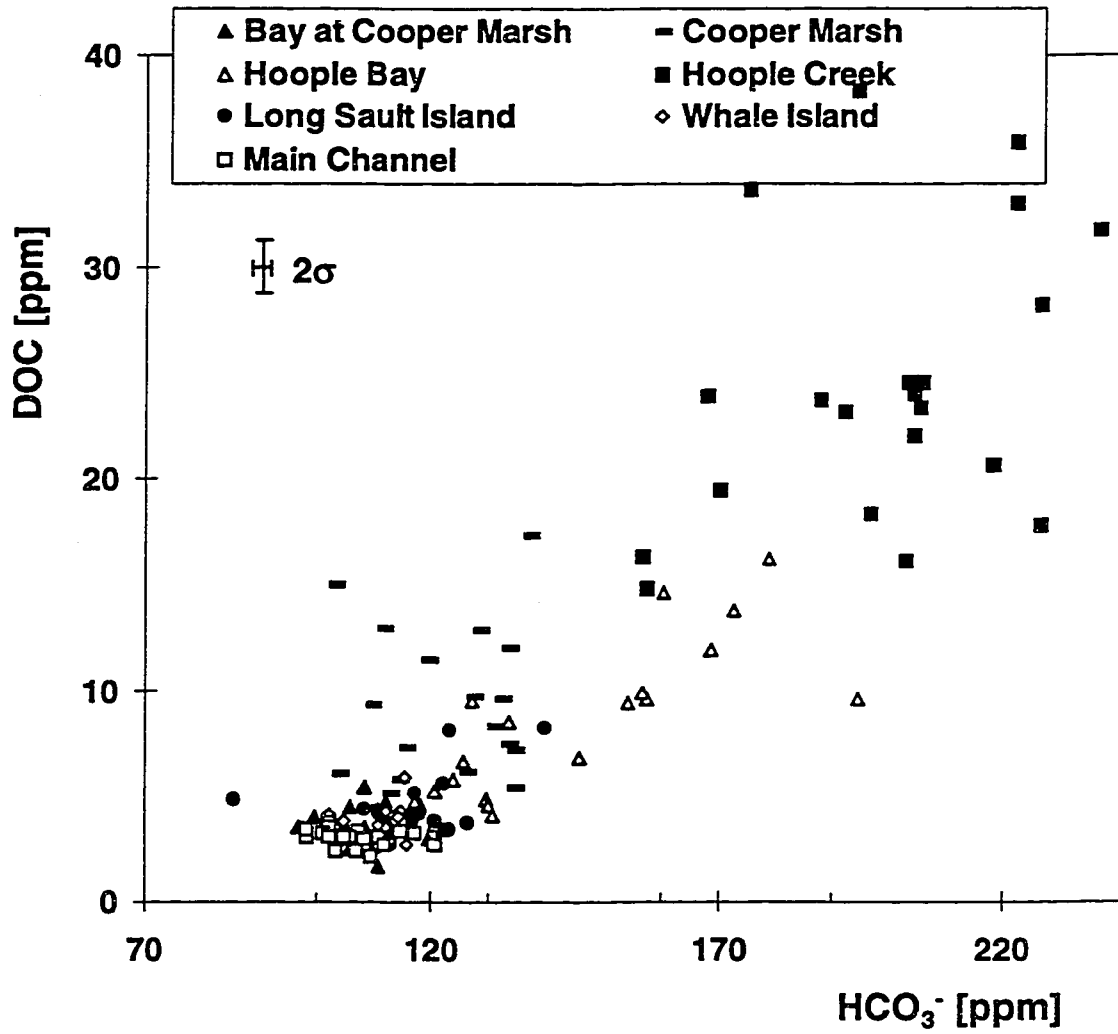


Fig. 5.7 Scatter plot of HCO_3^- versus DOC.

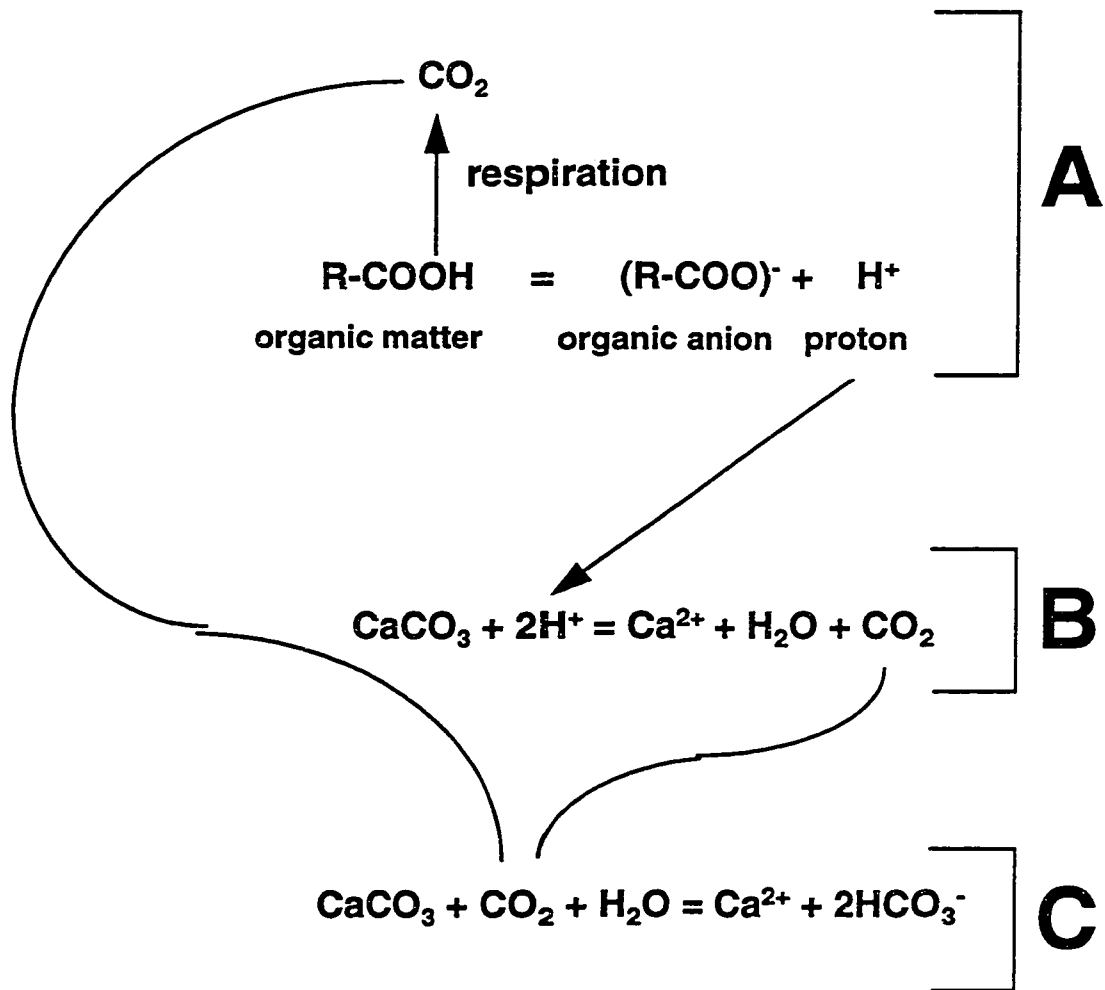


Fig. 5.8 Weathering model explaining the positive correlation between DOC and HCO_3^-

transported via interflow and baseflow to open aqueous systems. In this way the positive relationship between DOC and HCO_3^- concentrations can be explained without excluding mineral weathering.

5.6 Dissolved inorganic nitrogen species

In natural systems the inorganic nitrogen originates from leaching of organic nitrogen compounds in soils, whereas the anthropogenic nitrogen comes from fertilizers and sewage (Van Bennekom and Salomons, 1980). Once in the river, this nitrogen is assimilated by algae and macrophytes, particularly during warm seasons lowering its concentrations. Such seasonality is clearly evident in the NO_3^- distributions of the studied ecosystems in the Cornwall area (Fig. 5.9). These trends are repeated by other parameters, such as chlorophyll-a and carbon isotopes, particularly in the near-shore ecosystems, and the relevant processes will be discussed in Chapter 6.

The sources of dissolved nitrogen in precipitation are mainly nitrous oxides (NO_x), produced during combustion of fossil fuels in automobile engines. These oxides then react with atmospheric water to form nitric acid and other dissolved nitrogen species (Berner and Berner, 1996). It is of interest to compare the flux of the total dissolved nitrogen species ($\text{NO}_3^- + \text{NO}_2^- + \text{NH}_4^+$) in the 'Main Channel' to atmospheric inputs of total nitrogen over the Great Lakes. These calculations, performed in the same manner as for the major elements (Appendix 4.2A and B), show that the atmospheric contributions of total nitrogen amount from 401 % to 938 % of the river flux, depending whether the deposition over the Great Lakes or their entire watershed is taken into account.

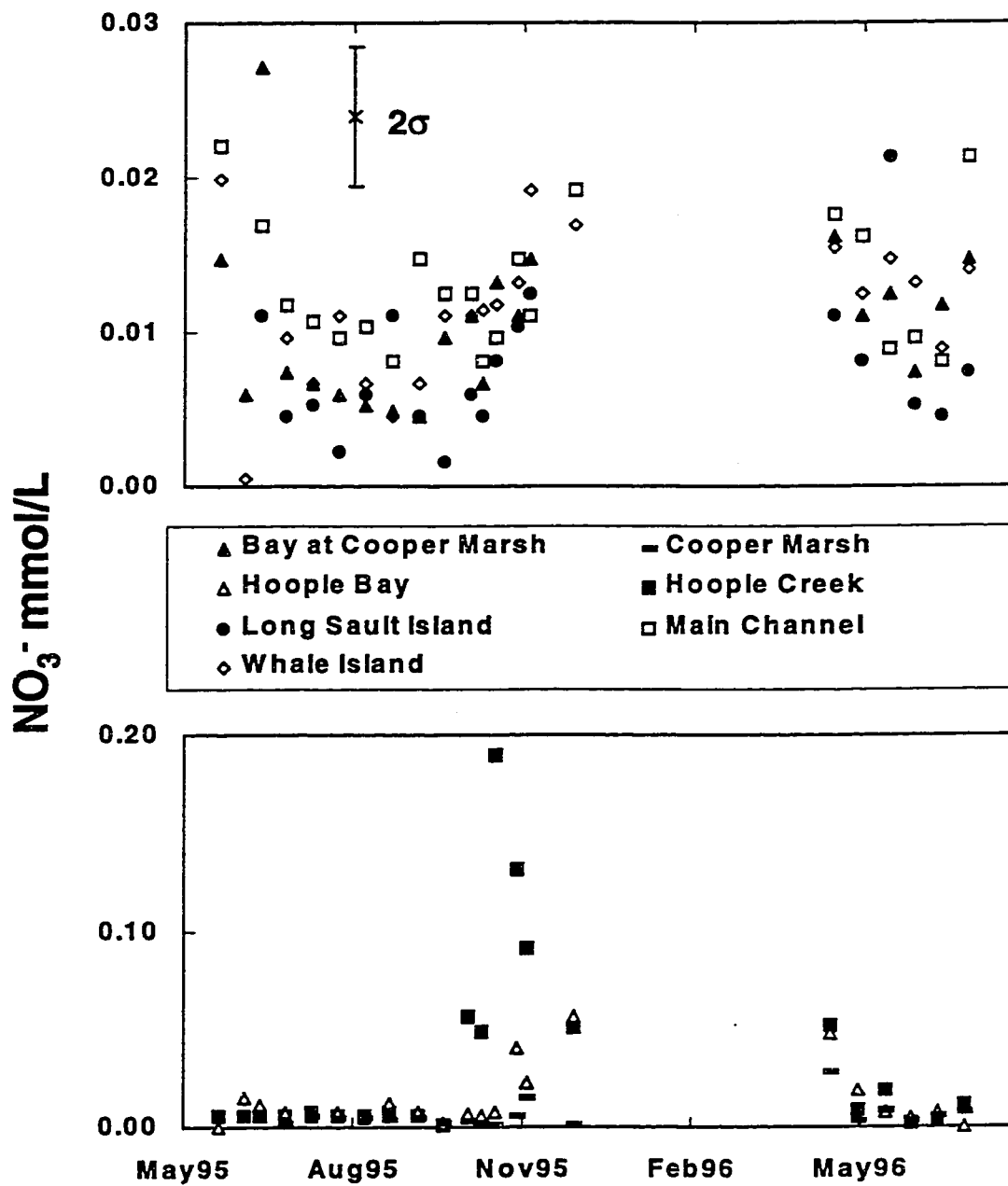


Fig. 5.9 Temporal trends of NO_3^- .

In other words, the total atmospheric N-input is up to 9.38 times larger than the output through the St. Lawrence River. At first sight, these numbers seem unrealistic, but they make sense if one considers that large amounts of nitrogen are consumed by land plants and algae.

Altogether, the above considerations have shown that mineral weathering plays a principal role in the major ion chemistry of all ecosystems studied. Due to involvement of soil CO_2 in most weathering reactions, the dominant anion in all river water samples is bicarbonate (HCO_3^-), the dominant species of the dissolved inorganic carbon. This indicates that a large part of the St. Lawrence carbon cycle is influenced by processes external to the river. In consideration the lithology of the catchment basin (Chapter 2), it becomes clear that carbonate weathering exerts a strong control on the river water chemistry.

However, if we are to better understand the complexity of the aquatic carbon cycle, it is also important to consider internal riverine processes. The stable isotopic composition of the dissolved inorganic carbon is an excellent tool that helps us to understand both, the external and internal components of this cycle (Chapter 6). Yet, the riverine carbon budget encompasses also organic components, such as dissolved and particulate organic carbon. All these will be discussed in the next chapter.

6. Carbon cycle

Previous reconnaissance work on the St. Lawrence River by Yang et al. (1996) has shown that biogeochemical parameters in the main stem of the river are relatively uniform along its entire length, from Kingston to Québec City. In this study, the 'Main Channel' partial pressures of CO₂ were found to vary from average values of 576 ppmV in the spring to 207 ppmV in the fall, while the $\delta^{13}\text{C}_{\text{DIC}}$ signal ranged between -4.3 to +0.7 ‰ VPDB. As will be seen, these variations are relatively small when compared those of the near-shore ecosystems and this stability reflects the influence of the Great Lakes, where the water resides for up to 127 years before entering the St. Lawrence fluvial system (United States Environmental Protection Agency and Government of Canada, 1995). This long lacustrine residence time causes the water to homogenize through biannual lake turnovers and favors CO₂ equilibration with the atmosphere. In order to investigate more closely the seasonal and spatial variations of this parameter in the St. Lawrence River, a detailed monitoring of seven ecosystems near the city of Cornwall (Fig. 6.1) was carried out in 1995 and 1996. The ecosystems studied include the center of the St. Lawrence River ('Main Channel'), several of its embayments with variable degrees of 'Main Channel' water input ('Bay at Cooper Marsh', 'Long Sault Island', 'Whale Island', 'Hoople Bay'), a creek that drains into the St. Lawrence ('Hoople Creek'), and a wetland ('Cooper Marsh').

In contrast to the relatively homogeneous down river evolution of the St. Lawrence, the results of this monitoring reveal strong biogeochemical gradients between

the 'Main Channel' and the near-shore ecosystems (Barth et al., 1996), as indicated for example by their differing annual $p\text{CO}_2$ values (Fig. 6.1).

These variations conceivably reflect not only spatial differences, but also seasonal changes in the aqueous carbon cycle. The latter, in turn, is influenced by differing rates of mineral dissolution, by equilibration with the atmosphere and by the balance of respiration and photosynthesis. Mineral dissolution, involving biogenic CO_2 , is the major contributor of bicarbonate to natural waters prior to their discharge into the Great Lakes-St. Lawrence system (Telmer, 1996). Subsequently, the DIC equilibrates with the atmosphere during the long residence time of water in the Great Lakes, a signal that is then transposed to the 'Main Channel' of the St. Lawrence (Yang et al., 1996). Yet, respiration and photosynthesis must also exert an important control on the carbon cycle in the studied ecosystems, and this control was further investigated via annual monitoring of proxy variables, such as the dissolved organic carbon (DOC), chlorophyll-a (chl-a) and the stable isotopic composition of the dissolved inorganic carbon ($\delta^{13}\text{C}_{\text{DIC}}$).

The vicinity of Cornwall is an ideal site for such biogeochemical studies, because the St. Lawrence water at this point originates entirely from Lake Ontario and is not influenced by discharge from any tributaries. The well mixed signal of the Great Lakes, presented at the 'Main Channel' sampling station, represents therefore a convenient baseline.

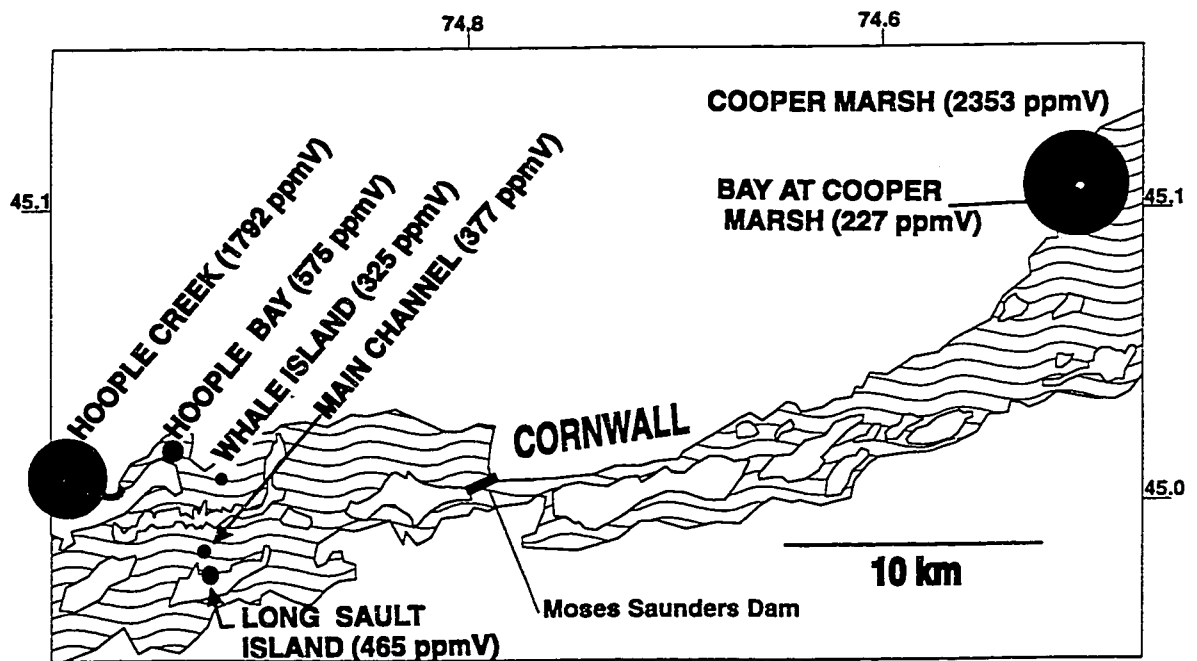


Fig. 6.1 Location of the studied ecosystems near Cornwall, with their average annual pCO₂ proportional to the circle size.

6.1 Seasonal dynamics of carbon dioxide and oxygen

Partial pressure of CO₂ was calculated from the activities of the DIC species, the H⁺ activity, the reaction constant between HCO₃⁻ and CO₂(aq) and Henry's law constant for the distribution between CO₂(aq) and CO₂(g). The activities of the species utilized in this calculation were determined with the Hydrowin program (Calmbach, 1995) with the input of alkalinity and pH and concentrations of other major ionic species. The precision of the calculated pCO₂ depends on two variables, the activity of H⁺ and the activity of HCO₃⁻, and was calculated to be ±15 % (2σ) by using a formula for the propagation of error with two variables (Kretz, 1985; Pantony, 1961; Miller and Miller, 1984). It should be noted that the calculated CO₂ partial pressures likely underestimate the true pCO₂ values, due to alkalinity decreases during titration (Hope et al., 1995).

The partial pressure of CO₂ is generally higher at near-shore sampling stations (Fig. 6.1), but shows considerable seasonal variations within each ecosystem. These variations are due to seasonally differing rates of ground- and soil water influx (baseflow), as well as to different rates of in situ biological activity, such as respiration and photosynthesis. The temporal pCO₂ variations between May (1995) and July (1996) in the seven ecosystems studied are displayed in Fig. 6.2, and will be described here in a succession from 'Hoople Creek' to 'Hoople Bay', 'Whale Island', 'Main Channel' and ending with the embayment at 'Long Sault Island'. The ecosystems 'Bay at Cooper Marsh' and 'Cooper Marsh' are described separately, since they are located 20 km further downstream and are not a part of the upstream transverse profile.

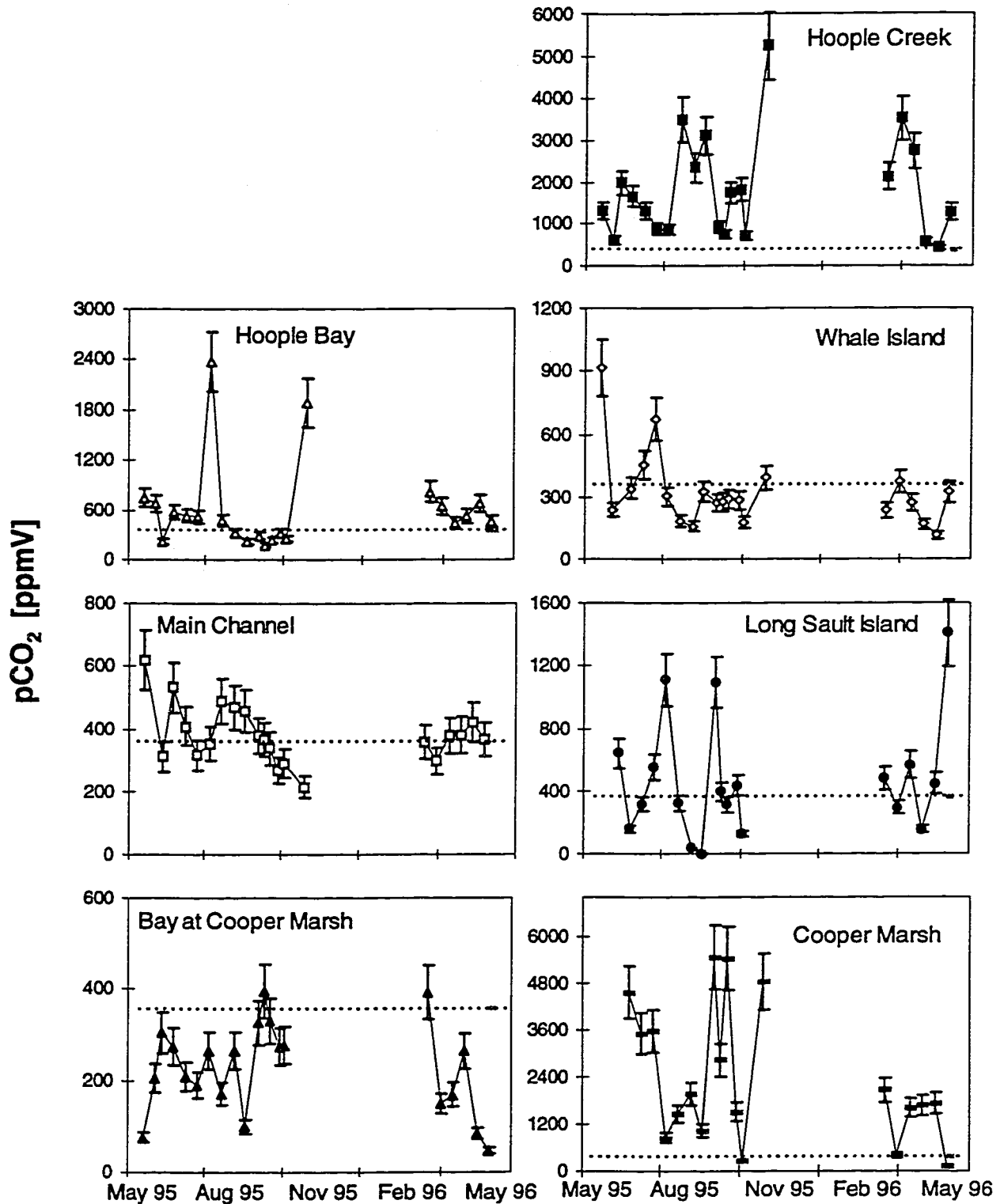


Fig. 6.2 Temporal variations of the $p\text{CO}_2$ in the ecosystems studied. The precision (2σ) is $\pm 15\%$ and depends on the absolute $p\text{CO}_2$ concentration. The dashed lines represent the $p\text{CO}_2$ of the atmosphere (358 ppmV; Houghton, 1996).

In 'Hoople Creek', the $p\text{CO}_2$ is subject to large variations throughout the year, with peak values as high as 5247 ppmV in the cold season. The $p\text{CO}_2$ variations in this ecosystem result from varying rates of respiration and photosynthesis as well as from seasonally differing rates of baseflow. The latter, with its CO_2 charged waters, dominates the water balance in the creek during the late fall, winter and early spring. Note that CO_2 may also originate from sediment water interaction. Specifically, seeping of pore waters with higher CO_2 contents may contribute to the overall CO_2 budget of the system. However, under anoxic conditions within sediments, CO_2 consumption via methane formation may be a process that influences the CO_2 budget.

As the water flows into 'Hoople Bay', the $p\text{CO}_2$ changes to values that, with two exceptions, range between 171 and 821 ppmV. One peak value, the 2368 ppmV in August 1995, is most likely a result of an increased influx of CO_2 -enriched 'Hoople Creek' waters following heavy rain events. The second high value, 1883 ppmV in December 1995, was observed under partial ice coverage, when respiration and decomposition of organic material dominated the ecosystem. During the late summer and fall, and during an algal bloom event in the spring of 1995, the $p\text{CO}_2$ in 'Hoople Bay' declined below the values expected for equilibrium with the atmosphere, due to algal consumption of CO_2 . In contrast, the $p\text{CO}_2$ in the spring and in early summer usually exceeds the 358 ppmV, because the ecosystem is dominated by respiration. In addition to these biogeochemical dynamics, 'Hoople Bay' is also influenced by mixing of waters with the 'Main Channel'.

The 'Whale Island' sampling station is strongly influenced by the waters of the 'Main Channel', as demonstrated by the similarity of seasonal $p\text{CO}_2$ curves.

Nonetheless, the 'Whale Island' curve often shows slightly lower $p\text{CO}_2$ values than the 'Main Channel', a result of higher photosynthetic activity.

The $p\text{CO}_2$ in the 'Main Channel' oscillates around 358 ppmV, indicating an approximate equilibration with the atmosphere. Values slightly lower than 358 ppmV in the spring and summer likely result from higher rates of photosynthesis in the Great Lakes-St. Lawrence system, but the lower values in October and November are not as easily explained. They could represent 'old' water that was depleted in CO_2 during the summer, but was held back at the upstream Iroquois Dam to be released only in the fall. Water regulations like these are common in the St. Lawrence seaway (Morin et al., 1994).

The $p\text{CO}_2$ in the elongated 'Long Sault Island' embayment varies strongly throughout the year. The waters in this embayment originate mostly from the 'Main Channel', but strong rain events, with subsequent increased baseflow, can cause peak CO_2 concentrations of 1408 ppmV. Values lower than atmospheric pressures in the spring and summer are again a consequence of prevailing photosynthetic activity.

The downstream ecosystem of the 'Bay at Cooper Marsh' must be the ecosystem most heavily influenced by photosynthesis, because its $p\text{CO}_2$ approaches an equilibrium with the atmosphere only during the cold seasons.

In contrast to this bay, the adjoining 'Cooper Marsh' shows the most elevated $p\text{CO}_2$ values, peaking at 5450 ppmV, with seasonal variations reflecting interactions of strong respiration versus photosynthesis and of varying rates of baseflow.

An effective way of representing the interaction of respiration and photosynthesis in these seven ecosystems is to subtract the atmospheric $p\text{CO}_2$ (358 ppmV) from the $p\text{CO}_2$ that has been calculated from the activities of HCO_3^- and H^+ in the water column (Fig.

6.3). Note that small changes in pH can cause large variations in the calculated CO_2 so that not all of the observed high CO_2 values may be caused by respiration. Nonetheless, one can argue that low pH values are a result of higher respiratory CO_2 , because after its dissolution in water it changes into the acid H_2CO_3 . If so, only inorganic addition of acid could raise the non-respiratory portion within the CO_2 pool. Values near zero indicate equilibration of the water with respect to atmospheric carbon dioxide, while positive differences demonstrate CO_2 overpressures that result in its evasion to the atmosphere. By the same token, negative differences imply undersaturation that causes ingassing of atmospheric CO_2 . In an analogous procedure, the partial pressure of atmospheric oxygen (209,500 ppmV; Keeling et al., 1996) was subtracted from the measured oxygen concentrations that were converted to pO_2 using Henry's law. Again these oxygen subtractions show equilibrium at zero, oversaturation at positive and undersaturation at negative differences. Assuming that oxygen oversaturation, coupled with CO_2 undersaturation, is caused by photosynthesis, and the inverse relationship by respiration, the quadrants in Fig. 6.3 can be interpreted as follows: (1) dominance of photosynthesis; (2) photosynthesis and respiration; and (3) prevalence of respiration. Most of the points cluster around the zero intersect, indicating that these water samples were close to equilibrium with the atmosphere. This is particularly true for water samples that are influenced by the Great Lakes, such as the 'Main Channel' and its related ecosystems, 'Whale Island' and 'Bay at Cooper Marsh'.

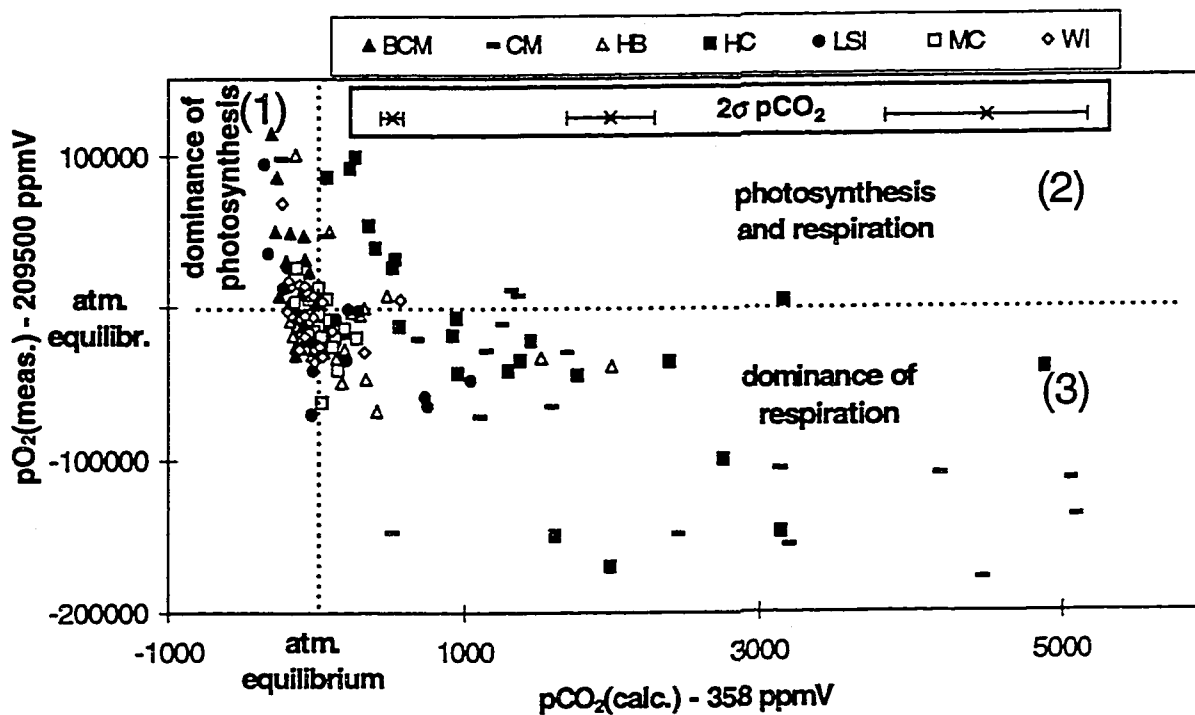


Fig. 6.3 Differences between calculated and atmospheric pCO_2 plotted versus the differences between measured pO_2 and atmospheric pO_2 . The 2σ precision for the pO_2 measurements ranges from 134 to 170 ppmV due to conversion from mg/L to ppmV and lies within the size of the symbols. The sampling stations are abbreviated as follows: BCM = 'Bay at Cooper Marsh', CM = 'Cooper Marsh', HB = 'Hoople Bay', HC = 'Hoople Creek', LSI = 'Long Sault Island', MC = 'Main Channel' and WI = 'Whale Island'.

The marginal ecosystems, 'Hoople Creek' and 'Cooper Marsh' and, at times, 'Hoople Bay' and 'Long Sault Island', show the general dominance of respiration. Nevertheless, they also show large seasonal $p\text{CO}_2$ and $p\text{O}_2$ variations, resulting from seasonal impact of photosynthesis. In general, it is in the warm seasons that photosynthesis prevails, resulting in oversaturation in O_2 and CO_2 undersaturation.

Photosynthesis in these aquatic systems is performed by macrophytes (submerged, immersed or floating plants) as well as by two separate aquatic plant communities, the phytoplankton and the periphyton. The periphyton represents benthic aquatic bacterial and algal mats that may become important in shallow water ecosystems, while the phytoplankton is composed of a large variety of taxonomic groups of free floating algae (e.g. Cyanophyceae, Chlorophyta or Xantophyceae; Lampert and Sommer, 1997), driving most of the photosynthetic activity in deep water ecosystems. Chlorophyll-a (chl-a) is a compound that is present in all oxygen evolving photosynthetic organisms (Wetzel, 1983), but because chl-a was only measured on the suspended particulate matter in the water column it is, in the present case, strictly a measure of phytoplankton biomass. In this study, oxygen supersaturation coupled with enhanced chl-a is therefore an indication of the phytoplankton photosynthesis, while the periphyton is characterized simply by oxygen oversaturation alone (Fig. 6.4). Based on these criteria, the oxygen oversaturations in the shallow water 'Hoople Creek', 'Whale Island', 'Long Sault Island', and the 'Bay at Cooper Marsh' ecosystems result mostly from the dominance of the periphyton community and perhaps macrophytes. The latter two groups should therefore be taken into account in any CO_2 and O_2 budgets of shallow aquatic systems.

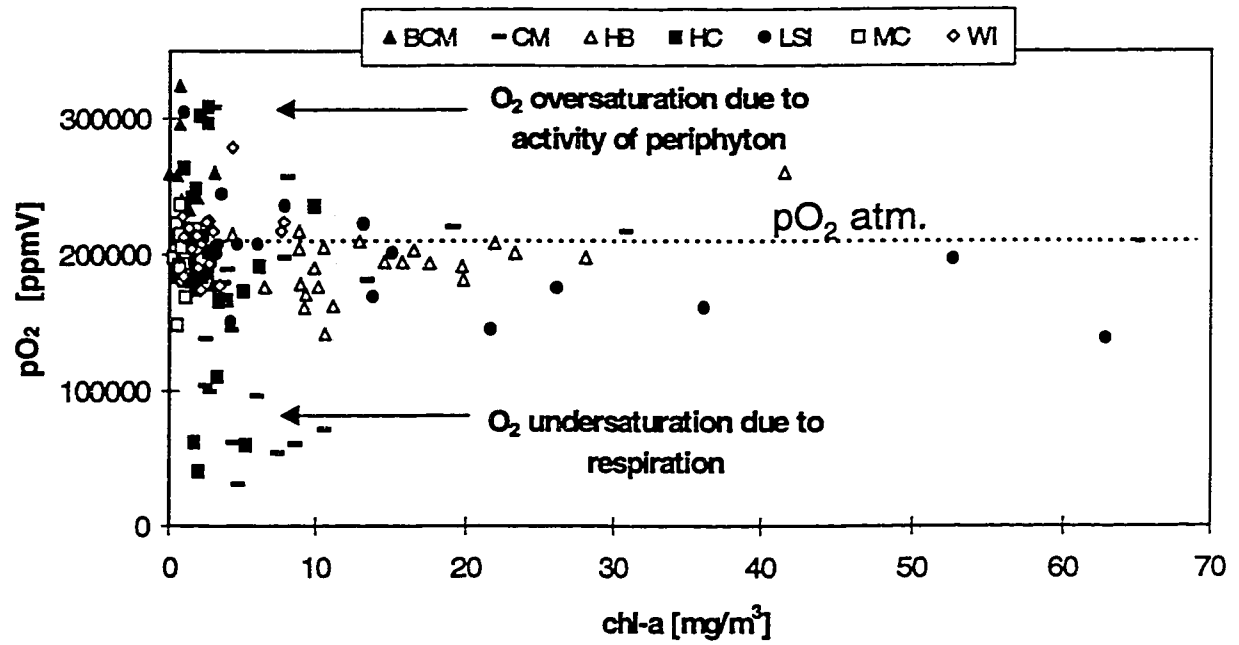


Fig. 6.4 Plot of chlorophyll-a versus the partial pressure of oxygen. The error bars for both parameters lie within the symbols. The abbreviations for the ecosystems are the same as in Fig.6.3.

6.2 Isotope constraints

Dissolved inorganic carbon is the largest carbon pool in most aquatic systems, with bicarbonate being the dominant species (Drever, 1988). In this study, the bicarbonate activities exceeded the sum of particulate and dissolved organic carbon by 5 to 57 times, depending on the season and the ecosystem studied. The isotopic signal of the dissolved inorganic carbon ($\delta^{13}\text{C}_{\text{DIC}}$) is therefore a useful tracer of processes that dominate the carbon cycle in aquatic systems. These processes occur along the pathway of water transport in catchment basins and can be divided into four groups: (1) generation of CO_2 and subsequent mineral dissolution in soils and aquifers; (2) respiration and decomposition of organic matter in the water column; (3) in situ photosynthesis; and (4) equilibration of the DIC with the CO_2 of the atmosphere. A fifth process affecting the $\delta^{13}\text{C}_{\text{DIC}}$ composition would be the generation of methane from $\text{CO}_2(\text{aq})$ in anoxic, organic rich sediments. However, in a pilot study on sedimentary gas evolution in the St. Lawrence River, this process was shown to have minor influences on the carbon budget and is ignored in the following discussion.

In the first process the $\delta^{13}\text{C}$ signal of organic matter is transferred to the CO_2 of soils by bacterial respiration and decay with little or no isotopic fractionation (Peterson and Fry, 1989; Fritz et al., 1978). Subsequently, this CO_2 becomes enriched in ^{13}C by 4.4 ‰, when a fraction of the gas diffuses from the soils (Cerling, 1991). The isotopic composition of soil CO_2 thus depends on the source material that is being decomposed (i.e. C_3 or C_4 plant remains) and on the rate of CO_2 diffusion.

Depending on the organic source material for CO_2 production, dissolution of calcite in soils and groundwaters results in $\delta^{13}\text{C}_{\text{DIC}}$ signals of -16 ‰ VPDB, if the soil CO_2

originates from decay of C₃ plants, and -13 ‰ VPDB, if from decomposition of C₄ plants (Salomons and Mook, 1986). These two examples are for typical soil pCO₂ values of 10,000 ppmV that assume calcite saturation at open system conditions. Note however, that closed system conditions (i.e. mineral dissolution in confined aquifers) can cause more positive δ¹³C_{DIC} signals in groundwaters. In contrast, more negative δ¹³C_{DIC} values can be an outcome of a lower pH, such as those caused by silicate dissolution and calcite undersaturation. This is due to the fact that, at low pH, CO₂(aq) becomes the more important species, and the fractionation between the soil CO₂ and the aqueous CO₂ thus dominates the δ¹³C_{DIC} signal. This fractionation is small (Mook et al., 1974), and the CO₂(aq) therefore resembles the ¹³C depleted soil CO₂ in its isotopic composition.

When the ground and soil waters enter the river, respiration and decomposition of organic matter (POC and DOC) results in a ¹³C depleted isotopic signal for the generated CO₂. The particulate organic matter investigated in this study had δ¹³C_{POC} values ranging from -16.3 to -31.5 ‰, with a median of -27 ‰ VPDB (Section 6.4). The isotopic composition of the DOC was not measured in this study, but Schiff et al. (1997) reported typical δ¹³C_{DOC} values of -27 ‰ VPDB from a lake and stream study in central Ontario. The CO₂ originating from the local organic matter (POC and DOC) should therefore retain an average isotopic composition of -27 ‰ VPDB with some scatter imposed by the variability of the source material.

In contrast to respiration, in situ photosynthesis has a ¹³C-enriching effect on the DIC, because algae preferentially remove light carbon (¹²C) from the DIC pool (Fry and Sherr, 1984). Carbon isotope discrimination by algae can be as large as 20 ‰ (Rau, 1978;

Herczeg and Fairbanks, 1987), but smaller fractionations of only 5 ‰ have also been reported (Fogel and Cifuentes, 1993).

A similar shift to more positive $\delta^{13}\text{C}_{\text{DIC}}$ signals in open water systems can also be generated by equilibration with atmospheric CO_2 . The latter has a $\delta^{13}\text{C}_{\text{CO}_2}$ of -7.6 ‰ VPDB (Zhang et al., 1995), but undergoes ^{13}C enrichment after its diffusion into water bodies. The equilibrium $\delta^{13}\text{C}_{\text{DIC}}$ depends on the temperature and the distribution of the DIC species ($\text{CO}_2(\text{aq})$, HCO_3^- and CO_3^{2-}), and Fig. 6.5 illustrates the comparison of the measured $\delta^{13}\text{C}_{\text{DIC}}$ values with the calculated theoretical ones. The theoretical values are usually heavier than the measured ones, except for the 'Main Channel'-controlled ecosystems during the warm season.

The ^{13}C depletion of DIC is particularly pronounced in near-shore ecosystems, such as 'Hoople Creek', 'Hoople Bay' and the 'Cooper Marsh'.

In a further step, one can consider the differences ($\Delta\delta^{13}\text{C}_{\text{DIC}}$) between the measured and the theoretical $\delta^{13}\text{C}_{\text{DIC}}$ signals for atmospheric equilibrium for the seven ecosystems studied to be a qualitative measure of biological activity (Fig. 6.6). Small $\Delta\delta^{13}\text{C}_{\text{DIC}}$ values indicate a ^{13}C enriched DIC signal that is closer to the one for atmospheric equilibrium, while large $\Delta\delta^{13}\text{C}_{\text{DIC}}$ values result from more negative $\delta^{13}\text{C}_{\text{DIC}}$ signals. All ecosystems have smaller $\Delta\delta^{13}\text{C}_{\text{DIC}}$ values in the warm seasons, likely a consequence of active photosynthesis, resulting in a drawdown of DIC by consumption of $\text{CO}_2(\text{aq})$ that,

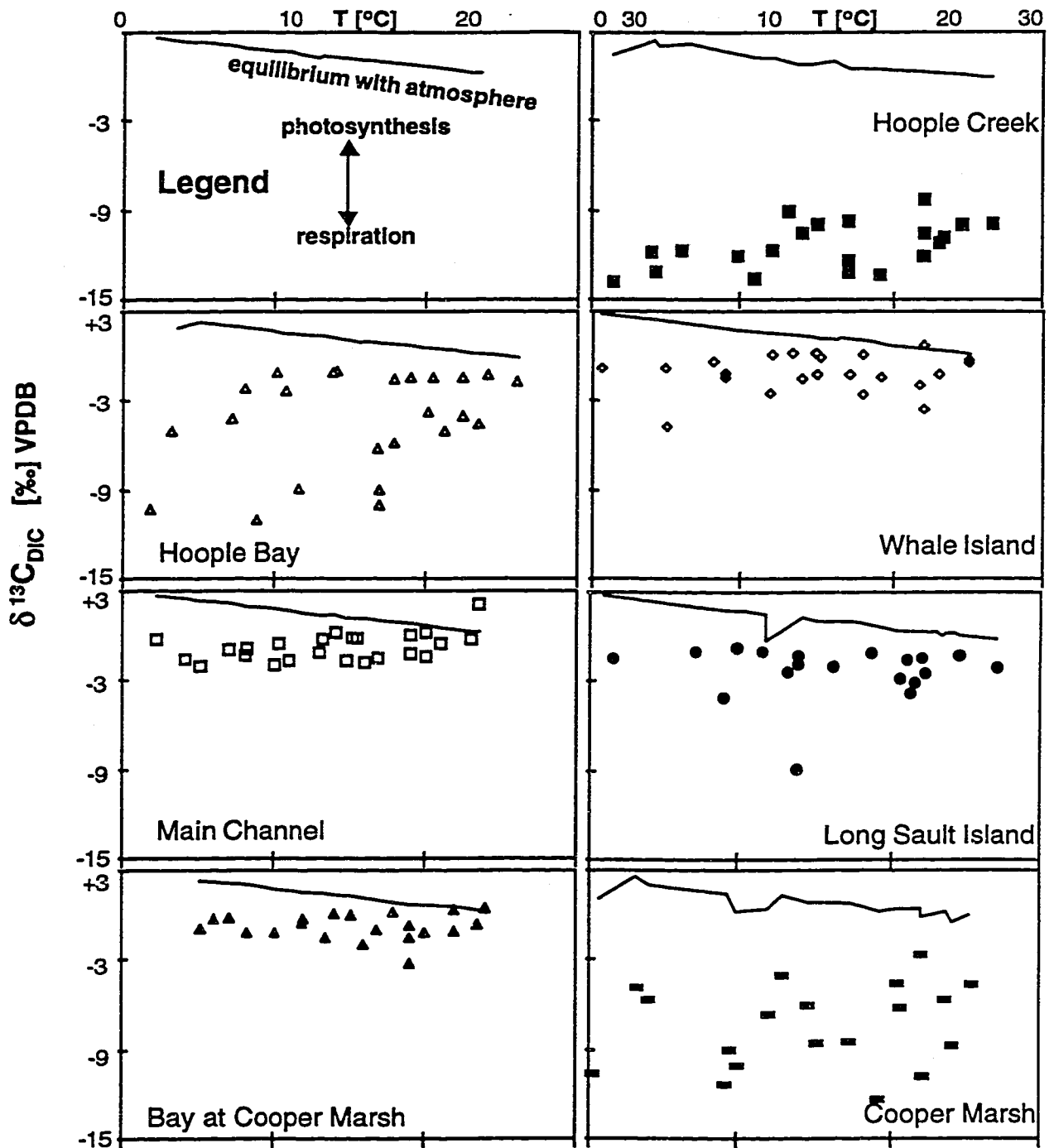


Fig. 6.5 Measured $\delta^{13}\text{C}_{\text{DIC}}$ compared to expected values for equilibrium with the atmospheric CO_2 (lines). The 2σ precision is less than the size of the symbols. The theoretical values for the $\delta^{13}\text{C}_{\text{DIC}}$ equilibrated with the atmosphere were calculated by computing the speciation of $\text{CO}_2(\text{aq})$, HCO_3^- , and CO_3^{2-} with Hydrowin program (Calmbach, 1995) and applying the following formula (Zhang et al., 1995)

$$\delta^{13}\text{C}_{\text{DIC atm. exchange}} = \sum f_i * \delta^{13}\text{C}_i$$

where ' f_i ' is the proportion of each DIC species and ' $\delta^{13}\text{C}_i$ ' its empirically determined, temperature dependent, isotopic composition at equilibrium with atmospheric CO_2 .

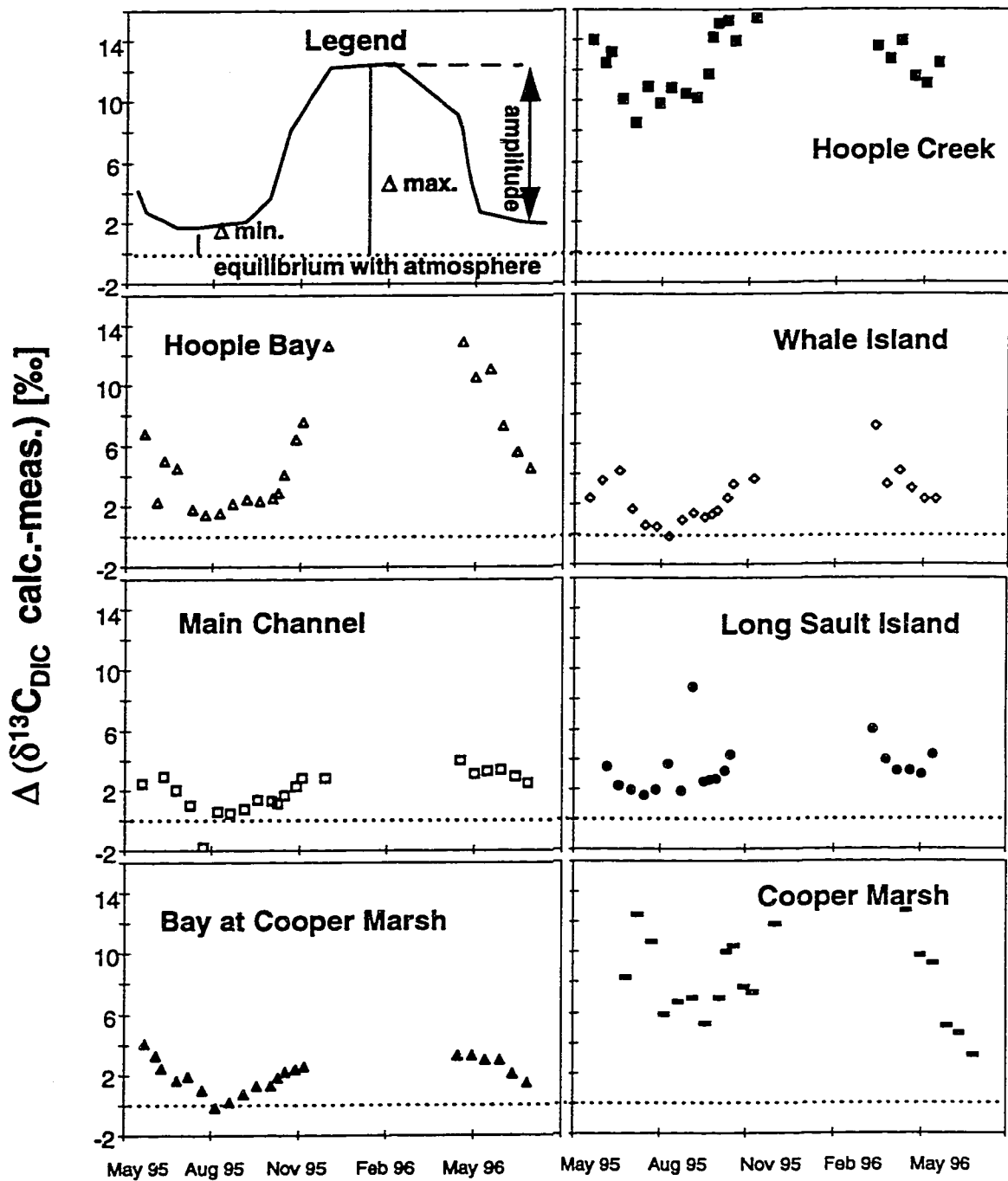


Fig. 6.6 Differences between the calculated and measured $\delta^{13}\text{C}_{\text{DIC}}$. The amplitudes of variations can serve as a qualitative measurement of biological activity, while the deviations from the calculated equilibrium, $\Delta \text{min.}$ and $\Delta \text{max.}$, demonstrate the completeness of the atmospheric equilibration.

if subject to strong photosynthetic utilization, has to be replenished by diffusion from atmospheric CO₂. Photosynthesis and atmospheric exchange may therefore both cause more positive $\delta^{13}\text{C}_{\text{DIC}}$ signals and consequently smaller $\Delta\delta^{13}\text{C}_{\text{DIC}}$ values during the warm season. Note, however, that the 'Hoople Creek' and 'Cooper Marsh' ecosystems still retain higher pCO₂ (Fig. 6.1) as well as larger $\Delta\delta^{13}\text{C}_{\text{DIC}}$ values (Fig. 6.6), even in the warm season. This may be a consequence of higher baseflow inputs and/or in situ bacterial respiration and decomposition of organic matter, all three resulting in more negative $\delta^{13}\text{C}_{\text{DIC}}$ signals that enlarge the $\Delta\delta^{13}\text{C}_{\text{DIC}}$ values.

The depleted $\delta^{13}\text{C}_{\text{DIC}}$ signals can be attenuated by mixing with water masses from the 'Main Channel'. The role of water balance, that is baseflow versus 'Main Channel' input, on the carbon budget of these ecosystems can be tested via the $\delta^{18}\text{O}_{\text{H}_2\text{O}}$ signal. The latter is known to range from -9.8 to -11.5 ‰ VSMOW for local groundwaters (Cane, 1996b), while in the Great Lakes dominated 'Main Channel' it ranges between -6.3 and -8.4 ‰ VSMOW (Appendix 5.1; c.f. Yang et al., 1996).

A plot of $\Delta\delta^{13}\text{C}_{\text{DIC}}$ versus $\delta^{18}\text{O}_{\text{H}_2\text{O}}$ therefore enables differentiation between soil and groundwater respiration signals that were transferred to the river by baseflow and those caused by in situ respiration (Fig. 6.7).

It is apparent that local baseflow, with typical $\delta^{18}\text{O}_{\text{H}_2\text{O}}$ values, can account for the highly depleted $\delta^{13}\text{C}_{\text{DIC}}$, hence elevated $\Delta\delta^{13}\text{C}_{\text{DIC}}$ values, in the 'Hoople Creek' ecosystem, particularly during winter and early spring. During these seasons the discharge of the creek is high and therefore the carbon isotopic composition in 'Hoople Bay' is influenced by mixing between the end members 'Hoople Creek' and 'Main Channel' (Fig. 6.7).

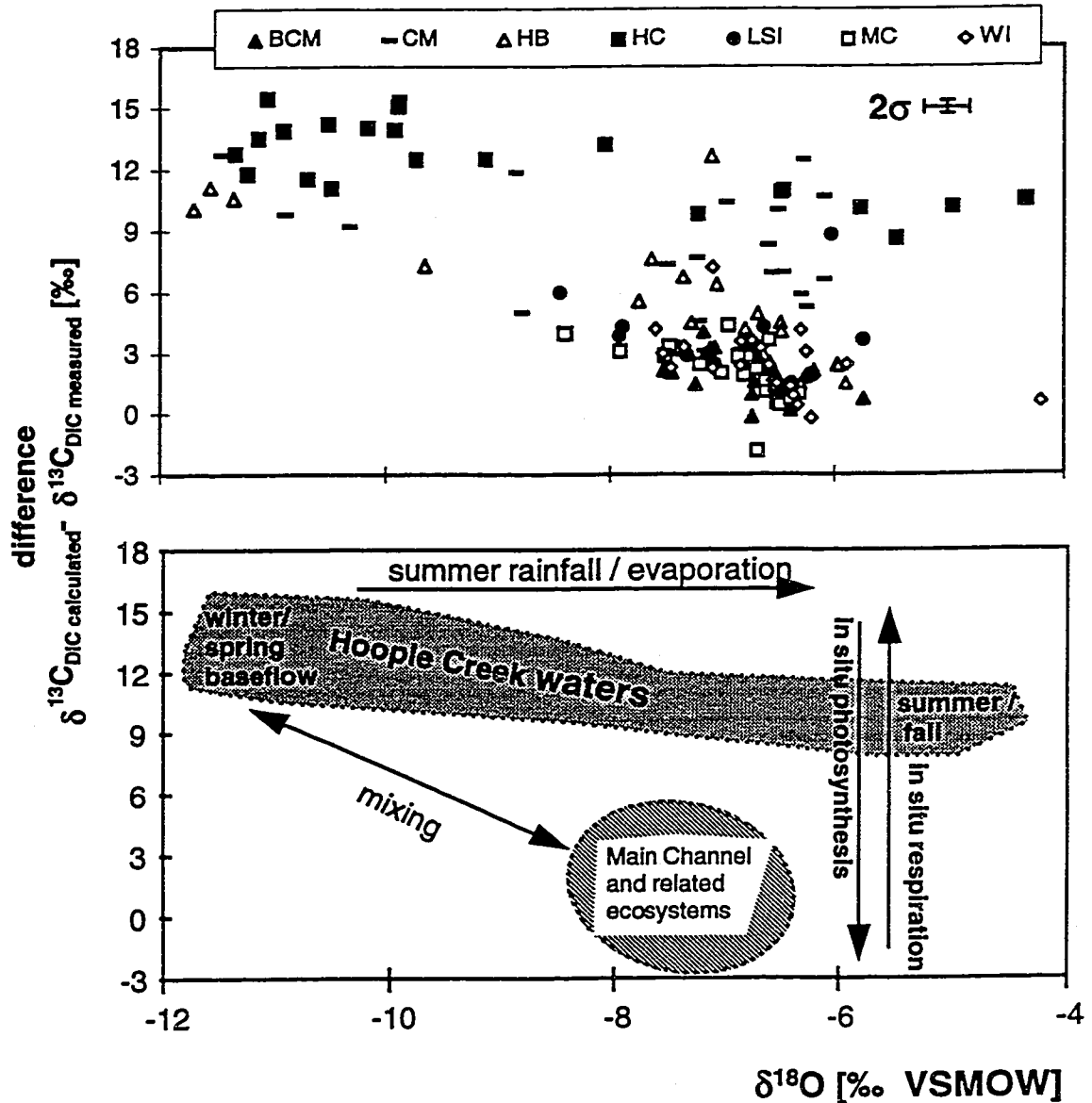


Fig. 6.7 Differences between the calculated and measured $\delta^{13}\text{C}_{\text{DIC}}$ plotted versus the $\delta^{18}\text{O}_{\text{H}_2\text{O}}$ signal of the water samples. Samples that have $\delta^{18}\text{O}$ signals of the 'Main Channel' but higher $\Delta\delta^{13}\text{C}_{\text{DIC}}$ values are dominated by in situ biological activity, respiration or photosynthesis, while samples with a different $\delta^{18}\text{O}$ signal are dominated by local groundwaters coupled with external respiration in soils. The abbreviations for the ecosystems are the same as in Fig.6.3.

Local baseflow and its mixing with the 'Main Channel' waters also influences the 'Hoople Bay' and 'Cooper Marsh' ecosystems during the spring, whereas for the remainder of the year, excessive in situ respiration appears to account for the larger $\Delta\delta^{13}\text{C}_{\text{DIC}}$ in these two ecosystems. For the ecosystems dominated by 'Main Channel' waters, photosynthesis coupled with atmospheric exchange appears to have been the main reason for their smaller $\Delta\delta^{13}\text{C}_{\text{DIC}}$ values. Overall, the interplay of respiration, photosynthesis and atmospheric exchange is best described by biogeochemical classification of these ecosystems.

6.3 Biogeochemical classification of ecosystems

A biogeochemical parameter that can help to classify the ecosystems is the dissolved organic carbon (DOC). DOC is composed mainly of humic substances, carbohydrates and amino acids (Volk et al., 1997), originating either from decaying terrestrial material (cellulose and lignin etc.), or from aquatic algae, diatoms and animals whose basic building materials are hemicellulose, proteins and chitinous substances (Aiken, 1985). If coming from outside the system, DOC may be added by soil solutions, rain or groundwater. The latter two sources were shown to have minimal DOC concentrations (Schiff et al., 1990). Anthropogenic influences, such as input of sewage or industrial wastewaters, can also contribute to the DOC in aquatic systems. This may be the case for the 'Hoople Creek' with its peak concentrations of 38.3 mg/L, since even streams that drain swamps and wetlands do not show DOC concentrations higher than 25 mg/L (Thurman, 1985). On the other hand, DOC of soil solutions can be as high as 105 ± 31 mg/L (Christ and David, 1994), so that these elevated DOC concentrations in 'Hoople Creek' may indicate a soil water dominated system. Additional sources of DOC are

leaching of plant material (macrophytes and phytoplankton) within the system. Generally, DOC is a food source for bacteria and enhances respiration, thereby increasing the $p\text{CO}_2$ and decreasing the $\delta^{13}\text{C}_{\text{DIC}}$ in aqueous systems. Another mechanism that decreases DOC, while having the same effect on the $\delta^{13}\text{C}_{\text{DIC}}$, would be the photo production of CO_2 , an effect that has recently caused many discussions, because it is linked to increased penetration of UV-B radiation (e.g. Scully and Lean 1994, Schindler et al. 1996, Lindel, 1996). Consideration of DOC and $\delta^{13}\text{C}_{\text{DIC}}$ signals may enable the grouping of ecosystems according to their decomposition of DOC (Fig. 6.8).

In such a perspective, the 'Hoople Creek' has the highest DOC and lowest $\delta^{13}\text{C}_{\text{DIC}}$ values, while the 'Main Channel' and its related ecosystems show the opposite characteristics. The ecosystems 'Cooper Marsh', 'Hoople Bay' and the embayment at 'Long Sault Island' lie between these two end members, with DOC concentrations ranging between 2.6 and 17.3 mg/L and $\delta^{13}\text{C}_{\text{DIC}}$ values as low as -12.3 ‰ VPDB. This trend may indicate mixing between the 'Main Channel' with low DOC concentration and a $\delta^{13}\text{C}_{\text{DIC}}$ composition of around 0 ‰ and near-shore ecosystems with higher DOC and lower $\delta^{13}\text{C}_{\text{DIC}}$ compositions. However, the decomposition of DOC may further decrease the $\delta^{13}\text{C}_{\text{DIC}}$ composition in near-shore sampling stations.

In order to elucidate the origin of the role of DOC on the $\delta^{13}\text{C}_{\text{DIC}}$ composition, temporal variations of these two parameters must be considered as well (Fig. 6.9). Decomposition of the DOC produces CO_2 with a fairly negative isotopic composition (~ -27 ‰). The isotopically depleted CO_2 is then incorporated into the DIC pool thus yielding more negative $\delta^{13}\text{C}_{\text{DIC}}$ values. This may be the reason for even more negative $\delta^{13}\text{C}_{\text{DIC}}$

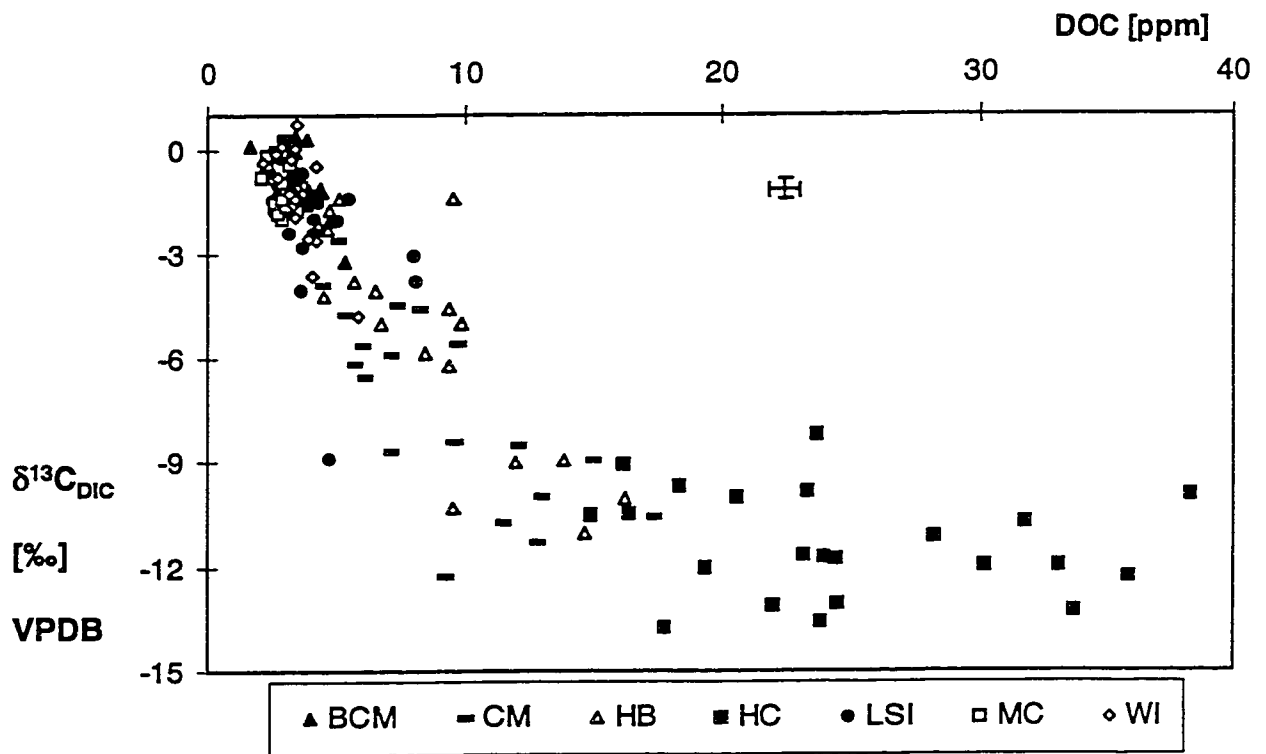


Fig. 6.8 Correlation between DOC and $\delta^{13}\text{C}_{\text{DIC}}$. The abbreviations of the ecosystems are the same as in Fig.6.3.

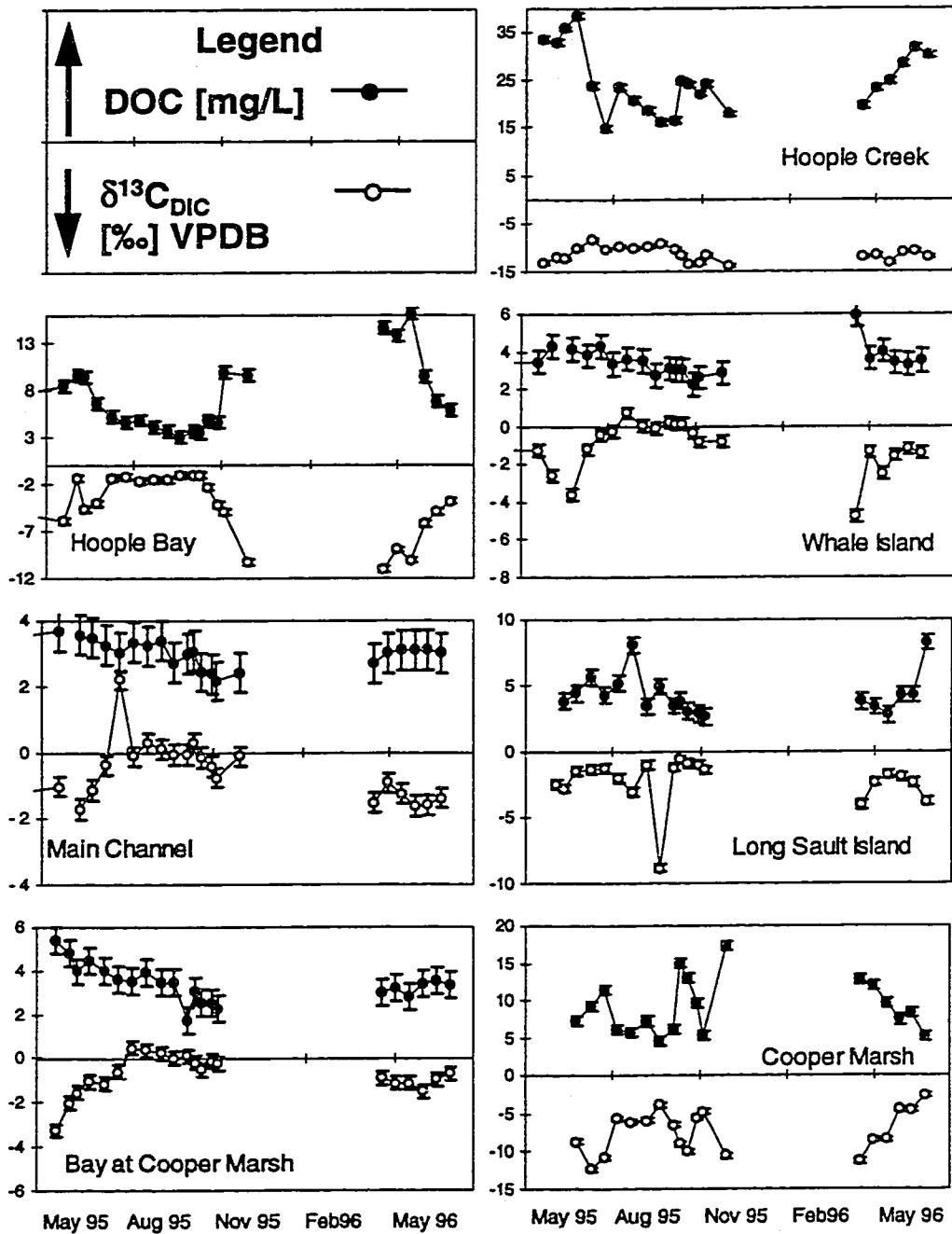


Fig. 6.9 Temporal variations of the $\delta^{13}\text{C}_{\text{DIC}}$ and DOC signals in the ecosystems studied.

In some ecosystems ('Hoople Creek', 'Long Sault Island', 'Bay at Cooper Marsh') the DOC concentrations are higher during the warm seasons, indicating either a stronger influence of soil water and/or in situ leaching of organic material. This fresh DOC is readily decomposed into CO₂ by either photo decomposition or respiration (Schiff et al. 1997), and it is therefore not surprising that the $\delta^{13}\text{C}_{\text{DIC}}$ becomes more negative. The same sampling stations show smaller DOC concentrations during the cold season, likely a result of increasing influx of groundwater.

The advected low concentration DOC is older and consists of fractions that are much more difficult to decompose (Schiff et al 1997) consequently leading to less negative $\delta^{13}\text{C}_{\text{DIC}}$ compositions. The 'Main Channel' and 'Whale Island' sampling stations, with DOC concentrations as low as 2.2 mg/L, mimic these temporal trends with much smaller amplitudes. Again, this is due to the influence of the Great Lakes, where DOC concentrations never exceed peak values of 6 mg/L (Eadie et al., 1990) and the $\delta^{13}\text{C}_{\text{DIC}}$ signal approaches 0 ‰ VPDB (Weiler and Nriagu, 1978). Compared to the above, the 'Hoople Bay' and 'Cooper Marsh' sampling stations have opposite DOC characteristics with low concentrations in the warm season and higher concentrations in the cold season (Fig. 6.9). In the fall this is likely a result of leaching of dying plant material, while in the spring higher influx of DOC enriched soil solutions may increase the DOC. Again the $\delta^{13}\text{C}_{\text{DIC}}$ compositions are more negative when the DOC is high, indicating that decomposition of fresh organic material influences the carbon cycle. In general the $\delta^{13}\text{C}_{\text{DIC}}$ response to the DOC concentrations shows that at fresh DOC is in part incorporated into the DIC pool, indicating that the river system does not only transport carbon but also actively recycles it. Evidently, the latter is more active in near-shore ecosystems.

A ternary plot combines the three most important parameters, 'respiration and decomposition of organic material', 'photosynthesis' and 'CO₂ exchange with the atmosphere', into a single picture (Fig. 6.10). In this projection, the length of the side is normalized to 100 % for a given end-member. The upper corner of the plot represents the end member 'respiration', with the most negative $\delta^{13}\text{C}_{\text{DIC}}$ readings, the highest DOC and the lowest chl-a concentrations.

As expected, the 'Hoople Creek' and cold season 'Cooper Marsh' and 'Hoople Bay' samples tend to assemble in this corner. The end member 'exchange with the atmosphere' occupies the lower right corner of the diagram and is characterized by the most positive $\delta^{13}\text{C}_{\text{DIC}}$ values, low chl-a and low DOC concentrations. The 'Main Channel' and 'Whale Island' ecosystems and the warm season 'Bay at Cooper Marsh', 'Hoople Bay' and 'Cooper Marsh' samples tend towards this end member. In contrast to the above two end members, photosynthesis-dominated ecosystems, although characterized by high chl-a and low DOC concentrations, may have variable $\delta^{13}\text{C}_{\text{DIC}}$ signals that reflect the degree of photosynthetic removal of ¹²C. Photosynthesis dominated ecosystems therefore plot across the lower part of the ternary diagram. The embayments 'Hoople Bay' and 'Long Sault Island' and, at times, the 'Cooper Marsh' belong to this group. It is in these ecosystems that the carbon cycle is most active, with a balanced interaction of respiration and photosynthesis (hence intermediate $\delta^{13}\text{C}_{\text{DIC}}$ signals).

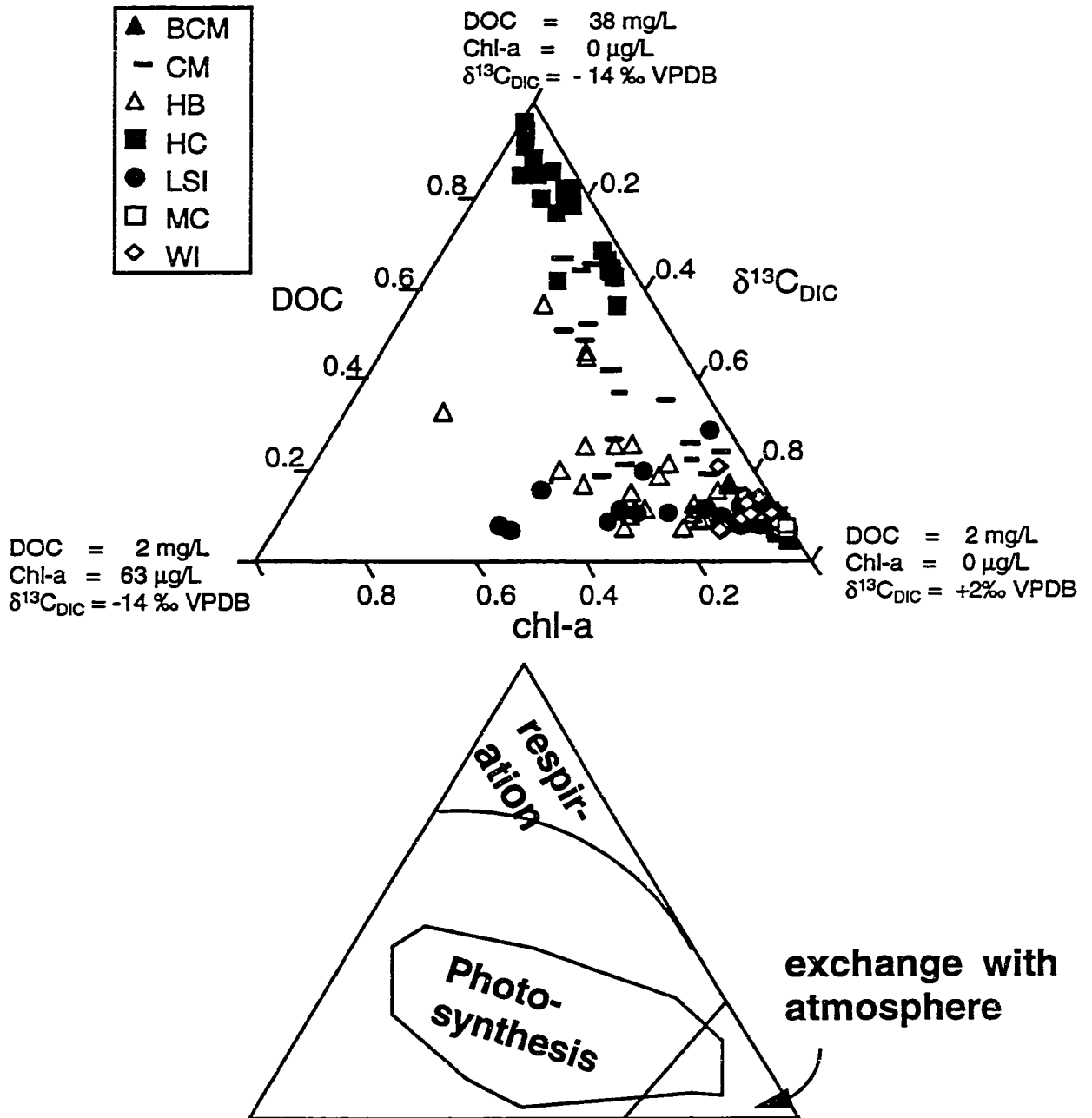


Fig. 6.10 Ternary plot of relative proportions of the DOC, $\delta^{13}C_{DIC}$ and chl-a. The associated end member processes are outlined in the bottom triangle. The abbreviations for the ecosystems are the same as in Fig.6.3.

6.4 Origin of particulate organic carbon in the upper St. Lawrence: Isotopic constraints

The study of organic carbon in rivers provides important information on the recycling of continental carbon (Ludwig et al., 1996). Riverine particulate organic carbon (POC) consists partly of detrital compounds, but can also be a product of in situ phytoplanktonic activity (Mook and Tan, 1991). Understanding the extent of in situ production of POC is essential, because it influences the aqueous carbon cycle by consuming dissolved inorganic carbon (DIC).

For the St. Lawrence River, the particulate organic carbon (POC) has been studied in detail, but only in the estuary (Pocklington, 1985; Pocklington and Tan, 1987; Tan and Strain, 1983; Lucotte, 1989; Lucotte et al. 1991). In these studies, the nature of the upstream riverine POC was conjectured to be mainly of terrestrial origin and to have isotopic compositions between -24.1 and -27 ‰. As yet no measurements on the isotopic composition of the upper St. Lawrence POC pool have been available. The present study provides the first overview of this parameter from a monitoring of seven aquatic ecosystems near the city of Cornwall (Ontario, Canada), ~150 km upstream of Montréal (Fig. 6.11). The ecosystems studied include the center of the St. Lawrence River ('Main Channel'), several of its embayments ('Bay at Cooper Marsh', 'Long Sault Island', 'Whale Island' and 'Hoople Bay'), a creek that drains into the St. Lawrence ('Hoople Creek') and a wetland ('Cooper Marsh').

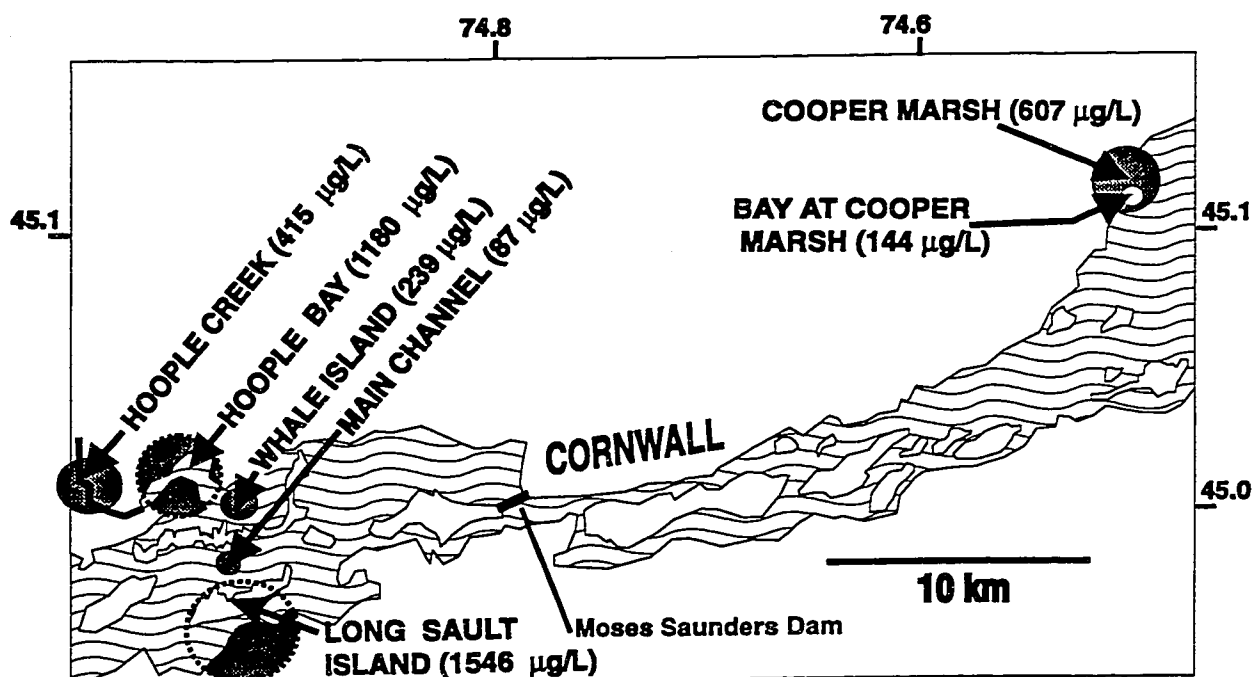


Fig. 6.11 Location map of the study area. Circles are proportional to the annual average concentrations of particulate organic carbon in the ecosystems studied.

The objectives of this research were:

- 1) to evaluate the relative importance of phytoplanktonic POC production versus detrital influx, seasonally and spatially, among the studied ecosystems; and
- 2) to test the proposition, based on estuarine studies, that the St. Lawrence is characterized by detrital POC.

The St. Lawrence is particularly suitable for this type of study, because its average discharge of 4×10^6 tonnes of suspended sediments per year ranks lowest among the major world rivers (Gleick, 1993). For comparison, the Mississippi has an average suspended load of 210×10^6 t/yr (Gleick, 1993). The low suspended sediment load of the St. Lawrence River implies small POC concentrations, minimizing the masking effect of the usually large allochthonous component on the overall balance of the riverine POC.

Our study area is typical of the upstream parts of the St. Lawrence River, because at this point the water originates directly from Lake Ontario without any influence from tributaries. As a result, the 'Main Channel' sampling station is characterized by well mixed POC from the Great Lakes and can thus serve as a baseline for comparison with the other ecosystems studied.

6.4.1 Results

The measured POC and chl-a concentrations range from 64 to 2663 and 0.3 to 26.1 $\mu\text{g/L}$, respectively (Appendix 5.2A). Samples with high chl-a concentrations also have high POC contents, with the 'Main Channel' waters representing the lowest

endmember and the 'Hoople Bay' and 'Long Sault Island' embayments having values up to an order of magnitude higher (Fig. 6.12). The waters of 'Hoople Creek', 'Whale Island', 'Bay at Cooper Marsh' and 'Cooper Marsh' are intermediate between the 'Main Channel' and the embayments in terms of their POC and chl-a levels.

The isotopic compositions of the POC ($\delta^{13}\text{C}_{\text{POC}}$) range from -31.5 to -16.3 ‰, while those of the dissolved inorganic carbon ($\delta^{13}\text{C}_{\text{DIC}}$) range between -13.7 and +0.3 ‰ (Appendix 5.2A). Although these two parameters yield only a somewhat diffuse spatial pattern, the samples from the 'Hoople Creek' and 'Cooper Marsh' ecosystems show the most negative $\delta^{13}\text{C}_{\text{POC}}$ and $\delta^{13}\text{C}_{\text{DIC}}$ values, indicating that these parameters are somewhat correlated (Appendix 5.2A).

The $\text{CO}_2(\text{aq})$ activities of most water samples scatter around a mean of 20 μM , reflecting the fact that the 'Main Channel' provides the bulk of the water to most of the studied ecosystems. Only the near-shore ecosystems 'Hoople Creek', 'Hoople Bay' and 'Cooper Marsh' deviated from this mean, reaching peak $\text{CO}_2(\text{aq})$ activities of 385 μM (Appendix 5.2A), an observation that will become important during the discussion of isotope discrimination between $\text{CO}_2(\text{aq})$ and phytoplanktonic POC.

6.4.2 Discussion

6.4.2.1 Sources of particulate organic carbon

Particulate organic carbon represents a variable mixture of living and dead phytoplankton and other components, such as detritus, bacteria and

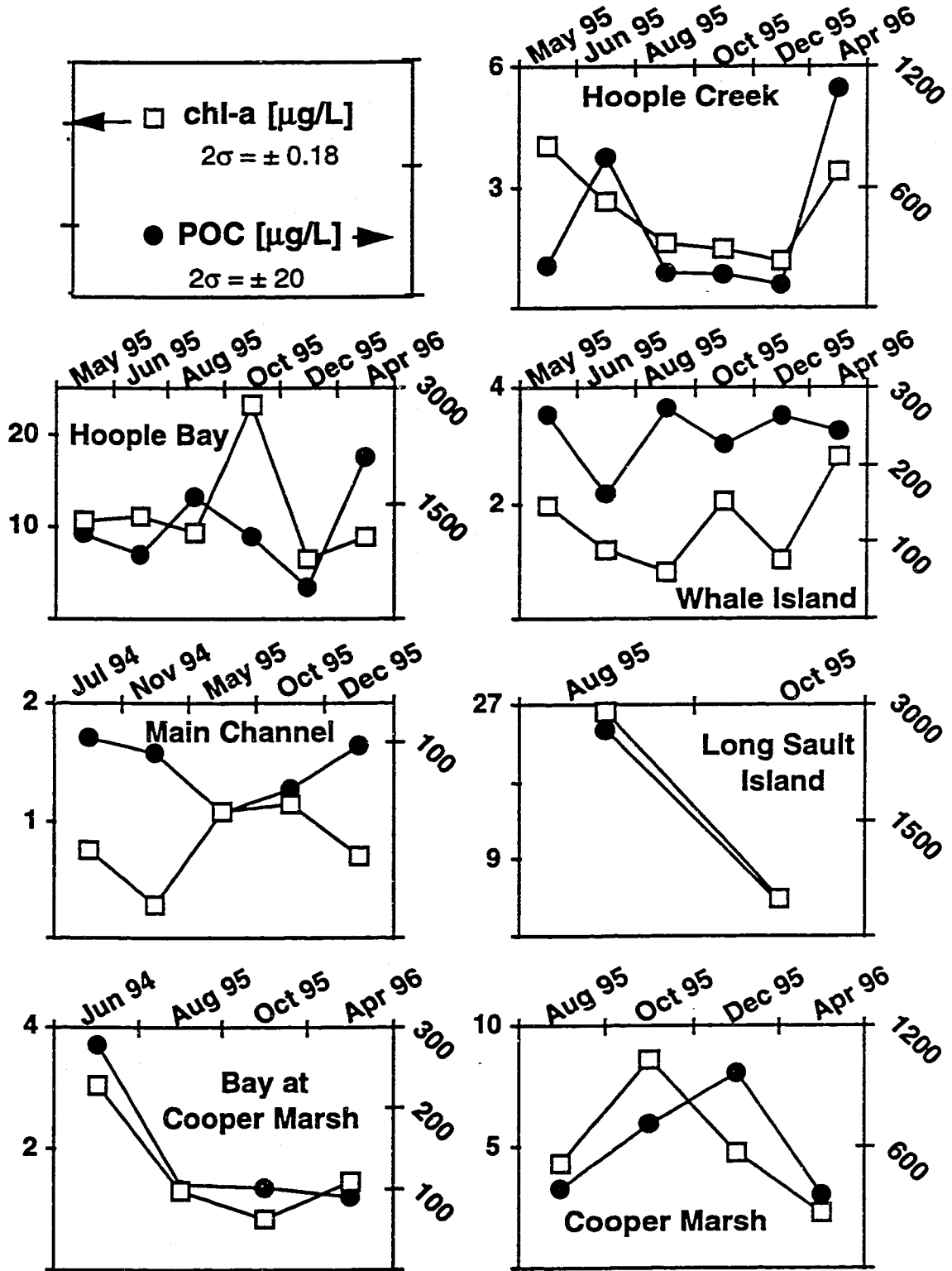


Fig. 6.12 Temporal distributions of chlorophyll-a contents and particulate organic carbon concentrations in the seven ecosystems studied.

zooplankton (Fogel, and Cifuentes, 1993; Fry and Sherr, 1984). Among all these components the major sources of riverine POC are (1) detrital matter, and (2) in situ produced phytoplankton. The latter changes the aqueous CO₂ content and the ¹³C/¹²C ratio of dissolved inorganic carbon and therefore can significantly influence the riverine carbon cycle. Although the proportion of phytoplankton in the POC pool is not easily quantified, it can be approximated by chl-a measurements on the suspended matter.

Seasonal variations of chl-a and POC contents that are specific to each ecosystem (Fig. 6.12) can yield insight into POC generation, because phytoplanktonic production should result in high POC contents during warm seasons (May to October). In contrast, cold season POC (November to April) should be dominated by allochthonous detrital material. We shall discuss the studied ecosystems in a traverse across the river from 'Hoople Creek' to 'Hoople Bay', 'Whale Island', 'Main Channel' and finally the embayment at 'Long Sault Island' (Fig. 6.11). The ecosystems 'Bay at Cooper Marsh' and 'Cooper Marsh' are described separately, since they are located 20 km further downstream.

The 'Hoople Creek' ecosystem shows two peak POC values in June 1995 and April 1996 (Fig. 6.12). These may be a consequence of either higher terrestrial runoff or of higher pelagic phytoplanktonic activity. The latter derives some support from concomitant high chl-a values, but both processes may have been involved, because the creek also receives input of terrestrial material, such as plant litter.

The isolated embayments of 'Hoople Bay' and 'Long Sault Island' derive the bulk of their elevated POC contents from pelagic algal activities, as indicated by their high chl-a concentrations (Fig. 6.12). Nevertheless, a subordinate terrestrial input cannot be entirely ruled out, because of their proximity to land. Furthermore, re-suspension of loosely

layered, organic rich bottom sediments, particularly during storm events, may be responsible for some of the POC peaks not supported by chl-a.

Higher flow velocities combined with low nutrient levels, as well as a larger distance from the shoreline may cause the generally low POC and chl-a levels in the 'Main Channel' (Fig. 6.12). Its POC concentrations in November 1994 and December 1995, when active photosynthesis must have been minimal, do not differ significantly from the warm-season values. This either means that most of this POC is of allochthonous origin, or that there is a constant low supply of phytoplanktonic POC from the Great Lakes. The latter scenario implies that, during the cold season, chl-a and POC are residual from the summer and arrive from the Great Lakes with some time delay. Essentially the same waters also dominate the 'Whale Island' and 'Bay at Cooper Marsh' ecosystems and, not surprisingly, their POC and chl-a characteristics are somewhat comparable to those of the 'Main Channel'.

The 'Cooper Marsh' seems to have higher POC concentrations due to terrestrial influences, particularly during cold seasons. During the warm season a portion of the POC likely is produced by situ photosynthetic activity, because POC and chl-a values move in parallel.

More frequent sampling may be required in order to decipher clearer seasonal patterns of chl-a and POC distributions. Nonetheless, their relative concentrations and temporal trends indicate that terrestrial organic matter dominates in near-shore ecosystems during cold seasons and storm surges. The in situ phytoplankton productivity is likely an important source for POC in the 'Hoop Bay', 'Long Sault Island' and 'Cooper Marsh' ecosystems, at least during the warm seasons. These tentative conclusions can be further

tested by isotopic techniques.

6.4.2.2 *Isotopic constraints*

Most $\delta^{13}\text{C}_{\text{POC}}$ values plot within the range of C_3 plants (-22 to -34 ‰; Vogel, 1993), thus indicating that this material contributes significant portions of the POC pool (Fig. 6.13). Both, allochthonous as well as in situ produced material can have this C_3 - $\delta^{13}\text{C}_{\text{POC}}$ composition (Fry and Sherr, 1984; Vogel, 1993), thus making a distinction between the two sources difficult. Deviations to more positive $\delta^{13}\text{C}_{\text{POC}}$ values (e.g. 'Whale Island', 'Long Sault Island', 'Bay at Cooper Marsh') indicate terrestrial influences, such as decomposition of lignin ($\delta^{13}\text{C}_{\text{POC}}$ ~-13 to -14 ‰; (Benner et al., 1987), or influx of detrital material from C_4 plants (-10 to -16 ‰; Vogel, 1983). The latter could originate from corn grown in the Cornwall area.

Although the $\delta^{13}\text{C}_{\text{POC}}$ compositions show no clear seasonal pattern, the POC/chl-a ratios of most samples are higher during the cold season (Fig. 6.13), thus indicating dominance of terrestrial material. Lower POC/chl-a ratios, typical for the warm season, on the other hand, are more indicative of photosynthetic activity when lower than 100 (Biggs, 1989; Søballe and Bachman, 1984). Nonetheless, exceptions to this pattern (i.e. warm season samples in the cold season field and vice versa) indicate that the POC budget in the study area is more complex.

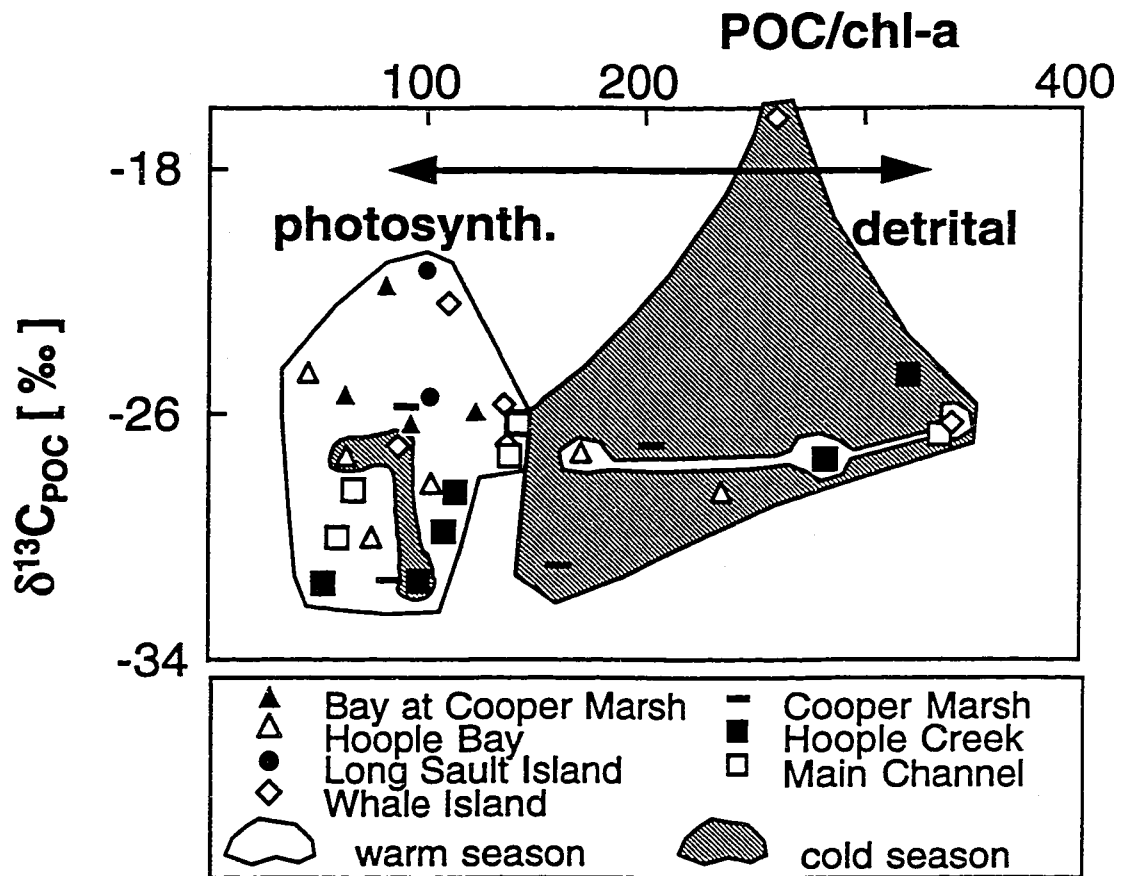


Fig. 6.13 POC/chl-a ratio versus $\delta^{13}\text{C}_{\text{POC}}$. The samples underlain by grey are from the cold season (November to April), while the samples underlain by white are from the warm season (May to October).

For example, the relatively low POC/chl-a ratios of most warm season 'Main Channel' data may hint at algal production as the source of POC, but higher ratios can be caused by infrequent flushing of detrital POC from the near-shore ecosystems that contain little chl-a. It is more difficult to explain the cold season samples with a low POC/chl-a ratio as perhaps containing residual amounts of chl-a or reflecting some contemporaneous algal activity. Note that, particularly in shallow water near-shore ecosystems, lower POC/chl-a ratios do not necessarily indicate phytoplanktonic POC generation, as chl-a containing plant debris from macrophytes may have lowered this ratio. The isotopic discrimination between POC and DIC may help to further elucidate the origin of the POC.

During photosynthesis, aquatic plants utilize aqueous CO_2 , a process that preferentially removes ^{12}C from the dissolved inorganic carbon pool. This mechanism explains the isotopic discrimination between DIC and phytoplankton (Fry and Sherr, 1984). The isotopic composition of POC ($\delta^{13}\text{C}_{\text{POC}}$), if resulting from algal photosynthetic activity, should therefore reflect that of DIC ($\delta^{13}\text{C}_{\text{DIC}}$), but at a more negative level. Based on this reasoning, the $\delta^{13}\text{C}_{\text{DIC}}$ and $\delta^{13}\text{C}_{\text{POC}}$ values should track each other. In general, the temporal $\delta^{13}\text{C}_{\text{POC}}$ and $\delta^{13}\text{C}_{\text{DIC}}$ curves for the seven ecosystems move in parallel, indicating some degree of participation of algal photosynthetic activity in the POC production (Fig. 6.14). Some $\delta^{13}\text{C}_{\text{POC}}$ peaks that do not have $\delta^{13}\text{C}_{\text{DIC}}$ counterparts are likely due to the influx of isotopically variable material, thus blurring the covariance.

The degree of isotopic discrimination between DIC and POC may therefore be useful in constraining the relative proportion of POC that originates from in situ photosynthetic activity as opposed to allochthonous detrital material in a given ecosystem and season.

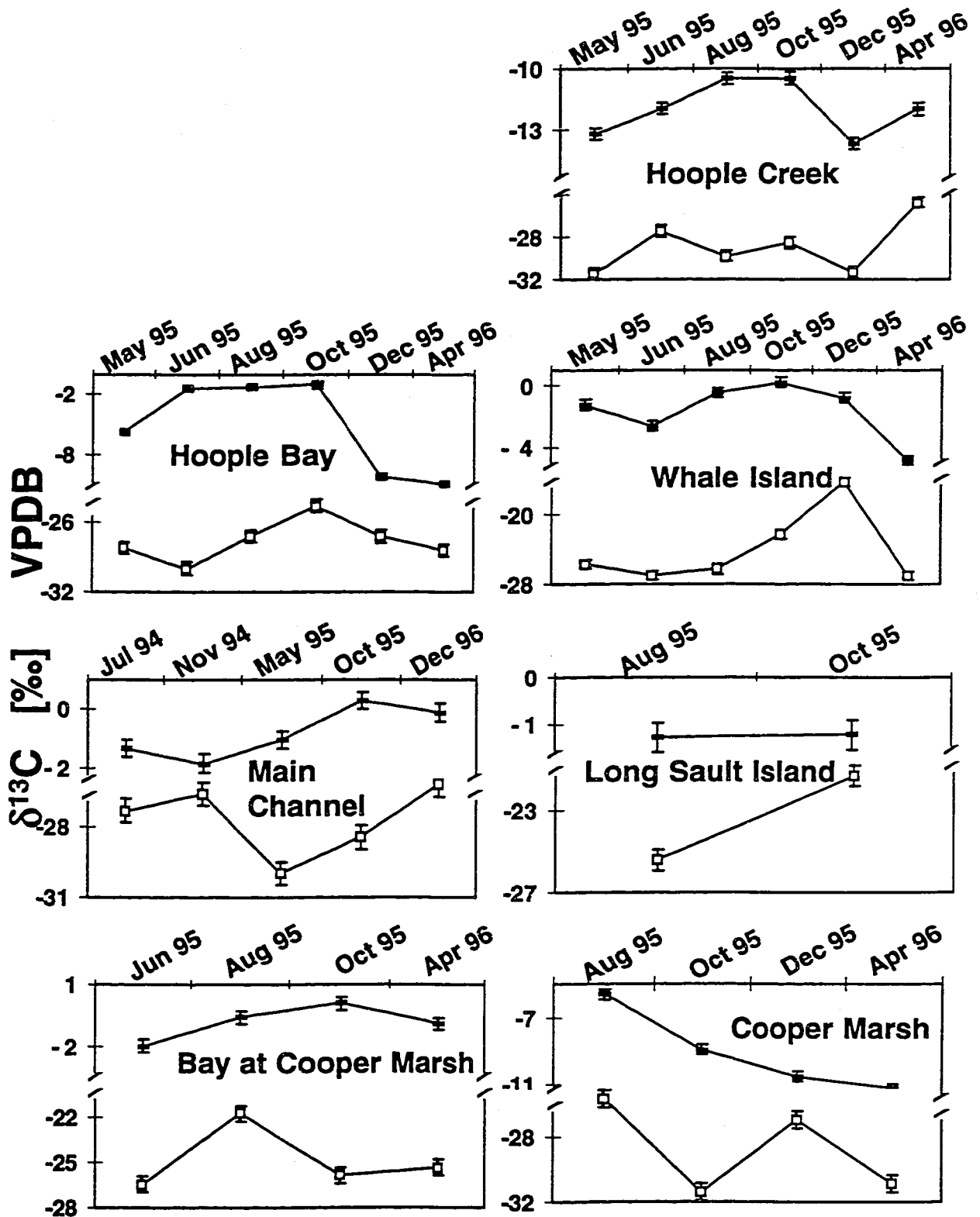


Fig. 6.14 Temporal variations of the $\delta^{13}\text{C}_{\text{DIC}}$ (upper curves) and $\delta^{13}\text{C}_{\text{POC}}$ (lower curves) in the seven ecosystems studied.

Theoretical considerations of carbon isotope fractionation by phytoplankton can perhaps further help with this task.

6.4.2.3 *Theoretical fractionation by algae*

Theoretically, carbon isotope fractionation by algae can be divided into two principal components: (1) aqueous diffusion of CO₂, and (2) enzymatic carboxylation reaction during carbon fixation (Vogel, 1993). The diffusion of CO₂ within water (ϵ_d) results in fractionation of 0.7 ‰ (O'Leary, 1984), whereas the enzymatic fractionation (ϵ_f) is caused by a catalyst known as Ribulose 1,5-bisphosphate carboxylase/oxygenase (RuBisCO) and has been described with values between 20 and 29 ‰ (Goericke et al., 1994; Wong et al., 1979; Roeske and O'Leary, 1984). For the subsequent modeling approach, we select an intermediate value of 25 ‰ for the latter process.

The fractionation of 0.7 ‰ occurs when low CO₂ concentrations are rate limiting during photosynthesis, causing utilization of all available CO₂ (¹²CO₂ and ¹³CO₂) and turning the carbon fixation by RuBisCO into a non-selective process. In contrast, at higher CO₂ concentrations, the isotopic fractionation is dominated by RuBisCO carbon fixation and approaches 25 ‰. One can therefore expect the phytoplanktonic carbon to be more negative (by 0.7 to 25 ‰) than CO₂(aq), depending on the activity of the latter. With respect to the phytoplanktonic growth rate, μ , this fractionation can be modeled utilizing the approach of Rau et al. (1996). Note that this model was developed for marine systems, but its application to freshwater systems is possible by modifying the relevant equation (Appendix 5.2.A). In order to use the model, the isotopic enrichment factor, ϵ , between the two reservoirs has to be defined.

$$\epsilon_{A-B} = [\alpha_{A-B} - 1] * 1000 = \left(\frac{1000 + \delta_A}{1000 + \delta_B} - 1 \right) * 1000 \approx \delta_A - \delta_B \quad \text{Clark and Fritz (1997)}$$

where α_{A-B} is the equilibrium isotopic fractionation factor and the subscripts A and B correspond to the isotopic composition of $\text{CO}_2(\text{aq})$ and the phytoplanktonic POC, respectively.

The isotopic enrichment factor between $\text{CO}_2(\text{aq})$ and phytoplanktonic POC ($\epsilon_{\text{CO}_2(\text{aq})\text{-POC}}$) varies with the growth rate, μ , over the range of the cell external $\text{CO}_2(\text{aq})$ concentration, C_e (Fig. 6.15). Most samples plot between the theoretically expected growth rates of 0.5 to 2, with some samples from near shore ecosystems ('Hoople Creek', 'Cooper Marsh', 'Hoople Bay', 'Whale Island' and 'Long Sault Island') plotting beyond this range. The latter are samples from ecosystems with elevated POC and chl-a concentrations (Fig. 6.12) and can plot into both, the 'photosynthetic' and 'detrital' fields in Fig. 6.13. For samples that plot in the photosynthetic field in Fig. 6.13, but do not conform to the given growth rates in Fig. 6.15 (i.e. 'Hoople Creek' and 'Cooper Marsh') two explanations may be given: (1) they derive their high chl-a contents from non-phytoplanktonic material (i.e. macrophytes) that does not fractionate according to the model.; (2) phytoplanktonic cells from these samples have a larger radius. For example increasing the radius from 10 μm to 50 μm , a still realistic proposition, would shift the isolines for the growth rate, μ , further to the right, causing all but six samples to conform to the model. The above considerations suggest that in the near-shore ecosystems both, enhanced in situ photosynthetic activity and allochthonous detrital input contribute at times to the elevated POC and chl-a values.

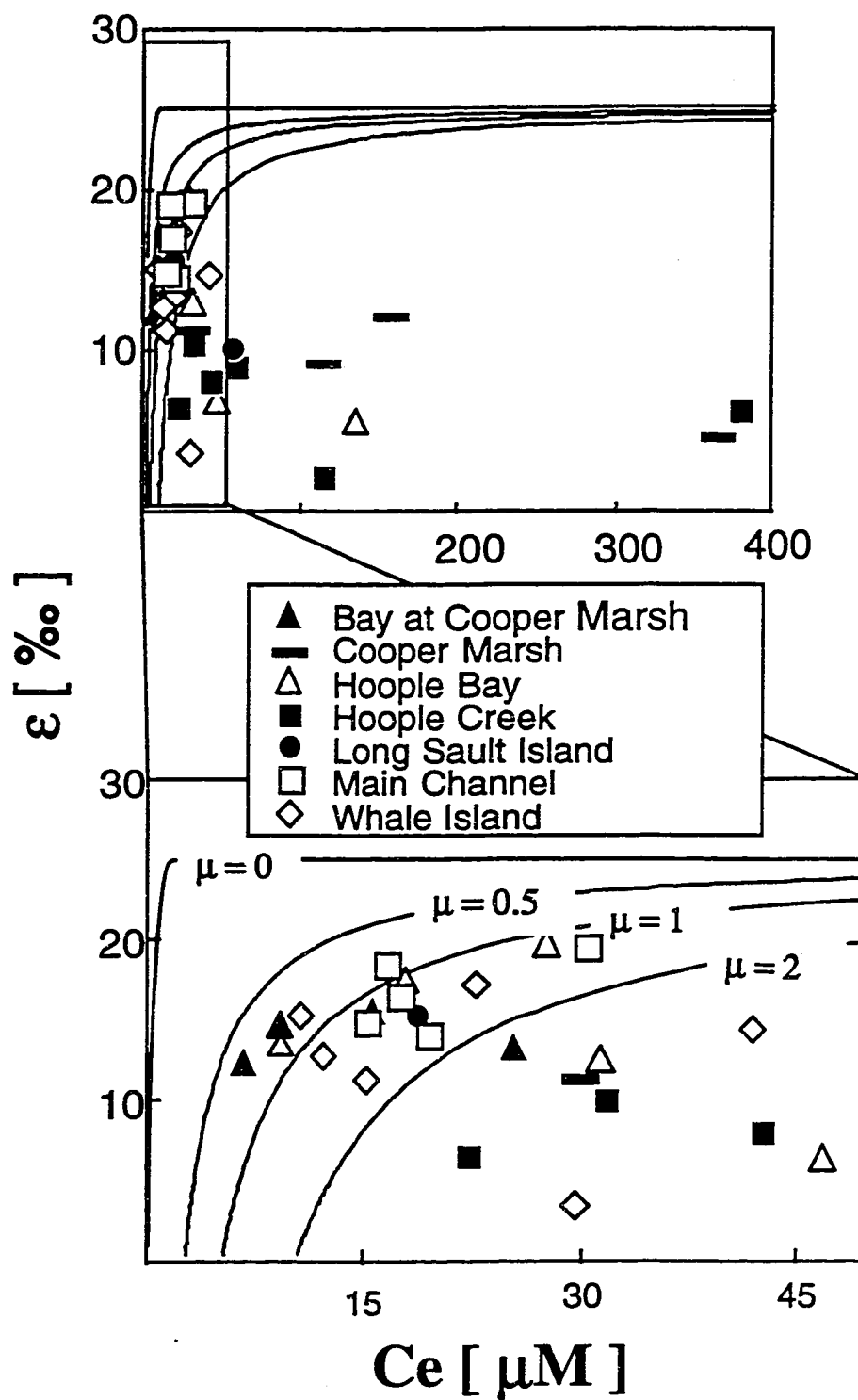


Fig. 6.15 Theoretical and measured fractionations, ε , between C_e ($= \text{CO}_2(\text{aq})$) and phytoplanktonic POC with varying growth rates, μ , following the model of Rau et al. (1996) (Appendix 5.2.B).

Note that the isotopic fractionation by diatoms exhibits a large scatter when plotted against the concentration of $\text{CO}_2(\text{aq})$ (Pancost et al., 1997). This may weaken the validity of the model, depending on the proportional amount of diatoms in the phytoplankton pool. Nevertheless, only insignificant amounts of diatoms were detected in the phytoplankton community of the 'Main Channel' in the Cornwall area (Hudon et al., 1996). Phytoplanktonic activity in the 'Main Channel' and related ecosystems ('Whale Island', 'Bay at Cooper Marsh', 'Long Sault Island') therefore likely conforms to the model by Rau et al. (1996). No estimates of the diatom proportions are available for the near-shore ecosystems ('Hoople Creek', 'Cooper Marsh' 'Long Sault Island'). If present, they also would cause the samples to plot in the photosynthetic field in Fig. 6.13, while deviating them from the model predictions in Fig.6.15.

This chapter has demonstrated that the peripheral ecosystems play an important role in the riverine carbon cycle. Compared to the 'Main Channel', these locations generally contain more organic and inorganic carbon and show much larger seasonal variations. If one takes the amount of carbon and its recycling as a measure of aquatic life, it is the near-shore locations, such as embayments, wetlands and creeks, that are the most active. Note, however, that the St. Lawrence may, in this respect, be an extreme example, because its 'Main Channel' waters are dominated by the Great Lakes that contain only small quantities of organic carbon (POC and DOC), thus enhancing the gradient between the main river and peripheral water masses.

Among the near-shore ecosystems, one can further differentiate between sites that are dominated by 'Main Channel' waters and by baseflow. The latter is important in the 'Hoople Creek', which receives most of its carbon from soil- and groundwaters, leading to high partial pressures of CO₂ and larger DOC contents. Ecosystems that are more influenced by the 'Main Channel' in many respects resemble the Great Lakes waters. Yet, some of the embayments, such as 'Hoople Bay', contain also the highest concentrations of particulate organic carbon, reflecting their importance for autochthonous POC generation.

7. Conclusions

The upper St. Lawrence River reflects the Great Lakes water masses, which are mixed homogeneously at Cornwall and appear with three typical characteristics that are caused by their long residence time in the lakes: (1) the water isotopic compositions ($\delta^{18}\text{O}_{\text{H}_2\text{O}}$, $\delta\text{D}_{\text{H}_2\text{O}}$) show clear signs of evaporation, (2) dissolved gases in the 'Main Channel' waters are equilibrated with the atmosphere, and (3) the waters are remarkably clear, due to sedimentation of large parts of the suspended load. Except for the sampling station 'Hoople Creek', these Great Lakes waters penetrate near-shore ecosystems at various degrees thus imposing their characteristics. Nevertheless, there is a considerable gradient between the 'Main Channel' and the near-shore ecosystems. Furthermore, substantial seasonal variations exist particularly in the near-shore ecosystems. It is obvious that the river does not only transport carbon, but also recycles it. Evidently this recycling is much more effective in near-shore ecosystems.

7.1 Water balance

The water isotopic composition proved to be useful conservative tracer for the estimate of mixing between the 'Main Channel' and near-shore ecosystems. Two principal water masses can be differentiated in the St. Lawrence River at Cornwall: (1) Great Lakes waters with average $\delta^{18}\text{O}_{\text{H}_2\text{O}}$ and $\delta\text{D}_{\text{H}_2\text{O}}$ isotopic compositions of -6.9 and -50 ‰, respectively, and (2) local baseflow with a typical $\delta^{18}\text{O}_{\text{H}_2\text{O}}$ signature of approximately -11 ‰. This revealed the following constraints:

- The 'Main Channel' is the dominant water body and carries essentially Great Lakes waters.
- Between 47 and 89 % of the water in 'Hoople Bay' originated from the 'Main Channel' during most of the sampling period. Only during spring, contributions of local waters (creek and baseflow) made up approximately 140 % in the 'Hoople Bay' sampling station, thus creating a strong outflow towards the 'Main Channel'.
- Similar local influences with even stronger influences from the 'Main Channel' are possible in the 'Cooper Marsh' and the 'Long Sault Island' sampling station, but were not quantified.
- The 'Hoople Creek' is the only ecosystem that is influenced by local precipitation and baseflow year round. In the spring, its waters are fairly homogenous in their water isotopic composition and match the $\delta^{18}\text{O}_{\text{H}_2\text{O}}$ values of the local groundwater. Snow melt and spring precipitation may have further contributed to this homogenous signal. During summer and fall, the creek is more influenced by precipitation with a time delay of about 5 days. During this time the 'Hoople Creek' waters are also subject to surface water evaporation.
- Temperature correlates with the isotopic composition of precipitation at Cornwall, a fact that becomes evident after weighing the $\delta^{18}\text{O}_{\text{H}_2\text{O}}$ values by their precipitation amounts.
- The similarity of the Cornwall meteoric water line to those of Simcoe and Ottawa indicates that the atmospheric waters must be distributed fairly homogeneously over this triangle of sampling stations.

- The similarity of the deuterium excess values among these 3 stations supports the estimate of Gat et al. (1994) that during summer and fall 4.6 to 16 % of the atmospheric moisture is contributed by direct evaporation from the Great Lakes surface.

7.2 Major element and nutrient chemistry

Due to its well mixed and homogenous water masses, the 'Main Channel' at Cornwall proves to be excellent site for the evaluation of major ion contribution of the Great Lakes to the average world river flux. Furthermore, contributions by precipitation to the 'Main Channel' major ion flux proved to be significant, particularly for SO_4^{2-} and total inorganic nitrogen. Anthropogenic influences, such as road salting are difficult to quantify in the 'Main Channel', but clearly observable in the near-shore ecosystems. The main conclusions of the major ion chemistry chapter are:

- The main ions in the upper St. Lawrence River are Ca^{2+} and Mg^{2+} and bicarbonate.
- Except for K^+ and SiO_2 , the upper St. Lawrence River carries a higher major ion load than average world river water. For the elements Ca^{2+} , Mg^{2+} and HCO_3^- this likely results from limestone weathering in the catchment area, while elevated Cl^- and SO_4^{2-} may originate from anthropogenic sources.
- SiO_2 in the 'Main Channel' is reduced due to diatom activity, mainly in the Great Lakes.

- SO_4^{2-} added by precipitation over the Great Lakes-upper St. Lawrence watershed is mostly of anthropogenic origin and accounts for 31.2 % of the 'Main Channel' flux at Cornwall.
- Total inorganic nitrogen contributions by precipitation over the catchment area almost ten times larger than the flux in the St. Lawrence 'Main Channel', indicating that the Great Lakes-St. Lawrence system must act as a nitrogen sink.
- Road salting influences the 'Cooper Marsh' sampling station, as evidenced by enhanced Na^+ contents during winter. In the 'Main Channel', no such increases were observed, but they cannot be excluded for the December to April period, because the frozen river was not sampled.
- The non-seasonal fluctuating pattern of Na^+ and SO_4^{2-} concentrations in 'Hoople Creek' is indicative of anthropogenic inputs, such as leakage from septic tanks, industrial or household discharges.

7.3 Upper St. Lawrence River carbon cycle

Although comparatively small by their water volume, the peripheral ecosystems play a significant role in the riverine carbon cycle. These are the sites where most of the net primary productivity, with its interplay between photosynthesis and respiration, takes place. This is indicated by higher DOC, POC, pCO_2 , chlorophyll-a, and variable isotopic compositions of the dissolved inorganic carbon ($\delta^{13}\text{C}_{\text{DIC}}$) and particulate organic carbon ($\delta^{13}\text{C}_{\text{POC}}$). The monitoring of the riverine carbon cycle at Cornwall has shown that:

- The seven ecosystems studied have their own biogeochemical characteristics, caused by varying rates of baseflow, differing degrees of atmospheric equilibration and fluctuating ratios of respiration to photosynthesis.
- In the spectrum of carbon recycling, the 'Main Channel' is the atmospherically equilibrated end member due to the long residence time of water in the Great Lakes. At the opposite end, the 'Hoople Creek' ecosystem is dominated by a respiratory signal inherited from soil- and groundwater systems (baseflow) that control the water balance in the creek.
- The remaining five ecosystems ('Hoople Bay', 'Whale Island', 'Long Sault Island', 'Cooper Marsh', 'Bay at Cooper Marsh') rank between these two end members with in situ respiration and photosynthesis acting as important secondary processes on the riverine carbon cycle.
- Strong oxygen oversaturations observed at low phytoplanktonic levels, such as in 'Hoople Creek', 'Cooper Marsh', and 'Bay at Cooper Marsh', result from the activities of either macrophytes or periphyton. It is therefore important to include these two plant communities into biogeochemical considerations, particularly for shallow water ecosystems.
- The study of the isotopic composition of POC in representative ecosystems of the upper St. Lawrence has shown that its near-shore ecosystems have a wide range of $\delta^{13}\text{C}_{\text{POC}}$ values. Nevertheless, their direct contribution to the POC flux in the main river channel is relatively minor and relegated mainly to high water flushing during storm events.
- With two exceptions, the 'Main Channel' POC has $\delta^{13}\text{C}$ at $-27 \pm 3\text{‰}$, confirming the

interpolations from earlier estuarine studies, with most of this POC originating from phytoplanktonic activity, likely in the Great Lakes.

- Our findings indicate that elevated phytoplanktonic activity and detrital sources are both contributors of POC in the near-shore sampling stations ('Hoople Creek', 'Cooper Marsh', 'Hoople Bay', 'Long Sault Island' and 'Bay at Cooper Marsh'), the latter during cold seasons, storm surges and snow melt episodes and the former likely dominant during warm seasons.

All these results reflect the importance of near-shore ecosystems if we are to understand the biogeochemical dynamics of major river systems. Most riverine biological activity takes place in these peripheral locations that are therefore most vulnerable to environmental influences and changes.

References

- Aiken, G.R. 1985. Humic Substances in Soil, Sediment, and Water: Geochemistry, Isolation, and Characterization. Wiley.
- Allègre, C.J., Dupré, B., Négrel, P. and Gaillardet, J. 1996. Sr-Nd-Pb isotopes systematics in Amazon and Congo river systems. Constraints about erosion processes. *Chemical Geology*, 131: 93-112.
- Amiotte Suchet, P. and Probst, J.L. 1995. A global model for present-day atmospheric/soil CO₂ consumption by chemical erosion of continental rocks (GEM- CO₂). *Tellus*, 47B, 273-280.
- Back, W. 1961. Techniques for mapping hydrochemical facies. U.S. Geological Survey Professional Paper, 424-D: 380-382.
- Baer, A.J., Poole, W.H. and Sanford, B.V. 1971. Rivière Gatineau / MAP 1334 A, sheet 31. Geological Survey of Canada, scale 1 : 1 000 000.
- Bally, A.W. 1989. Phanerozoic Basins of North America. In: *The Geology of North America: An Overview* (eds. A.W. Bally and A.R. Palmer), Vol. A, pp. 397-446. The Geological Society of America.
- Barnett, P.J. 1991. Quaternary Geology of Ontario. In: *Geology of Ontario, Part 2* (eds. P.C. Thurston, H.R. Williams, R.H. Sutcliffe and G.M. Stott), Special Vol. 4, pp. 1011-1082. Ministry of Northern Development and Mines.
- Barth, J.A.C., Veizer, J. and Hall, G.E.M. 1996. Geochemical monitoring of the St. Lawrence River in the Cornwall area. Ecosystem recovery on the St. Lawrence. IREE Research Paper, 23. Institut for Research on Environment and Economy, University of Ottawa, Canada.
- Barth, J.A.C., Veizer, J. and Mayer, B. submitted. Sources and origin of particulate organic carbon and its relation to dissolved inorganic carbon in the upper St. Lawrence: Isotopic constraints. *Earth and Planetary Science Letters*.
- Barth, J.A.C. and Veizer, J. submitted. Carbon cycle in St. Lawrence aquatic ecosystems at Cornwall (Ontario), Canada: Annual monitoring. *Chemical Geology Special Issue 'The Global Carbon Cycle'*. (eds. J.L. Probst, H. Faure and J. Veizer).
- Benner, R., Fogel, M.L., Sprague, E.K. and Hodson, R.E. 1987. Depletion of ¹³C in lignin and its implications for stable carbon isotope studies. *Nature*, 329: 708-710.
- Bennett, G., Dressler, B.O. and Robertson, J.A. 1991. The Huronian Supergroup and associated intrusive rocks. In: *Geology of Ontario, Part 1* (eds. P.C. Thurston, H.R. Williams, R.H. Sutcliffe and G.M. Stott), Special Vol. 4, pp. 549-542. Ministry of Northern Development and Mines.

- Berner, E.K. and Berner, R.A. 1987. *The Global Water Cycle: Geochemistry and Environment*. Prentice-Hall.
- Berner, E.K. and Berner, R.A. 1996. *Global Environment: Water, Air, and Geochemical Cycles*. Prentice-Hall.
- Biggs, B.J.F. 1989. Biomonitoring of organic pollution using periphyton, South Branch, Canterbury, New Zealand. *New Zealand Journal of Marine and Freshwater Research*, 29, 263-274.
- Blackburn, C.E., Johns, G.W., Ayer, J. and Davis, D.W. 1991. Wabigoon Subprovince. In: *Geology of Ontario, Part 1* (eds. P.C. Thurston, H.R. Williams, R.H. Sutcliffe and G.M. Stott), Special Vol. 4, pp. 303-382. Ministry of Northern Development and Mines.
- Bolsenga, S.J. and Herdendorf, C.E. 1993. *Lake Erie and Lake St. Clair Handbook*. Wayne State University Press.
- Buhl, D., Neuser, R.D., Richter, D.K., Riedel, D., Roberts, B., Strauss, H. and Veizer, J. 1991. Nature and nurture: environmental isotope story of the river Rhine. *Naturwissenschaften*, 78: 337-346.
- Burgman, J.O., Calles, B. and Westman, F. 1987. Conclusions from a ten year study of oxygen-18 in precipitation and runoff in Sweden. In: *Isotope Techniques in Water Resources Development*, International Atomic Energy Agency; 1987; Vienna, Austria: pp. 579-590. International Atomic Energy (IAEA).
- Burnison, B.K. 1980. Modified dimethyl sulfoxide (DMSO) extraction for chlorophyll analysis of phytoplankton. *Canadian Journal of Fisheries and Aquatic Sciences*, 37: 729-733.
- Calmbach, L. 1995. *Hydrowin (Computer Program)*. Version: 3.0. Institut de Minéralogie BSFH2, 1050 Lausanne, Switzerland.
- Cameron, E.M., Hall, G.E.M., Veizer, J. and Krouse, H.R. 1995. Isotopic and elemental hydrochemistry of a major river system: Fraser River, British Columbia, Canada. *Chemical Geology (Isotope Geoscience Section)*, 122: 149-169.
- Canadian & World Encyclopedia 1997. (CD-ROM). McClelland & Stewart Inc.
- Cane, G. 1996a. General geology of the St. Lawrence Lowland. Ecosystem recovery on the St. Lawrence. IREE Research Paper, 2. Institut for Research on Environment and Economy, University of Ottawa, Canada.
- Cane, G. 1996b. Groundwater quality and contaminant pathways in the Raisin River agricultural watershed: susceptibility to groundwater contamination, Cornwall, Ontario. Ecosystem recovery on the St. Lawrence. IREE Research Paper, 18. Institut for Research on Environment and Economy, University of Ottawa, Canada.

Carignan, R., Lorrain, S. and Lum, K. 1994. A fifty-year record of pollution by nutrients, trace metals and organic chemicals in the St. Lawrence River. *Canadian Journal of Aquatic Science*, 51: 1088-1100.

Cerling, T.E. 1991. Carbon dioxide in the atmosphere; evidence from Cenozoic and Mesozoic Paleosols. *American Journal of Science*, 291: 377-400.

Charron, J.E. 1978. Hydrochemical study of groundwater flow in the interstream area between the Ottawa and St. Lawrence Rivers. Ottawa, Canada: Inland Waters Directorate, Water Resources Branch.

Christ, M. and David, M.B. 1994. Fractionation of dissolved organic carbon in soil water: Effects of extraction and storage methods. *Commun. Soil Sci. Plant Anal.*, 25, 3305-3319.

Clark, I.D. and Fritz, P. 1997. *Environmental Isotopes in Hydrogeology*. Lewis.

Clark, P. and Karrow, P.F. 1984. Late Pleistocene water bodies in the St. Lawrence Lowland, New York and regional correlations. *Geological Society of America, Bulletin*, 95: 805-830.

Cluis, D., Bourgeault, C., Laberge, C., Guimont, C. and Potvin, D. 1990. Analyse statistique des données de qualité de l'eau du fleuve Saint-Laurent (1978-1988) INRS-Eau pour Environnement Canada. Rapport scientifique 289. Direction des eaux intérieures, Région du Québec.

Comer, N.T. and McKendry, I.G. 1993. Observations and numerical modelling of Lake Ontario Breezes. *Atmosphere-Ocean*, 31: 481-499.

Compilation of EPA's Sampling and Analysis Methods 1996 (ed. L.H. Keith). Lewis.

Compton's Encyclopedia 1994. Compton's Interactive Encyclopedia (CD-ROM) / Webster's New World Dictionary, 3rd College Edition. Compton's New Media, Inc.

Craig, H. 1961. Isotopic variations in meteoric waters. *Science*, 133, 1833-1834.

Dansgaard, W. 1964. Stable isotopes in precipitation. *Tellus*, 16: 436-468.

Davis, J.C. 1986. *Statistics and Data Analysis in Geology*. Wiley.

Degens, E.T., Guillard, R.R.L., Sackette, W.M. and Hellebust, J.A. 1968. Metabolic fractionation of carbon isotopes in marine plankton. Temperature and respiration experiments. *Deep Sea Research*, 15: 1-9.

Degens, E.T., Kempe, S. and Richey, J. 1991. *Biogeochemistry of Major World Rivers*, SCOPE 42. Wiley.

- Désilets, L. and Langlois, C. 1989. Variabilité spatiale et saisonnière de la qualité de l'eau du fleuve Saint-Laurent. Environnement Canada. Direction des eaux intérieures, Région du Québec.
- Dionex 1992. DX-100 Ion Chromatograph with SRS Control Operator's Manual. Dionex Corporation.
- Dredge, L.A. and Cowan, W.R. 1989. Quaternary geology of the southwestern Canadian Shield. In: Chapter 3 of Quaternary Geology of Canada and Greenland (ed. R.J. Foulton), Vol. K-1, pp. 214-235. The Geological Society of America.
- Dreimanis, A. 1982. Genetic classification of tills and criteria for their differentiation. ETH Zurich, Progress report on activities 1977-1982. INQUA, Commission on Genesis and Lithology of Quaternary Deposits.
- Dreimanis, A. 1985. Till stratigraphy in the St. Lawrence Valley near Malone, New York: Revised glacial history and stratigraphic nomenclature: Discussion and Reply. Geological Society of America, Bulletin, 96: 155-156.
- Dressler, B.O., Gupta, V.K. and Muir, T.L. 1991. The Sudbury Structure. In: Geology of Ontario, Part 1 (eds. P.C. Thurston, H.R. Williams, R.H. Sutcliffe and G.M. Stott), Special Vol. 4, pp. 593-625. Ministry of Northern Development and Mines.
- Drever, J.I. 1988. The Geochemistry of Natural Waters. Prentice-Hall.
- Dyke, A.S., Vincent, J.S., Andrews, J.T., Dredge, L.A. and Cowan, W.R. 1989. Quaternary geology of the southwestern Canadian Shield. In: Chapter 3 of Quaternary Geology of Canada and Greenland. (ed. R.J. Foulton), Vol. K-1, pp. 178-189. The Geological Society of America.
- Eadie, B.J., Morehead N.R. and Landrum P.F. 1990. Three-phase partitioning of hydrophobic organic compounds in Great Lakes US- waters. Chemosphere, 20: 161-178.
- Easton, R.M. 1991. The Grenville Province and the proterozoic history of central and southern Ontario. In: Geology of Ontario, Part 2 (eds. P.C. Thurston, H.R. Williams, R.H. Sutcliffe and G.M. Stott), Special Vol. 4, pp. 715-886. Ministry of Northern Development and Mines.
- Edmond, J.M., Palmer, M.R., Measures, C.I., Grant, B. and Stallard, R.F. 1995. The fluvial geochemistry and denudation rate of the Guyana Shield in Venezuela, Colombia, Brazil. *Geochimica et Cosmochimica Acta*, 59: 3301-3325.
- Environment Canada 1992. Envirodat Water Quality Database. Canadian Inland Waters Directorate, Water Quality Branch.

Environment Canada 1994. Great Lakes precipitation network: A ten year data summary 1980-1989: Environment Canada. Great Lakes Studies Aquatic Environmental Quality Division, Environmental Conservation.

Epstein, S. and Mayeda, T. 1953. Variation of ^{18}O content from natural sources. *Geochimica et Cosmochimica Acta*, 4: 213-224.

Farquhar, G.D., O'Leary, M.H., Berry, J.H. 1982. On the relationship between carbon isotope discrimination and the intracellular carbon dioxide concentration in leaves. *Australian Journal of Plant Physiology*, 9: 121-137.

Farrand, W.R. and Bell, D.L. 1982. Quaternary Geology of Southern Michigan. State of Michigan Department of Natural Resources, scale 1 : 500,000.

Farvolden, R.N. and Cherry, J.A. 1988. St. Lawrence Lowland. In: *The Geology of North America: Hydrogeology* (eds. W. Back, J.S. Rosenheim and P.R. Saeber), Vol. O-2 , pp. 133-141. The Geological Society of America.

Faure, G. 1986. *Principles of Isotope Geology*. Wiley.

Fisher, J.H., Barratt, M.H., Droste, J.B. and Shaver, R.H. 1988. Michigan Basin. In: *The Geology of North America: Sedimentary Cover-North American Craton: U.S.* (ed. L.L. Sloss), Vol. D-2 , pp. 361-382. The Geological Society of America.

Flintrop, C., Hohlmann, B., Jasper, T., Korte, C., Podlaha, O.G., Scheele, S. and Veizer, J. 1996. Anatomy of pollution: rivers of North Rhine-Westphalia, Germany. *American Journal of Science*., 296: 55-98.

Fogel, M.L. and Cifuentes, L.A. 1993. Isotope fractionation during primary production. In: *Organic Geochemistry: Principles and Applications* (eds. M.H. Engel and S.A. Macko), pp. 73-98. Plenum Press.

Fritz, P., Cherry, J.A., Weyer, K.U. and Sklash, M.G. 1976. Storm runoff analyses using environmental isotopes and major ions. In: *Interpretation of Environmental Isotope and Hydrochemical Data in Groundwater Hydrology*, pp. 111-130. International Atomic Energy Agency (IAEA), Vienna, Austria.

Fritz, P., Drimmie, R.J., Frappe, S.K. and O'Shea, K.J. 1987. The isotopic composition of precipitation and groundwater in Canada. In: *Isotope Techniques in Water Resources Development*, International Atomic Energy Agency; 1987; Vienna, Austria: pp. 539-550. International Atomic Energy Agency (IAEA).

Fritz, P., Reardon, E.J., Barker, J., Brown, R.M., Cherry, J.A., Killey, R.W.D. and McNaughton, D. 1978. The carbon isotope geochemistry of a small groundwater system in northeastern Ontario. *Water Resources Research*, 14: 1059-1067.

- Fry, B. and Sherr, E.B. 1984. $\delta^{13}\text{C}$ measurements as indicators of carbon flow in marine and freshwater ecosystems. *Contributions in Marine Science*, 27: 13-47.
- Fullerton, D.S. 1980. Preliminary correlation of post-Erie interstadial events (16,000 to 10,000 radiocarbon years before present), central and eastern Great Lakes region, and Hudson, Champlain and St. Lawrence Lowlands, United States and Canada. Professional Paper 1089. United States Geological Survey.
- Fullerton, D.S. and Richmond, G.M. 1991. Quaternary geologic map of the Lake Erie 4°X6° Quadrangle / Quaternary Geologic Atlas of the United States. United States Geological Survey, scale 1: 1000,000.
- Gadd, N.R. 1986. Lithofacies of the Leda Clay in the Ottawa Basin of the Champlain Sea. Ottawa, Canada. Paper 85-21. Geological Survey of Canada.
- Gao, W. and Kempe, S. 1987. The Changjiang: its long-term changes in pCO_2 and carbonate mineral saturation. In: *Transport of Carbon and Minerals in Major World Rivers, Part 4* (eds. E.T. Degens, S. Kempe and W. Gan), SCOPE/UNEP, Vol. 64, pp. 207-216. *Mitteilungen aus dem Geologisch-Paläontologischen Institut der Universität Hamburg*.
- Garrels, R.M. 1976. A survey of low temperature water-mineral relations. In: *Interpretation of Environmental Isotope and Hydrochemical Data in Groundwater Hydrology*, pp. 65-84. International Atomic Energy Agency (IAEA).
- Garrels, R.M. and Mackenzie, F.T. 1971. *Evolution of Sedimentary Rocks*. W.W. Norton.
- Gat, J.R. 1996. Oxygen and hydrogen isotopes in the hydrologic cycle. *Annual Review of Earth and Planetary Science*, 24: 225-262.
- Gat, J.R., Bowser, C.J. and Kendall, C. 1994. The contribution of evaporation from the Great Lakes to the continental atmosphere: Estimate based on stable isotope data. *Geophysical Research Letters*, 21: 557-560.
- Gearing, J.N., Gearing, P.J., Rudnick, D.T., Requejo, A.D. and Hutchins, M.J. 1984. Isotopic variability of organic carbon in a phytoplankton-based temperate estuary. *Geochimica et Cosmochimica Acta*, 48: 1089-1098.
- Gibbs, R.J. 1970. Mechanisms controlling world water chemistry. *Science*, 170: 1088-1090.
- Gleick, P.H. 1993. *Water in Crisis: A Guide to the World's Fresh Water Resources*. Oxford University Press.
- Goericke, R., Montoya, J.P., Fry, B. 1994. Physiology of isotope fractionation in algae and cyanobacteria. In: *Stable Isotopes in Ecology* (eds. K. Lathja and B. Michener). Blackwell Scientific.

- Hach Company 1989. Company Manual, Model 44600 Conductivity / TDS Meter. Hach.
- Hach Company 1992. Digital Titrator Model 169001-01 Manual. Hach
- Hach Company 1993a. Spectrophotometer Handbook. Hach
- Hach Company 1993b. portable Hach one pH Meter Model 43800-00 Manual. Hach.
- Haeussler, E.F. (Jr.) and Paul, R.S. 1987. Introductory Mathematical Analysis. Prentice-Hall.
- Herczeg, A.L. and Fairbanks, R.I. 1987. Anomalous carbon isotope fractionation between atmospheric CO₂ and dissolved inorganic carbon induced by intense photosynthesis. *Geochimica et Cosmochim. Acta*, 51: 895-899.
- Hewitt, D.F. 1972. Palaeozoic geology of southern Ontario. Geological Report 105. Ottawa: Ministry of Natural Resources / Ontario Division of Mines.
- Hoffman, P.F. 1993. Precambrian geology and tectonic history of North America. In: *The Geology of North America-Overview* (eds. Bally A.W. and Palmer A.R.), Vol. A , pp. 447-513. The Geological Society of America.
- Hofmann, H.J. 1972 Stratigraphy of the Montreal area. XXIV International Geological Congress, Excursion B-03, 27-59.
- Holland, H.D. 1978. *The Chemistry of the Atmosphere and Oceans*. Wiley.
- Hope, D., Dawson, J.C.D., Cresser, M.S. and Billet, M.F. 1995. A method for measuring free CO₂ in upland streamwater using headspace analysis. *Journal of Hydrology*, 166: 1-14.
- Houghton, J. and Intergovernmental Panel on Climate Change. Working Group-1 1996. *Climate change 1995: The Science of Climate Change*. Cambridge University Press.
- Houle, D., Dupras, D. and Sylvestre, A. 1995. Évaluation et bilan du programme de la qualité de l'eau. Montréal: Centre Saint-Laurent / Environment Canada.
- Hudon, C., Paquet, S. and Jarry, V. 1996. Downstream variations of phytoplankton in the St. Lawrence River (Québec, Canada), *Hydrobiologia*, 337, 11-26.
- Illingworth, J.A. 1981. A common source of error in pH measurements. *Biochemical Journal*, 195: 259-262.
- Jackson, S.L. and Fyon, J.A. 1991. The western Abitibi Subprovince in Ontario. In: *Geology of Ontario, Part 1* (eds. P.C. Thurston, H.R. Williams, R.H. Sutcliffe and G.M. Stott), Special Vol. 4, pp. 405-482. Ministry of Northern Development and Mines.

- Jeffrey, S.W. and Humphrey, G.F. 1975. New spectrometric equations for determining chlorophylls a, b, c₁ and c₂ in equal amounts in higher plants, algae and natural phytoplankton. *Biochemie und Physiologie der Pflanzen (BPP)*, 167: 191-194.
- Johnson, M.D., Armstrong, D.K., Sanford, B.V., Telford, B.G. and Rutka, M.A. 1992. Paleozoic and Mesozoic Geology of Ontario. In: *Geology of Ontario, Part 2* (eds. P.C. Thurston, H.R. Williams, R.H. Sutcliffe and G.M. Stott), Special Vol. 4, pp. 907-1011. Ministry of Northern Development and Mines.
- Jouzel, J. and Merlivat, M. 1984. Deuterium and oxygen-18 in precipitation: Modelling of the isotopic effects during snow formation. *Journal of Geophysical Research*, 89: 11749-11757.
- Karrow, P.F. 1984. Quaternary stratigraphy and history, Great Lakes-St. Lawrence region. In: *Quaternary Stratigraphy of Canada-A Canadian Contribution to IGCP Project 24*, Geological Survey of Canada Paper 84-10, pp. 137-153.
- Keeling, R.F., Piper, C.P. and Heiman, M. 1996. Global and hemispheric CO₂ sinks deduced from changes in atmospheric O₂ concentration. *Nature*, 381: 218-221.
- Kempe, S. 1982. Long-term records of CO₂ pressure fluctuations in fresh water. In: *Transport of Carbon and Minerals in Major World Rivers, Part 1* (ed. E.T. Degens), SCOPE/UNEP Vol. 52, pp. 91-332. *Mitteilungen aus dem Geologischen-Paläontologischen Institut der Universität Hamburg*.
- Kendall, C., Sklash, M.G. and Bullen, T.D. 1995. Isotope tracers of water and solute sources in catchments. In: *Solute Modelling in Catchment Systems* (ed. S.T. Trudgill), pp. 261-303. Wiley.
- Kretz, R. 1985. Calculation and illustration of uncertainty in geochemical data analyses. *Journal of Geological Education*, 33: 40-44.
- Lamarche, A. 1992. Quality of water for direct human consumption. Assessment of St. Lawrence River water, Conwall-Île d'Orleans section, 1978 to 1988. Montréal: St. Lawrence Centre / Environment Canada.
- Lampert, W. and Sommer, U. 1997. *Limnoecology: The Ecology of Lakes and Streams*. Oxford University Press.
- Leopoldo, P.R., Martinez, J.C. and Moratti, J.C. 1992. Estimation using ¹⁸O of the water residence time in small watersheds. In: *Isotope Techniques in Water Resources Development 1991*, International Atomic Energy Agency, 1991, Vienna, Austria, pp. 75-84. International Atomic Energy (IAEA).
- Lindel, M. 1996. Effects of sunlight on organic matter and bacteria in lakes. Ph.D. thesis, Department of Ecology/Limnology, Lund University, Sweden.

Livingstone, D.A. 1963. Chemical composition of rivers and Lakes. U.S.G.S. Professional Paper no. 440G. United States Geological Survey.

Louvat, P. and Allègre, C. 1997. Present denudation rates on the island of Réunion determined by river geochemistry: Basalt weathering and mass budget between chemical and mechanical erosions. *Geochimica et Cosmochimica Acta*, 61: 3645-3669.

Lucas, W.J. 1983. Photosynthetic assimilation of exogeneous HCO_3^- by aquatic plants. *Annual Review of Plant Physiology*, 34: 71-104.

Lucotte, M. 1989. Organic carbon isotope ratios and implications for the maximum turbidity zone of the St. Lawrence upper estuary. *Estuarine Coastal and Shelf Science*, 29: 293-304.

Lucotte, M., Hillaire-Marcel, C. and Louchouart, P. 1991. First-order organic carbon budget in the St. Lawrence lower estuary from ^{13}C data. *Estuarine Coastal and Shelf Science*, 32: 297-312.

Ludwig, W., Probst, J.L. and Kempe, S. 1996. Predicting the oceanic input of organic carbon by continental erosion. *Global Biogeochemical Cycles*, 10: 23-41.

MacClintock, P. 1958. *Glacial Geology of the St. Lawrence Seaway and Power Project*. New York State Museum and Science Service.

Machavaram, M.V. and Krishnamurthy, R.V. 1995. Earth surface evaporative process: A case study from Great Lakes region of the United States based on deuterium excess in precipitation. *Geochimica et Cosmochimica Acta*, 59: 4279-4283.

Mc Gaha Miller, G. 1988. pH measurement problems solved. *American Laboratory News Edition #6088*.

Messier D., Legendre P., Delisle C.E., Bouchard M.A. 1990. Symposium on the Saint Lawrence-A River to be Reclaimed; Nov. 3 1989 à Montréal. Environment Canada, Centre Saint-Laurent.

Meybeck, M. 1979. Concentrations des eaux fluviales en éléments majeures et apports en solution aux océans. *Revue Dynamique de Géologie et de Géographie Physique*, 21: 215-246.

Meybeck, M. 1980. Pathways of major elements from land to ocean through rivers. In: *Proceedings of the Review and Workshop on River Inputs to Ocean Systems, 1980*; Rome, FAO (eds. United Nations Educational Scientific and Cultural Organization and United Nations Environment Program), pp. 18-30. UNEP/UNESCO.

Meybeck, M. 1984. *Les fleuves et les cycle géochimique des éléments*. Paris, France: Ph.D. thesis no 84-35. Université Pierre et Marie Curie, Paris 6, France.

- Meybeck, M. 1986. Composition chimique des ruisseaux non pollués de France. *Sci. Geo. Bull.*, 39: 3-77.
- Miller, J.C. and Miller, J.N. 1984. *Statistics for Analytical Chemistry*. Chichester.
- Mizutani, H. and Wada, E. 1982. Effect of high atmospheric CO₂ concentration on $\delta^{13}\text{C}$ of algae. *Origins Life*, 12: 377-390.
- Mook, W.G., Bommerson, J.C. and Staverman, W.H. 1974. Carbon isotope fractionation between dissolved bicarbonate and gaseous carbon dioxide. *Earth and Planetary Science Letters*, 22: 169-176.
- Mook, W.G. and Tan, F.C. 1991. Stable carbon isotopes in rivers and estuaries. In: *Biogeochemistry of Major World Rivers*. Scope 42 (eds. E.T. Degens, S. Kempe and J. Richey), pp. 245-264. Wiley.
- Morin, J., Boudreau, P. and Leclerc, M. 1994. Lac Saint-Francois: Les bases de la modélisation hydrodynamique. Ecosystem recovery on the St. Lawrence. IREE Research Paper, 1. Institut for Research on Environment and Economy, University of Ottawa, Canada.
- Négrel, P., Allègre, C.J., Dupré, B. and Lewin, E. 1993. Erosion sources determined by inversion of major and trace element ratios and strontium isotopic ratios in river water: The Congo River Case. *Earth and Planetary Science Letters*, 120: 59-76.
- National Atlas Information Service 1993. *The National Atlas of Canada / Canada Vegetation Cover*. Energy, Mines and Resources Canada.
- O'Leary, M.H. 1984. Measurement of the isotopic fractionation associated with diffusion of carbon dioxide in aqueous solution. *Journal of Physical Chemistry*, 88: 823-825.
- Ochietti, S. 1989. Quaternary geology of the St. Lawrence Valley and adjacent Appalachian subregion. In: Chapter 4 of *Quaternary Geology of Canada and Greenland* (ed. R.J. Foulton), Vol. K-1, pp. 350-389. The Geological Society of America.
- Ontario Geological Survey 1991. *Bedrock geology of Ontario, southern sheet / Map 2544*. Ontario Geological Survey, scale 1 : 1 000 000.
- Pancost, R.D., Freeman, K.H., Wakeham, S.G., Robertson, C.Y. 1997. Controls on carbon isotope fractionation by diatoms in the Peru upwelling region. *Geochimica et Cosmochimica Acta*, 61, 4983-4991.
- Pantony, D.A. 1961. *A Chemist's Introduction to Statistics, Theory of Error and Design of Experiment*. Lecture Series, 1961, No. 2. The Royal Institute of Chemistry, London.
- Pawellek, F. and Veizer, J. 1995. Carbon cycle in the upper Danube and its tributaries: $\delta^{13}\text{C}_{\text{DIC}}$ constraints. *Israel Journal of Earth Sciences.*, 43: 187-194.

- Payne, B.R. 1992. On the statistical treatment of environmental isotope data in hydrology. In: *Isotope Techniques in Water Resources Development 1991*, International Atomic Energy Agency; 1991 Mar 11-15, Vienna, Austria, pp. 273-290. International Atomic Energy (IAEA).
- Pearce, A.J., Stewart, M.K. and Sklash, M.K. 1986. Storm runoff generation in humid headwater catchments, 1. Where does the water come from? *Water Resources Research*, 22: 1263-1273.
- Percival, J.A. and Sullivan, R.W. 1988. Age constraints on the evolution of the Quetico Belt, Superior Province, Ontario. In: *Radiogenic and Isotopic Studies, report 2, Paper 88-2*, pp. 97-107. Geological Survey of Canada.
- Peterson, B.J. and Fry, B. 1989. Stable isotopes in ecosystems studies. *Annual Review of Ecology and Systematics*, 18: 293-320.
- Pocklington, R. 1985. The contribution of organic matter by the St. Lawrence River to the Gulf of the St. Lawrence, 1981-1983. In: *Transport of Carbon and Minerals in Major World Rivers, Part 3* (eds. E.T. Degens, S. Kempe and R. Herrera), SCOPE/UNEP Vol. 58, pp. 323-328. *Mitteilungen aus dem Geologisch-Paläontologischen Institut der Universität Hamburg*.
- Pocklington, R. and Tan, F.C. 1987. Seasonal and annual variations in the organic matter contributed by the St. Lawrence River to the Gulf of St. Lawrence. *Geochimica et Cosmochimica Acta*, 51: 2579-2586.
- Porter, S. 1996. Groundwater / surface water interaction in the Raisin River watershed near Cornwall, Ontario. M.Sc. Thesis. Department of Geology, University of Ottawa, Canada.
- Probst, J.L., Amiotte, S.P. and Tardy, Y. 1992. Global continental erosion and fluctuations of atmospheric CO₂ consumed during the last 100 years. In: *Proceedings of the 7th international symposium on water-rock interaction, Vol. 1, Low temperature environments. Proceedings-International Symposium on Water-Rock Interaction* (eds. Y.K. Kharaka and A.S. Maest), pp. 483-486.
- Quémerais, B., Lum, K. and Lemieux, C. 1996. Concentrations and transport of trace metals in the St. Lawrence River. *Aquatic Sciences*, 58: 52-68.
- Ramesh, R. and Anglejan, B. 1995. Mineralogy, chemistry and particle size interrelationships in some post-glacial marine deposits of the St. Lawrence Lowlands. *Journal of Coastal Research*, 11: 1167-1179.
- Rau, G. 1978. Carbon-13 depletion in a subalpine lake: Carbon flow implications. *Science*, 201: 901-902.

- Rau, G.H., Riebesell, U.H., Wolf-Gladrow, D. 1996. A model of photosynthetic ^{13}C fractionation by marine phytoplankton based on diffusible molecular CO_2 uptake. *Marine Ecology Progress Series*, 133, 275-285.
- Richmond, G.M. and Fullerton, D.S. 1983a. Quaternary geologic map of the Minneapolis 4°X6° Quadrangle / Quaternary Geologic Atlas of the United States. United States Geological Survey, scale 1: 1000,000.
- Richmond, G.M. and Fullerton, D.S. 1983b. Quaternary geologic map of the Chicago 4°X6° Quadrangle / Quaternary Geologic Atlas of the United States. United States Geological Survey, scale 1: 1000,000.
- Robin, M.J.L. 1996. Geological Data Analyses. Notes for GEO 3152. Department of Geology, University of Ottawa, Canada.
- Roeske, C.A. and O'Leary, M.H. 1984. Carbon isotope effect on carboxylation of ribulose biphosphate. *Biochemistry*, 23: 6275-6284.
- Rondeau, B. 1993. Qualité des eaux du fleuve Saint-Laurent 1985-1990, Tronçon Cornwall-Québec. Montréal: Centre Saint-Laurent / Environment Canada.
- Rust, B.R. 1977. Mass flow deposits in a Quaternary succession near Ottawa. Canada: Diagnostic criteria for subaqueous outwash. *Canadian Journal of Earth Sciences*, 14: 175-184.
- Salomons, W. and Mook, W. G. 1986. Isotope Geochemistry of Carbonates in the Weathering Zone. In: *Handbook of Environmental Isotope Geochemistry* (eds. P. Fritz and J. Ch. Fontes), Vol. 2. The Terrestrial Environment, pp. 239-269. Elsevier.
- Sanford, B.V. 1993. St. Lawrence Platform-Introduction. In: *The Geology of North America: Sedimentary Cover of the Craton in Canada* (eds. D.F. Stott and J.D. Aitken), Vol. D-1, pp. 725-786. The Geological Society of America.
- Schiff, S.L., Aravena, R., Trumbore, S.E., Dillon, P.J. 1990. Dissolved organic carbon cycling in forested watersheds: A carbon isotope approach. *Water Resources Research*, 12, 2949-2957.
- Schiff, S.L., Aravena, R., Trumbore, S.E., Hinton, M.J., Elgood, R. and Dillon, P.J. 1997. Export of DOC from forested catchments on the Precambrian Shield of Central Ontario: Clues from ^{13}C and ^{14}C . *Biogeochemistry*, 36: 43-65.
- Schindler, D.W., Jefferson Curtis, P., Parker, B.R., and Stainton 1996. Consequences of climate warming and lake acidification for UV-B penetration in North American boreal lakes. *Nature*, 379, 705-708.
- Scully, N.M. and Lean, D.R.S. 1994. The attenuation of ultraviolet radiation in temperate lakes. *Arch. Beih. Ergebn. Limnol*, 43, 135-144.

Shannon, J.D. and Voldner, E.C. 1992. Deposition of S and NO_x nitrogen to the Great Lakes estimated with a regional deposition model. *Environmental Science and Technology*, 26: 970-978.

Shimadzu Corporation 1991. Shimadzu Total Organic Carbon Analyzer TOC-5000 P/N 638-9026 Instruction Manual. Shimadzu.

Sims, P.K., Anderson, J.L., Bauer, R.L., Chandler, V.W., Hanson, G.N., Kolliokoski, J., Morey, G.B., Mudrey, M.G. (Jr.), Ojakangas, R.W., Peterman, Z.E., Schulz, K.J., Shirley, S.B., Smith, E.I., Southwick, D.L., Van Schmus, R.W. and Weiblen, P.W. 1993. The Lake Superior Region and Trans-Hudson orogen. In: *The Geology of North America. Precambrian: Counterminous U.S.* (eds. J.C. Reed (Jr.), M.E. Bickfort, R.S. Houston, P.K. Link, D.W Rankin, P.K. Sims and W.R. Van Schmus), Vol. C-2 , pp. 11-121. The Geological Society of America.

Sklash M.G., Farvolden, R.N. and Fritz P. 1976. A conceptual model of watershed response to rainfall developed through the use of oxygen-18 as a natural tracer. *Canadian Journal of Earth Sciences*, 13, 271-283.

Sklash M.G. 1978. Isotope studies of runoff from small headwater basins. Ph.D. thesis, University of Waterloo, Canada.

Sloss, L.L. 1963. Sequences in the cratonic interior of North America. *Geological Society of America, Bulletin*, 74: 93-114.

Sloterdijk, H. 1991. Mercury and organochlorinated hydrocarbons in surficial sediments of the St. Lawrence River (Lake S. Francis). *Water Pollution Research Journal of Canada*, 26: 41-60.

Søballe, D.M. and Bachman, R.W. 1984. Influence of reservoir transit on riverine algal transport and abundance. *Canadian Journal of Fisheries and Aquatic Sciences*, 41, 1803-1813.

Sørensen, S.P.L. 1909. Enzymstudien II. Über die Messung und Bedeutung der Wasserstoffionenkonzentration bei enzymatischen Prozessen. *Biochemische Zeitung*, 21: 131.

St. Lawrence Centre 1993. St. Lawrence Update, the River at a Glance. Environment Canada, Québec Region.

Stallard, R.F. and Edmond, J.M. 1983. Geochemistry of the Amazon 2: The influence of the geology and weathering environment on the dissolved load. *Journal of Geophysical Research*, 88: 9671-9688.

Stumm, W. and Morgan, J.J. 1996. *Aquatic chemistry: Chemical Equilibria and Rates in Natural Waters*. Wiley.

Tan, F.C. 1987. Discharge and carbon isotope composition of particulate organic carbon from the St. Lawrence River, Canada. In: *Transport of Carbon and Minerals in Major World Rivers, Part 4* (eds. E.T. Degens, S. Kempe, W. Gan), SCOPE/UNEP Vol. 64, pp. 301-310. *Mitteilungen aus dem Geologisch-Paläontologischen Institut der Universität Hamburg*.

Tan, F.C. and Edmond, J.M. 1992. Sources and transport of organic carbon in the Orinoco Basin. In: *29th International Geological Congress, Abstracts-Congrès Géologique Internationale, Resumes* (ed. Anonymous), p. 68. *International Geological Congress*.

Tan, F.C. and Strain, P.M. 1983. Sources, sinks and distribution of organic carbon in the St. Lawrence Estuary, Canada. *Geochimica et Cosmochimica Acta*, 47: 125-123.

Tardy, Y., Mortatti, J. and Probst, J.L. 1995. Chemical and mechanical erosion in the Amazon Basin; surface runoff estimation by using the method of reservoirs of variable contribution and constant load over time. *Comptes Rendus de L'Academie des Sciences, Serie II, Sciences de la Terre et des Planètes*. 320: 853-860.

Tardy, Y., Mortatti, J., Victoria, R., Martinelli, L., Ribeiro, A., Cerri, C., Piccolo, M., de Moraes, J.L., Probst, J. L., Andreux, F. and Volkoff, B. (1993) Hydroclimatology and biogeochemistry of the Amazon; 2, Geochemical cycles. In: *Geochemistry of the Earth Surface; Abstracts for the Third International Symposium on the Geochemistry of the Earth Surface. Chemical Geology* (ed. L.R. Kump), pp. 411-414.

Telmer, K.H. 1996. Biogeochemistry and water balance of the Ottawa River basin. Ph.D. thesis. Department of Geology, University of Ottawa, Canada.

Terasmae, J. 1965. Surficial geology of the Cornwall and St. Lawrence seaway project areas. *Geological Survey of Canada Bulletin 121*. Geological Survey of Canada.

Thomas, R.L., Kemp, A.L.W. and Lewis, C.F.M. 1972. Report on the surficial sediment distribution of the Great Lakes. Part 1- Lake Ontario. Burlington, Ontario. Paper 72-17. Geological Survey of Canada/Canada Centre for Inland Waters.

Thurman, E.M. 1985. *Organic Geochemistry of Natural Waters*. Kluwer Academic.

Thurston, P.C. 1991a. Archean Geology of Ontario: Introduction. In: *Geology of Ontario, Part 1* (eds. P.C. Thurston, H.R. Williams, R.H. Sutcliffe and G.M. Stott), Special Vol. 4, pp. 73-81. Ministry of Northern Development and Mines.

Thurston, P.C. 1991b. Geology of Ontario: Introduction. In: *Geology of Ontario, Part 1* (eds. P.C. Thurston, H.R. Williams, R.H. Sutcliffe and G.M. Stott), Special Vol. 4, pp. 3-26. Ministry of Northern Development and Mines.

U.S. Department of Commerce/ NCDC/ NOAA 1998. (Internet site)
<http://www.ncdc.noaa.gov/ol/ncdc.html>: National Climatic Data Center/ National Oceanic and Atmospheric Administration.

United States Environmental Protection Agency and Government of Canada 1995. The Great Lakes. An Environmental Atlas and Resource Book. Environment Canada.

Van Bennekom, A.J. and Salomons, W. (1980) Pathways of nutrients and organic matter from land to ocean. In: Proceedings of the Review and Workshop on River Inputs to Ocean Systems, 1980, Rome, FAO (ed. United Nations Educational Scientific and Cultural Organization, and United Nations Environment Program), pp. 33-51. UNEP/UNESCO.

Vogel, J.C. 1993. Variability of carbon isotope fractionation during photosynthesis. In: Stable Isotopes and Plant Carbon-Water relations (eds. J.R. Ehleringer, A.H. Hall and G.D. Farquhar), pp. 29-45. Academic Press.

Volk, C.R., Volk, C.B. and Kaplan, L.A. 1997. Chemical composition of biodegradable dissolved organic matter in streamwater. *Limnology and Oceanography*, 42: 39-44.

Wadleigh, M.A., Veizer, J. and Brooks, C. 1985. Strontium isotopes in Canadian rivers: fluxes and global implications. *Geochimica et Cosmochimica Acta*, 49: 1727-1736.

Wallace B. and Millvard K. 1985. Great Lakes-St. Lawrence catchment area. Toxics, Great Lakes Hotspots [Information map]. Toronto, Ontario: Pollution Probe.

Weiler, R.R. and Chawla, V.K. 1969. Dissolved mineral quality of Great Lakes waters. In: Proceedings of the 12th conference of Great Lakes Research, 1969, pp. 801-818. International Association of Great Lakes Research.

Weiler, R.R. and Nriagu, J.O. 1978. Isotopic composition of dissolved inorganic carbon in the Great Lakes. *Journal of the Fisheries Research Board of Canada*, 35: 422-430.

Wetzel, R.G. 1983. *Limnology*. Saunders.

Wetzel, R.G. and Likens, G.E. 1991. *Limnological Analyses*. Springer Verlag .

Williams, D.A., Wolf, R.R. and Carson, D.M. 1985. Geology of the Cornwall-Huntington area, Southern Ontario, Map P. 2720. Ontario Geological Survey, scale 1 : 50,000.

Williams, H.R., Stott, G.M., Heather, K.B., Muir, T.L. and Sage, R.P. 1991. Wawa Subprovince. In: *Geology of Ontario, Part 1* (eds. P.C. Thurston, H.R. Williams, R.H. Sutcliffe and G.M. Stott), Special Vol. 4, pp. 485-539. Ministry of Northern Development and Mines.

Wilson, A.E. 1946. Geology of the St. Lawrence Lowland, Ontario and Québec. Memoir 241. Department of Mines and Technical Surveys, Canada, Geological Survey of Canada.

Wong, W.W., Benedict, C.R. and Kohel, R.J. 1979. Enzymatic fractionation of the stable carbon isotopes of carbon dioxide by ribulose-1.5-bisphosphate carboxylase. *Plant Physiology*, 63: 852-856.

Yang, C., Telmer, K. and Veizer, J. 1996. Chemical dynamics of the "St. Lawrence" riverine system: δD_{H_2O} , $\delta^{18}O_{H_2O}$, $\delta^{13}C_{DIC}$, $\delta^{34}S_{Sulfate}$, and dissolved $^{87/86}Sr$. *Geochimica et Cosmochimica Acta*, 60: 851-866.

Zhang, J., Quay, P.D. and Wilbour, D.O. 1995. Carbon isotope fractionation during gas-water exchange and dissolution of CO_2 . *Geochimica et Cosmochimica Acta*, 59: 107-114.

Appendices

Appendix 1

Trace- and rare earth element data

Appendix 1 Trace and rare earth element data. All concentrations in ppb ($\mu\text{g/L}$)

Sample ID	date	Li	Be	Al	Ti	V	Cr	Fe	Mn	Co	Ni	Cu	Zn	As	Se	Rb
Bay at Cooper Marsh																
JB25	5/29/95	2.031	0.012	12.53	0.46	0.50	0.33	31.94	4.39	0.05	0.91	0.88	0.53	1.02	1.00	0.92
JB27	6/12/95	1.935	0.005	7.83	0.50	0.40	0.41	11.49	6.45	0.10	2.72	0.78	0.71	1.30	1.00	0.95
JB32	6/20/95	1.914	0.005	7.33	0.50	0.31	0.32	10.56	3.85	0.06	0.58	0.85	0.50	1.23	1.00	0.95
JB43	7/3/95	1.932	0.005	5.69	0.50	0.37	0.34	9.90	3.27	0.05	0.62	0.79	0.72	1.39	1.00	0.98
JB45	7/18/95	1.915	0.005	6.12	0.50	0.33	0.32	9.20	2.31	0.06	0.66	1.11	0.96	1.44	1.00	0.96
JB52	8/1/95	1.932	0.005	9.44	0.50	0.37	0.22	6.81	3.08	0.07	2.23	0.94	1.84	1.27	1.00	0.95
JB59	8/15/95	1.957	0.005	5.48	0.50	0.34	0.38	8.68	3.16	0.06	1.08	0.73	1.70	1.20	1.00	0.96
JB66	8/29/95	1.436	0.005	50.04	1.01	1.42	0.20	25.33	1.83	0.08	0.55	0.58	2.33	1.08	1.00	0.79
JB73	9/13/95	2.310	0.076	3.54	0.84	0.46	0.54	20.25	1.66	0.05	0.84	1.10	1.69	1.19	1.00	1.05
JB80	9/26/95	2.277	0.083	3.45	1.33	0.27	0.19	5.86	1.40	0.05	1.27	0.93	5.28	1.20	1.00	1.08
JB87	10/10/95	2.126	0.054	4.69	1.38	0.47	0.45	10.31	3.93	0.05	1.30	0.97	3.57	1.14	1.00	1.01
JB99	10/17/95	2.244	0.075	3.60	1.47	0.28	0.32	7.40	1.72	0.05	1.07	0.92	1.23	0.93	1.00	1.10
JB106	10/24/95	2.150	0.046	3.92	1.50	0.29	0.25	13.43	1.85	0.05	1.14	0.89	0.96	0.97	1.00	1.08
JB113	11/4/95	2.366	0.077	5.28	1.66	0.44	0.52	11.23	1.31	0.05	1.17	0.98	0.88	1.06	1.00	1.06
JB120	11/10/95	2.217	0.092	6.17	1.78	0.42	0.32	7.33	0.95	0.05	1.07	1.05	1.39	1.13	1.00	1.03
JB127	4/20/96	2.352	0.005	8.00	0.50	0.20	0.60	5.00	1.50	0.05	0.80	1.20	1.70	1.30	1.00	1.21
JB134	5/4/96	2.444	0.005	9.00	0.50	0.20	0.60	9.00	2.40	0.05	0.90	1.20	1.80	1.20	1.00	1.23
JB141	5/18/96	1.895	0.005	7.00	0.50	0.30	0.50	21.00	2.30	0.05	0.80	1.00	0.60	1.00	1.00	1.01
JB148	6/1/96	1.644	0.005	7.00	0.50	0.30	0.60	19.00	3.40	0.05	0.60	0.80	0.70	0.90	1.00	0.93
JB155	6/15/96	1.660	0.005	6.00	0.50	0.20	0.50	23.00	2.20	0.05	0.70	0.80	0.80	0.90	1.00	0.95
JB162	6/29/96	1.701	0.005	6.00	0.50	0.30	0.30	12.00	2.30	0.05	0.50	0.70	0.90	0.90	1.00	0.88
Cooper Marsh																
JB42	7/3/95	1.942	0.005	19.31	0.70	0.93	0.27	43.50	10.02	0.08	0.40	0.40	2.67	1.24	1.00	0.67
JB44	7/18/95	2.070	0.005	8.31	0.56	0.34	0.32	85.11	20.25	0.10	0.23	0.26	8.88	1.30	1.00	0.69
JB51	8/1/95	1.984	0.005	12.38	0.60	0.43	0.41	43.43	6.56	0.08	0.35	0.48	3.00	1.07	1.00	0.53
JB58	8/15/95	1.881	0.005	7.11	0.50	0.42	0.28	18.83	4.98	0.18	0.44	0.40	3.95	1.05	1.00	0.83
JB65	8/29/95	2.100	0.005	10.07	0.50	0.36	0.24	15.35	4.91	0.06	0.40	0.46	6.85	1.09	1.00	0.79
JB72	9/13/95	2.494	0.068	5.92	1.02	0.52	0.45	31.39	3.55	0.05	0.55	0.71	2.52	0.85	1.23	1.09
JB79	9/26/95	2.068	0.060	4.86	1.03	0.34	0.42	11.34	2.16	0.05	0.71	0.68	3.46	0.81	1.00	1.03
JB86	10/10/95	1.911	0.060	9.81	1.84	0.51	0.49	113.17	15.90	0.10	0.84	0.54	24.00	0.67	1.00	1.42
JB98	10/17/95	1.808	0.022	17.32	1.96	0.24	0.40	242.36	12.22	0.15	0.65	0.35	3.69	0.45	1.00	1.61
JB105	10/24/95	1.916	0.027	15.96	2.15	0.20	0.42	141.61	10.46	0.14	0.62	0.32	4.96	0.49	1.00	1.69
JB112	11/4/95	2.117	0.043	22.40	2.98	0.47	0.43	73.77	3.13	0.07	0.81	0.81	3.30	0.81	1.00	1.89
JB119	11/10/95	2.140	0.063	16.71	2.66	0.30	0.47	34.53	5.59	0.06	1.12	0.97	5.83	0.82	1.00	1.11
JB125	12/4/95	1.860	0.039	26.41	2.81	0.11	0.50	640.49	200.89	0.28	0.69	0.50	6.89	0.58	1.00	1.96
JB126	4/20/96	0.895	0.011	54.00	3.00	0.60	0.60	91.00	20.90	0.12	0.50	1.90	5.60	0.70	1.00	1.37
JB133	5/4/96	1.569	0.005	25.00	1.60	0.90	0.70	87.00	13.50	0.08	0.60	1.00	18.20	1.00	1.00	1.38
JB140	5/18/96	1.591	0.005	29.00	1.80	0.90	0.80	86.00	17.60	0.08	0.80	1.10	4.50	1.00	1.00	1.32
JB147	6/1/96	1.658	0.005	22.00	2.60	0.90	0.60	64.00	9.70	0.06	0.80	0.50	5.90	0.80	1.00	0.84
JB154	6/15/96	1.734	0.011	41.00	1.90	1.20	0.50	73.00	12.70	0.07	0.50	0.50	6.40	1.10	1.00	0.92
JB161	6/29/96	1.720	0.005	30.00	0.70	0.50	0.40	26.00	2.60	0.05	0.40	0.80	11.50	1.00	1.00	0.82
JB6	5/5/94	2.000	0.200	15.50	2.10	0.40	1.10	5.00	1.00	0.09	0.90	1.30	0.40	0.80	1.00	1.00
JB19	11/3/94	1.588	0.005	9.64	0.61	1.01	0.54	12.46	0.54	0.05	0.21	1.18	0.50	0.67	1.00	0.61

Sample II	date	Li	Be	Al	Ti	V	Cr	Fe	Mn	Co	Ni	Cu	Zn	As	Se	Rb
Hoople Bay																
JB22	5/29/95	1.529	0.017	10.63	0.54	1.69	0.21	16.76	2.34	0.08	0.78	1.36	3.08	0.65	1.00	0.70
JB28	6/12/95	1.535	0.005	135.76	5.64	2.20	0.45	79.98	6.28	0.14	0.84	1.33	2.82	1.36	1.00	1.08
JB33	6/20/95	1.564	0.005	133.94	4.37	2.14	0.40	75.38	1.73	0.13	0.47	1.36	0.56	1.31	1.00	0.93
JB40	7/3/95	1.561	0.005	23.79	0.74	3.07	0.33	12.08	0.80	0.09	0.56	1.43	1.65	1.42	1.00	0.78
JB49	7/18/95	1.505	0.005	89.20	3.04	3.18	0.20	41.16	1.51	0.10	0.97	1.03	3.39	1.51	1.00	0.83
JB56	8/1/95	1.373	0.005	25.83	0.78	2.62	0.44	26.93	1.03	0.10	2.23	0.79	2.48	1.34	1.00	0.74
JB63	8/15/95	1.405	0.005	44.35	1.09	2.60	0.58	16.22	0.88	0.69	7.33	0.89	2.21	1.34	1.00	0.78
JB70	8/29/95	1.602	0.005	21.20	0.50	2.06	0.21	6.48	0.81	0.08	0.53	1.20	2.30	1.30	1.00	0.68
JB77	9/13/95	1.848	0.079	34.87	2.00	1.87	0.50	30.25	1.20	0.05	0.78	0.97	2.15	1.01	1.00	0.74
JB84	9/26/95	1.687	0.094	22.21	1.87	1.81	0.40	14.25	0.65	0.06	1.00	0.89	5.75	0.94	1.00	0.62
JB91	10/10/95	1.693	0.062	9.55	1.50	1.66	0.37	11.55	0.91	0.07	0.98	0.99	4.70	0.87	1.98	0.75
JB97	10/17/95	1.620	0.061	37.49	2.92	1.65	0.41	30.04	1.28	0.07	1.08	1.09	3.27	0.81	1.00	0.64
JB100	10/24/95	1.550	0.047	16.07	2.52	1.48	0.33	19.89	1.76	0.10	1.10	1.44	3.65	0.69	1.00	0.70
JB107	11/4/95	1.982	0.043	25.52	3.23	0.82	0.26	33.82	4.56	0.08	1.16	1.30	14.08	0.83	1.00	0.94
JB117	11/10/95	1.743	0.064	24.78	3.70	1.29	2.32	76.81	6.43	0.16	5.06	1.75	3.08	0.78	1.00	0.95
JB123	12/4/95	1.859	0.085	17.89	3.46	0.54	0.50	45.35	13.16	0.13	1.56	1.82	5.94	0.79	1.00	1.14
JB131	4/20/96	0.665	0.006	34.00	2.30	1.10	0.90	81.00	31.80	0.15	0.70	2.00	4.70	0.60	1.00	0.85
JB138	5/4/96	0.948	0.005	53.00	3.50	1.60	0.70	73.00	12.20	0.17	0.70	1.60	4.40	0.70	1.00	0.84
JB145	5/18/96	0.728	0.005	40.00	3.20	1.30	0.70	72.00	3.20	0.12	0.60	1.50	5.00	0.60	1.00	0.73
JB152	6/1/96	1.148	0.007	63.00	3.90	1.50	0.60	49.00	1.60	0.08	0.60	1.40	2.40	0.70	1.00	0.68
JB159	6/15/96	1.328	0.012	143.00	8.30	1.80	0.60	109.00	3.40	0.09	0.60	1.20	3.80	0.80	1.00	1.03
JB166	6/29/96	1.349	0.005	77.00	4.50	2.00	0.40	59.00	1.80	0.07	0.50	1.20	3.20	0.90	1.00	0.88
Hoople Creek																
JB23	5/29/95	1.951	0.033	28.73	1.86	0.94	0.33	294.28	62.83	0.22	1.42	1.73	1.65	0.68	1.00	0.80
JB30	6/12/95	2.323	0.013	30.49	1.61	1.30	0.82	321.10	86.12	0.30	0.96	1.34	1.34	1.08	1.00	0.96
JB36	6/20/95	2.407	0.011	16.53	1.46	1.27	0.83	278.00	457.96	0.44	0.91	1.19	1.77	1.40	1.00	1.53
JB41	7/3/95	2.502	0.011	13.12	2.08	1.40	0.60	237.38	175.68	0.44	0.99	0.91	2.30	1.87	1.00	1.47
JB50	7/18/95	2.370	0.009	7.45	1.32	0.85	0.66	111.37	61.08	0.16	0.53	0.60	1.79	1.66	1.00	1.81
JB57	8/1/95	3.056	0.005	3.86	0.50	0.45	0.40	28.47	3.16	0.19	0.37	0.48	1.12	0.81	1.00	2.23
JB64	8/15/95	3.273	0.005	7.22	0.53	0.81	0.51	54.07	9.75	0.20	0.74	1.10	1.53	1.04	1.00	2.34
JB71	8/29/95	3.001	0.005	3.03	0.50	0.52	0.51	71.71	66.64	0.35	0.61	0.54	2.06	1.19	1.00	2.60
JB78	9/13/95	3.816	0.073	5.60	3.01	0.52	0.57	56.56	206.58	0.16	1.18	0.96	2.59	1.06	1.00	3.44
JB85	9/26/95	3.392	0.083	7.92	3.05	0.63	0.44	62.49	118.47	0.16	1.47	0.88	4.46	1.30	1.00	3.18
JB92	10/10/95	4.840	0.140	16.16	5.56	0.84	0.52	99.98	20.71	0.17	1.89	2.28	2.58	0.63	1.00	2.14
JB93	10/17/95	2.744	0.036	17.54	5.72	0.90	0.85	145.07	13.42	0.18	2.17	2.59	5.70	0.80	1.08	1.93
JB101	10/24/95	1.311	0.048	40.60	5.18	0.83	0.65	131.58	14.09	0.22	2.05	3.37	6.86	0.54	1.00	1.77
JB108	11/4/95	1.777	0.044	35.66	6.42	0.89	0.72	114.40	10.95	0.18	2.19	2.91	4.63	0.70	1.00	1.33
JB118	11/10/95	1.857	0.054	37.98	5.86	0.81	0.68	150.68	14.10	0.23	2.24	2.55	3.87	0.71	1.00	0.80
JB122	12/4/95	1.407	0.045	34.10	5.67	0.74	0.70	102.76	12.96	0.18	1.79	2.10	5.80	0.68	1.00	0.69
JB132	4/20/96	0.525	0.007	71.00	3.00	0.80	1.00	110.00	12.50	0.13	0.70	1.70	40.80	0.60	1.00	1.26
JB139	5/4/96	1.162	0.006	42.00	1.60	0.90	1.10	255.00	45.20	0.19	0.80	1.60	3.50	0.70	1.00	0.75
JB146	5/18/96	0.949	0.005	42.00	2.10	0.90	0.90	238.00	30.80	0.17	0.80	1.50	4.40	0.70	1.00	0.82
JB153	6/1/96	1.523	0.012	35.00	1.60	1.20	0.80	298.00	32.20	0.22	1.00	1.40	1.60	0.80	1.00	0.78
JB160	6/15/96	2.263	0.015	28.00	2.00	1.30	0.80	314.00	37.80	0.22	1.10	1.50	2.10	1.00	1.00	1.04
JB167	6/29/96	2.223	0.010	13.00	1.80	1.20	0.80	194.00	50.80	0.21	0.90	1.10	2.30	1.00	1.00	1.16

Sample ID	date	Li	Be	Al	Ti	V	Cr	Fe	Mn	Co	Ni	Cu	Zn	As	Se	Rb
Long Sault Island																
JB35	6/20/95	1.835	0.005	17.78	0.50	0.54	0.32	13.15	5.45	0.06	0.47	0.87	0.50	1.09	1.00	0.94
JB37	7/3/95	1.802	0.005	31.08	0.61	0.85	0.29	19.29	2.57	0.06	0.78	0.69	0.88	1.21	1.00	1.00
JB47	7/18/95	1.711	0.005	42.64	1.57	0.69	0.23	49.61	10.05	0.07	0.53	0.52	3.52	1.62	1.00	1.33
JB54	8/1/95	1.621	0.005	29.69	0.65	0.88	0.25	23.39	1.53	0.08	0.43	0.52	0.50	1.46	1.00	0.96
JB61	8/15/95	1.521	0.005	48.04	1.46	0.92	0.33	39.68	1.86	0.08	0.59	0.55	1.21	1.21	1.00	1.03
JB67	8/29/95	1.331	0.005	34.79	0.58	1.30	0.45	26.01	1.67	0.05	0.66	0.67	2.60	0.83	1.00	0.76
JB74	9/13/95	1.884	0.088	29.76	0.92	1.18	0.45	38.10	4.36	0.05	0.75	0.80	3.97	1.15	1.00	0.85
JB81	9/26/95	1.187	0.082	34.48	1.77	2.99	0.21	35.02	4.21	0.07	0.84	1.01	1.63	1.35	1.00	0.58
JB88	10/10/95	1.625	0.088	17.60	2.01	0.66	0.41	45.74	24.89	0.05	0.89	0.66	6.74	0.89	1.00	0.66
JB94	10/17/95	1.877	0.084	14.33	2.07	0.53	0.39	41.32	9.54	0.05	0.93	0.66	3.31	0.85	1.00	0.89
JB102	10/24/95	1.774	0.063	15.63	1.98	0.56	0.40	42.12	17.54	0.06	0.94	1.20	6.08	0.67	1.00	0.80
JB109	11/4/95	1.947	0.060	19.82	2.52	0.44	0.37	55.91	7.29	0.05	1.15	0.98	6.23	0.72	1.00	0.87
JB114	11/10/95	1.899	0.071	13.96	1.99	0.44	0.52	31.83	8.40	0.05	1.07	0.92	7.40	0.74	1.00	0.81
JB128	4/20/96	1.506	0.005	11.00	0.70	0.40	0.60	5.00	18.10	0.05	0.50	0.70	5.10	0.70	1.00	1.04
JB135	5/4/96	1.640	0.008	13.00	0.50	0.50	0.50	15.00	23.10	0.05	0.50	1.10	6.00	0.80	1.00	0.79
JB142	5/18/96	1.631	0.005	12.00	0.50	0.50	0.50	28.00	18.20	0.05	0.60	0.80	1.90	0.70	1.00	0.79
JB149	6/1/96	1.491	0.005	32.00	0.80	0.80	0.50	31.00	2.90	0.05	0.60	0.80	2.60	0.80	1.00	0.72
JB156	6/15/96	1.417	0.005	51.00	2.20	0.90	0.40	78.00	2.10	0.05	0.50	0.60	1.80	0.80	1.00	0.74
JB163	6/29/96	1.448	0.005	62.00	2.80	0.60	0.40	92.00	3.00	0.05	0.50	0.60	6.40	0.90	1.00	1.65
Main Channel																
JB4	5/5/94	2.200	0.200	2.00	2.10	0.50	1.30	5.00	1.00	0.05	0.80	1.40	0.60	0.80	1.00	1.10
JB12	7/14/94	2.077	0.005	4.44	0.96	0.34	0.44	5.00	1.83	0.05	0.74	1.00	0.63	0.92	1.00	0.95
JB17	11/3/94	2.214	0.005	2.00	0.30	0.35	0.67	9.24	1.14	0.05	0.32	1.47	0.60	0.85	1.00	1.03
JB21	5/29/95	2.038	0.009	3.33	0.31	0.13	0.20	11.75	1.98	0.06	0.83	0.98	0.50	0.83	1.00	0.94
JB34	6/20/95	1.929	0.005	2.94	0.50	0.19	0.23	5.00	2.17	0.05	0.65	1.01	0.50	1.02	1.00	0.93
JB38	7/3/95	1.942	0.005	3.64	0.50	0.29	0.38	6.30	1.55	0.06	0.69	1.49	0.91	1.44	1.00	0.95
JB46	7/18/95	1.906	0.005	4.38	0.50	0.27	0.39	5.00	1.09	0.05	0.56	0.80	0.51	1.34	1.00	0.92
JB53	8/1/95	1.956	0.005	4.90	0.50	0.32	0.38	5.00	1.11	0.05	0.77	0.98	2.03	1.24	1.00	0.94
JB60	8/15/95	1.973	0.005	4.35	0.50	0.32	0.84	9.13	1.29	0.06	1.13	0.82	1.69	1.16	1.00	0.97
JB68	8/29/95	2.056	0.005	3.40	0.50	0.33	0.33	5.00	1.44	0.05	0.81	3.10	2.99	1.09	1.00	1.03
JB75	9/13/95	2.265	0.063	3.93	0.77	0.50	0.59	13.54	1.72	0.05	1.00	1.09	2.08	1.20	1.34	1.03
JB82	9/26/95	2.227	0.046	2.67	1.11	0.36	0.44	6.91	1.39	0.05	1.18	0.96	1.72	1.19	1.00	1.01
JB89	10/10/95	2.003	0.075	2.93	1.30	0.40	0.50	5.04	1.46	0.05	1.07	0.96	1.61	1.05	1.00	1.00
JB95	10/17/95	2.252	0.059	5.35	1.68	0.25	0.52	10.64	1.95	0.05	1.16	1.02	3.13	0.99	1.00	1.06
JB103	10/24/95	2.182	0.060	3.07	1.51	0.30	0.49	15.51	1.48	0.05	1.14	1.02	1.22	0.99	1.00	1.01
JB110	11/4/95	2.345	0.075	3.96	1.43	0.49	0.50	13.43	1.19	0.05	1.11	1.04	1.07	1.08	1.59	1.09
JB115	11/10/95	2.254	0.074	5.28	1.67	0.29	0.50	10.94	1.21	0.05	1.03	1.01	1.20	0.99	1.00	1.03
JB121	12/4/95	2.262	0.098	4.65	1.56	0.42	0.46	12.55	1.73	0.05	1.17	1.01	7.53	1.07	1.00	0.97
JB129	4/20/96	2.450	0.005	7.00	0.50	0.20	0.20	5.00	1.60	0.05	1.10	1.30	1.10	1.20	1.00	1.23
JB136	5/4/96	2.052	0.005	7.00	0.50	0.20	0.60	28.00	1.60	0.05	0.80	1.10	1.20	1.10	2.00	1.07
JB143	5/18/96	1.782	0.005	11.00	0.50	0.20	0.50	22.00	2.00	0.05	0.70	1.00	1.50	1.00	1.00	0.97
JB150	6/1/96	1.793	0.005	5.00	0.50	0.30	0.50	10.00	1.80	0.05	0.70	0.90	1.20	1.00	1.00	1.02
JB157	6/15/96	1.594	0.005	7.00	0.50	0.10	0.30	20.00	1.80	0.05	0.60	0.90	0.70	0.80	1.00	0.90
JB164	6/29/96	1.742	0.005	5.00	0.50	0.20	0.40	8.00	1.50	0.05	0.60	0.80	1.40	0.90	1.00	0.84

Sample II	date	Li	Be	Al	Ti	V	Cr	Fe	Mn	Co	Ni	Cu	Zn	As	Se	Rb
Whale Island																
JB11	7/14/94	1.994	0.005	23.73	1.37	0.66	0.49	15.31	0.10	0.05	0.78	1.57	6.42	0.86	1.00	0.99
JB18	11/3/94	1.996	0.005	6.87	0.51	0.40	0.59	20.40	3.10	0.05	0.44	0.86	0.50	0.77	1.00	0.95
JB20	5/29/95	1.899	0.008	8.01	0.28	0.25	0.12	13.32	1.83	0.05	0.89	0.93	0.50	0.69	1.00	0.86
JB29	6/12/95	1.852	0.005	29.16	0.75	0.47	0.40	25.74	4.25	0.12	0.63	0.95	0.50	1.23	1.00	0.96
JB39	7/3/95	1.903	0.005	18.40	0.50	0.68	0.32	15.43	1.76	0.05	0.52	0.81	0.50	1.35	1.00	0.98
JB48	7/18/95	1.853	0.005	26.37	0.63	0.86	0.31	15.70	2.96	0.06	0.54	0.77	4.24	1.25	1.00	1.01
JB55	8/1/95	1.816	0.005	17.15	0.50	0.47	0.27	13.90	1.41	0.06	0.47	0.64	1.27	1.33	1.00	0.93
JB62	8/15/95	1.832	0.005	19.61	0.50	0.61	0.34	8.71	0.65	0.05	0.78	0.63	1.03	1.26	1.00	0.91
JB69	8/29/95	1.964	0.005	25.86	0.50	0.57	0.27	12.67	0.97	0.06	0.63	0.81	0.84	1.25	1.00	0.93
JB76	9/13/95	2.069	0.058	21.10	1.18	0.77	0.41	29.37	1.20	0.05	0.86	0.84	0.85	1.10	1.50	0.94
JB83	9/26/95	2.042	0.057	9.32	1.14	0.67	0.35	11.20	1.68	0.05	1.18	0.84	2.51	1.08	1.00	0.96
JB90	10/10/95	2.141	0.074	11.29	1.61	0.53	0.34	26.28	3.14	0.05	1.13	0.97	1.77	1.05	1.34	1.04
JB96	10/17/95	2.141	0.072	12.92	1.78	0.53	0.37	27.57	3.24	0.05	1.17	0.91	1.94	1.02	1.17	1.02
JB104	10/24/95	2.142	0.070	14.55	1.95	0.52	0.40	28.86	3.35	0.05	1.21	0.85	2.11	0.99	1.00	1.00
JB111	11/4/95	2.238	0.053	14.13	2.04	0.44	0.22	40.93	3.99	0.05	1.11	1.45	1.42	0.95	1.30	0.98
JB116	11/10/95	2.106	0.080	11.02	1.88	0.44	0.50	35.81	2.97	0.06	1.85	0.98	2.77	0.88	1.00	0.95
JB124	12/4/95	2.210	0.065	6.54	1.75	0.29	0.47	21.70	2.26	0.05	1.17	1.00	0.50	0.94	1.00	1.01
JB130	4/20/96	1.901	0.005	13.00	1.10	0.40	0.70	15.00	5.20	0.07	1.00	1.40	1.60	0.90	1.00	1.04
JB137	5/4/96	1.916	0.005	12.00	0.50	0.20	0.40	24.00	6.00	0.05	0.60	0.90	0.90	0.90	1.00	0.95
JB144	5/18/96	1.677	0.005	12.00	0.50	0.40	0.50	26.00	2.00	0.05	0.60	0.90	0.70	0.80	1.00	0.86
JB151	6/1/96	1.662	0.005	12.00	0.50	0.40	0.50	25.00	4.80	0.05	0.60	0.90	3.80	0.80	1.00	0.88
JB158	6/15/96	1.572	0.007	12.00	0.50	0.30	0.40	10.00	2.20	0.05	0.50	0.80	0.50	0.80	1.00	0.89
JB165	6/29/96	1.653	0.005	20.00	0.80	0.50	0.30	23.00	2.10	0.05	0.50	0.70	0.80	0.90	1.00	0.88
Flannigans Point																
JB3	5/4/94	1.000	0.200	2.50	4.10	1.80	1.70	55.00	5.00	0.05	0.70	2.80	0.40	0.50	1.00	0.70
JB9	7/13/94	2.016	0.005	5.89	0.86	0.39	0.40	5.28	3.04	0.05	0.77	1.06	0.50	0.93	1.00	0.98
JB15	10/30/94	2.189	0.005	2.26	0.35	0.42	0.75	9.76	2.09	0.05	0.42	1.05	0.50	0.99	1.00	1.06
North and South of Cornwall Island																
JB2	5/4/94	2.200	0.200	2.50	1.30	0.50	1.90	5.00	3.00	0.05	0.80	1.30	1.10	0.90	1.00	1.00
JB1	5/2/94	2.200	0.200	2.00	1.60	0.50	1.40	5.00	1.00	0.05	0.75	1.10	0.50	0.80	1.00	1.00
JB8	7/12/94	1.867	0.005	4.76	0.67	0.35	0.46	5.00	2.15	0.05	0.55	1.06	0.50	0.81	1.00	0.97
JB14	10/30/94	2.170	0.005	2.00	0.31	0.39	0.67	9.57	1.47	0.05	0.32	1.07	0.50	0.99	1.00	1.08
Thompson Island																
JB7	7/11/94	1.885	0.005	2.00	0.67	0.29	0.51	5.00	3.43	0.05	0.62	1.42	1.18	0.87	1.00	0.95
JB13	10/30/94	2.210	0.005	2.00	0.35	0.49	0.72	12.06	2.15	0.05	0.35	1.15	0.50	1.07	1.00	1.08
Hoople Island																
JB5	5/5/94	2.200	0.200	2.00	2.00	0.50	1.20	5.00	2.00	0.05	0.85	1.20	0.70	0.80	1.00	1.10
JB10	7/14/94	1.961	0.005	11.05	0.99	0.47	0.41	14.09	11.55	0.05	0.69	1.44	0.50	0.93	1.00	1.01
JB16	11/3/94	2.228	0.005	2.34	0.38	0.41	0.71	14.25	3.39	0.05	0.57	1.37	0.50	0.88	1.00	1.05

Sample II	date	Mo	Ag	Cd	In	Sb	Ba	La	Ce	Pr	Nd	Sm	Eu	Gd	Tb	Dy
Bay at Cooper Marsh																
JB25	5/29/95	1.17	0.05	0.05	0.01	0.15	20.21	0.02	0.03	0.005	0.021	0.005	0.005	0.008	0.005	0.005
JB27	6/12/95	1.15	0.05	0.05	0.01	0.17	20.09	0.01	0.02	0.005	0.014	0.005	0.005	0.005	0.005	0.005
JB32	6/20/95	1.23	0.05	0.05	0.01	0.18	16.37	0.01	0.02	0.005	0.013	0.005	0.005	0.005	0.005	0.005
JB43	7/3/95	1.16	0.05	0.05	0.01	0.17	17.45	0.01	0.02	0.005	0.010	0.005	0.005	0.005	0.005	0.005
JB45	7/18/95	1.16	0.05	0.05	0.01	0.18	18.88	0.01	0.01	0.005	0.008	0.005	0.005	0.005	0.005	0.005
JB52	8/1/95	1.21	0.05	0.08	0.01	0.20	21.61	0.01	0.01	0.005	0.012	0.005	0.005	0.005	0.005	0.005
JB59	8/15/95	1.27	0.05	0.05	0.01	0.19	23.00	0.01	0.01	0.005	0.007	0.005	0.005	0.005	0.005	0.005
JB66	8/29/95	1.58	0.05	0.05	0.01	0.20	21.17	0.03	0.06	0.007	0.032	0.005	0.005	0.005	0.005	0.005
JB73	9/13/95	1.59	0.05	0.05	0.01	0.20	21.94	0.01	0.01	0.005	0.005	0.005	0.005	0.005	0.005	0.005
JB80	9/26/95	1.37	0.05	0.05	0.01	0.20	22.97	0.01	0.01	0.005	0.012	0.016	0.005	0.005	0.005	0.005
JB87	10/10/95	1.40	0.05	0.05	0.01	0.20	24.06	0.01	0.01	0.005	0.005	0.005	0.005	0.005	0.008	0.005
JB99	10/17/95	1.33	0.05	0.05	0.01	0.19	23.41	0.01	0.01	0.005	0.007	0.010	0.005	0.005	0.007	0.012
JB106	10/24/95	1.40	0.05	0.05	0.01	0.20	23.57	0.01	0.01	0.005	0.005	0.005	0.005	0.005	0.005	0.007
JB113	11/4/95	1.39	0.05	0.05	0.01	0.19	23.16	0.01	0.01	0.005	0.005	0.005	0.005	0.005	0.005	0.005
JB120	11/10/95	1.38	0.05	0.05	0.01	0.21	23.23	0.01	0.01	0.005	0.009	0.005	0.005	0.005	0.005	0.005
JB127	4/20/96	1.51	0.05	0.05	0.01	0.21	27.30	0.01	0.02	0.005	0.014	0.005	0.005	0.005	0.007	0.005
JB134	5/4/96	1.45	0.05	0.05	0.01	0.21	25.30	0.02	0.03	0.005	0.028	0.012	0.005	0.005	0.006	0.005
JB141	5/18/96	1.20	0.05	0.05	0.01	0.18	17.50	0.01	0.02	0.005	0.020	0.014	0.005	0.005	0.006	0.005
JB148	6/1/96	0.98	0.05	0.05	0.01	0.15	18.70	0.01	0.02	0.005	0.013	0.007	0.005	0.005	0.005	0.005
JB155	6/15/96	1.01	0.05	0.05	0.01	0.15	18.80	0.01	0.02	0.005	0.016	0.005	0.005	0.005	0.006	0.005
JB162	6/29/96	1.01	0.05	0.05	0.01	0.15	16.10	0.01	0.01	0.005	0.017	0.005	0.005	0.005	0.005	0.005
Cooper Marsh																
JB42	7/3/95	0.97	0.05	0.05	0.01	0.15	13.35	0.03	0.06	0.005	0.044	0.005	0.005	0.005	0.005	0.005
JB44	7/18/95	0.42	0.05	0.05	0.01	0.08	16.39	0.03	0.07	0.005	0.035	0.005	0.005	0.005	0.005	0.005
JB51	8/1/95	0.49	0.05	0.05	0.01	0.09	17.72	0.02	0.04	0.005	0.021	0.005	0.005	0.005	0.005	0.005
JB58	8/15/95	0.95	0.05	0.05	0.01	0.14	22.31	0.01	0.02	0.005	0.013	0.005	0.005	0.005	0.005	0.005
JB65	8/29/95	0.99	0.05	0.06	0.01	0.14	20.12	0.01	0.01	0.005	0.011	0.005	0.005	0.005	0.005	0.005
JB72	9/13/95	0.82	0.05	0.05	0.01	0.10	20.84	0.02	0.03	0.005	0.018	0.005	0.005	0.005	0.005	0.006
JB79	9/26/95	0.98	0.05	0.05	0.01	0.14	19.71	0.01	0.01	0.005	0.027	0.009	0.005	0.005	0.005	0.005
JB86	10/10/95	0.42	0.05	0.05	0.01	0.08	17.10	0.04	0.07	0.010	0.053	0.006	0.005	0.005	0.016	0.011
JB98	10/17/95	0.14	0.05	0.05	0.01	0.05	14.35	0.06	0.09	0.011	0.051	0.019	0.005	0.005	0.008	0.014
JB105	10/24/95	0.21	0.05	0.05	0.01	0.04	15.34	0.05	0.07	0.012	0.041	0.005	0.005	0.005	0.005	0.011
JB112	11/4/95	0.59	0.05	0.05	0.01	0.09	19.43	0.06	0.09	0.012	0.044	0.007	0.005	0.005	0.006	0.015
JB119	11/10/95	1.04	0.05	0.05	0.01	0.14	23.59	0.03	0.04	0.009	0.039	0.010	0.005	0.005	0.005	0.012
JB125	12/4/95	0.14	0.05	0.05	0.01	0.05	15.19	0.06	0.12	0.016	0.063	0.010	0.005	0.005	0.005	0.013
JB126	4/20/96	0.45	0.05	0.05	0.01	0.08	22.30	0.14	0.24	0.036	0.127	0.025	0.005	0.005	0.023	0.015
JB133	5/4/96	0.51	0.05	0.05	0.01	0.09	18.60	0.11	0.19	0.026	0.115	0.019	0.005	0.005	0.021	0.015
JB140	5/18/96	0.85	0.05	0.05	0.01	0.12	18.00	0.11	0.19	0.021	0.101	0.030	0.005	0.005	0.015	0.010
JB147	6/1/96	0.88	0.05	0.05	0.01	0.12	17.40	0.05	0.09	0.008	0.037	0.012	0.005	0.005	0.005	0.005
JB154	6/15/96	0.86	0.05	0.05	0.01	0.15	20.00	0.06	0.11	0.013	0.055	0.009	0.005	0.005	0.008	0.005
JB161	6/29/96	1.01	0.05	0.05	0.01	0.16	14.30	0.03	0.05	0.006	0.022	0.005	0.005	0.005	0.005	0.005
JB6	5/5/94	1.30	0.05	0.05	0.01	0.28	31.50	0.01	0.03	0.005	0.005	0.005	0.005	0.005	0.005	0.005
JB19	11/3/94	1.38	0.05	0.05	0.01	0.28	22.55	0.02	0.03	0.005	0.018	0.005	0.005	0.008	0.005	0.005

Sample II	date	Mo	Ag	Cd	In	Sb	Ba	La	Ce	Pr	Nd	Sm	Eu	Gd	Tb	Dy
Hoople Bay																
JB22	5/29/95	1.33	0.05	0.05	0.01	0.15	27.92	0.05	0.06	0.008	0.047	0.011	0.005	0.006	0.005	0.007
JB28	6/12/95	1.30	0.05	0.05	0.01	0.14	29.98	0.11	0.22	0.023	0.097	0.015	0.005	0.020	0.005	0.009
JB33	6/20/95	1.31	0.05	0.05	0.01	0.14	25.27	0.10	0.22	0.025	0.126	0.017	0.005	0.013	0.005	0.011
JB40	7/3/95	1.34	0.05	0.05	0.01	0.16	24.06	0.04	0.04	0.005	0.018	0.005	0.005	0.005	0.005	0.005
JB49	7/18/95	1.30	0.05	0.05	0.01	0.18	24.23	0.13	0.11	0.009	0.048	0.005	0.005	0.008	0.005	0.006
JB56	8/1/95	1.29	0.05	0.05	0.01	0.16	22.23	0.02	0.03	0.005	0.018	0.005	0.005	0.005	0.005	0.005
JB63	8/15/95	1.42	0.05	0.05	0.01	0.16	23.99	0.04	0.05	0.005	0.037	0.005	0.005	0.005	0.005	0.005
JB70	8/29/95	1.47	0.05	0.05	0.01	0.19	23.09	0.01	0.02	0.005	0.022	0.005	0.005	0.005	0.005	0.005
JB77	9/13/95	1.50	0.05	0.05	0.01	0.21	19.26	0.04	0.07	0.011	0.025	0.005	0.005	0.005	0.007	0.005
JB84	9/26/95	1.48	0.05	0.05	0.01	0.19	19.04	0.02	0.03	0.007	0.029	0.011	0.005	0.005	0.005	0.005
JB91	10/10/95	1.54	0.05	0.05	0.01	0.17	21.93	0.01	0.02	0.005	0.013	0.009	0.005	0.005	0.007	0.005
JB97	10/17/95	1.48	0.05	0.05	0.01	0.17	22.93	0.04	0.08	0.009	0.020	0.009	0.005	0.005	0.005	0.012
JB100	10/24/95	1.53	0.05	0.05	0.01	0.17	24.49	0.03	0.05	0.009	0.011	0.009	0.005	0.005	0.005	0.012
JB107	11/4/95	1.50	0.05	0.05	0.01	0.17	26.00	0.05	0.08	0.011	0.061	0.012	0.005	0.005	0.005	0.007
JB117	11/10/95	1.47	0.05	0.05	0.01	0.15	34.16	0.09	0.14	0.022	0.092	0.011	0.005	0.005	0.008	0.016
JB123	12/4/95	1.18	0.05	0.05	0.01	0.14	33.02	0.05	0.08	0.013	0.074	0.005	0.005	0.005	0.012	0.009
JB131	4/20/96	0.86	0.05	0.05	0.01	0.08	31.70	0.18	0.34	0.039	0.196	0.045	0.006	0.005	0.037	0.023
JB138	5/4/96	1.10	0.05	0.05	0.01	0.10	30.40	0.15	0.25	0.036	0.168	0.016	0.009	0.006	0.028	0.026
JB145	5/18/96	0.93	0.05	0.05	0.01	0.07	29.00	0.13	0.25	0.031	0.155	0.033	0.006	0.006	0.031	0.023
JB152	6/1/96	1.12	0.05	0.05	0.01	0.13	24.00	0.08	0.14	0.025	0.075	0.012	0.005	0.005	0.018	0.012
JB159	6/15/96	1.15	0.05	0.05	0.01	0.13	25.20	0.13	0.26	0.030	0.139	0.018	0.005	0.005	0.016	0.016
JB166	6/29/96	1.18	0.05	0.05	0.01	0.15	23.10	0.11	0.20	0.024	0.108	0.012	0.005	0.005	0.015	0.013
Hoople Creek																
JB23	5/29/95	1.27	0.05	0.05	0.01	0.07	49.19	0.13	0.26	0.034	0.132	0.032	0.007	0.019	0.005	0.018
JB30	6/12/95	1.24	0.05	0.05	0.01	0.07	62.66	0.13	0.26	0.035	0.144	0.027	0.005	0.018	0.005	0.021
JB36	6/20/95	1.39	0.05	0.05	0.01	0.07	54.36	0.10	0.25	0.028	0.144	0.026	0.005	0.023	0.005	0.019
JB41	7/3/95	1.13	0.05	0.05	0.01	0.07	43.58	0.09	0.17	0.016	0.091	0.024	0.005	0.015	0.005	0.012
JB50	7/18/95	0.88	0.05	0.05	0.01	0.06	39.89	0.03	0.07	0.008	0.043	0.006	0.005	0.005	0.005	0.008
JB57	8/1/95	1.20	0.05	0.05	0.01	0.07	62.23	0.01	0.02	0.005	0.015	0.005	0.005	0.005	0.005	0.005
JB64	8/15/95	1.65	0.05	0.05	0.01	0.09	57.52	0.02	0.04	0.005	0.028	0.008	0.005	0.005	0.005	0.005
JB71	8/29/95	0.98	0.05	0.05	0.01	0.06	55.22	0.02	0.05	0.006	0.022	0.005	0.005	0.008	0.005	0.009
JB78	9/13/95	0.98	0.05	0.05	0.01	0.06	66.19	0.02	0.03	0.005	0.028	0.009	0.005	0.005	0.007	0.009
JB85	9/26/95	0.88	0.05	0.05	0.01	0.06	52.06	0.02	0.04	0.007	0.027	0.014	0.005	0.005	0.005	0.005
JB92	10/10/95	3.17	0.05	0.05	0.01	0.15	67.25	0.05	0.08	0.013	0.043	0.018	0.007	0.005	0.015	0.013
JB93	10/17/95	1.70	0.05	0.05	0.01	0.10	63.14	0.07	0.11	0.022	0.071	0.015	0.007	0.005	0.015	0.032
JB101	10/24/95	1.42	0.05	0.05	0.01	0.10	57.30	0.12	0.18	0.029	0.118	0.037	0.005	0.005	0.025	0.042
JB108	11/4/95	1.21	0.05	0.05	0.01	0.09	62.87	0.10	0.13	0.025	0.107	0.011	0.005	0.005	0.010	0.021
JB118	11/10/95	1.37	0.05	0.05	0.01	0.09	60.27	0.10	0.11	0.023	0.108	0.021	0.005	0.005	0.015	0.032
JB122	12/4/95	0.86	0.05	0.05	0.01	0.07	50.33	0.06	0.10	0.013	0.079	0.018	0.005	0.005	0.005	0.005
JB132	4/20/96	0.78	0.05	0.05	0.01	0.10	75.60	0.13	0.24	0.030	0.154	0.032	0.005	0.005	0.028	0.033
JB139	5/4/96	1.05	0.05	0.05	0.01	0.06	46.50	0.10	0.18	0.026	0.125	0.034	0.005	0.005	0.026	0.020
JB146	5/18/96	0.99	0.05	0.05	0.01	0.08	43.10	0.13	0.21	0.032	0.134	0.029	0.005	0.005	0.021	0.023
JB153	6/1/96	1.09	0.05	0.05	0.01	0.05	45.90	0.13	0.22	0.030	0.131	0.026	0.006	0.005	0.024	0.021
JB160	6/15/96	1.33	0.05	0.05	0.01	0.09	49.60	0.13	0.24	0.036	0.150	0.026	0.006	0.005	0.033	0.029
JB167	6/29/96	0.88	0.05	0.05	0.01	0.07	54.30	0.08	0.16	0.025	0.108	0.015	0.005	0.005	0.013	0.024

Sample II	date	Mo	Ag	Cd	In	Sb	Ba	La	Ce	Pr	Nd	Sm	Eu	Gd	Tb	Dy
Whale Island																
JB11	7/14/94	1.25	0.05	0.05	0.01	0.21	22.36	0.01	0.01	0.005	0.023	0.005	0.005	0.005	0.005	0.005
JB18	11/3/94	1.28	0.05	0.05	0.01	0.21	22.69	0.02	0.03	0.005	0.014	0.005	0.005	0.005	0.005	0.005
JB20	5/29/95	1.12	0.05	0.05	0.01	0.17	20.82	0.01	0.02	0.005	0.017	0.005	0.005	0.006	0.005	0.005
JB29	6/12/95	1.18	0.05	0.05	0.01	0.17	20.22	0.03	0.06	0.006	0.029	0.005	0.005	0.005	0.005	0.005
JB39	7/3/95	1.20	0.05	0.05	0.01	0.17	20.53	0.01	0.03	0.005	0.015	0.005	0.005	0.005	0.005	0.005
JB48	7/18/95	1.28	0.05	0.05	0.01	0.17	24.77	0.02	0.04	0.005	0.012	0.005	0.005	0.005	0.005	0.005
JB55	8/1/95	1.18	0.05	0.05	0.01	0.16	22.69	0.01	0.02	0.005	0.017	0.005	0.005	0.005	0.005	0.005
JB62	8/15/95	1.28	0.05	0.05	0.01	0.16	21.99	0.01	0.02	0.005	0.012	0.005	0.005	0.005	0.005	0.005
JB69	8/29/95	1.40	0.05	0.05	0.01	0.20	19.78	0.02	0.12	0.005	0.019	0.005	0.005	0.006	0.005	0.005
JB76	9/13/95	1.48	0.05	0.05	0.01	0.19	16.98	0.02	0.04	0.006	0.021	0.005	0.005	0.005	0.005	0.005
JB83	9/26/95	1.40	0.05	0.05	0.01	0.20	19.43	0.01	0.02	0.005	0.019	0.013	0.007	0.005	0.005	0.005
JB90	10/10/95	1.49	0.05	0.05	0.01	0.18	21.59	0.02	0.04	0.005	0.017	0.013	0.005	0.005	0.005	0.005
JB96	10/17/95	1.42	0.05	0.05	0.01	0.18	22.36	0.02	0.04	0.005	0.015	0.011	0.005	0.005	0.005	0.011
JB104	10/24/95	1.35	0.05	0.05	0.01	0.19	23.13	0.03	0.04	0.005	0.013	0.009	0.005	0.005	0.005	0.018
JB111	11/4/95	1.42	0.05	0.05	0.01	0.20	23.00	0.03	0.04	0.005	0.033	0.010	0.005	0.005	0.005	0.012
JB116	11/10/95	1.43	0.05	0.05	0.01	0.18	23.24	0.03	0.04	0.006	0.017	0.005	0.005	0.005	0.006	0.005
JB124	12/4/95	1.40	0.05	0.05	0.01	0.19	22.69	0.01	0.02	0.005	0.022	0.006	0.005	0.005	0.005	0.008
JB130	4/20/96	1.34	0.05	0.05	0.01	0.17	24.20	0.39	0.07	0.010	0.046	0.010	0.005	0.005	0.016	0.005
JB137	5/4/96	1.26	0.05	0.05	0.01	0.17	20.60	0.03	0.05	0.005	0.023	0.008	0.005	0.005	0.009	0.005
JB144	5/18/96	1.17	0.05	0.05	0.01	0.15	20.10	0.03	0.06	0.005	0.039	0.008	0.005	0.005	0.005	0.007
JB151	6/1/96	1.04	0.05	0.05	0.01	0.17	17.80	0.03	0.05	0.006	0.018	0.007	0.005	0.005	0.006	0.008
JB158	6/15/96	0.99	0.05	0.05	0.01	0.14	16.50	0.02	0.03	0.005	0.017	0.005	0.005	0.005	0.005	0.008
JB165	6/29/96	1.05	0.05	0.05	0.01	0.16	16.80	0.03	0.06	0.009	0.035	0.005	0.005	0.005	0.005	0.007
Flannigans Point																
JB3	5/4/94	0.90	0.05	0.05	0.01	0.30	24.50	0.01	0.18	0.030	0.140	0.040	0.005	0.020	0.005	0.010
JB9	7/13/94	1.25	0.05	0.05	0.01	0.21	19.07	0.01	0.01	0.005	0.013	0.005	0.005	0.005	0.005	0.005
JB15	10/30/94	1.36	0.05	0.05	0.01	0.21	23.42	0.01	0.01	0.005	0.007	0.005	0.005	0.005	0.005	0.005
North and South of Cornwall Island																
JB2	5/4/94	1.20	0.05	0.05	0.01	0.24	25.50	0.01	0.03	0.005	0.005	0.005	0.005	0.005	0.005	0.005
JB1	5/2/94	1.20	0.05	0.05	0.01	0.21	25.00	0.01	0.03	0.005	0.005	0.005	0.005	0.005	0.005	0.005
JB8	7/12/94	1.24	0.05	0.05	0.01	0.19	21.08	0.01	0.01	0.005	0.011	0.005	0.005	0.005	0.005	0.005
JB14	10/30/94	1.37	0.05	0.05	0.01	0.23	22.99	0.01	0.01	0.005	0.011	0.005	0.005	0.005	0.005	0.005
Thompson Island																
JB7	7/11/94	1.19	0.05	0.11	0.01	0.18	19.36	0.01	0.01	0.005	0.005	0.005	0.005	0.005	0.005	0.005
JB13	10/30/94	1.45	0.05	0.05	0.01	0.23	24.14	0.01	0.01	0.005	0.005	0.005	0.005	0.005	0.005	0.005
Hoople Island																
JB5	5/5/94	1.30	0.05	0.05	0.01	0.20	25.50	0.01	0.03	0.005	0.005	0.005	0.005	0.005	0.005	0.005
JB10	7/14/94	1.26	0.05	0.05	0.01	0.28	21.09	0.01	0.01	0.005	0.023	0.005	0.005	0.005	0.005	0.005
JB16	11/3/94	1.46	0.05	0.05	0.01	0.40	23.50	0.01	0.02	0.005	0.007	0.005	0.005	0.005	0.005	0.005

Sample ID	date	Ho	Yb	Lu	Tl	Pb	U
Bay at Cooper Marsh							
JB25	5/29/95	0.005	0.005	0.005	0.005	0.10	0.371
JB27	6/12/95	0.005	0.005	0.005	0.007	0.10	0.313
JB32	6/20/95	0.005	0.005	0.005	0.005	0.10	0.334
JB43	7/3/95	0.005	0.005	0.005	0.006	0.10	0.308
JB45	7/18/95	0.005	0.005	0.005	0.009	0.10	0.316
JB52	8/1/95	0.005	0.005	0.005	0.005	0.10	0.320
JB59	8/15/95	0.005	0.005	0.005	0.005	0.10	0.328
JB66	8/29/95	0.005	0.005	0.005	0.005	0.10	0.400
JB73	9/13/95	0.005	0.005	0.005	0.005	0.10	0.393
JB80	9/26/95	0.005	0.005	0.005	0.009	0.10	0.375
JB87	10/10/95	0.005	0.007	0.005	0.011	0.10	0.379
JB99	10/17/95	0.005	0.005	0.005	0.007	0.10	0.370
JB106	10/24/95	0.005	0.005	0.005	0.007	0.10	0.408
JB113	11/4/95	0.005	0.005	0.005	0.009	0.10	0.406
JB120	11/10/95	0.005	0.005	0.005	0.005	0.10	0.415
JB127	4/20/96	0.005	0.005	0.005	0.007	0.10	0.422
JB134	5/4/96	0.005	0.005	0.005	0.007	0.10	0.402
JB141	5/18/96	0.005	0.005	0.005	0.005	0.10	0.344
JB148	6/1/96	0.005	0.005	0.005	0.005	0.10	0.295
JB155	6/15/96	0.005	0.005	0.005	0.005	0.10	0.285
JB162	6/29/96	0.005	0.005	0.005	0.005	0.10	0.301
Cooper Marsh							
JB42	7/3/95	0.005	0.005	0.005	0.005	0.10	0.162
JB44	7/18/95	0.005	0.005	0.005	0.005	0.10	0.053
JB51	8/1/95	0.005	0.005	0.005	0.005	0.10	0.077
JB58	8/15/95	0.005	0.005	0.005	0.005	0.10	0.136
JB65	8/29/95	0.005	0.005	0.005	0.005	0.10	0.163
JB72	9/13/95	0.005	0.005	0.005	0.005	0.10	0.145
JB79	9/26/95	0.005	0.005	0.005	0.005	0.12	0.200
JB86	10/10/95	0.005	0.008	0.005	0.005	0.14	0.075
JB98	10/17/95	0.005	0.005	0.005	0.005	0.10	0.025
JB105	10/24/95	0.005	0.005	0.005	0.005	0.10	0.048
JB112	11/4/95	0.005	0.005	0.005	0.005	0.13	0.209
JB119	11/10/95	0.005	0.005	0.005	0.005	0.10	0.385
JB125	12/4/95	0.005	0.006	0.005	0.005	0.19	0.058
JB126	4/20/96	0.005	0.009	0.005	0.005	0.20	0.364
JB133	5/4/96	0.005	0.008	0.005	0.005	0.18	0.340
JB140	5/18/96	0.005	0.009	0.005	0.005	0.13	0.364
JB147	6/1/96	0.005	0.005	0.005	0.005	0.10	0.263
JB154	6/15/96	0.005	0.009	0.005	0.005	0.11	0.239
JB161	6/29/96	0.005	0.005	0.005	0.005	0.10	0.283
JB6	5/5/94	0.005	0.005	0.005	0.005	0.10	0.360
JB19	11/3/94	0.005	0.007	0.005	0.006	0.10	0.425

Sample ID	date	Ho	Yb	Lu	Tl	Pb	U
Hoople Bay							
JB22	5/29/95	0.005	0.005	0.005	0.005	0.13	0.627
JB28	6/12/95	0.005	0.005	0.005	0.005	0.10	0.577
JB33	6/20/95	0.005	0.007	0.005	0.006	0.10	0.523
JB40	7/3/95	0.005	0.005	0.005	0.007	0.10	0.465
JB49	7/18/95	0.005	0.005	0.005	0.005	0.10	0.459
JB56	8/1/95	0.005	0.005	0.005	0.005	0.10	0.402
JB63	8/15/95	0.005	0.005	0.005	0.005	0.10	0.417
JB70	8/29/95	0.005	0.005	0.005	0.005	0.10	0.443
JB77	9/13/95	0.005	0.005	0.005	0.005	0.10	0.419
JB84	9/26/95	0.005	0.008	0.005	0.005	0.10	0.454
JB91	10/10/95	0.005	0.010	0.005	0.008	0.10	0.439
JB97	10/17/95	0.005	0.005	0.005	0.005	0.10	0.450
JB100	10/24/95	0.005	0.005	0.005	0.005	0.10	0.492
JB107	11/4/95	0.005	0.007	0.005	0.005	0.12	0.473
JB117	11/10/95	0.005	0.009	0.005	0.005	0.10	0.874
JB123	12/4/95	0.005	0.005	0.005	0.005	0.10	0.969
JB131	4/20/96	0.006	0.014	0.005	0.005	0.10	0.986
JB138	5/4/96	0.005	0.016	0.005	0.005	0.10	0.934
JB145	5/18/96	0.005	0.011	0.005	0.005	0.79	0.834
JB152	6/1/96	0.005	0.009	0.005	0.005	0.10	0.614
JB159	6/15/96	0.005	0.008	0.005	0.005	0.10	0.481
JB166	6/29/96	0.005	0.007	0.005	0.005	0.10	0.429
Hoople Creek							
JB23	5/29/95	0.006	0.015	0.005	0.006	0.10	1.123
JB30	6/12/95	0.005	0.013	0.005	0.005	0.12	1.323
JB36	6/20/95	0.005	0.012	0.005	0.005	0.11	1.080
JB41	7/3/95	0.005	0.009	0.005	0.005	0.10	0.851
JB50	7/18/95	0.005	0.005	0.005	0.005	0.10	0.477
JB57	8/1/95	0.005	0.005	0.005	0.005	0.10	0.550
JB64	8/15/95	0.005	0.008	0.005	0.005	0.10	1.560
JB71	8/29/95	0.005	0.007	0.005	0.005	0.10	1.010
JB78	9/13/95	0.005	0.006	0.005	0.005	0.10	0.707
JB85	9/26/95	0.005	0.016	0.005	0.005	0.10	0.745
JB92	10/10/95	0.005	0.008	0.005	0.005	0.10	1.410
JB93	10/17/95	0.005	0.017	0.005	0.005	0.10	1.481
JB101	10/24/95	0.005	0.017	0.005	0.005	0.10	1.126
JB108	11/4/95	0.005	0.013	0.005	0.005	0.10	2.147
JB118	11/10/95	0.005	0.015	0.005	0.005	0.10	2.066
JB122	12/4/95	0.006	0.010	0.005	0.005	0.10	1.966
JB132	4/20/96	0.006	0.016	0.005	0.005	0.10	1.146
JB139	5/4/96	0.005	0.012	0.005	0.005	0.10	1.090
JB146	5/18/96	0.005	0.016	0.005	0.005	0.10	0.964
JB153	6/1/96	0.005	0.015	0.005	0.005	0.10	0.837
JB160	6/15/96	0.005	0.022	0.005	0.005	0.14	1.042
JB167	6/29/96	0.005	0.012	0.005	0.005	0.10	0.816

Sample ID	date	Ho	Yb	Lu	Tl	Pb	U
Long Sault Island							
JB35	6/20/95	0.005	0.005	0.005	0.005	0.10	0.345
JB37	7/3/95	0.005	0.005	0.005	0.005	0.10	0.310
JB47	7/18/95	0.005	0.005	0.005	0.005	0.10	0.245
JB54	8/1/95	0.005	0.005	0.005	0.005	0.10	0.273
JB61	8/15/95	0.005	0.005	0.005	0.005	0.10	0.256
JB67	8/29/95	0.005	0.005	0.005	0.005	0.10	0.326
JB74	9/13/95	0.005	0.005	0.005	0.005	0.10	0.367
JB81	9/26/95	0.005	0.005	0.005	0.005	0.10	0.412
JB88	10/10/95	0.005	0.007	0.005	0.005	0.10	0.331
JB94	10/17/95	0.005	0.005	0.005	0.005	0.10	0.380
JB102	10/24/95	0.005	0.005	0.005	0.005	0.10	0.405
JB109	11/4/95	0.005	0.005	0.005	0.005	0.10	0.434
JB114	11/10/95	0.005	0.005	0.005	0.008	0.10	0.435
JB128	4/20/96	0.005	0.005	0.005	0.005	0.10	0.462
JB135	5/4/96	0.005	0.005	0.005	0.005	0.13	0.398
JB142	5/18/96	0.005	0.005	0.005	0.005	0.10	0.353
JB149	6/1/96	0.005	0.005	0.005	0.005	0.10	0.390
JB156	6/15/96	0.005	0.007	0.005	0.005	0.11	0.319
JB163	6/29/96	0.005	0.005	0.005	0.005	0.15	0.258
Main Channel							
JB4	5/5/94	0.005	0.005	0.005	0.005	0.10	0.350
JB12	7/14/94	0.005	0.005	0.005	0.005	0.10	0.325
JB17	11/3/94	0.005	0.005	0.005	0.017	0.10	0.354
JB21	5/29/95	0.005	0.005	0.005	0.005	0.10	0.316
JB34	6/20/95	0.005	0.005	0.005	0.007	0.10	0.325
JB38	7/3/95	0.005	0.005	0.005	0.009	0.10	0.319
JB46	7/18/95	0.005	0.005	0.005	0.008	0.10	0.318
JB53	8/1/95	0.005	0.005	0.005	0.005	0.10	0.313
JB60	8/15/95	0.005	0.005	0.005	0.005	0.10	0.310
JB68	8/29/95	0.005	0.005	0.005	0.005	0.10	0.358
JB75	9/13/95	0.005	0.005	0.005	0.005	0.10	0.367
JB82	9/26/95	0.005	0.008	0.005	0.008	0.10	0.395
JB89	10/10/95	0.005	0.005	0.005	0.006	0.10	0.348
JB95	10/17/95	0.005	0.005	0.005	0.008	0.10	0.374
JB103	10/24/95	0.005	0.005	0.005	0.007	0.10	0.393
JB110	11/4/95	0.005	0.005	0.005	0.006	0.10	0.423
JB115	11/10/95	0.005	0.005	0.005	0.008	0.10	0.373
JB121	12/4/95	0.005	0.005	0.005	0.005	0.10	0.402
JB129	4/20/96	0.005	0.006	0.005	0.005	0.10	0.452
JB136	5/4/96	0.005	0.005	0.005	0.005	0.10	0.345
JB143	5/18/96	0.005	0.005	0.005	0.005	0.10	0.316
JB150	6/1/96	0.005	0.006	0.005	0.005	0.10	0.320
JB157	6/15/96	0.005	0.005	0.005	0.005	0.10	0.282
JB164	6/29/96	0.005	0.005	0.005	0.005	0.10	0.293

Sample ID	date	Ho	Yb	Lu	Tl	Pb	U
Whale Island							
JB11	7/14/94	0.005	0.005	0.005	0.005	0.10	0.339
JB18	11/3/94	0.005	0.005	0.005	0.013	0.10	0.349
JB20	5/29/95	0.005	0.005	0.005	0.008	0.10	0.330
JB29	6/12/95	0.005	0.005	0.005	0.005	0.10	0.349
JB39	7/3/95	0.005	0.005	0.005	0.006	0.10	0.332
JB48	7/18/95	0.005	0.005	0.005	0.008	0.10	0.362
JB55	8/1/95	0.005	0.005	0.005	0.005	0.10	0.320
JB62	8/15/95	0.005	0.005	0.005	0.005	0.10	0.326
JB69	8/29/95	0.005	0.006	0.005	0.005	0.10	0.382
JB76	9/13/95	0.005	0.005	0.005	0.006	0.10	0.359
JB83	9/26/95	0.005	0.006	0.005	0.005	0.10	0.347
JB90	10/10/95	0.005	0.006	0.005	0.005	0.10	0.371
JB96	10/17/95	0.005	0.005	0.005	0.007	0.16	0.373
JB104	10/24/95	0.005	0.005	0.005	0.008	0.21	0.374
JB111	11/4/95	0.005	0.005	0.005	0.008	0.15	0.420
JB116	11/10/95	0.005	0.005	0.005	0.005	0.10	0.385
JB124	12/4/95	0.005	0.005	0.005	0.005	0.10	0.353
JB130	4/20/96	0.005	0.006	0.005	0.005	0.10	0.545
JB137	5/4/96	0.005	0.005	0.005	0.005	0.10	0.374
JB144	5/18/96	0.005	0.005	0.005	0.005	0.10	0.370
JB151	6/1/96	0.005	0.005	0.005	0.005	0.10	0.290
JB158	6/15/96	0.005	0.005	0.005	0.005	0.10	0.287
JB165	6/29/96	0.005	0.005	0.005	0.005	1.49	0.294
Flannigans Point							
JB3	5/4/94	0.005	0.010	0.005	0.005	0.10	0.800
JB9	7/13/94	0.005	0.005	0.005	0.005	0.10	0.352
JB15	10/30/94	0.005	0.005	0.005	0.016	0.10	0.355
North and South of Cornwall Island							
JB2	5/4/94	0.005	0.005	0.005	0.005	0.10	0.350
JB1	5/2/94	0.005	0.005	0.005	0.005	0.10	0.370
JB8	7/12/94	0.005	0.005	0.005	0.005	0.10	0.373
JB14	10/30/94	0.005	0.005	0.005	0.019	0.10	0.353
Thompson Island							
JB7	7/11/94	0.005	0.005	0.005	0.005	0.10	0.344
JB13	10/30/94	0.005	0.005	0.005	0.014	0.10	0.345
Hoople Island							
JB5	5/5/94	0.005	0.005	0.005	0.005	0.10	0.340
JB10	7/14/94	0.005	0.005	0.005	0.005	0.10	0.332
JB16	11/3/94	0.005	0.005	0.005	0.014	0.10	0.366

Appendix 2

Field measurements

Appendix 2 Field data

Sample ID	date	T [°C]	pH	diss. oxygen [mg/L]	conductivity [µS/cm]	Eh [mV]	Alkalinity [mg/L]
Bay at Cooper Marsh							
JB25	5/29/95	19.0	9.10	12.5	334.0	358.0	108.2
JB27	6/12/95	16.0	8.66	9.0	335.0	414.9	112.0
JB32	6/20/95	19.0	8.51	11.2	299.0	380.9	112.0
JB43	7/3/95	22.0	8.55	11.1	299.0	361.0	105.7
JB45	7/18/95	20.0	8.63	8.7	300.0	350.5	99.4
JB52	8/1/95	23.5	8.71	9.5	299.0	436.9	103.1
JB59	8/15/95	24.0	8.54	10.0	296.0	377.8	96.8
JB66	8/29/95	22.0	8.78	9.8	289.0	399.1	112.0
JB73	9/13/95	18.0	8.60	9.7	293.0	429.0	122.1
JB80	9/26/95	15.2	8.97	11.1	301.0	403.4	112.0
JB87	10/10/95	14.1	8.44	9.8	302.0	380.6	110.6
JB99	10/17/95	12.0	8.32	9.8	306.0	429.6	105.1
JB106	10/24/95	11.9	8.40	9.9	312.0	415.1	105.7
JB113	11/4/95	7.0	8.47	11.9	311.0	441.2	109.3
JB120	11/10/95	6.0	8.46	11.6	309.5	438.2	109.3
JB127	4/20/96	5.1	8.31	12.5	308.0	366.2	110.6
JB134	5/4/96	8.2	8.73	14.1	303.0	360.3	106.9
JB141	5/18/96	10.1	8.69	14.6	294.0	373.5	108.1
JB148	6/1/96	13.5	8.50	13.6	288.0	349.9	103.3
JB155	6/15/96	16.9	9.04	14.7	287.0	360.4	108.1
JB162	6/29/96	19.0	9.29	15.6	291.0	350.4	104.5
Cooper Marsh							
JB42	7/3/95	24.0	7.38	4.5	322.0	426.0	115.8
JB44	7/18/95	19.0	7.44	5.0	315.0	349.8	109.5
JB51	8/1/95	22.0	7.49	2.5	305.0	444.4	119.6
JB58	8/15/95	23.5	8.06	2.8	300.0	374.9	103.8
JB65	8/29/95	20.5	7.85	6.5	296.0	396.5	114.5
JB72	9/13/95	14.5	7.75	7.5	313.0	430.4	134.7
JB79	9/26/95	12.8	7.93	10.1	301.0	412.2	110.7
JB86	10/10/95	11.9	7.26	4.0	314.0	409.0	126.4
JB98	10/17/95	9.4	7.45	3.5	269.0	391.5	103.3
JB105	10/24/95	9.9	7.20	5.5	300.0	411.2	111.8
JB112	11/4/95	3.8	7.78	11.7	407.0	409.0	127.6
JB119	11/10/95	3.1	8.60	11.8	408.0	424.3	134.9
JB125	12/4/95	0.1	7.30	2.2	395.0	325.3	137.4
JB126	4/20/96	9.1	7.67	10.4	392.0	362.0	128.8
JB133	5/4/96	15.1	8.43	13.2	468.0	366.9	133.7
JB140	5/18/96	17.2	7.84	9.8	368.0	379.5	132.5
JB147	6/1/96	20.3	7.85	10.4	335.0	365.6	133.7
JB154	6/15/96	25.3	7.86	9.6	337.0	362.6	131.3
JB161	6/29/96	21.9	8.98	14.2	296.0	337.3	113.0

Sample ID	date	T [°C]	pH	diss. oxygen [mg/L]	conductivity [µS/cm]	Eh [mV]	Alkalinity [mg/L]
Hoople Bay							
JB6	5/5/94	17.0	8.83	15.4	340.0	452.0	168.8
JB19	11/3/94	8.0	8.64	11.3	321.0	384.0	110.7
JB22	5/29/95	18.0	8.18	7.0	386.0	419.0	133.7
JB28	6/12/95	19.0	8.30	7.8	405.0	409.6	157.5
JB33	6/20/95	23.5	8.73	8.9	358.0	379.8	127.1
JB40	7/3/95	22.5	8.30	9.4	331.0	382.0	125.9
JB49	7/18/95	22.5	8.32	8.30	338.0	370.7	120.8
JB56	8/1/95	24.1	8.33	7.2	326.0	378.0	118.3
JB63	8/15/95	26.0	7.72	7.5	333.0	407.1	129.7
JB70	8/29/95	20.5	8.39	8.3	329.0	361.5	130.9
JB77	9/13/95	18.0	8.51	8.7	315.0	417.9	120.8
JB84	9/26/95	14.2	8.63	10.9	314.0	405.2	119.6
JB91	10/10/95	13.9	8.46	10.0	315.0	389.4	104.5
JB97	10/17/95	10.2	8.70	11.3	333.0	411.2	112.4
JB100	10/24/95	10.8	8.58	11.3	351.0	440.3	117.3
JB107	11/4/95	7.1	8.46	12.9	328.0	427.6	130.1
JB117	11/10/95	3.2	8.64	12.7	448.0	441.0	156.9
JB123	12/4/95	1.8	7.85	11.9	371.0	374.1	194.7
JB131	4/20/96	8.8	8.16	12.6	385.0	403.2	160.5
JB138	5/4/96	11.6	8.31	11.2	401.0	392.1	172.7
JB145	5/18/96	17.0	8.53	12.9	388.0	394.2	178.8
JB152	6/1/96	16.9	8.39	9.6	362.0	359.6	154.4
JB159	6/15/96	21.3	8.29	9.7	354.0	328.9	145.9
JB166	6/29/96	20.2	8.38	9.2	337.0	364.5	124.0
Hoople Creek							
JB23	5/29/95	19.0	8.05	8.0	491.0	418.0	175.1
JB30	6/12/95	22.0	8.50	14.2	504.5	384.7	221.9
JB36	6/20/95	17.0	7.96	3.0	518.0	380.2	221.9
JB41	7/3/95	24.5	8.03	7.5	463.0	364.8	194.1
JB50	7/18/95	22.0	8.11	9.30	526.0	376.3	187.8
JB57	8/1/95	22.0	8.19	11.1	589.0	368.4	157.5
JB64	8/15/95	26.5	8.34	10.3	559.0	407.0	205.4
JB71	8/29/95	15.0	7.69	3.2	586.5	371.4	218.1
JB78	9/13/95	17.0	7.82	2.0	614.0	413.1	196.6
JB85	9/26/95	13.1	7.69	5.9	673.0	387.7	202.9
JB92	10/10/95	14.0	8.11	10.3	707.0	367.6	156.9
JB93	10/17/95	3.9	8.26	16.0	657.0	431.6	203.2
JB101	10/24/95	10.9	7.85	9.7	530.0	438.6	167.8
JB108	11/4/95	4.2	7.88	12.0	618.0	431.7	204.4
JB118	11/10/95	6.0	8.30	16.2	610.0	441.1	204.4
JB122	12/4/95	1.4	7.46	11.5	586.0	381.5	226.3
JB132	4/20/96	9.8	7.78	9.4	351.0	406.3	170.3
JB139	5/4/96	12.0	7.62	11.6	404.0	391.9	192.2
JB146	5/18/96	17.0	7.79	8.6	410.0	385.5	205.6
JB153	6/1/96	23.0	8.55	13.7	425.0	375.0	226.3
JB160	6/15/96	23.3	8.70	13.4	455.0	358.4	236.1
JB167	6/29/96	21.9	8.27	8.8	520.0	355.6	272.7

Sample ID	date	T [°C]	pH	diss. oxygen [mg/L]	conductivity [µS/cm]	Eh [mV]	Alkalinity [mg/L]
Long Sault Island							
JB1	6/12/95	18.0	8.46	10.0	312.0	389.0	109.5
JB35	6/20/95	20.5	8.23	9.7	310.0	380.5	120.8
JB37	7/3/95	21.0	8.79	11.0	295.0	366.4	108.2
JB47	7/18/95	22.0	8.55	6.4	322.0	361.0	122.1
JB54	8/1/95	24.5	8.31	7.8	306.0	423.2	118.3
JB61	8/15/95	27.0	8.01	6.3	321.0	389.3	117.0
JB67	8/29/95	21.5	8.54	7.8	308.0	380.0	123.4
JB74	9/13/95	18.7	9.45	11.8	260.0	418.6	102.5
JB81	9/26/95	13.8	10.59	16.0	244.0	366.9	85.5
JB88	10/10/95	13.9	7.96	7.9	307.0	414.3	123.4
JB94	10/17/95	9.9	8.35	11.4	315.0	431.5	116.7
JB102	10/24/95	11.5	8.42	11.4	313.0	431.0	105.7
JB109	11/4/95	7.1	8.28	11.6	318.0	426.6	111.8
JB114	11/10/95	1.5	8.79	15.1	326.0	450.9	110.6
JB128	4/20/96	9.0	8.30	11.6	307.0	375.2	126.4
JB135	5/4/96	13.2	8.46	11.0	303.0	386.1	105.7
JB142	5/18/96	13.9	8.21	10.9	304.0	397.4	113.0
JB149	6/1/96	16.2	8.77	11.2	299.0	360.6	110.6
JB156	6/15/96	22.2	8.38	9.0	311.0	337.4	116.7
JB163	6/29/96	21.2	7.95	7.5	344.0	359.6	139.8
Main Channel upstream							
JB4	5/5/94	5.0	8.55	13.4	294.0	462.3	103.1
JB12	7/14/94	20.0	8.28	8.9	280.0	396.4	98.1
JB17	11/3/94	10.0	8.36	11.2	299.0	424.0	108.2
JB21	5/29/95	13.0	8.12	10.1	316.0	416.3	101.9
JB34	6/20/95	16.0	8.44	11.0	299.0	376.3	101.9
JB38	7/3/95	19.0	8.21	9.4	302.0	364.8	98.1
JB46	7/18/95	21.0	8.35	9.4	305.0	366.0	101.0
JB53	8/1/95	23.5	8.49	8.7	300.0	426.1	104.0
JB60	8/15/95	23.0	8.45	8.9	305.0	388.0	106.9
JB68	8/29/95	20.0	8.33	8.0	302.0	382.6	117.0
JB75	9/13/95	19.0	8.33	9.1	305.0	427.5	114.5
JB82	9/26/95	15.2	8.34	9.4	299.0	408.5	120.8
JB89	10/10/95	15.5	8.36	9.4	301.0	399.9	104.5
JB95	10/17/95	14.1	8.39	10.3	300.0	416.8	110.6
JB103	10/24/95	13.2	8.39	10.3	301.0	420.5	103.3
JB110	11/4/95	10.3	8.49	11.9	304.0	433.7	108.1
JB115	11/10/95	8.1	8.45	11.3	307.0	470.8	109.3
JB121	12/4/95	2.2	8.55	15.8	309.0	375.2	106.9
JB129	4/20/96	4.0	8.35	14.3	316.0	370.7	111.8
JB136	5/4/96	6.9	8.42	13.0	292.0	371.4	105.7
JB143	5/18/96	8.0	8.32	11.2	291.0	405.0	105.7
JB150	6/1/96	11.0	8.33	8.2	292.0	368.4	104.5
JB157	6/15/96	14.8	8.30	11.1	283.0	363.3	102.0
JB164	6/29/96	16.9	8.40	10.2	298.0	343.8	108.1

Sample ID	date	T [°C]	pH	diss. oxygen [mg/L]	conductivity [µS/cm]	Eh [mV]	Alkalinity [mg/L]
Whale Island							
JB11	7/14/94	21.7	8.38	8.2	305.0	394.5	103.1
JB18	11/3/94	9.0	8.38	10.5	249.0	391.0	106.9
JB20	5/29/95	15.0	8.00	11.0	297.0	445.5	111.2
JB29	6/12/95	18.0	8.61	8.9	316.0	396.3	112.0
JB39	7/3/95	22.0	8.44	8.0	306.0	378.2	101.9
JB48	7/18/95	23.0	8.33	8.8	310.0	364.2	104.4
JB55	8/1/95	25.0	8.21	8.0	301.0	408.3	114.5
JB62	8/15/95	25.0	8.49	9.1	299.0	388.0	98.1
JB69	8/29/95	22.0	8.75	9.4	296.0	370.5	110.7
JB76	9/13/95	18.0	8.79	10.1	294.0	415.1	112.0
JB83	9/26/95	15.2	8.47	10.4	295.0	460.8	115.8
JB90	10/10/95	14.9	8.50	9.8	291.0	402.0	103.3
JB96	10/17/95	13.5	8.48	10.80	293.5	395.3	103.3
JB104	10/24/95	12.0	8.45	11.8	296.0	388.5	103.3
JB111	11/4/95	8.2	8.46	12.9	306.5	394.1	109.3
JB116	11/10/95	4.9	8.65	14.1	317.0	428.4	110.6
JB124	12/4/95	0.6	8.31	14.8	321.0	374.5	113.0
JB130	4/20/96	5.0	8.55	14.1	303.0	370.3	115.4
JB137	5/4/96	9.0	8.35	10.6	303.5	372.1	110.6
JB144	5/18/96	11.9	8.52	12.2	304.0	399.2	114.2
JB151	6/1/96	14.0	8.70	11.9	286.0	358.0	103.3
JB158	6/15/96	17.1	8.88	13.8	290.0	343.9	102.0
JB165	6/29/96	19.1	8.45	10.4	293.0	326.4	103.3
Flannigans Point							
JB3	5/4/94	5.0	8.32	13.3	262.0	457.5	100.6
JB9	7/13/94	21.0	8.36	10.9	295.0	430.8	90.5
JB15	10/30/94	10.0	8.57	9.9	289.0	437.1	101.9
North and south of Cornwall Island							
JB2	5/4/94	5.5	8.66	12.8	302.0	486.0	101.9
JB1	5/2/94	4.0	8.42		290.0	520.0	101.9
JB8	7/12/94	19.8	8.19	9.7	297.0	430.0	90.5
JB14	10/30/94	11.0	8.12	8.3	300.0	419.0	95.6
Thompson Island							
JB7	7/11/94	23.0	8.61	11.8	280.0	428.0	100.6
JB13	10/30/94	11.0	8.28	10.8	333.0	407.0	98.1
Hoople Island							
JB5	5/5/94	7.0	8.25	12.8	289.0	472.1	110.7
JB10	7/14/94	20.9	8.36	8.9	297.0	406.0	104.4
JB16	11/3/94	10.0	8.57	11.0	297.0	385.0	100.6

Appendix 3

Deuterium and Oxygen data and calculations

Appendix 3.1 Precipitation heights, air temperature, $\delta^{18}\text{O}_{\text{H}_2\text{O}}$ and $\delta\text{D}_{\text{H}_2\text{O}}$ values in precipitation at Cornwall . The bold dates mark the end of a precipitation sample, while 'R' and 'S' signify rain and snow, respectively.

Date	[mm]	[°C]	$\delta^{18}\text{O}$	δD	Date	[mm]	[°C]	$\delta^{18}\text{O}$	δD	Date	[mm]	[°C]	$\delta^{18}\text{O}$	δD
R	7/18/95	2.03	23.9		R	10/24/95	5.08	13.0		S	2/11/96	2.54	-3.1	-12.7 -100
R	7/19/95		21.9	-8.9 -57	R	10/25/95	0.51	9.7		S	2/20/96	13.46	5.3	
R	7/20/95	1.02	21.1		R	10/26/95	0.00	9.2		S	2/21/96	6.35	4.2	-5.6 -28
R	7/21/95		23.3		R	10/27/95	0.51	12.5		S	2/24/96	11.18	3.9	
R	7/22/95		23.6		R	10/28/95	1.27	12.5		S	2/25/96	1.52	1.7	-16.5 -128
R	7/23/95	26.16	22.5	-7.5 -47	R	10/29/95	1.02	4.4	-4.2 -20	S	2/28/96	7.11	-4.5	-5.9 -62
R	7/26/95	1.52	25.8		R	11/1/95	2.79	1.9		S	3/3/96	1.02	-5.8	
R	7/27/95	0.00	24.2		R	11/2/95	6.60	9.4	-11.2 -75	S	3/4/96	0.00	-9.7	
R	7/28/95	3.56	23.6		R	11/7/95	5.33	5.8	-10.9 -72	S	3/5/96	0.51	-5.6	
R	7/29/95	8.89	27.5	-4.2 -19	R	11/8/95	2.03	0.8	-10.5 -81	S	3/6/96	0.00	-9.2	
R	8/1/95	0.25	24.4		R	11/11/95	10.16	13.6	-13.2 -86	S	3/7/96	0.76	-13.1	
R	8/2/95	0.00	20.0		S	11/12/95	12.45	1.9	-20.9 -156	S	3/8/96	1.27	-12.5	-26.8 -207
R	8/3/95	37.85	20.8		S	11/13/95	5.08	-4.5	-19.8 -148	S	3/20/96	0.76	1.7	
R	8/4/95	22.86	24.2	-5.5 -28	S	11/14/95	12.70	0.5		S	3/21/96	3.05	0.5	
R	8/5/95	41.91	20.5	-8.4 -48	S	11/15/95	2.79	0.3	-15.0 -114	S	3/22/96	1.52	-2.5	-19.2 -141
R	8/14/95	2.29	23.0		S	11/19/95	1.27	-1.7	-14.2 -106	R	4/1/96	0.51	3.6	-6.9 -63
R	8/15/95	2.03	27.2		S	11/21/95	1.52	2.5		S	4/8/96	13.72	1.9	-18.6 -142
R	8/16/95	0.00	24.7		S	11/22/95	0.00	-1.7		R	4/15/96	9.65	5.8	
R	8/17/95	0.00	24.7		S	11/23/95	1.52	-1.1		R	4/16/96	8.89	5.0	
R	8/18/95	0.00	21.9		S	11/24/95	0.00	-9.2		R	4/17/96	3.56	2.2	-10.5 -74
R	8/19/95	0.00	20.5		S	11/25/95	0.00	-6.4		R	4/20/96	19.30	10.5	-2.0 -19
R	8/20/95	0.00	22.8		S	11/26/95	0.00	0.0		R	4/22/96	4.06	10.0	
R	8/21/95	0.00	26.4		S	11/27/95	15.24	-5.0		R	4/23/96	6.35	7.5	
R	8/22/95	0.00	18.9		S	11/28/95	6.35	-7.5	-15.2 -98	R	4/24/96	0.25	5.3	-8.1 -67
R	8/23/95	1.52	18.0		S	12/1/95	11.43	0.5		R	5/10/96	17.27	13.3	
R	8/24/95	0.00	16.7	-5.8 -35	S	12/2/95	0.00	-6.4		R	5/11/96	22.10	9.2	
R	8/27/95	1.27	17.8		S	12/3/95	6.60	-9.7		R	5/12/96	9.20	3.3	-16.0 -123
R	8/28/95	0.00	17.5		S	12/4/95	2.79	-2.5	-17.0 -118	R	5/18/96	5.33	20.3	
R	8/29/95	0.00	20.8		S	12/14/95	21.08	-14.7	-9.5 -57	R	5/19/96	0.00	23.3	
R	8/30/95	0.00	16.9		S	12/16/95	2.79	-5.6	-16.4 -117	R	5/20/96	9.65	23.9	3.1 -4
R	8/31/95	4.57	17.2	-3.5 -17	S	12/20/95	3.81	-13.3		R	6/7/96	9.14	15.5	-7.2 -40
R	9/7/95	14.99	16.1	-9.3 -23	S	12/21/95	0.76	-9.7	-14.0 -109	R	6/8/96	10.16	14.4	-7.9 -56
R	9/13/95	2.79	21.9		S	12/25/95	0.00	-5.6		R	6/10/96	1.78	23.3	-3.9 -27
R	9/14/95	1.78	15.3	-5.3 -29	S	12/26/95	0.00	-8.1		R	6/12/96	0.00	23.3	
R	9/21/95	1.52	14.4		S	12/27/95	0.00	-8.9		R	6/13/96	3.56	22.2	-2.2 -29
R	9/22/95	16.26	15.5		S	12/28/95	0.00	-8.6		R	6/22/96	13.72	17.2	-7.2 -49
R	9/23/95	0.00	7.5		S	12/29/95	0.76	-7.2		R	6/29/96	1.27	21.1	
R	9/24/95	0.00	7.2		S	12/30/95	0.25	-3.6		R	6/30/96	1.02	24.4	
R	9/25/95	1.02	8.9		S	12/31/95	1.78	-3.3	-19.2 -141	R	7/1/96	0.00	23.3	
R	9/26/95	1.02	13.0		S	1/3/96	1.52	-19.5		R	7/2/96	0.00	22.0	
R	9/27/95	1.78	15.5	-10.6 -70	S	1/4/96	0.25	-23.6	-29.6 -216	R	7/3/96	37.50	27.0	
R	10/5/95	9.91	11.1		S	1/9/96	2.79	-9.7		R	7/4/96	31.60	17.0	-10.4 -72
R	10/6/95	72.64	11.4		S	1/10/96	1.27	-13.3	-18.3 -129	R	7/16/96	14.20	20.8	-11.3 -91
R	10/7/95	4.06	17.5	-12.5 -90	S	1/21/96	1.27	-7.2	-10.5 -72	R	7/19/96	18.40	22.3	-7.3 -48
R	10/14/95	14.48	16.4	-9.3 -64	S	1/29/96	0.76	-7.8	-11.7 -72	R	7/30/96	18.10	19.8	
R	10/21/95	50.29	13.9	-10.0 -60	S	2/8/96	7.37	3.9	-23.5 -175	R	7/31/96	1.90	19.0	-9.4 -59

Appendix 3.2 $\delta^{18}\text{O}_{\text{H}_2\text{O}}$, $\delta\text{D}_{\text{H}_2\text{O}}$ and Cl^- for surface water samples

Sample ID	date	$\delta^{18}\text{O}_{\text{H}_2\text{O}}$ [‰]	$\delta\text{D}_{\text{H}_2\text{O}}$ [‰]	Cl^- mmol/L
Bay at Cooper Marsh				
JB25	5/29/95	-7.2	-51.5	0.609
JB27	6/12/95	-6.7	-48.2	0.550
JB32	6/20/95	-6.8	-44.4	0.532
JB43	7/3/95	-6.7	-48.9	0.528
JB45	7/18/95	-6.6	-48.3	0.519
JB52	8/1/95	-6.8	-46.7	0.538
JB59	8/15/95	-6.8	-44.6	0.540
JB66	8/29/95	-6.4	-45.6	0.540
JB73	9/13/95	-5.7	-46.5	0.552
JB80	9/26/95	-6.5	-59.9	0.535
JB87	10/10/95	-6.5	-49.0	0.571
JB99	10/17/95	-6.5	-48.5	0.578
JB106	10/24/95	-7.5	-54.3	0.579
JB113	11/4/95	-7.1	-52.1	0.599
JB120	11/10/95	-6.6	-49.9	0.585
JB127	4/20/96	-7.1	-50.7	0.588
JB134	5/4/96	-7.1	-52.0	0.610
JB141	5/18/96	-7.2	-53.3	0.600
JB148	6/1/96	-7.3	-51.5	0.565
JB155	6/15/96	-7.5	-49.7	0.548
JB162	6/29/96	-7.3	-51.0	0.615
Cooper Marsh				
JB42	7/3/95	-6.6	-48.8	0.588
JB44	7/18/95	-6.3	-47.9	0.612
JB51	8/1/95	-6.1	-43.2	0.581
JB58	8/15/95	-6.3	-45.1	0.573
JB65	8/29/95	-6.1	-47.0	0.578
JB72	9/13/95	-6.6	-46.9	0.658
JB79	9/26/95	-6.3	-48.3	0.575
JB86	10/10/95	-6.5	-51.5	0.652
JB98	10/17/95	-6.5	-52.3	0.613
JB105	10/24/95	-7.0	-50.7	0.718
JB112	11/4/95	-7.2	-51.8	1.141
JB119	11/10/95	-7.5	-52.8	0.980
JB125	12/4/95	-8.8	-65.1	1.248
JB126	4/20/96	-11.5	-81.4	1.165
JB133	5/4/96	-10.9	-78.3	1.950
JB140	5/18/96	-10.3	-75.1	0.997
JB147	6/1/96	-8.8	-64.1	0.732
JB154	6/15/96	-7.2	-53.1	0.626
JB161	6/29/96	-7.2	-46.4	0.623

Sample ID	date	$\delta^{18}\text{O}_{\text{H}_2\text{O}}$ [‰]	$\delta\text{D}_{\text{H}_2\text{O}}$ [‰]	Cl^- mmol/L
Hoople Bay				
JB6	5/5/94	-11.7	-78.5	0.532
JB19	11/3/94	-6.8	-49.4	0.765
JB22	5/29/95	-7.4	-54.8	0.648
JB28	6/12/95	-7.0	-50.2	0.681
JB33	6/20/95	-6.7	-49.7	0.627
JB40	7/3/95	-6.5	-46.6	0.608
JB49	7/18/95	-6.6	-48.5	0.591
JB56	8/1/95	-6.3	-46.7	0.591
JB63	8/15/95	-5.9	-45.8	0.659
JB70	8/29/95	-6.2	-44.9	0.612
JB77	9/13/95	-6.0	-42.0	0.588
JB84	9/26/95	-6.0	-44.8	0.601
JB91	10/10/95	-6.6	-52.4	0.617
JB97	10/17/95	-6.8	-45.5	0.700
JB100	10/24/95	-6.5	-50.2	0.748
JB107	11/4/95	-7.1	-53.1	0.653
JB117	11/10/95	-7.6	-55.9	0.806
JB123	12/4/95	-7.5	-51.6	0.800
JB131	4/20/96	-12.2	-86.6	0.709
JB138	5/4/96	-11.3	-82.1	0.719
JB145	5/18/96	-11.6	-82.3	0.559
JB152	6/1/96	-9.7	-70.1	0.582
JB159	6/15/96	-7.8	-57.8	0.562
JB166	6/29/96	-7.3	-48.9	0.606
Hoople Creek				
JB23	5/29/95	-10.2	-70.7	0.288
JB30	6/12/95	-9.1	-64.4	0.282
JB36	6/20/95	-8.1	-58.1	0.305
JB41	7/3/95	-5.8	-51.8	0.638
JB50	7/18/95	-5.5	-50.6	0.684
JB57	8/1/95	-6.5	-49.4	0.406
JB64	8/15/95	-7.2	-51.6	0.372
JB71	8/29/95	-6.5	-53.7	0.500
JB78	9/13/95	-4.3	-39.5	0.690
JB85	9/26/95	-5.0	-43.5	1.206
JB92	10/10/95	-11.2	-79.7	0.866
JB93	10/17/95	-10.5	-71.6	0.730
JB101	10/24/95	-9.9	-63.4	0.622
JB108	11/4/95	-9.9	-66.6	0.678
JB118	11/10/95	-9.9	-70.3	0.569
JB122	12/4/95	-11.0	-73.9	0.701
JB132	4/20/96	-11.1	-76.9	0.335
JB139	5/4/96	-11.3	-73.7	0.408
JB146	5/18/96	-10.9	-71.5	0.434
JB153	6/1/96	-10.7	-71.5	0.248
JB160	6/15/96	-10.5	-71.4	0.283
JB167	6/29/96	-9.7	-64.6	0.320

Sample ID	date	$\delta^{18}\text{O}_{\text{H}_2\text{O}}$ [‰]	$\delta\text{D}_{\text{H}_2\text{O}}$ [‰]	Cl^- mmol/L
Long Sault Island				
JB1	6/12/95	-6.9	-53.0	xx
JB35	6/20/95	-6.8	-49.7	0.531
JB37	7/3/95	-6.6	-48.4	0.531
JB47	7/18/95	-6.2	-47.5	0.524
JB54	8/1/95	-6.4	-44.2	0.523
JB61	8/15/95	-6.2	-45.1	0.523
JB67	8/29/95	-5.7	-46.6	0.547
JB74	9/13/95	-6.2	-43.6	0.521
JB81	9/26/95	-6.0	-46.3	0.477
JB88	10/10/95	-7.1	-53.8	0.604
JB94	10/17/95	-6.7	-42.8	0.561
JB102	10/24/95	-6.8	-51.4	0.609
JB109	11/4/95	-7.4	-55.0	0.555
JB114	11/10/95	-7.9	-58.7	0.570
JB128	4/20/96	-8.4	-62.3	0.399
JB135	5/4/96	-7.9	-56.4	0.547
JB142	5/18/96	-7.4	-50.4	0.549
JB149	6/1/96	-7.4	-50.5	0.551
JB156	6/15/96	-7.3	-50.6	0.504
JB163	6/29/96	-6.6	-49.3	0.538
Main Channel				
JB4	5/5/94	-7.0	-50.5	0.584
JB12	7/14/94	-7.0	-52.8	0.601
JB17	11/3/94	-6.6	-47.8	0.606
JB21	5/29/95	-6.8	-47.1	0.517
JB34	6/20/95	-6.9	-46.4	0.532
JB38	7/3/95	-6.8	-52.4	0.524
JB46	7/18/95	-6.3	-49.5	0.521
JB53	8/1/95	-6.7	-43.6	0.528
JB60	8/15/95	-6.5	-45.5	0.533
JB68	8/29/95	-6.5	-48.9	0.537
JB75	9/13/95	-6.4	-47.4	0.539
JB82	9/26/95	-6.5	-48.4	0.549
JB89	10/10/95	-6.4	-48.2	0.559
JB95	10/17/95	-6.6	-51.1	0.561
JB103	10/24/95	-6.6	-49.9	0.570
JB110	11/4/95	-6.7	-50.4	0.579
JB115	11/10/95	-6.8	-50.9	0.574
JB121	12/4/95	-6.9	-51.4	0.582
JB129	4/20/96	-8.4	-61.0	0.540
JB136	5/4/96	-7.9	-56.4	0.590
JB143	5/18/96	-7.4	-51.7	0.551
JB150	6/1/96	-7.5	-49.4	0.564
JB157	6/15/96	-7.5	-47.0	0.545
JB164	6/29/96	-7.2	-50.7	0.615

Sample ID	date	$\delta^{18}\text{O}_{\text{H}_2\text{O}}$ [‰]	$\delta\text{D}_{\text{H}_2\text{O}}$ [‰]	Cl^- mmol/L
Whale Island				
JB11	7/14/94	-5.9	-47.8	0.603
JB18	11/3/94	-6.3	-49.1	0.610
JB20	5/29/95	-6.9	-49.1	0.536
JB29	6/12/95	-6.8	-49.1	0.534
JB39	7/3/95	-6.3	-47.1	0.539
JB48	7/18/95	-6.6	-45.8	0.536
JB55	8/1/95	-6.4	-44.4	0.532
JB62	8/15/95	-6.3	-48.4	0.539
JB69	8/29/95	-6.2	-45.8	0.543
JB76	9/13/95	-6.4	-45.0	0.550
JB83	9/26/95	-6.4	-49.1	0.535
JB90	10/10/95	-6.6	-49.6	0.564
JB96	10/17/95	-6.5	-49.2	0.568
JB104	10/24/95	-6.5	-48.7	0.572
JB111	11/4/95	-6.6	-49.0	0.590
JB116	11/10/95	-6.7	-49.3	0.587
JB124	12/4/95	-6.8	-49.7	0.611
JB130	4/20/96	-7.1	-54.4	0.616
JB137	5/4/96	-7.4	-54.6	0.552
JB144	5/18/96	-7.6	-54.7	0.611
JB151	6/1/96	-7.5	-51.9	0.565
JB158	6/15/96	-7.5	-49.0	0.553
JB165	6/29/96	-7.1	-43.4	0.581
Flannigans Point				
JB3	5/4/94	-7.1	-52.0	0.594
JB9	7/13/94	-7.2	-51.4	0.609
JB15	10/30/94	-6.6	-49.2	0.599
North and South of Cornwall Island				
JB2	5/4/94	-7.0	-50.6	0.624
JB1	5/2/94	-6.9	-51.5	0.587
JB8	7/12/94	-7.1	-49.3	0.597
JB14	10/30/94	-6.6	-50.3	0.590
Thompson Island				
JB7	7/11/94	-7.0	-52.8	0.600
JB13	10/30/94	-6.9	-49.0	0.590
Hoople Island				
JB5	5/5/94	-7.0	-48.1	0.598
JB10	7/14/94	-6.9	-51.4	0.610
JB16	11/3/94	-6.9	-47.9	0.600

Appendix 3.3 Calculation of the mixing of water masses in 'Hoople Bay'

The mixing between the 'Main Channel', 'Hoople Creek' and groundwater should be reflected by an intermediate composition of isotopic and chemical parameters in the 'Hoople Bay' mixing pool. The conditions for estimating the proportions of the endmembers are:

- (1) the parameters used for calculation are conservative, that is, they are not influenced by any other processes unrelated to mixing, such as chemical precipitation or biological consumption;
- (2) the isotopic or chemical composition of each source must be distinct from the other two sources;
- (3) the parameters used must be uncorrelated to each other;
- (4) all three components add up to 100 %.

With these conditions, an equation system can be established as follows:

$$\begin{array}{rcccccc}
 X * \delta^{18}O_x & + & Y * \delta^{18}O_y & + & Z * \delta^{18}O_z & = & \delta^{18}O_w \\
 X * Cl_x & + & Y * Cl_y & + & Z * Cl_z & = & Cl_w \\
 X & + & Y & + & Z & = & 1
 \end{array}$$

with

X, Y, Z = the relative proportions of groundwater, 'Hoople Creek' and the 'Main Channel'.

$\delta^{18}O_{x,y,z,w}$ and $Cl_{x,y,z,w}$ = oxygen isotope and chloride compositions of the groundwater, 'Hoople Creek', 'Main Channel' and 'Hoople Bay' waters, respectively.

The left side of this equation system can be transformed into a 3*3 matrix. Subsequently, its determinant ('Det A') can be calculated. In three other steps, each column of

the original 3*3 matrix is replaced with the result column of 'Hoople Bay' (i.e. the right side of the equation system), thus yielding the determinants 'Det B', 'Det C', and 'Det E'. According to Cramer's rule (Haeussler and Paul, 1987), the ratios of 'Det B'/'Det A', 'Det C'/'Det A' and 'Det E'/'Det A' yield the relative proportions of groundwater, 'Hoople Creek' and 'Main Channel' for the mixing in 'Hoople Bay'. Multiplying these proportions by 100 gives the percent contributions of these three endmembers.

Several calculations with various time intervals were attempted, but, except for the late summer, only mixing with monthly averages of the parameters yielded reasonable results, indicating that this is the necessary time for achieving a homogenous mixture in 'Hoople Bay'. The $\delta^{18}\text{O}_{\text{H}_2\text{O}}$ of the local groundwater was chosen to be -11.1 ‰ (Cane, 1996b), while its Cl⁻ concentration was estimated to be 100 mg/L, an intermediate value from Charron's (1978) report.

Appendix 4

Major ion and nutrient data and calculations

Appendix 4.1 Concentration of major ions and nutrients in mmol/L
including charge balance in percent (last column)

	date	HCO ₃ ⁻	SO ₄ ²⁻	Cl ⁻	NO ₃ ⁻	NO ₂ ⁻	NH ₄ ⁺	Ca ²⁺	Mg ²⁺	Na ⁺	K ⁺	SiO ₂	%
Bay at Cooper Marsh													
JB25	5/29/95	1.774	0.251	0.609	0.015	0.000	0.006	0.957	0.352	0.533	0.034	0.014	4.8
JB27	6/12/95	1.836	0.251	0.550	0.006	0.002	0.003	0.882	0.329	0.492	0.034	0.011	0.9
JB32	6/20/95	1.836	0.267	0.532	0.027	0.001	0.000	0.868	0.333	0.483	0.035	0.009	-0.2
JB43	7/3/95	1.732	0.262	0.528	0.007	0.001	0.001	0.843	0.337	0.476	0.032	0.010	1.4
JB45	7/18/95	1.629	0.251	0.519	0.007	0.001	0.002	0.813	0.333	0.476	0.034	0.007	2.7
JB52	8/1/95	1.691	0.258	0.538	0.006	0.001	0.002	0.847	0.337	0.481	0.033	0.009	2.3
JB59	8/15/95	1.587	0.263	0.540	0.005	0.001	0.008	0.833	0.335	0.478	0.032	0.012	3.6
JB66	8/29/95	1.836	0.264	0.540	0.005	0.001	0.001	0.800	0.342	0.483	0.034	0.012	-1.9
JB73	9/13/95	2.001	0.267	0.552	0.004	0.001	0.003	0.865	0.364	0.502	0.036	0.008	-1.6
JB80	9/26/95	1.836	0.285	0.535	0.010	0.000	0.001	0.897	0.360	0.507	0.037	0.011	1.8
JB87	10/10/95	1.813	0.287	0.571	0.011	0.000	0.006	0.912	0.363	0.507	0.040	0.006	2.2
JB99	10/17/95	1.723	0.285	0.578	0.007	0.000	0.000	0.917	0.362	0.505	0.039	0.009	3.7
JB106	10/24/95	1.733	0.288	0.579	0.013	0.000	0.001	0.904	0.355	0.500	0.039	0.010	2.7
JB113	11/4/95	1.793	0.286	0.599	0.011	0.000	0.002	0.926	0.357	0.494	0.039	0.014	2.1
JB120	11/10/95	1.793	0.289	0.585	0.015	0.000	0.002	0.921	0.359	0.498	0.038	0.008	2.1
JB127	4/20/96	1.813	0.262	0.588	0.016	0.000	0.001	0.933	0.333	0.509	0.036	0.006	2.3
JB134	5/4/96	1.753	0.255	0.610	0.011	0.000	0.003	0.911	0.329	0.492	0.033	0.006	2.1
JB141	5/18/96	1.773	0.253	0.600	0.013	0.001	0.001	0.898	0.325	0.487	0.033	0.010	1.3
JB148	6/1/96	1.693	0.233	0.565	0.007	0.000	0.000	0.893	0.309	0.470	0.036	0.007	3.2
JB155	6/15/96	1.773	0.242	0.548	0.012	0.000	0.000	0.911	0.309	0.478	0.033	0.014	2.3
JB162	6/29/96	1.713	0.252	0.615	0.015	0.000	0.003	0.878	0.309	0.509	0.031	0.015	1.2
Cooper Marsh													
JB42	7/3/95	1.898	0.225	0.588	0.002	0.001	0.000	0.833	0.354	0.552	0.018	0.017	0.1
JB44	7/18/95	1.794	0.160	0.612	0.005	0.001	0.000	0.822	0.354	0.622	0.021	0.033	4.6
JB51	8/1/95	1.960	0.146	0.581	0.004	0.000	0.001	0.858	0.360	0.587	0.012	0.054	3.4
JB58	8/15/95	1.701	0.239	0.573	0.004	0.001	0.006	0.817	0.348	0.520	0.025	0.021	2.2
JB65	8/29/95	1.877	0.243	0.578	0.004	0.001	0.003	0.777	0.356	0.522	0.020	0.013	-2.3
JB72	9/13/95	2.209	0.216	0.658	0.004	0.002	0.003	0.876	0.388	0.579	0.028	0.018	-2.6
JB79	9/26/95	1.815	0.275	0.575	0.002	0.000	0.001	0.907	0.376	0.542	0.039	0.008	3.4
JB86	10/10/95	2.072	0.173	0.652	0.003	0.000	0.000	0.908	0.353	0.594	0.047	0.018	1.4
JB98	10/17/95	1.693	0.070	0.613	0.002	0.000	0.000	0.776	0.309	0.559	0.045	0.062	6.2
JB105	10/24/95	1.833	0.095	0.718	0.001	0.000	0.000	0.815	0.329	0.642	0.050	0.051	4.2
JB112	11/4/95	2.092	0.233	1.141	0.006	0.000	0.003	1.023	0.409	0.972	0.069	0.020	2.7
JB119	11/10/95	2.212	0.331	0.980	0.015	0.000	0.003	1.131	0.431	0.772	0.048	0.022	1.0
JB125	12/4/95	2.252	0.131	1.248	0.001	0.000	0.004	0.943	0.396	1.035	0.056	0.047	0.1
JB126	4/20/96	2.112	0.180	1.165	0.028	0.000	0.006	1.083	0.354	1.031	0.056	0.047	4.0
JB133	5/4/96	2.192	0.224	1.950	0.003	0.000	0.002	1.093	0.432	1.544	0.051	0.029	0.6
JB140	5/18/96	2.172	0.196	0.997	0.009	0.001	0.000	1.068	0.370	0.883	0.043	0.041	3.1
JB147	6/1/96	2.192	0.202	0.732	0.003	0.000	0.003	0.956	0.358	0.687	0.031	0.006	0.3
JB154	6/15/96	2.152	0.188	0.626	0.006	0.001	0.016	1.020	0.362	0.639	0.028	0.044	4.4
JB161	6/29/96	1.852	0.239	0.623	0.007	0.004	0.005	0.896	0.321	0.526	0.028	0.010	0.5

	date	HCO ₃ ⁻	SO ₄ ²⁻	Cl ⁻	NO ₃ ⁻	NO ₂ ⁻	NH ₄ ⁺	Ca ²⁺	Mg ²⁺	Na ⁺	K ⁺	SiO ₂	%
Hoople Bay													
JB6	5/5/94	2.768	0.219	0.532	0.007	0.000		0.885	0.327	0.411	0.035		
JB19	11/3/94	1.815	0.318	0.765	0.003	0.000		0.855	0.327	0.953	0.042		
JB22	5/29/95	2.192	0.313	0.648	0.000	0.000	0.007	1.180	0.337	0.631	0.041	0.005	3.4
JB28	6/12/95	2.581	0.288	0.681	0.015	0.001	0.013	1.155	0.340	0.670	0.045	0.029	-1.8
JB33	6/20/95	2.084	0.279	0.627	0.011	0.004	0.002	1.087	0.344	0.633	0.044	0.008	3.7
JB40	7/3/95	2.064	0.268	0.608	0.007	0.004	0.003	1.002	0.340	0.598	0.043	0.015	1.6
JB49	7/18/95	1.981	0.253	0.591	0.005	0.006	0.003	0.967	0.337	0.600	0.042	0.023	2.6
JB56	8/1/95	1.939	0.248	0.591	0.007	0.001	0.005	0.898	0.325	0.589	0.040	0.017	0.8
JB63	8/15/95	2.126	0.259	0.659	0.004	0.001	0.003	0.904	0.331	0.663	0.041	0.014	-2.0
JB70	8/29/95	2.146	0.271	0.612	0.012	0.006	0.005	0.877	0.344	0.600	0.041	0.010	-3.6
JB77	9/13/95	1.981	0.269	0.588	0.007	0.002	0.003	0.884	0.366	0.572	0.039	0.004	0.0
JB84	9/26/95	1.960	0.288	0.601	0.002	0.000	0.003	0.886	0.362	0.605	0.039	0.007	0.0
JB91	10/10/95	1.713	0.287	0.617	0.007	0.001	0.004	0.877	0.348	0.650	0.042	0.005	3.9
JB97	10/17/95	1.842	0.326	0.700	0.005	0.000	0.000	0.921	0.344	0.681	0.045	0.001	0.8
JB100	10/24/95	1.922	0.360	0.748	0.007	0.001	0.006	1.004	0.350	0.761	0.051	0.005	1.8
JB107	11/4/95	2.132	0.357	0.653	0.040	0.000	0.002	1.042	0.364	0.581	0.046	0.014	-1.4
JB117	11/10/95	2.572	0.532	0.806	0.023	0.000	0.010	1.493	0.390	0.739	0.055	0.024	1.2
JB123	12/4/95	3.191	0.519	0.800	0.056	0.000	0.019	1.643	0.402	0.724	0.051	0.035	-2.0
JB131	4/20/96	2.632	0.189	0.709	0.048	0.001	0.007	1.452	0.243	0.622	0.051	0.076	3.9
JB138	5/4/96	2.832	0.209	0.719	0.018	0.001	0.001	1.509	0.284	0.657	0.051	0.020	3.7
JB145	5/18/96	2.931	0.180	0.559	0.007	0.000	0.003	1.524	0.267	0.574	0.049	0.029	4.3
JB152	6/1/96	2.532	0.216	0.582	0.004	0.002	0.003	1.285	0.309	0.596	0.043	0.001	3.8
JB159	6/15/96	2.392	0.223	0.562	0.007	0.001	0.004	1.125	0.300	0.596	0.043	0.018	1.2
JB166	6/29/96	2.032	0.237	0.606	0.000	0.014	0.003	1.065	0.300	0.605	0.041	0.016	3.9
Hoople Creek													
JB23	5/29/95	2.871	0.467	0.288	0.005	0.000	0.001	2.129	0.348	0.294	0.026	0.033	12.6
JB30	6/12/95	3.637	0.501	0.282	0.005	0.000	0.000	2.378	0.412	0.254	0.030	0.009	8.7
JB36	6/20/95	3.637	0.372	0.305	0.005	0.001	0.000	2.250	0.428	0.270	0.049	0.029	9.5
JB41	7/3/95	3.182	0.148	0.638	0.005	0.001	0.000	1.727	0.504	0.511	0.061	0.033	9.9
JB50	7/18/95	3.078	0.100	0.684	0.007	0.001	0.001	1.412	0.479	0.496	0.084	0.033	4.7
JB57	8/1/95	2.581	1.364	0.406	0.005	0.001	0.000	2.277	0.586	0.337	0.105	0.021	3.8
JB64	8/15/95	3.368	0.895	0.372	0.005	0.001	0.001	2.241	0.527	0.250	0.092	0.015	3.0
JB71	8/29/95	3.575	0.496	0.500	0.007	0.001	0.003	1.849	0.617	0.328	0.115	0.048	2.9
JB78	9/13/95	3.223	1.258	0.690	0.006	0.001	0.004	2.274	0.772	0.507	0.177	0.028	2.6
JB85	9/26/95	3.327	0.780	1.206	0.001	0.000	0.000	1.951	0.686	1.344	0.200	0.040	5.6
JB92	10/10/95	2.572	1.802	0.866	0.056	0.001	0.001	2.868	0.633	0.644	0.100	0.086	4.4
JB93	10/17/95	3.331	1.307	0.730	0.049	0.000	0.000	2.964	0.508	0.524	0.092	0.089	5.9
JB101	10/24/95	2.752	0.860	0.622	0.189	0.000	0.003	2.275	0.349	0.452	0.105	0.112	4.7
JB108	11/4/95	3.351	0.959	0.678	0.131	0.000	0.001	2.707	0.421	0.465	0.076	0.077	5.6
JB118	11/10/95	3.351	1.110	0.569	0.091	0.000	0.001	2.808	0.434	0.396	0.045	0.060	5.3
JB122	12/4/95	3.711	0.727	0.701	0.051	0.000	0.001	2.546	0.402	0.563	0.044	0.075	4.7
JB132	4/20/96	2.792	0.152	0.335	0.052	0.000	0.006	1.529	0.198	0.231	0.064	0.076	3.8
JB139	5/4/96	3.151	0.261	0.408	0.008	0.000	0.001	1.826	0.263	0.274	0.036	0.020	4.7
JB146	5/18/96	3.371	0.203	0.434	0.019	0.000	0.001	1.794	0.263	0.326	0.041	0.005	2.9
JB153	6/1/96	3.711	0.253	0.248	0.002	0.000	0.001	2.091	0.313	0.200	0.031	0.022	6.0
JB160	6/15/96	3.870	0.279	0.283	0.004	0.000	0.001	2.158	0.362	0.213	0.033	0.042	5.7
JB167	6/29/96	4.470	0.244	0.320	0.011	0.000	0.001	2.428	0.387	0.226	0.038	0.064	5.4

	date	HCO ₃ ⁻	SO ₄ ²⁻	Cl ⁻	NO ₃ ⁻	NO ₂ ⁻	NH ₄ ⁺	Ca ²⁺	Mg ²⁺	Na ⁺	K ⁺	SiO ₂	%
Long Sault Island													
JB T	6/12/95	1.794											
JB35	6/20/95	1.981	0.264	0.531	0.011	0.002	0.003	0.884	0.337	0.474	0.035	0.008	-1.6
JB37	7/3/95	1.774	0.259	0.531	0.004	0.001	0.004	0.887	0.342	0.470	0.036	0.006	2.4
JB47	7/18/95	2.001	0.238	0.524	0.005	0.001	0.011	0.919	0.350	0.468	0.038	0.026	0.8
JB54	8/1/95	1.939	0.247	0.523	0.002	0.001	0.001	0.883	0.342	0.470	0.036	0.014	0.0
JB61	8/15/95	1.919	0.255	0.523	0.006	0.004	0.000	0.919	0.350	0.468	0.034	0.008	1.3
JB67	8/29/95	2.022	0.266	0.547	0.011	0.004	0.001	0.862	0.356	0.485	0.034	0.021	-2.6
JB74	9/13/95	1.681	0.259	0.521	0.004	0.000	0.004	0.732	0.362	0.489	0.034	0.016	-0.2
JB81	9/26/95	1.401	0.255	0.477	0.002	0.000	0.004	0.564	0.336	0.441	0.026	0.013	-2.5
JB88	10/10/95	2.022	0.251	0.604	0.006	0.002	0.000	0.932	0.377	0.450	0.038	0.012	-0.5
JB94	10/17/95	1.912	0.276	0.561	0.004	0.000	0.001	0.954	0.381	0.483	0.041	0.014	2.7
JB102	10/24/95	1.733	0.271	0.609	0.008	0.000	0.003	0.947	0.372	0.463	0.038	0.014	4.2
JB109	11/4/95	1.833	0.280	0.555	0.010	0.000	0.003	0.944	0.373	0.468	0.038	0.006	3.0
JB114	11/10/95	1.813	0.289	0.570	0.013	0.000	0.003	0.964	0.377	0.459	0.036	0.007	3.4
JB128	4/20/96	2.072	0.269	0.399	0.011	0.001	0.011	0.986	0.407	0.348	0.031	0.016	2.5
JB135	5/4/96	1.733	0.270	0.547	0.008	0.000	0.001	0.933	0.358	0.452	0.031	0.010	4.0
JB142	5/18/96	1.852	0.263	0.549	0.021	0.002	0.004	0.923	0.354	0.448	0.033	0.012	1.5
JB149	6/1/96	1.813	0.256	0.551	0.005	0.001	0.003	0.946	0.342	0.457	0.036	0.002	3.2
JB156	6/15/96	1.912	0.249	0.504	0.004	0.001	0.001	0.978	0.358	0.444	0.031	0.013	3.8
JB163	6/29/96	2.292	0.262	0.538	0.007	0.001	0.035	1.075	0.383	0.465	0.036	0.013	1.3
Main Channel													
JB4	5/5/94	1.691	0.260	0.584	0.023	0.001		0.882	0.327	0.405	0.035		
JB12	7/14/94	1.608	0.266	0.601	0.016	0.000	0.001	0.820	0.329	0.474	0.036		
JB17	11/3/94	1.774	0.315	0.606				0.823	0.329	0.465	0.035		
JB21	5/29/95	1.670	0.258	0.517	0.022	0.000	0.004	0.841	0.325	0.455	0.033	0.010	1.8
JB34	6/20/95	1.670	0.265	0.532	0.017	0.003	0.001	0.876	0.335	0.474	0.035	0.010	3.2
JB38	7/3/95	1.608	0.261	0.524	0.012	0.002	0.001	0.857	0.335	0.472	0.035	0.010	4.0
JB46	7/18/95	1.656	0.254	0.521	0.011	0.001	0.000	0.851	0.335	0.474	0.035	0.010	3.3
JB53	8/1/95	1.704	0.255	0.528	0.010	0.001	0.001	0.822	0.340	0.465	0.034	0.009	1.3
JB60	8/15/95	1.753	0.259	0.533	0.010	0.002	0.000	0.835	0.342	0.468	0.033	0.011	0.6
JB68	8/29/95	1.919	0.259	0.537	0.008	0.002	0.000	0.815	0.340	0.470	0.036	0.013	-2.9
JB75	9/13/95	1.877	0.261	0.539	0.015	0.000	0.000	0.877	0.359	0.496	0.037	0.011	0.8
JB82	9/26/95	1.981	0.268	0.549	0.013	0.000	0.002	0.892	0.358	0.492	0.038	0.008	-0.8
JB89	10/10/95	1.713	0.275	0.559	0.013	0.001	0.006	0.879	0.355	0.487	0.038	0.008	2.9
JB95	10/17/95	1.813	0.282	0.561	0.008	0.000	0.003	0.898	0.356	0.483	0.038	0.013	1.4
JB103	10/24/95	1.693	0.279	0.570	0.010	0.000	0.001	0.891	0.356	0.485	0.037	0.010	3.2
JB110	11/4/95	1.773	0.279	0.579	0.015	0.000	0.001	0.899	0.355	0.481	0.038	0.007	1.7
JB115	11/10/95	1.793	0.280	0.574	0.011	0.000	0.001	0.913	0.354	0.481	0.037	0.011	1.9
JB121	12/4/95	1.753	0.279	0.582	0.019	0.000	0.000	0.903	0.349	0.472	0.036	0.009	1.7
JB129	4/20/96	1.833	0.253	0.540	0.018	0.000	0.001	0.931	0.337	0.492	0.036	0.007	2.8
JB136	5/4/96	1.733	0.249	0.590	0.016	0.000	0.001	0.906	0.329	0.483	0.033	0.006	2.6
JB143	5/18/96	1.733	0.236	0.551	0.009	0.001	0.000	0.871	0.313	0.431	0.033	0.014	1.2
JB150	6/1/96	1.713	0.238	0.564	0.010	0.001	0.003	0.903	0.309	0.452	0.033	0.014	2.6
JB157	6/15/96	1.673	0.233	0.545	0.008	0.000	0.003	0.888	0.296	0.448	0.033	0.007	2.9
JB164	6/29/96	1.773	0.253	0.615	0.021	0.000	0.003	0.866	0.305	0.500	0.036	0.007	-0.6

	date	HCO ₃ ⁻	SO ₄ ²⁻	Cl ⁻	NO ₃ ⁻	NO ₂ ⁻	NH ₄ ⁺	Ca ²⁺	Mg ²⁺	Na ⁺	K ⁺	SiO ₂	%
Whale Island													
JB11	7/14/94	1.691	0.264	0.603	0.015	0.000	0.001	0.848	0.325	0.478	0.036		
JB18	11/3/94	1.753	0.311	0.610				0.841	0.327	0.478	0.036		
JB20	5/29/95	1.823	0.261	0.536	0.020	0.000	0.000	0.907	0.325	0.465	0.036	0.009	1.1
JB29	6/12/95	1.836	0.258	0.534	0.000	0.001	0.005	0.858	0.325	0.472	0.035	0.011	-0.2
JB39	7/3/95	1.670	0.260	0.539	0.010	0.001	0.004	0.862	0.335	0.485	0.037	0.011	3.2
JB48	7/18/95	1.712	0.252	0.536	0.007	0.002	0.003	0.870	0.335	0.489	0.036	0.012	3.1
JB55	8/1/95	1.877	0.251	0.532	0.011	0.000	0.001	0.835	0.337	0.470	0.035	0.010	-1.2
JB62	8/15/95	1.608	0.259	0.539	0.007	0.001	0.003	0.812	0.340	0.478	0.033	0.011	2.7
JB69	8/29/95	1.815	0.261	0.543	0.004	0.001	0.001	0.797	0.342	0.481	0.035	0.011	-1.6
JB76	9/13/95	1.836	0.264	0.550	0.007	0.000	0.001	0.835	0.361	0.505	0.036	0.011	0.2
JB83	9/26/95	1.898	0.275	0.535	0.011	0.000	0.008	0.866	0.357	0.496	0.037	0.006	-0.1
JB90	10/10/95	1.693	0.279	0.564	0.011	0.000	0.001	0.862	0.355	0.492	0.037	0.004	2.4
JB96	10/17/95	1.693	0.279	0.568	0.011	0.000	0.002	0.873	0.355	0.494	0.038	0.006	2.7
JB104	10/24/95	1.693	0.280	0.572	0.012	0.000	0.002	0.883	0.355	0.496	0.038	0.007	3.0
JB111	11/4/95	1.793	0.285	0.590	0.013	0.000	0.001	0.921	0.365	0.492	0.039	0.006	2.2
JB116	11/10/95	1.813	0.308	0.587	0.019	0.000	0.003	0.976	0.365	0.520	0.040	0.007	3.3
JB124	12/4/95	1.852	0.298	0.611	0.017	0.000	0.003	0.964	0.364	0.502	0.038	0.006	2.0
JB130	4/20/96	1.892	0.229	0.616	0.015	0.000	0.004	0.998	0.296	0.531	0.036	0.024	2.9
JB137	5/4/96	1.813	0.231	0.552	0.013	0.000	0.000	0.946	0.325	0.500	0.036	0.005	4.0
JB144	5/18/96	1.872	0.243	0.611	0.015	0.000	0.000	0.963	0.321	0.500	0.036	0.015	1.9
JB151	6/1/96	1.693	0.236	0.565	0.013	0.000	0.000	0.878	0.313	0.461	0.033	0.011	2.4
JB158	6/15/96	1.673	0.232	0.553	0.009	0.000	0.001	0.901	0.296	0.461	0.033	0.007	3.4
JB165	6/29/96	1.693	0.247	0.581	0.014	0.000	0.001	0.886	0.288	0.483	0.028	0.007	1.4
Flannigans Point													
JB3	5/4/94	1.650	0.261	0.594	0.027	0.000		0.898	0.272	0.457	0.040		0.8
JB9	7/13/94	1.484	0.273	0.609	0.011	0.000	0.002	0.827	0.329	0.498	0.035		3.6
JB15	10/30/94	1.670	0.314	0.599				0.841	0.327	0.489	0.037		-0.6
North and south of Cornwall Island													
JB2	5/4/94	1.670	0.272	0.624	0.023	0.000		0.931	0.333	0.411	0.036		2.0
JB1	5/2/94	1.670	0.260	0.587	0.024	0.000		0.891	0.321	0.405	0.035		1.1
JB8	7/12/94	1.484	0.268	0.597	0.024			0.846	0.327	0.481	0.035		4.0
JB14	10/30/94	1.567	0.309	0.590				0.847	0.333	0.481	0.036		1.8
Thompson Island													
JB7	7/11/94	1.650	0.262	0.600	0.014	0.000		0.832	0.331	0.478	0.035		0.9
JB13	10/30/94	1.608	0.305	0.590	0.013	0.000	0.000	0.836	0.331	0.472	0.038		0.4
Hoople Island													
JB5	5/5/94	1.815	0.263	0.598	0.026	0.000		0.908	0.327	0.424	0.036		-0.6
JB10	7/14/94	1.712	0.262	0.610	0.019	0.001	0.003	0.842	0.331	0.478	0.035		0.0
JB16	11/3/94	1.650	0.310	0.600				0.833	0.327	0.461	0.035		-0.9

Appendix 4.2A Calculation of precipitation flux for major elements and nutrients over the Great Lakes

In order to calculate the percentage of major elements in the St. Lawrence River that originate from precipitation over the Great Lakes, its precipitation fluxes have to be compared to those of the river. The following tables illustrate how the fluxes of precipitation and 'Main Channel' water at Cornwall are related to each other. No data for Lake Michigan were available from the Environment Canada data set, but by averaging precipitation and concentration values of Lake Superior and Lake Huron a good estimate could be obtained. These averages should be realistic, because Lake Michigan lies between these two lakes.

Multiplying the average precipitation height (in m) of the Great Lakes by their surface area (in m²) yields the annual average volume of precipitation over each lake (Table 1A). The latter was multiplied by 1000 to convert from m³ to L.

lake	Superior	Michigan	Huron	Erie	Ontario
precip. (10 year av.) [m] (1)	0.823	0.85	0.877	0.837	0.8105
lake surface [m ²] (2)	8.210E+10	5.780E+10	5.960E+10	2.570E+10	1.896E+10
volume precip [L]	6.75683E+13	4.91300E+13	5.22692E+13	2.15109E+13	1.53671E+13

Table 1A Average precipitation heights for each of the 5 Great Lakes and the lake surface areas, yielding the average annual volume of precipitation for each lake. Sources (1) = (Environment Canada, 1994), (2) = (United States Environmental Protection Agency and Government of Canada, 1995).

Multiplying the annual precipitation volumes of each lake (Table 1A) with their average molar concentrations (Table 2A) yields the average flux of each major element in mol per year (Table 3A). The flux of each lake is then summarized for each element to yield the cumulative annual flux of major elements to the Great Lakes via precipitation (Table 3A, last column).

	Superior mol/L	Michigan mol/L	Huron mol/L	Erie mol/L	Ontario mol/L
Ca ²⁺	2.021E-05	2.345E-05	2.670E-05	2.520E-05	2.520E-05
Mg ²⁺	4.115E-06	6.584E-06	9.053E-06	6.173E-06	8.230E-06
Na ⁺	7.395E-06	1.196E-05	1.653E-05	8.699E-06	1.261E-05
K ⁺	2.302E-06	4.092E-06	5.882E-06	2.813E-07	3.836E-06
Cl ⁻	1.213E-05	1.763E-05	2.313E-05	1.608E-05	2.116E-05
SO ₄ ²⁻	2.958E-05	3.817E-05	4.676E-05	5.332E-05	5.166E-05
SiO ₂	8.822E-07	8.239E-07	7.656E-07	8.322E-07	9.987E-07
Inorg. N	6.038E-05	4.601E-05	1.006E-04	9.350E-05	9.334E-05

Table 2A Ten year averages of major element concentrations in Great Lakes precipitation from Environment Canada (1994).

	Superior mol/year	Michigan mol/year	Huron mol/year	Erie mol/year	Ontario mol/year	total mol/year
Ca ²⁺	1.366E+09	1.152E+09	1.395E+09	5.421E+08	3.872E+08	4.842E+09
Mg ²⁺	2.781E+08	3.235E+08	4.732E+08	1.328E+08	1.265E+08	1.334E+09
Na ⁺	4.996E+08	5.877E+08	8.640E+08	1.871E+08	1.938E+08	2.332E+09
K ⁺	1.555E+08	2.010E+08	3.075E+08	6.052E+06	5.895E+07	7.290E+08
Cl ⁻	8.196E+08	8.662E+08	1.209E+09	3.459E+08	3.251E+08	3.566E+09
SO ₄ ²⁻	1.998E+09	1.875E+09	2.444E+09	1.147E+09	7.938E+08	8.259E+09
SiO ₂	5.961E+07	4.048E+07	4.002E+07	1.790E+07	1.535E+07	1.734E+08
Inorg. N	4.079E+09	2.260E+09	5.256E+09	2.011E+09	1.434E+09	1.504E+10

Table 3A Annual average fluxes of major elements to the Great Lakes via precipitation.

The St. Lawrence River flux is calculated by multiplying the average annual discharge of the St. Lawrence River (2.35872×10^{14} L; Morin et al., 1994) with the annual average molar concentrations of the 'Main Channel'. Dividing the last column of Table 3A by the average St. Lawrence flux and multiplying this ratio by 100 yields the percent contribution of major elements added to the river via precipitation over the Great Lakes (Table 4A).

	average mol/L	Flux mol/year	% contribution from Precip in GL
Ca ²⁺	8.724E-04	2.058E+11	2.4
Mg ²⁺	3.362E-04	7.930E+10	1.7
Na ⁺	4.709E-04	1.111E+11	2.1
K ⁺	3.540E-05	8.350E+09	8.7
Cl ⁻	5.584E-04	1.317E+11	2.7
SO ₄ ²⁻	2.632E-04	6.209E+10	13.3
SiO ₂	9.766E-06	2.304E+09	7.5
Inorg. N	1.590E-05	3.751E+09	401.0

Table 4A Average molar concentrations and fluxes in the 'Main Channel' at Cornwall. The last column indicates the percent contribution of each element by precipitation over the Great Lakes.

Appendix 4.2B Calculation of precipitation flux for major elements and nutrients over the Great Lakes catchment area

These calculations are very similar to the ones above, except that the Great Lakes surface areas were substituted by of their catchment areas (Table 1B). Additionally, the size of the catchment area of the upper St. Lawrence between Kingston and Cornwall was estimated with GIS (Spans). The amount of precipitation over this sub-catchment area was assumed to be the same as over Lake Ontario.

catchment	Superior	Michigan	Huron	Erie	Ontario	upper St. Lawrence
precip. (10 year av.) [m] (1)	0.823	0.85	0.877	0.837	0.8105	0.8105
lake surface [m ²] (2)	1.277E+11	1.180E+11	1.341E+11	7.800E+10	6.403E+10	1.898E+10
volume precip [L]	1.05097E+14	1.003E+14	1.17606E+14	6.5286E+13	5.18963E+13	1.53833E+13

Table 1B Average precipitation heights for each of the 6 sub-catchment basins yielding their average annual volume. Sources are (1) = (Environment Canada, 1994), (2) = (United States Environmental Protection Agency and Government of Canada, 1995).

The molar concentrations of the major ions and nutrients are the same as in table 2A, with identical precipitation concentrations for the upper St. Lawrence catchment and Lake Ontario. This yields the molar fluxes in Table 2B.

	Superior mol/year	Michigan mol/year	Huron mol/year	Erie mol/year	Ontario mol/year	upper St. Lawrence mol/year	Sum mol/year
Ca ²⁺	2.124E+09	2.352E+09	3.140E+09	1.645E+09	1.308E+09	3.877E+08	1.096E+10
Mg ²⁺	4.325E+08	6.604E+08	1.065E+09	4.030E+08	4.271E+08	1.266E+08	3.114E+09
Na ⁺	7.771E+08	1.200E+09	1.944E+09	5.680E+08	6.546E+08	1.940E+08	5.337E+09
K ⁺	2.419E+08	4.104E+08	6.918E+08	1.837E+07	1.991E+08	5.902E+07	1.621E+09
Cl ⁻	1.275E+09	1.768E+09	2.720E+09	1.050E+09	1.098E+09	3.255E+08	8.237E+09
SO ₄ ²⁻	3.108E+09	3.828E+09	5.499E+09	3.481E+09	2.681E+09	7.946E+08	1.939E+10
SiO ₂	9.271E+07	8.264E+07	9.004E+07	5.433E+07	5.183E+07	1.536E+07	3.869E+08
inorg. N	6.345E+09	4.615E+09	1.183E+10	6.104E+09	4.844E+09	1.436E+09	3.517E+10

Table 2B Annual average fluxes of major elements to the Great Lakes catchment via precipitation.

Dividing the last column of Table 2B by the average St. Lawrence flux and multiplying this ratio by 100 yields the percent contribution of major elements added to the river via precipitation over the entire Great Lakes catchment (Table 3B).

	average mol/L	Flux mol/year	% contribution from precip. in GL-catchment
Ca ²⁺	8.724E-04	2.058E+11	5.3
Mg ²⁺	3.362E-04	7.930E+10	3.9
Na ⁺	4.709E-04	1.111E+11	4.8
K ⁺	3.540E-05	8.350E+09	19.4
Cl ⁻	5.584E-04	1.317E+11	6.3
SO ₄ ²⁻	2.632E-04	6.209E+10	31.2
SiO ₂	9.766E-06	2.304E+09	16.8
Inorg. N	1.590E-05	3.751E+09	937.6

Table 3B Average molar concentrations and fluxes in the 'Main Channel' at Cornwall. The last column indicates the percent contribution of each element by precipitation over the entire catchment area up to Cornwall.

Appendix 4.2C Atmospheric corrections for major ions

These corrections were performed by subtracting the precipitation fluxes of Ca^{2+} , Mg^{2+} , Na^+ , Cl^- , SO_4^{2-} , SiO_2 (Table 3B) from those of the 'Main Channel' and its related ecosystems. Because potassium is utilized excessively by land plants, the correction for the atmospheric K^+ contribution of table 4A was used. The precipitation input of major elements to 'Hoople Creek' is negligible, because of the small catchment area and higher total dissolved solids. The latter indicate that baseflow processes dominate the major ion chemistry of the creek. The 'Hoople Bay' samples were corrected according to the calculated proportional influences of the 'Main Channel' (Chapter 4, Fig. 4.6), and the 'Cooper Marsh' water samples were corrected only during the cold seasons (December 95 to May 96), with their contributions reduced by 50%. The latter is an estimate for the influences of the 'Main Channel' on 'Cooper Marsh' during these times.

Appendix 5

Carbon cycle and calculations

Appendix 5.1 List of parameters relevant for the carbon cycle (section 6.1 to 6.3).

	Date	T [°C]	pH	aCO ₃ ²⁻ [mol/L]	aHCO ₃ ⁻ [mol/L]	aCO ₂ (aq) [mol/L]	pCO ₂ [ppmV]	O ₂ [mg/L]	δ ¹³ C _(DIC) [‰]	chl-a [mg/m ³]	DOC [mg/L]	δ ¹⁸ O _{H2O} [‰]
Bay at Cooper Marsh												
JB25	5/29/95	19.0	9.10	9.19E-05	1.65E-03	2.99E-06	75	12.5	-3.3	3.18	5.4	-7.2
JB27	6/12/95	16.0	8.66	3.21E-05	1.71E-03	9.01E-06	205	9.0	-2.0	3.03	4.8	-6.7
JB32	6/20/95	19.0	8.51	2.45E-05	1.71E-03	1.21E-05	304	11.2	-1.5	1.36	4.0	-6.8
JB43	7/3/95	22.0	8.55	2.71E-05	1.62E-03	9.95E-06	274	11.1	-1.1	1.97	4.4	-6.7
JB45	7/18/95	20.0	8.63	2.93E-05	1.52E-03	8.04E-06	208	8.7	-1.2	2.00	4.0	-6.6
JB52	8/1/95	23.5	8.71	3.94E-05	1.58E-03	6.58E-06	189	9.5	-0.6	1.30	3.6	-6.8
JB59	8/15/95	24.0	8.54	2.53E-05	1.48E-03	9.09E-06	264	10.0	0.5	1.01	3.5	-6.8
JB66	8/29/95	22.0	8.78	4.87E-05	1.71E-03	6.21E-06	171	9.8	0.3	1.25	3.9	-6.4
JB73	9/13/95	18.0	8.60	3.20E-05	1.86E-03	1.09E-05	264	9.7	0.2	1.00	3.5	-5.7
JB80	9/26/95	15.2	8.97	6.42E-05	1.71E-03	4.47E-06	99	11.1	0.0	0.94	3.5	-6.5
JB87	10/10/95	14.1	8.44	1.82E-05	1.69E-03	1.53E-05	325	9.8	0.1	0.83	1.7	-6.5
JB99	10/17/95	12.0	8.32	1.24E-05	1.61E-03	2.00E-05	395	9.8	-0.2	1.02	3.0	-6.5
JB106	10/24/95	11.9	8.40	1.49E-05	1.61E-03	1.68E-05	330	9.9	-0.5	1.47	2.5	-7.5
JB113	11/4/95	7.0	8.47	1.57E-05	1.67E-03	1.65E-05	273	11.9	-0.2	1.18	2.5	-7.1
JB120	11/10/95	6.0	8.46	1.49E-05	1.67E-03	1.73E-05	276	11.6	-0.3	1.56	2.3	-6.6
JB127	4/20/96	5.1	8.31	1.04E-05	1.69E-03	2.54E-05	392	12.5	-0.9	1.47	3.0	-7.1
JB134	5/4/96	8.2	8.73	2.90E-05	1.63E-03	8.63E-06	149	14.1	-1.2	0.84	3.2	-7.1
JB141	5/18/96	10.1	8.69	2.83E-05	1.65E-03	9.15E-06	169	14.6	-1.1	0.03	2.8	-7.2
JB148	6/1/96	13.5	8.50	1.92E-05	1.58E-03	1.26E-05	264	13.6	-1.5	0.59	3.4	-7.3
JB155	6/15/96	16.9	9.04	7.60E-05	1.65E-03	3.57E-06	84	14.7	-1.0	0.73	3.5	-7.5
JB162	6/29/96	19.0	9.29	1.37E-04	1.60E-03	1.87E-06	47	15.6	-0.7	0.70	3.3	-7.3
Cooper Marsh												
JB42	7/3/95	24.0	7.38	2.09E-06	1.77E-03	1.57E-04	4548	4.5	-8.7	2.80	7.2	-6.6
JB44	7/18/95	19.0	7.44	2.03E-06	1.68E-03	1.39E-04	3499	5.0	-12.3	2.49	9.3	-6.3
JB51	8/1/95	22.0	7.49	2.67E-06	1.83E-03	1.29E-04	3557	2.5	-10.7	7.38	11.4	-6.1
JB58	8/15/95	23.5	8.06	8.88E-06	1.59E-03	2.96E-05	848	2.8	-5.6	4.30	6.1	-6.3
JB65	8/29/95	20.5	7.85	5.66E-06	1.75E-03	5.53E-05	1456	6.5	-6.2	2.52	5.8	-6.1
JB72	9/13/95	14.5	7.75	4.57E-06	2.05E-03	9.02E-05	1950	7.5	-5.9	4.23	7.2	-6.6
JB79	9/26/95	12.8	7.93	5.43E-06	1.69E-03	5.08E-05	1034	10.1	-3.9	3.95	4.5	-6.3
JB86	10/10/95	11.9	7.26	1.29E-06	1.93E-03	2.76E-04	5450	4.0	-6.6	10.52	6.1	-6.5
JB98	10/17/95	9.4	7.45	1.53E-06	1.59E-03	1.56E-04	2812	3.5	-9.0	8.61	14.9	-6.5
JB105	10/24/95	9.9	7.20	9.42E-07	1.71E-03	2.95E-04	5419	5.5	-10.0	5.98	12.9	-7.0
JB112	11/4/95	3.8	7.78	3.38E-06	1.94E-03	1.01E-04	1500	11.7	-5.6	13.38	9.7	-7.2
JB119	11/10/95	3.1	8.60	2.31E-05	2.04E-03	1.65E-05	238	11.8	-4.7	3.74	5.4	-7.5
JB125	12/4/95	0.1	7.30	1.06E-06	2.09E-03	3.69E-04	4827	2.2	-10.6	4.75	17.3	-8.8
JB126	4/20/96	9.1	7.67	3.13E-06	1.96E-03	1.15E-04	2055	10.4	-11.3	2.26	12.8	-11.5
JB133	5/4/96	15.1	8.43	2.21E-05	2.02E-03	1.81E-05	400	13.2	-8.5	8.05	12.0	-10.9
JB140	5/18/96	17.2	7.84	5.92E-06	2.01E-03	6.81E-05	1613	9.8	-8.4	7.82	9.6	-10.3
JB147	6/1/96	20.3	7.85	6.58E-06	2.04E-03	6.42E-05	1680	10.4	-4.5	19.04	7.4	-8.8
JB154	6/15/96	25.3	7.86	7.36E-06	2.00E-03	5.74E-05	1720	9.6	-4.6	30.78	8.3	-7.2
JB161	6/29/96	21.9	8.98	7.77E-05	1.73E-03	3.95E-06	108	14.2	-2.6	3.03	5.1	-7.2

	Date	T [°C]	pH	aCO ₃ ²⁻ [mol/L]	aHCO ₃ ⁻ [mol/L]	aCO ₂ (aq) [mol/L]	pCO ₂ [ppmV]	O ₂ [mg/L]	δ ¹³ C _(DIC) [‰]	chl-a [mg/m ³]	DOC [mg/L]	δ ¹⁸ O _{H2O} [‰]
Hoople Bay												
JB6	5/5/94	17.0	8.83	7.34E-05	2.57E-03	8.98E-06	211	15.4	-9.0		12.0	-11.7
JB19	11/3/94	8.0	8.64	2.43E-05	1.69E-03	1.10E-05	188	11.3	-2.1	19.73	4.4	-6.8
JB22	5/29/95	18.0	8.18	1.33E-05	2.03E-03	3.09E-05	753	7.0	-5.8	10.66	8.5	-7.4
JB28	6/12/95	19.0	8.30	2.12E-05	2.39E-03	2.71E-05	682	7.8	-1.4	11.15	9.6	-7.0
JB33	6/20/95	23.5	8.73	5.09E-05	1.93E-03	7.65E-06	219	8.9	-4.6	28.02	9.5	-6.7
JB40	7/3/95	22.5	8.30	1.83E-05	1.92E-03	2.08E-05	579	9.4	-4.1	10.56	6.6	-6.5
JB49	7/18/95	22.5	8.32	1.84E-05	1.84E-03	1.91E-05	532	8.3	-1.4	19.78	5.2	-6.6
JB56	8/1/95	24.1	8.33	1.91E-05	1.80E-03	1.79E-05	521	7.2	-1.2	9.28	4.6	-6.3
JB63	8/15/95	26.0	7.72	5.34E-06	1.98E-03	7.78E-05	2368	7.5	-1.7	9.39	4.8	-5.9
JB70	8/29/95	20.5	8.39	2.24E-05	2.00E-03	1.81E-05	477	8.3	-1.5	10.21	4.1	-6.2
JB77	9/13/95	18.0	8.51	2.58E-05	1.84E-03	1.32E-05	321	8.7	-1.5	8.97	3.6	-6.0
JB84	9/26/95	14.2	8.63	3.05E-05	1.82E-03	1.06E-05	227	10.9	-1.0	12.94	3.0	-6.0
JB91	10/10/95	13.9	8.46	1.79E-05	1.60E-03	1.38E-05	293	10.0	-1.1	9.90	3.6	-6.6
JB97	10/17/95	10.2	8.70	3.02E-05	1.71E-03	9.23E-06	171	11.3	-1.1	23.29	3.5	-6.6
JB100	10/24/95	10.8	8.58	2.43E-05	1.78E-03	1.25E-05	236	11.3	-2.3	16.54	4.8	-6.5
JB107	11/4/95	7.1	8.46	1.83E-05	1.98E-03	1.99E-05	330	12.9	-4.2	4.31	4.6	-7.1
JB117	11/10/95	3.2	8.64	2.95E-05	2.36E-03	1.72E-05	249	12.7	-5.0	14.64	9.9	-7.6
JB123	12/4/95	1.8	7.85	5.66E-06	2.92E-03	1.36E-04	1883	11.9	-10.3	6.53	9.6	-7.1
JB131	4/20/96	8.8	8.16	1.19E-05	2.43E-03	4.66E-05	821	12.6	-11.0	8.92	14.6	-12.2
JB138	5/4/96	11.6	8.31	1.97E-05	2.61E-03	3.32E-05	647	11.2	-8.9	8.91	13.8	-11.3
JB145	5/18/96	17.0	8.53	3.90E-05	2.70E-03	1.87E-05	439	12.9	-10.1	41.64	16.2	-11.6
JB152	6/1/96	16.9	8.39	2.43E-05	2.34E-03	2.24E-05	526	9.6	-6.2	17.53	9.4	-9.7
JB159	6/15/96	21.3	8.29	2.02E-05	2.22E-03	2.50E-05	673	9.7	-5.0	21.87	6.8	-7.8
JB166	6/29/96	20.2	8.38	2.06E-05	1.89E-03	1.76E-05	459	9.2	-3.8	15.81	5.8	-7.3
Hoople Creek												
JB23	5/29/95	19.0	8.05	1.33E-05	2.62E-03	5.24E-05	1316	8.0	-13.3	4.01	33.7	-10.2
JB30	6/12/95	22.0	8.50	5.07E-05	3.30E-03	2.22E-05	612	14.2	-12.0	2.64	33.0	-9.1
JB36	6/20/95	17.0	7.96	1.30E-05	3.31E-03	8.39E-05	1976	3.0	-12.3	5.31	35.9	-8.1
JB41	7/3/95	24.5	8.03	1.58E-05	2.92E-03	5.65E-05	1661	7.5	-10.0	3.39	38.3	-5.8
JB50	7/18/95	22.0	8.11	1.75E-05	2.83E-03	4.75E-05	1306	9.3	-8.2	2.68	23.8	-5.5
JB57	8/1/95	22.0	8.19	1.76E-05	2.33E-03	3.18E-05	875	11.1	-10.5	1.60	14.8	-6.5
JB64	8/15/95	26.5	8.34	3.56E-05	3.05E-03	2.79E-05	857	10.3	-9.8	9.88	23.4	-7.2
JB71	8/29/95	15.0	7.69	6.53E-06	3.26E-03	1.60E-04	3507	3.2	-10.0	1.74	20.7	-6.5
JB78	9/13/95	17.0	7.82	8.35E-06	2.90E-03	1.00E-04	2359	2.0	-9.7	2.00	18.4	-4.3
JB85	9/26/95	13.1	7.69	5.78E-06	3.01E-03	1.52E-04	3120	5.9	-9.1	3.33	16.1	-5.0
JB92	10/10/95	14.0	8.11	1.20E-05	2.30E-03	4.28E-05	908	10.3	-10.5	1.44	16.3	-11.2
JB93	10/17/95	3.9	8.26	1.63E-05	2.99E-03	5.01E-05	743	16.0	-11.8	1.82	24.5	-10.5
JB101	10/24/95	10.9	7.85	6.50E-06	2.50E-03	9.14E-05	1740	9.7	-13.6	1.88	23.9	-9.9
JB108	11/4/95	4.2	7.88	6.91E-06	3.02E-03	1.21E-04	1815	12.0	-13.1	2.64	22.0	-9.9
JB118	11/10/95	6.0	8.30	1.93E-05	3.02E-03	4.38E-05	699	16.2	-11.7	1.04	24.0	-9.9
JB122	12/4/95	1.4	7.46	2.64E-06	3.36E-03	3.85E-04	5247	11.5	-13.7	1.17	17.7	-11.0
JB132	4/20/96	9.8	7.78	5.44E-06	2.58E-03	1.16E-04	2125	9.4	-12.0	3.40	19.4	-11.1
JB139	5/4/96	12.0	7.62	4.52E-06	2.90E-03	1.78E-04	3528	11.6	-11.7	2.36	23.2	-11.3
JB146	5/18/96	17.0	7.79	8.15E-06	3.10E-03	1.17E-04	2755	8.6	-13.1	5.08	24.6	-10.9
JB153	6/1/96	23.0	8.55	5.92E-05	3.39E-03	2.02E-05	571	13.7	-11.1	2.11	28.2	-10.7
JB160	6/15/96	23.3	8.70	8.78E-05	3.53E-03	1.48E-05	422	13.4	-10.7	2.68	31.7	-10.5
JB167	6/29/96	21.9	8.27	3.66E-05	4.06E-03	4.65E-05	1276	8.8	-12.0	6.21	30.1	-9.7

	Date	T [°C]	pH	aCO ₃ ²⁻ [mol/L]	aHCO ₃ ⁻ [mol/L]	aCO ₂ (aq) [mol/L]	pCO ₂ [ppmV]	O ₂ [mg/L]	δ ¹³ C _(DIC) [‰]	chl-a [mg/m ³]	DOC [mg/L]	δ ¹⁸ O _{H2O} [‰]
Long Sault Island												
JB35	6/20/95	20.5	8.23	1.43E-05	1.84E-03	2.42E-05	638	9.7	-2.8	3.23	3.8	-6.8
JB37	7/3/95	21.0	8.79	4.71E-05	1.65E-03	5.94E-06	159	11.0	-1.5	7.98	4.4	-6.6
JB47	7/18/95	22.0	8.55	3.13E-05	1.86E-03	1.15E-05	315	6.4	-1.4	62.96	5.6	-6.2
JB54	8/1/95	24.5	8.31	1.84E-05	1.81E-03	1.87E-05	549	7.8	-1.3	26.11	4.2	-6.4
JB61	8/15/95	27.0	8.01	9.57E-06	1.78E-03	3.57E-05	1109	6.3	-2.1	21.65	5.1	-6.2
JB67	8/29/95	21.5	8.54	3.06E-05	1.88E-03	1.19E-05	324	7.8	-3.1	13.84	8.1	-5.7
JB74	9/13/95	18.7	9.45	1.94E-04	1.57E-03	1.28E-06	32	11.8	-1.1	3.57	3.4	-6.2
JB81	9/26/95	13.8	10.59	1.97E-03	1.32E-03	8.55E-08	2	16.0	-8.9	1.01	4.9	-6.0
JB88	10/10/95	13.9	7.96	6.68E-06	1.88E-03	5.16E-05	1091	7.9	-1.2	4.28	3.4	-7.1
JB94	10/17/95	9.9	8.35	1.39E-05	1.78E-03	2.16E-05	397	11.4	-0.7	3.33	3.8	-6.7
JB102	10/24/95	11.5	8.42	1.55E-05	1.61E-03	1.61E-05	313	11.4	-0.9	3.45	3.0	-6.8
JB109	11/4/95	7.1	8.28	1.04E-05	1.71E-03	2.60E-05	432	11.6	-1.0	2.92	2.8	-7.4
JB114	11/10/95	1.5	8.79	2.77E-05	1.69E-03	9.27E-06	127	15.1	-1.5	0.87	2.6	-7.9
JB128	4/20/96	9.0	8.30	1.31E-05	1.93E-03	2.68E-05	477	11.6	-4.1	15.18	3.7	-8.4
JB135	5/4/96	13.2	8.46	1.78E-05	1.61E-03	1.42E-05	293	11.0	-2.4	6.14	3.3	-7.9
JB142	5/18/96	13.9	8.21	1.09E-05	1.73E-03	2.66E-05	563	10.9	-1.8	4.67	2.7	-7.4
JB149	6/1/96	16.2	8.77	4.10E-05	1.69E-03	6.87E-06	157	11.2	-2.0	13.27	4.2	-7.4
JB156	6/15/96	22.2	8.38	2.03E-05	1.78E-03	1.61E-05	446	9.0	-2.4	52.75	4.2	-7.3
JB163	6/29/96	21.2	7.95	8.84E-06	2.12E-03	5.24E-05	1408	7.5	-3.8	36.25	8.2	-6.6
Main Channel												
JB4	5/5/94	5.0	8.55	1.67E-05	1.58E-03	1.37E-05	211	13.4	-2.0	1.01	3.0	-7.0
JB12	7/14/94	20.0	8.28	1.29E-05	1.50E-03	1.77E-05	460	8.9	-1.3	0.75	3.1	-7.0
JB17	11/3/94	10.0	8.36	1.32E-05	1.65E-03	1.97E-05	362	11.2	-1.8	0.28	2.8	-6.6
JB21	5/29/95	13.0	8.12	7.79E-06	1.56E-03	3.02E-05	619	10.1	-1.0	1.08	3.7	-6.8
JB34	6/20/95	16.0	8.44	1.76E-05	1.56E-03	1.36E-05	310	11.0	-1.7	1.88	3.6	-6.9
JB38	7/3/95	19.0	8.21	1.07E-05	1.50E-03	2.12E-05	532	9.4	-1.1	0.99	3.5	-6.8
JB46	7/18/95	21.0	8.35	1.60E-05	1.54E-03	1.53E-05	409	9.4	-0.4	0.95	3.3	-6.3
JB53	8/1/95	23.5	8.49	2.40E-05	1.59E-03	1.10E-05	316	8.7	2.2	0.98	3.0	-6.7
JB60	8/15/95	23.0	8.45	2.22E-05	1.63E-03	1.25E-05	353	8.9	-0.1	1.04	3.3	-6.5
JB68	8/29/95	20.0	8.33	1.73E-05	1.79E-03	1.88E-05	488	8.0	0.3	1.09	3.2	-6.5
JB75	9/13/95	19.0	8.33	1.65E-05	1.75E-03	1.87E-05	469	9.1	0.1	1.15	3.4	-6.4
JB82	9/26/95	15.2	8.34	1.62E-05	1.84E-03	2.06E-05	455	9.4	-0.1	0.60	2.7	-6.5
JB89	10/10/95	15.5	8.36	1.48E-05	1.60E-03	1.69E-05	379	9.4	-0.1	0.76	3.0	-6.4
JB95	10/17/95	14.1	8.39	1.62E-05	1.69E-03	1.72E-05	366	10.3	0.3	1.15	3.1	-6.6
JB103	10/24/95	13.2	8.39	1.48E-05	1.58E-03	1.63E-05	337	10.3	-0.2	1.05	2.4	-6.6
JB110	11/4/95	10.3	8.49	1.80E-05	1.65E-03	1.44E-05	268	11.9	-0.4	0.64	2.4	-6.7
JB115	11/10/95	8.1	8.45	1.55E-05	1.67E-03	1.68E-05	289	11.3	-0.8	0.65	2.2	-6.8
JB121	12/4/95	2.2	8.55	1.58E-05	1.63E-03	1.53E-05	214	15.8	-0.1	0.70	2.4	-6.9
JB129	4/20/96	4.0	8.35	1.11E-05	1.71E-03	2.41E-05	359	14.3	-1.5	0.48	2.7	-8.4
JB136	5/4/96	6.9	8.42	1.35E-05	1.62E-03	1.80E-05	297	13.0	-0.9	0.79	3.0	-7.9
JB143	5/18/96	8.0	8.32	1.11E-05	1.62E-03	2.21E-05	379	11.2	-1.3	0.74	3.1	-7.4
JB150	6/1/96	11.0	8.33	1.23E-05	1.60E-03	1.99E-05	380	8.2	-1.6	0.58	3.1	-7.5
JB157	6/15/96	14.8	8.30	1.24E-05	1.56E-03	1.93E-05	421	11.1	-1.6	0.76	3.1	-7.5
JB164	6/29/96	16.9	8.40	1.74E-05	1.65E-03	1.56E-05	366	10.2	-1.4	0.79	3.0	-7.2

	Date	T [°C]	pH	aCO ₃ ²⁻ [mol/L]	aHCO ₃ ⁻ [mol/L]	aCO ₂ (aq) [mol/L]	pCO ₂ [ppmV]	O ₂ [mg/L]	δ ¹³ C _(DIC) [‰]	chl-a [mg/m ³]	DOC [mg/L]	δ ¹⁸ O _{H2O} [‰]
Whale Island												
JB11	7/14/94	21.7	8.38	1.77E-05	1.58E-03	1.44E-05	393	8.2	-1.9	3.55	3.5	-5.9
JB18	11/3/94	9.0	8.38	1.33E-05	1.63E-03	1.90E-05	337	10.5	-1.1	0.65	3.3	-6.3
JB20	5/29/95	15.0	8.00	6.80E-06	1.70E-03	4.16E-05	916	11.0	-1.3	1.95	3.4	-6.9
JB29	6/12/95	18.0	8.61	3.01E-05	1.71E-03	9.77E-06	238	8.9	-2.6	1.18	4.3	-6.8
JB39	7/3/95	22.0	8.44	2.03E-05	1.56E-03	1.24E-05	340	8.0	-3.6	2.19	4.1	-6.3
JB48	7/18/95	23.0	8.33	1.65E-05	1.60E-03	1.61E-05	455	8.8	-1.2	2.80	3.8	-6.6
JB55	8/1/95	25.0	8.21	1.43E-05	1.75E-03	2.26E-05	674	8.0	-0.4	0.81	4.3	-4.2
JB62	8/15/95	25.0	8.49	2.33E-05	1.50E-03	1.02E-05	304	9.1	-0.2	2.28	3.4	-6.3
JB69	8/29/95	22.0	8.75	4.49E-05	1.69E-03	6.58E-06	181	9.4	0.7	2.07	3.6	-6.2
JB76	9/13/95	18.0	8.79	4.55E-05	1.71E-03	6.45E-06	157	10.1	0.1	2.17	3.5	-6.4
JB83	9/26/95	15.2	8.47	2.10E-05	1.77E-03	1.46E-05	324	10.4	-0.1	1.93	2.7	-6.4
JB90	10/10/95	14.9	8.50	1.99E-05	1.58E-03	1.23E-05	269	9.8	0.2	2.05	3.1	-6.6
JB96	10/17/95	13.5	8.48	1.83E-05	1.58E-03	1.32E-05	275	10.8	0.2	1.55	3.0	-6.5
JB104	10/24/95	12.0	8.45	1.64E-05	1.58E-03	1.46E-05	288	11.8	0.1	7.72	3.0	-6.5
JB111	11/4/95	8.2	8.46	1.59E-05	1.67E-03	1.64E-05	283	12.9	-0.4	1.36	2.3	-6.6
JB116	11/10/95	4.9	8.65	2.25E-05	1.69E-03	1.16E-05	178	14.1	-0.8	7.90	2.6	-6.7
JB124	12/4/95	0.6	8.31	9.09E-06	1.72E-03	2.94E-05	391	14.8	-0.8	1.01	2.8	-6.8
JB130	4/20/96	5.0	8.55	1.87E-05	1.76E-03	1.53E-05	235	14.1	-4.8	2.81	5.9	-7.1
JB137	5/4/96	9.0	8.35	1.28E-05	1.69E-03	2.10E-05	373	10.6	-1.4	1.01	3.6	-7.4
JB144	5/18/96	11.9	8.52	2.13E-05	1.74E-03	1.37E-05	270	12.2	-2.5	2.57	4.0	-7.6
JB151	6/1/96	14.0	8.70	3.08E-05	1.58E-03	7.89E-06	168	11.9	-1.6	0.89	3.4	-7.5
JB158	6/15/96	17.1	8.88	4.99E-05	1.56E-03	4.86E-06	115	13.8	-1.2	4.38	3.3	-7.5
JB165	6/29/96	19.1	8.45	1.97E-05	1.58E-03	1.28E-05	323	10.4	-1.4	3.10	3.5	-7.1
Flannigans Point												
JB3	5/4/94	5.0	8.32	9.61E-06	1.54E-03	2.27E-05	350	13.3	-2.0	0.70	3.1	-7.05
JB9	7/13/94	21.0	8.36	1.46E-05	1.38E-03	1.34E-05	358	10.9	-2.5	1.07	3.2	-7.15
JB15	10/30/94	10.0	8.57	2.02E-05	1.56E-03	1.14E-05	210	9.9	-1.3	0.47	3.2	-6.64
North and south of Cornwall Island												
JB2	5/4/94	5.5	8.66	2.16E-05	1.56E-03	1.03E-05	162	12.8	-0.8 xx		3.2	-6.95
JB1	5/2/94	4.0	8.42	1.19E-05	1.56E-03	1.87E-05	279		0.7	1.01	2.7	-6.92
JB8	7/12/94	19.8	8.19	9.63E-06	1.38E-03	2.02E-05	521	9.7	0.1	0.68	3.1	-7.07
JB14	10/30/94	11.0	8.12	6.91E-06	1.46E-03	2.95E-05	564	8.3	-0.6	0.49	3.1	-6.62
Thompson Island												
JB7	7/11/94	23.0	8.61	3.02E-05	1.54E-03	8.14E-06	230	11.8	-1.0	1.01	3.6	-7.01
JB13	10/30/94	11.0	8.28	1.03E-05	1.50E-03	2.10E-05	400	10.8	-1.0	0.77	3.1	-6.93
Hoople Island												
JB5	5/5/94	7.0	8.25	9.59E-06	1.69E-03	2.78E-05	459	12.8		0.84	2.9	-6.95
JB10	7/14/94	20.9	8.36	1.69E-05	1.60E-03	1.55E-05	412	8.9	-2.1	1.82	3.2	-6.89
JB16	11/3/94	10.0	8.57	1.99E-05	1.54E-03	1.13E-05	208	11.0	-0.3	0.64	2.8	-6.86

Appendix 5.2A List of parameters studied for POC study (section 6.4)

Sample ID	Date	chl-A [$\mu\text{g/L}$]	POC [$\mu\text{g/L}$]	POC/chl-a -	$\delta^{13}\text{C}_{\text{POC}}$ [‰]	$\delta^{13}\text{C}_{\text{DIC}}$ [‰]	aHCO_3^- μM	aCO_3^- μM	$\text{aCO}_2(\text{aq})$ μM	DIC μM
Bay at Cooper Marsh										
JB27	6/12/95	3.0	277	91.6	-26.5	-2.0	1711	32	9	1752
JB52	8/1/95	1.3	105	81.3	-21.8	-0.6	1576	39	7	1622
JB87	10/10/95	0.8	102	122.6	-25.9	0.1	1688	18	15	1721
JB127	4/20/96	1.5	91	62.3	-25.3	-0.9	1690	10	25	1726
Cooper Marsh										
JB58	8/15/95	4.3	391	90.7	-25.7	-5.6	1587	9	30	1625
JB98	10/17/95	8.6	711	82.6	-31.4	-9.0	1587	2	156	1745
JB125	12/4/95	4.8	964	202.7	-27.0	-10.6	2090	1	369	2460
JB126	4/20/96	2.3	361	159.6	-30.9	-11.3	1955	3	115	2073
Hoople Bay										
JB22	5/29/95	10.7	1095	102.7	-28.2	-5.8	2028	13	31	2072
JB28	6/12/95	11.2	832	74.6	-30.0	-1.4	2386	21	27	2434
JB56	8/1/95	9.3	1578	170.0	-27.3	-1.2	1804	19	18	1841
JB97	10/17/95	23.3	1056	45.3	-24.7	-1.1	1713	30	9	1752
JB123	12/4/95	6.5	415	63.7	-27.3	-10.3	2921	6	136	3063
JB131	4/20/96	8.9	2107	236.2	-28.5	-11.0	2430	12	47	2489
Hoople Creek										
JB23	5/29/95	4.0	211	52.7	-31.5	-13.3	2622	13	52	2688
JB30	6/12/95	2.6	747	283.3	-27.4	-12.0	3303	51	22	3376
JB57	8/1/95	1.6	173	108.3	-29.8	-10.5	2329	18	32	2378
JB92	10/10/95	1.4	162	112.9	-28.5	-10.5	2298	12	43	2353
JB122	12/4/95	1.2	112	95.5	-31.3	-13.7	3358	3	385	3745
JB132	4/20/96	3.4	1087	320.1	-24.7	-12.0	2583	5	116	2705
Long Sault Island										
JB54	8/1/95	26.1	2663	102.0	-25.4	-1.3	1806	18	19	1843
JB88	10/10/95	4.3	429	100.3	-21.4	-1.2	1882	7	52	1940
Main Channel										
JB12	7/14/94	0.7	102	136.6	-27.4	-1.3	1500	13	18	1531
JB17	11/3/94	0.3	95	334.7	-26.7	-1.8	1654	13	20	1687
JB21	5/29/95	1.1	64	59.1	-30.0	-1.0	1559	8	30	1597
JB95	10/17/95	1.1	76	66.2	-28.5	0.3	1689	16	17	1722
JB121	12/4/95	0.7	99	141.7	-26.3	-0.1	1634	16	15	1665
Whale Island										
JB20	5/29/95	2.0	264	135.4	-25.7	-1.3	1699	7	42	1747
JB29	6/12/95	1.2	162	136.6	-27.0	-2.6	1712	30	10	1752
JB55	8/1/95	0.8	274	340.0	-26.3	-0.4	1749	14	23	1786
JB90	10/10/95	2.1	226	110.1	-22.4	0.2	1579	20	12	1611
JB124	12/4/95	1.0	264	261.1	-16.3	-0.8	1724	9	29	1762
JB130	4/20/96	2.8	245	87.2	-27.0	-4.8	1762	19	15	1796

Appendix 5.2B Calculation of theoretical fractionation by algae (section 6.4.2.3)

Determination of the theoretical carbon isotope fractionation by algae:

The isotopic composition of plant material, $\delta^{13}\text{C}_{\text{phyto}}$, can be written as:

$$\delta^{13}\text{C}_{\text{phyto}} = \delta^{13}\text{C}_{\text{Ce}} - \epsilon_d - (\epsilon_f - \epsilon_d) * C_i / C_e \quad \text{Farquhar, et al. (1982)}$$

where $\delta^{13}\text{C}_{\text{Ce}}$ is the $\delta^{13}\text{C}$ of the ambient $\text{CO}_2(\text{aq})$ ($\approx C_e$), ϵ_d is the isotopic fractionation associated with diffusive transport of $\text{CO}_2(\text{aq})$ in water ($\approx 0.7 \text{ ‰}$; O'Leary, 1984), ϵ_f is the isotope fractionation associated with enzymatic, intracellular carbon fixation ($\approx 25 \text{ ‰}$ in this model; Rau et al., 1996). While most of these independent variables are known, the cell internal CO_2 concentration, C_i , is unknown. It can however be expressed as:

$$C_i = C_e - Q_s * \left(\frac{r}{D_r * \left(1 + \frac{r}{r_k}\right)} + \frac{1}{P} \right) \quad \text{Rau et al. (1996)}$$

with:

$$Q_s = \text{CO}_2(\text{aq}) \text{ uptake rate per unit cell surface area} = \frac{\gamma_c * 2\mu}{4\pi r^2} \quad [\text{mol C m}^{-2} \text{ s}^{-1}]$$

with

$$\gamma_c = \text{carbon content per cell} (= 1.76 * 10^{-11} [\text{mol C}])$$

μ = specific growth rate (varies between 0 and 2 [d^{-1}] and is always < 2.3 ; Rau et al., 1996)

r = average cell radius (assumed to be $10 \mu\text{m} = 10^{-5} \text{ [m]}$)

D_T = Temperature sensitive diffusivity of $\text{CO}_2(\text{aq})$ in freshwater ($= 1.543 * 10^{-9} \text{ [m}^2 \text{ s}^{-1}]$ @ 17 °C)

r_k = Reacto diffusive length ($= 2.06 * 10^{-4} \text{ [m]}$)

P = Cell wall permeability to $\text{CO}_2(\text{aq}) \text{ [m s}^{-1}]$

For a detailed derivation of these parameters refer to Rau et al. (1996). By substituting various values for μ ($= 0, 0.5, 1$ and 2), the equation can be solved explicitly for C_e and the isotopic fractionation between $\text{CO}_2(\text{aq})$ and phytoplankton, ϵ , with:

$$C_e = \frac{(\epsilon_f - \epsilon_d) * \left(\frac{\gamma_c * 2\mu}{4\pi r^2}\right) * \left[\frac{r}{(D_T * (1 + r/r_k))} + \frac{1}{P}\right]}{\delta^{13}\text{C}_{\text{Phyto}} - \delta^{13}\text{C}_{C_e} + \epsilon_d + (\epsilon_d - \epsilon_f)}$$

Temperature and pH influence the parameters D_T and r_k , but the model results proved to be essentially the same even under dramatic changes of these two parameters (i.e. change of temperature ± 10 °C and change of ± 1 pH unit). The model is, however, very sensitive to the cell radius, r , because it also changes cell carbon content, γ_c . Increasing r causes the isolines for μ to plot further to the right in Fig. 6.15, thus integrating more samples into the model. However an average cell radius of $10 \mu\text{m}$ seems a reasonable assumption for the phytoplankton community in the 'Main Channel' at Cornwall (Hudon et al., 1996).

Determination of the $\delta^{13}\text{C}_{\text{CO}_2(\text{aq})}$:

The $\delta^{13}\text{C}_{\text{CO}_2(\text{aq})}$ values were evaluated by using the temperature dependent isotopic discrimination between HCO_3^- and $\text{CO}_2(\text{aq})$. This isotopic discrimination changes linearly from -12 ‰ VPDB at 0 °C to -8.4 ‰ at 30 °C (Mook et al., 1974). The $\delta^{13}\text{C}$ value of the $\text{CO}_2(\text{aq})$ can be calculated by setting the $\delta^{13}\text{C}_{\text{DIC}}$ equal to the isotopic composition of the HCO_3^- ($\delta^{13}\text{C}_{\text{HCO}_3^-}$). It is safe to assume that isotopic compositions of DIC and HCO_3^- are identical, as long as the dissolved HCO_3^- is the major species of the DIC, which is true for the pH conditions found in this study. The activities of the aqueous CO_2 (= C_e) for the samples displayed in Fig. 6.15 were calculated from pH and alkalinity by using the program Hydrowin Calmbach (1995).